

Comparative analysis of methods for producing nanocellulose from wheat straw and bran, with co-extraction of valuable products

by

Regan Ceaser

Thesis presented in partial fulfilment

of the requirements for the Degree

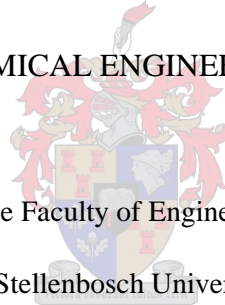
of

MASTER OF ENGINEERING

(CHEMICAL ENGINEERING)

in the Faculty of Engineering

at Stellenbosch University



The financial assistance of the of the Department of Science and Innovation (DSI) /Council of Scientific and Industrial Research (CSIR)- Waste Road Map and National Research Foundation (NRF) towards this research is hereby acknowledged. Opinions expressed and conclusions arrived at, are those of the author and are not necessarily to be attributed to the DSI/CSIR or NRF.

Supervisor

Prof. AFA Chimphango

Co-Supervisor

Prof. JF Görgens

December 2019

DECLARATION

By submitting this thesis electronically, I declare that the entirety of the work contained therein is my own, original work, that I am the sole author thereof (save to the extent explicitly otherwise stated), that reproduction and publication thereof by Stellenbosch University will not infringe any third party rights and that I have not previously in its entirety or in part submitted it for obtaining any qualification.

Date: *December 2019*

Copyright © 2019 Stellenbosch University

All rights reserved

PLAGIARISM DECLARATION

1. Plagiarism is the use of ideas, material, and other intellectual property of another's work and to present is as my own.
2. I agree that plagiarism is a punishable offence because it constitutes theft.
3. I also understand that direct translations are plagiarism.
4. Accordingly, all quotations and contributions from any source whatsoever (including the internet) have been cited fully. I understand that the reproduction of text without quotation marks (even when the source is cited) is plagiarism.
5. I declare that the work contained in this assignment, except where otherwise stated, is my original work and that I have not previously (in its entirety or in part) submitted it for grading in this module/assignment or another module/assignment.

Initials and surname: R Ceaser

Signature:

Date: December 2019

ABSTRACT

Nanocellulose production has recently attracted much attention from most researchers due to its variable applications in fields such as food, packaging, and medicine. Nanocellulose production from agricultural residues requires cellulose-rich pulp as the precursor which is mainly obtained by bleaching the biomass after pretreatment. Bleaching of the agricultural residues results in the loss and disruption of other cell wall components such as hemicellulose, hydroxycinnamic acid and lignin. However, these cell wall components are valuable products that when extracted can improve the treatment process. It is therefore necessary to develop a method to obtain a cellulose-rich pulp for nanocellulose production while co-extracting these other cell wall components as value-added products.

This study focused on developing and optimising a method to produce cellulose-rich pulp to further produce nanocellulose while co-extracting hemicellulose, lignin, ferulic and *p*-coumaric acid from wheat bran and wheat straw, which are agricultural residues from the wheat production industry. A two-stage alkaline treatment was the selected method for the extraction of hemicellulose, lignin, ferulic and *p*-coumaric acid while producing a cellulose-rich pulp. The first alkaline treatment stage was termed as a mild alkaline treatment stage due to the mild process conditions (1.5-2.5 wt. % NaOH conc., 20-40°C at 16 hours) used. The mild alkaline treatment was optimised by a central composite design with a response surface methodology targeted at extracting high yields of hemicelluloses and ferulic acid (for wheat bran) or *p*-coumaric acid (for wheat straw) with the extraction of lignin as a by-product of the treatment. The second stage alkaline treatment termed as the alkaline delignification step was conducted and optimised at treatment conditions of 6-10 wt. % NaOH for wheat bran and 8-12 wt. % NaOH for wheat straw for 30-90 min at 121°C. The alkaline delignification optimisation was focused on obtaining a cellulose-rich pulp with minimal lignin content for nanocellulose production whereas extracting as much lignin as possible with hemicelluloses as by-product. The hemicelluloses, lignin and cellulose-rich pulp obtained were analysed by compositional analysis, Fourier Transform Infrared Spectroscopy (FTIR) and a thermogravimetric analysis (TGA) whereas the extracted hydroxycinnamic acids (ferulic and *p*-coumaric acid) were analysed by compositional analysis and their antioxidant activity determined.

The total yield of hemicelluloses and lignin obtained after the two-stage alkaline treatment from wheat straw was 77% and 68%, respectively whereas the *p*-coumaric yield was 85% with an antioxidant activity of 45%. In addition, the wheat straw cellulose-rich pulp obtained after the two-stage alkaline treatment had a cellulose recovery, cellulose content, hemicelluloses content, lignin content and crystallinity of 97%, 76%, 3%, 5% and 55%, respectively which were within the range for application in nanocellulose production. The results indicated that two-stage alkaline treatment was beneficial for producing cellulose-rich wheat straw with a high crystallinity for nanocellulose production.

Yields of 52% and 94% were obtained for the two-stage alkaline treatment of hemicelluloses and lignin, respectively for wheat bran whereas a ferulic acid yield of 65% with a 15% antioxidant activity was obtained. Furthermore, the wheat bran cellulose-pulp obtained had cellulose recovery, cellulose content, hemicellulose content, lignin content and crystallinity of 83%, 48%, 31%, 6% and 41%, respectively. The cellulose recovery indicated cellulose loss during the delignification step whereas the hemicellulose content was high enough to inhibit enzymatic hydrolysis to produce nanocellulose. The alkaline delignified wheat bran cellulose produced required further treatment to be applied in nanocellulose production and was therefore not used in the nanocellulose production stage of this study.

Results from nanocellulose production from delignified wheat straw using sulfuric acid, hydrochloric acid and enzymatic treatment indicated that although sulfuric acid produced cellulose nanoparticles presented the highest yield (34%) and crystallinity (75%), it resulted in the lowest maximum thermal decomposition temperature (309⁰C) as compared to both hydrochloric acid and enzymatic treatment. In addition, the yield, zeta potential and maximum thermal decomposition temperature for nanoparticles produced by enzymatic treatment ($17.16 \pm 2.30\%$, -15.2 ± 0.6 mV and 378⁰C, respectively) were similar to that of hydrochloric acid treatment ($20.31 \pm 1.24\%$, -16.3 ± 1.50 mV and 380⁰C, respectively). It was interesting to note that, the yield, zeta potential and maximum thermal degradation temperature were obtained at a shorter time (4.64 h) for enzymatic treatment than the hydrochloric acid treatment (7.41 h), resolving the issue of extended enzymatic treatment times for nanocellulose production. Furthermore, the crystallinity obtained for hydrochloric acid produced nanoparticles (70%) was closer to that of sulfuric acid (75%) produced nanoparticles and higher than enzymatic hydrolysis produced nanoparticles (48%). Hydrochloric acid produced cellulose nanoparticles resulted in improved polydispersity index (0.53 ± 0.20) and fiber morphology (514 ± 50 length) as compared to enzymatic produce nanoparticles (0.92 ± 0.13 PdI and >1 μ m length). It can be concluded that between enzymatic and hydrochloric acid treatments, the latter resulted in nanoparticles with improved properties than the former.

KEYWORDS

Wheat straw; Wheat bran; Alkaline treatment; Hemicellulose; Lignin; *p*-Coumaric acid; Ferulic acid; Nanocellulose

OPSOMMING

Die produksie van nanocellulose het die afgelope tyd baie aandag gekry van die meeste navorsers as gevolg van die wisselvallige toepassings op gebiede soos voedsel, verpakking en medisyne. Die produksie van nanocellulose uit landboukoshuise benodig sellulose-ryke pulp as die voorloper wat hoofsaaklik verkry word deur die biomassa na behandeling met blykmiddels. Behandeling van die landboureste lei tot die verlies van ander selwandkomponente soos hemicellulose, hidroksisinnamiensuur en lignien. Hierdie selwandkomponente is egter waardevolle produkte wat die behandelingsproses kan verbeter wanneer dit ontgin word. Dit is dus nodig om 'n metode te ontwikkel om 'n sellulose-ryke eindproduk van nanocellulose-produksie te verkry, terwyl hierdie ander selwandkomponente as waardetoevoegingsprodukte saamgewerk kan word.

Hierdie studie het gefokus op die ontwikkeling en optimalisering van 'n metode om sellulose-ryke pulp te vervaardig waarvan nanocellulose verder geproduseer word, terwyl dit hemicellulose, lignien, feruline en p-coumaric acid van koring semels en koringstrooi, wat landbou-residu's uit die koringproduksiebedryf is, saamwerk. 'N Alkaliëse behandeling met twee fases was die geselekteerde metode vir die ekstraksie van hemicellulose, lignien, feruline en p-coumaric acid, terwyl 'n sellulose-ryke pulp geproduseer word. Die eerste alkaliese behandelingsfase word as ligte alkaliese behandelingsfase gedoen as gevolg van die ligte prosesstoestand (1,5-2,5 wt.% Konsentrasie NaOH, 20-40 °C op 16 uur). Die ligte alkaliese behandeling is geoptimaliseer deur 'n sentrale saamgestelde ontwerp met 'n responsoppervlak-metodologie wat daarop gemik is om hoë opbrengste van hemicelluloses en ferulienesuur (vir koring semels) of p-coumaric acid (vir koringstrooi) te onttrek met die ekstraksie van lignien as 'n by- produk van die behandeling. Die tweede fase alkaliese behandeling, wat as die alkaliese delignifikasie-stap bekend staan, is uitgevoer en geoptimaliseer tydens behandelingsstoestand van 6-10 wt.% NaOH vir koring semels en 8-12 wt.% NaOH vir koringstrooi vir 30-90 min by 121°C. Die optimalisering van die alkaliese delignifikasie was daarop gefokus om 'n sellulose-ryke pulp met 'n minimale lignieninhoud vir nanocellulose-produksie te verkry, terwyl soveel as moontlik lignien met hemicelluloses as neweproduk verkry word. Die hemicelluloses, lignien en sellulose-ryke pulp wat verkry is, is met behulp van samestellingsanalise, Fourier Transform Infrared Spectroscopy (FTIR) en 'n termogravimetrieë analise (TGA) geanaliseer, terwyl die onttrekte hidrosikannamiese sure (feruline en p-coumaric acid) deur middel van komposisie-analise en hul antioksidant aktiwiteit bepaal.

Die totale opbrengs van hemicelluloses en lignien wat na die tweestap-alkaliese behandeling van koringstrooi verkry is, was onderskeidelik 77% en 68%, terwyl die p-coumaric acid opbrengs 85% was met 'n antioksidantaktiwiteit van 45%. Boonop het die koringstrooi sellulose-ryke pulp wat na die tweestap-alkaliese behandeling verkry is, 'n sellulose-herstel, sellulose-inhoud, hemicellulose-inhoud, lignieninhoud en kristaliniteit van onderskeidelik 97%, 76%, 3%, 5% en 55% gehad. wat binne die

reeks vir toediening in nanocellulose-produksie was. Die resultate het aangedui dat tweestadige alkaliese behandeling voordelig was vir die produksie van sellulose-ryk koringstrooi met 'n hoë kristaliniteit vir nanocellulose-produksie.

Opbrengste van 52% en 94% is behaal vir die tweestap-alkaliese behandeling van hemicelluloses en lignien, onderskeidelik vir koring semels, terwyl 'n feruline suuropbrengs van 65% met 'n 15% antioksidant aktiwiteit verkry is. Verder het die koring semelselle sellulose-pulp sellulose herstel, sellulose-inhoud, hemicellulose-inhoud, lignieninhoud en kristaliniteit van onderskeidelik 83%, 48%, 31%, 6% en 41% gehad. Die sellulose-herstel het sellulose-verlies tydens die delignifikasiestap aangedui, terwyl die hemicellulose-inhoud hoog genoeg was om ensimatiëse hidrolise te inhibeer om nanocellulose te produseer. Die alkaliese delignifiseerde koring semelsellulose wat geproduseer is, het verdere behandeling toegepas in die produksie van nanocellulose en is daarom nie in die nanocellulose-produksiestadium van hierdie studie gebruik nie.

Resultate uit die produksie van nanocellulose uit delignifiseerde koringstrooi met behulp van swawelsuur, soutsuur en ensiembehandeling het aangedui dat hoewel swaelsuur geproduseerde sellulose-nanodeeltjies die hoogste opbrengs (34%) en kristaliniteit (75%) lewer, dit tot die laagste maksimum temperatuur vir ontbinding van die temperatuur gelei het (309°C) in vergelyking met beide soutsuur en ensimatiëse behandeling. Daarbenewens was die opbrengs, zeta-potensiaal en maksimum termiese ontbindingstemperatuur vir nanodeeltjies wat geproduseer word deur ensimatiëse behandeling (onderskeidelik $17,16 \pm 2,30\%$, $-15,2 \pm 0,6$ mV en 378°C) soortgelyk aan dié van soutsuurbehandeling ($20,31 \pm 1,24\%$, $-16,3 \pm 1,50$ mV en 380°C, onderskeidelik). Dit was interessant om daarop te let dat die opbrengs, die zeta-potensiaal en die maksimum termiese afbrekingstemperatuur op 'n korter tyd (4,64 uur) verkry is vir ensimatiëse behandeling as die soutsuurbehandeling (7,41 uur), wat die kwessie van verlengde ensimatiëse behandelingstye vir nanocellulose opgelos het. Verder was die kristaliniteit wat verkry is vir soutsuur geproduseerde nanopartikels (70%) nader aan dié van swaelsuur (75%) geproduseer nanodeeltjies en hoër as ensimatiëse hidrolise geproduseer nanodeeltjies (48%). Soutsuur geproduseerde sellulose-nanodeeltjies het gelei tot 'n verbeterde polydispersiteitsindeks ($0,53 \pm 0,20$) en veselmorfologie (514 ± 50 lengte) in vergelyking met die ensimatiëse produkte van nanopartikels ($0,92 \pm 0,13$ PdI en > 1 µm lengte). Die gevolgtrekking kan gemaak word dat laasgenoemde tussen ensimatiëse en soutsuurbehandelings nanodeeltjies tot gevolg gehad het met beter eienskappe as eersgenoemde.

ACKNOWLEDGEMENTS

I thank the Almighty God, for his gift of life, health, care, and strength throughout this research study.

I would also like to thank my parents and siblings for their unrelenting support, motivation and prayers throughout the course of this research study.

I am thankful to the following people for their support as well during this research studies:

- ❖ Prof. Annie F.A. Chiphango and Prof. Johann F. Görgens for their supervision throughout my study in Stellenbosch University.
- ❖ The National Research Foundation (NRF), DST/CSIR Waste Roadmap programme for their financial support.
- ❖ The analytical staff (Mr Jaco van Rooyen, Mrs Levine Simmers, Mrs Hanlie Botha) and the technical staff (Mr Alvin Peterson) of the Process Engineering Department for all their help with analysis and instruments, respectively.
- ❖ The staff of Forestry and Wood Science Department (Mr Henry Solomon and Mr Wilmour Hendrikse) for direction, training, and permission to use their facilities.
- ❖ Dr Helen Pfukwa and Dr Leigh Loots from the Department of Chemistry of Polymer Science and the Chemistry Department, respectively for training and help with FTIR and XRD, respectively.
- ❖ Prof. Lydia Joubert and Dr Erika Harmzen-Pretorius at the Central Analytical Facility for their assistance with SEM analysis.
- ❖ Friends and colleagues for their academic and social support, motivation, and friendship.

I really appreciate you all and would like to say a big thank you!

ABBREVIATIONS

AP	Alkaline Pretreatment
CC	Combination of Chemical Treatments
CCD	Central Composite Design
CI	Crystallinity Index
CM	Combination of Chemical and Mechanical Treatments
CMB	Combination of Chemical, Mechanical and Biological Treatments
CNC	Cellulose Nanocrystals
CNW	Cellulose Nanowhiskers
CNF	Nano Fibrillated Cellulose or Cellulose Nanofibers
DAP	Dilute Acid Pretreatment
DLS	Dynamic Light Scattering
DP	Degree of Polymerisation
EGU	Endoglucanase Unit
FTIR	Fourier Transform Infrared Spectroscopy
HMF	5-hydroxymethyl-2-furfural
HPLC	High Performance Liquid Chromatography
M ₀	Combined Severity Factor for Alkaline Pretreatment
N/R	Not Recorded
SE	Steam Explosion
SEM	Scanning Electron Microscopy
TEMPO	2, 2, 6, 6- tetramethylpiperidiny-1-oxyl
TGA	Thermogravimetric Analysis
WB	Wheat Bran
WS	Wheat Straw
XRD	X-Ray Diffraction

TABLE OF CONTENTS

DECLARATION.....	I
PLAGIARISM DECLARATION.....	II
ABSTRACT	III
OPSOMMING.....	V
ACKNOWLEDGEMENTS.....	VII
ABBREVIATIONS	VIII
TABLE OF CONTENTS.....	IX
LIST OF FIGURES	XIII
LIST OF TABLES	XVII
CHAPTER ONE.....	1
<i>1.1 INTRODUCTION.....</i>	<i>1</i>
CHAPTER TWO	3
LITERATURE REVIEW	3
<i>2.1 Composition of Wheat Straw and Bran.....</i>	<i>3</i>
2.1.1 Cellulose	4
2.1.1.1 Nanocellulose.....	6
2.1.1.2 Nanofibrillated cellulose (CNF)	6
2.1.1.3 Cellulose Nanocrystals (CNC).....	7
2.1.2 Hemicelluloses.....	8
2.1.3 Lignin.....	10
2.1.4 Starch	11
2.1.5 Proteins	13
2.1.6 Hydroxycinnamic acids (p-coumaric and ferulic acid)	14
<i>2.2 Fractionation of Wheat Straw and Wheat Bran into Hemicellulose, Lignin, Cellulose and Hydroxycinnamic Acids.....</i>	<i>15</i>
2.2.1 Starch Removal from wheat bran	16
2.2.2 Fractionation Methods for the Extraction of Hemicelluloses, Lignin and Producing Cellulose-Rich Pulp	17
2.2.2.1 Alkaline Pretreatment (AP)	18
2.2.2.2 Dilute Acid Pretreatment (DAP).....	24
2.2.2.3 Steam Explosion (SE).....	25
<i>2.3 Nanocellulose Treatment Methods.....</i>	<i>26</i>
2.3.1 Mechanical Methods.....	27
2.3.1.1 Microfluidization	27
2.3.1.2 Homogenizer.....	27
2.3.2 Chemical Methods	28
2.3.2.1 Oxidation	28
2.3.2.2 Acid hydrolysis.....	28

2.3.3	Biological Reaction	31
2.3.3.1	Enzymatic Treatment.....	31
2.4	<i>Production of Nanocellulose</i>	34
2.5	<i>Research Gaps</i>	38
2.6	<i>Aims and Objectives of the Study</i>	40
CHAPTER THREE		41
EXPERIMENTAL PROCEDURES		41
3.1	<i>Materials and Chemicals</i>	41
3.2	<i>Statistical analysis</i>	41
3.3	<i>Fractionation of Wheat Straw and Bran</i>	42
3.3.1	Milling	42
3.3.2	Starch Removal.....	42
3.3.3	Mild Alkaline Treatment for Extraction of Hemicelluloses and Hydroxycinnamic Acids (Ferulic and <i>p</i> -Coumaric Acids)	44
3.3.4	Alkaline Delignification Treatment for Producing Cellulose-rich Fiber with Minimal Lignin Content and Extraction of Lignin	45
3.4	<i>Nanocellulose Production with Cellulose-Rich Fibers</i>	46
3.4.1	Sulfuric Acid Hydrolysis of Cellulose-Rich Fibers.....	46
3.4.2	Hydrochloric Acid Hydrolysis of Cellulose-Rich Fibers	46
3.4.3	Enzymatic Treatment of Cellulose-Rich Fibers	47
3.5	<i>Characterization</i>	48
3.5.1	Sample Preparation.....	48
3.5.2	Compositional Analysis.....	48
3.5.2.1	Determination of moisture content	48
3.5.2.2	Determination of ash content.....	49
3.5.2.3	Determination of extractives.....	49
3.5.2.4	Determination of structural carbohydrates and lignin.	49
3.5.2.5	Determination of protein content.....	50
3.5.2.6	Determination of starch content.....	51
3.5.2.7	Determination of antioxidant DPPH free radical scavenging activity.....	51
3.5.3	Fourier Transform Infrared Spectroscopy (FTIR).....	51
3.5.4	X-Ray Diffraction and Crystallinity	52
3.5.5	Scanning Electron Microscopy.....	52
3.5.6	Thermogravimetric Analysis (TGA)	52
3.5.7	Particle Morphology and Surface Charge	52
CHAPTER FOUR.....		54
TWO-STAGE ALKALINE TREATMENT OF WHEAT STRAW AND WHEAT BRAN TO EXTRACT HEMICELLULOSE, LIGNIN, <i>P</i> -COUMARIC ACID (FROM WHEAT STRAW), FERULIC ACID (FROM WHEAT BRAN) AND PRODUCE CELLULOSE-RICH FIBERS FOR NANOCELLULOSE PRODUCTION		54
4.1	<i>Introduction</i>	54

4.1.1	Outline of two-stage alkaline treatment of wheat and wheat bran to extract hemicellulose, lignin, <i>p</i> -Coumaric acid (from wheat straw), ferulic acid (from wheat bran) and produce cellulose-rich fibers for nanocellulose production	55
4.2	<i>Chemical Composition of Wheat Straw and Wheat Bran</i>	56
4.3	<i>Destarching of wheat bran</i>	57
4.4	<i>Mild Alkaline Treatment of Untreated Wheat Straw and Destarched Wheat Bran for Hemicellulose, p-Coumaric Acid and Ferulic Acid Extraction</i>	59
4.4.1	Extraction of Recovered Alkali Soluble Hemicelluloses and Lignin at the Optimum Mild Alkaline Conditions	62
4.4.1.1	Yield and Composition of Recovered Hemicelluloses and Lignin at the Optimum Mild Alkaline Conditions	62
4.4.1.2	Fourier Transform Infrared Spectroscopy (FTIR) of Recovered Alkali Soluble Hemicelluloses and Lignin at the Optimum Alkaline Delignification Conditions.....	67
4.4.1.3	Thermal Stability of Recovered Alkali Soluble Hemicelluloses and Lignin at the Optimum Mild Alkaline Conditions.....	69
4.4.2	Mild Alkaline Extraction of <i>p</i> -coumaric Acid (from Wheat Straw) and Ferulic Acid (from Wheat Bran). 72	
4.4.2.1	Yield of Alkali Soluble P-Coumaric and Ferulic Acid.....	72
4.4.2.2	<i>p</i> -Coumaric Acid and Ferulic Acid Composition	72
4.5	<i>Alkaline Delignification Treatment of Mild Alkaline Treated Residues for Lignin Extraction and Production of Cellulose-Rich Pulp</i>	73
4.5.1	Extraction of Recovered Alkali Soluble Hemicelluloses and Lignin at the Optimum Alkaline Delignification Conditions	78
4.5.1.1	Yield and Composition of Recovered Alkali Soluble Hemicelluloses and Lignin at the Optimum Alkaline Delignification Conditions	78
4.5.1.2	Fourier Transform Infrared Spectroscopy (FTIR) of Recovered Alkali Soluble Hemicelluloses and Lignin at the Optimum Alkaline Delignification Conditions.....	80
4.5.1.3	Thermal Stability of Recovered Alkali Soluble Hemicelluloses and Lignin at the Optimum Alkaline Delignification Conditions	82
4.6	<i>Cellulose Isolation</i>	83
4.6.1	Fourier Transform Infrared Spectroscopy of Wheat Straw and Wheat Bran Treated and Untreated Samples	85
4.6.2	X-Ray Diffraction and Crystallinity of Wheat Straw and Wheat Bran Treated and Untreated Samples.....	87
4.6.3	Structural Changes of Wheat Straw and Wheat Bran Treated and Untreated Samples	89
4.6.4	Thermal Stability of Wheat Straw and Wheat Bran Treated and Untreated Samples.....	91
4.7	<i>Summary of Results</i>	93
CHAPTER FIVE		95
NANOCELLULOSE PRODUCTION		95
<i>Introduction</i>		95
5.1	<i>Yield, Particle Morphology and Surface Charge for Nanocellulose Production</i>	96
5.1.1	Commercial Cellulose Nanocrystals (CNC) and Cellulose Nanofibers (CNF)	96
5.1.2	Sulfuric Acid Hydrolysis of Cellulose-Rich Fibers from Two-step Alkaline Treatment of Wheat Straw ..	97
5.1.3	Optimisation of Hydrochloric Acid Hydrolysis of Cellulose-Rich Fibers from Two-step Alkaline Treatment of Wheat Straw	97

5.1.4	Optimisation of Enzymatic Hydrolysis of Cellulose-Rich Fibers from Two-step Alkaline Treatment of Wheat Straw	101
5.2	<i>Fourier Transform Infrared Spectroscopy of Functional Group Changes of Produced Nanocelluloses and Commercial Nanocelluloses</i>	105
5.3	<i>X-Ray Diffraction and Crystallinity of Produced Nanocelluloses and Commercial Nanocelluloses</i>	106
5.4	<i>Thermal Stability of Produced Nanocelluloses and Commercial Nanocelluloses</i>	107
5.5	<i>Conclusions</i>	109
CHAPTER SIX.....		111
CONCLUSIONS AND RECOMMENDATION.....		111
6.1	<i>Conclusions</i>	111
6.2	<i>Recommendations and future work</i>	113
REFERENCES.....		115
APPENDIX A: INFRARED BAND ASSIGNMENT.....		142
APPENDIX B: ANOVA ANALYSIS TABLES		144
APPENDIX C: MODELS AT DIFFERENT STAGES FOR WHEAT STRAW AND WHEAT BRAN TREATMENTS.....		155
APPENDIX D: CRYSTALLINITY AND THERMOGRAVIMETRIC ANALYSIS AT DIFFERENT TREATMENT STAGES		159
APPENDIX E: SEM IMAGES		162

LIST OF FIGURES

Figure 2.1 Structure of cellulose (Giri and Adhikari, 2013).....	4
Figure 2.2 Structure of hemicelluloses (arabinoxylan) (Sinha et al., 2012)	8
Figure 2.3 Structure of base unit alcohols (p-coumaryl alcohol, coniferyl alcohol and sinapyl alcohol) (Krogh and Olsson, 2008).	10
Figure 2.4 Structure of starch amylose (top) and amylopectin (bottom) (Visakh et al., 2014)	12
Figure 2.5 Structure of amino acid (basic unit of protein).....	13
Figure 2.6 Structure of ferulic acid (right) and <i>p</i> -Coumaric acid (left) (Saad et al., 2019)	14
Figure 2.7 Mechanism of sulfuric acid treatment of cellulose to produce nanocellulose (Malladi et al., 2018) ...	30
Figure 2.8 Mechanism of hydrochloric acid treatment of cellulose to produce nanocellulose (Islam et al., 2013)	31
Figure 2.9 Mechanism of enzymatic treatment (with endoglucanase, exoglucanase and β -glucosidase) of cellulose (Pino et al., 2018)	33
Figure 2.10 Chemical Treatment Combination (CC) for the production of CNC (adapted from Johar et al. (2012))	35
Figure 2.11 Chemical-Mechanical combination (CM) method for the production of CNF (adapted from Kaushik and Singh, (2011)).....	36
Figure 2.12 Chemical-Mechanical-Biological combination (CMB) method for the production of CNF(adapted from de Campos et al. (2013))	37
Figure 3.1 Process flow diagram for comparative analysis of methods for producing nanocellulose from wheat straw and bran, with co-extraction of valuable products	43
Figure 4.1 Pareto charts for mild alkaline treatment of wheat straw for hemicelluloses and <i>p</i> -coumaric acid extraction A) Hemicelluloses yield B) Hemicelluloses purity C) <i>p</i> -Coumaric acid yield.....	59
Figure 4.2 Pareto charts for mild alkaline treatment of wheat bran for hemicelluloses and ferulic acid extraction A) Hemicelluloses yield B) Hemicelluloses purity C) Ferulic acid yield.....	61
Figure 4.3 Surface plot of optimisation of wheat straw mild alkaline extracted A) Hemicelluloses purity B) Hemicelluloses yield/ original hemicelluloses C) <i>p</i> -Coumaric acid yield D) Desirability (54.14 °C, 2.35 wt.% NaOH) with NaOH concentration and temperature as independent variables	63

Figure 4.4 Yield and chemical composition of recovered lignin for mild alkaline wheat straw (MAWS), alkaline delignified wheat straw (SAWS), mild alkaline wheat bran (MAWB) and alkaline delignified wheat bran (SAWSB) at optimum conditions	64
Figure 4.5 Surface plot of optimisation of wheat bran mild alkaline extracted A) Hemicelluloses purity B) Hemicelluloses yield/ original hemicelluloses C) Ferulic acid yield D) Desirability (68.28°C, 2.71 wt. % NaOH) with NaOH concentration and temperature as independent variables.	66
Figure 4.6 Yield and chemical composition of recovered hemicelluloses for mild alkaline wheat straw (MAWS), alkaline delignified wheat straw (SAWS), mild alkaline wheat bran (MAWB) and alkaline delignified wheat bran (SAWSB) at optimum conditions.	67
Figure 4.7 FTIR spectra of functional group changes of mild alkaline wheat straw extracted hemicelluloses (MAWS Hemis) and mild alkaline wheat bran hemicelluloses (MAWB Hemis).....	68
Figure 4.8 FTIR spectra of functional group changes of mild alkaline wheat straw extracted lignin (MAWS Lignin) and mild alkaline wheat bran lignin (MAWB Lignin).....	69
Figure 4.9 Thermal stability of mild alkaline wheat bran hemicelluloses (MAWB); mild alkaline wheat straw hemicelluloses (MAWS); alkaline delignified wheat bran hemicelluloses (SAWB); alkaline delignified wheat straw hemicelluloses (SAWS).....	71
Figure 4.10 Thermal stability of mild alkaline wheat straw extracted lignin (MAWS); mild alkaline wheat bran extracted lignin (MAWB); alkaline delignified wheat straw extracted lignin (SAWS); alkaline delignified wheat bran extracted lignin (SAWB)	71
Figure 4.11 Surface plot of optimisation of alkaline delignified (SA) wheat straw A) Cellulose content in residue after SA treatment B) Lignin content in residue after SA treatment C) Extracted lignin yield/ lignin in mild alkaline wheat straw (MAWS) residue D) Desirability (10 wt.% NaOH, 60 min) with NaOH concentration and time as independent variables.....	74
Figure 4.12 Surface plot of optimisation of alkaline delignified (SA) wheat bran A) Cellulose content in residue after SA treatment B) Lignin content in residue after SA treatment C) Extracted lignin yield/ lignin in mild alkaline treated wheat bran (MAWB) residue D) Desirability(9.41 wt.% NaOH, 81.2 min) with NaOH concentration and time as independent variables	75
Figure 4.13 Pareto Charts A) Cellulose in residue B) Lignin in residue after alkaline delignification of mild alkaline treated wheat straw	76
Figure 4.14 Pareto Charts A) Cellulose in residue B) Lignin in residue after alkaline delignification of mild alkaline treated wheat bran.....	77
Figure 4.15 FTIR spectra of functional group changes of alkaline delignified wheat straw extracted hemicelluloses (SAWS Hemis) and alkaline delignified wheat bran hemicelluloses (SAWB Hemis).....	81

Figure 4.16 FTIR spectra of functional group changes of alkaline delignified wheat straw extracted lignin (SAWS Lignin) and alkaline delignified wheat bran lignin (SAWB Lignin)	82
Figure 4.17 Chemical composition and crystallinity of wheat straw at different treatment stages with comparison with the set literature parameters.	84
Figure 4.18 Chemical composition and crystallinity of wheat bran at different treatment stages with comparison with the set literature parameters.	84
Figure 4.19 FTIR spectra of functional group changes of untreated wheat straw (WS), mild alkaline wheat straw (MAWS) residues and alkaline delignified wheat straw (SAWS) residues.....	86
Figure 4.20 FTIR spectra of functional group changes for untreated wheat bran (WB), mild alkaline wheat bran (MAWB) residues and alkaline delignified wheat bran (SAWB) residues.	87
Figure 4.21 Scanning electron micrographs for a) untreated wheat straw b) mild alkaline treated wheat straw c) alkaline delignified wheat straw d) untreated wheat bran e) destarched wheat bran f) mild alkaline treated wheat bran g) alkaline delignified wheat bran.....	90
Figure 4.22 Thermal stability of untreated wheat straw (WS), mild alkaline wheat straw (MAWS) and alkaline delignified wheat straw (SAWS)	92
Figure 4.23 Thermal stability of untreated wheat bran (WB), destarched wheat bran (WB), mild alkaline wheat bran (MAWB) and alkaline delignified wheat bran (SAWB)	92
Figure 5.1 Pareto chart of optimisation of hydrochloric acid produced nanocellulose (a) yield (b) zeta potential (c) polydispersity index (d) particle length.....	98
Figure 5.2 Surface plot of optimisation of HCN process conditions A) Yield B) Zeta Potential (ZP) C) Polydispersity Index (PdI) D) Nanocellulose Length E) Desirability with time (7.41 hours) and temperature (114.14 ⁰ C) as dependent variables.....	100
Figure 5.3 Pareto chart of optimisation of enzymatic treatment produced nanocellulose (a) glucose concentration (b) zeta potential (c) polydispersity index (d) particle diameter	102
Figure 5.4 Yield, diameter, zeta potential and crystallinity for commercial nanocelluloses, sulphuric acid produced nanocelluloses (SCN), hydrochloric acid produced nanocelluloses (HCN), and enzymatic treatment produced nanocelluloses (ECN).....	103
Figure 5.5 Surface plot of optimisation of ECN (A) Glucose Concentration (B-C) Zeta Potential (ZP) (D-E) Polydispersity Index (PdI) (F-H) Nanocellulose Diameter (I-K) Desirability with time (4.64 h), FiberCare Dosage (75 ECU/g) and Viscozyme Dosage (10.8 FBG/g) as dependent variables	104

Figure 5.6 Polydispersity index of commercial nanocelluloses, sulphuric acid produced nanocelluloses (SCN), hydrochloric acid produced nanocelluloses (HCN), and enzymatic treatment produced nanocelluloses (ECN) 105

Figure 5.7 FTIR spectra of chemical group changes of nanofibrillated cellulose (CNF), cellulose nanocrystals (CNC), sulfuric acid nanoparticles (SCN), hydrochloric acid nanoparticles (HCN) and enzymatic cellulose nanoparticles (ECN).....106

Figure 5.8 Thermogravimetric analysis of sulfuric acid nanoparticles (SCN), hydrochloric acid nanoparticles (HCN), nanofibrillated cellulose (CNF), cellulose nanocrystals (CNC), enzymatic cellulose nanoparticles (ECN)108

Figure 6.1 SEM image of SCN162

Figure 6.2 SEM image of HCN at optimum conditions.....162

Figure 6.3 SEM image of ECN at optimum conditions163

LIST OF TABLES

Table 2.1 Chemical composition of wheat straw and bran on dry matter (dm) basis.....	3
Table 2.2 Effects of NaOH pretreatment conditions on various biomass and its effect on cellulose, hemicelluloses and lignin (continued on next page).....	22
Table 3.1 Parameters used for optimisation of mild alkaline treatment of wheat straw and wheat bran for the extraction of hemicelluloses and hydroxycinnamic acids (p-coumaric and ferulic acid).....	44
Table 3.2 Parameters used for optimisation of severe treatment of mild alkaline treated wheat straw solid residues	45
Table 3.3 Parameters used for optimisation of severe treatment of mild alkaline treated wheat bran solid residues	45
Table 3.4 Parameters to be considered for hydrochloric acid hydrolysis nanocellulose production of wheat straw and bran cellulose.....	47
Table 3.5 Parameters to be considered for enzymatic hydrolysis nanocellulose production of wheat straw and bran cellulose.....	47
Table 4.1 Chemical composition of untreated wheat straw, untreated wheat bran and destarched wheat bran. ...	57
Table 4.2 Mass balance for destarching of wheat bran	58
Table 4.3 Treatment conditions and response from mild alkaline treatment of wheat straw for hemicellulose and <i>p</i> -Coumaric acid extraction.....	60
Table 4.4 Treatment conditions and response from mild alkaline treatment of destarched wheat bran for hemicellulose and ferulic acid extraction.....	62
Table 4.5 Predicted and experimental values at optimised conditions for mild alkaline treated wheat straw for hemicellulose and <i>p</i> -coumaric acid extraction.....	63
Table 4.6 Predicted and experimental values at optimised conditions for mild alkaline treated wheat bran for hemicellulose and ferulic acid extraction.....	65
Table 4.7 Predicted and experimental values from optimised conditions for alkaline delignification treatment of wheat straw for production of cellulose-rich pulp and lignin extraction	77
Table 4.8 Predicted and experimental values from optimised conditions for alkaline delignification treatment of wheat bran for production of cellulose-rich pulp and lignin extraction.....	78

Table 5.1 Dimension, zeta potential (ZP) and polydispersity index (PdI) of produced commercial and sulfuric acid cellulose nanocrystal from wheat straw	96
Table 5.2 Optimised conditions for hydrochloric acid treated wheat straw cellulose nanoparticles (HCN).....	99
Table 6.1 Potential applications of various treatment products based on analysed characteristics	113
Table 6.2 Peak assignments for various functional groups found in various extracts	142
Table 6.3 ANOVA table for hemicellulose purity of mild alkaline treatment optimisation of wheat straw	144
Table 6.4 ANOVA table for hemicellulose yield of mild alkaline treatment optimisation of wheat straw.....	144
Table 6.5 ANOVA table for <i>p</i> -coumaric acid yield of mild alkaline treatment optimisation of wheat straw	144
Table 6.6 ANOVA table for hemicellulose purity of mild alkaline treatment optimisation of wheat bran.....	145
Table 6.7 ANOVA table for hemicellulose yield of mild alkaline treatment optimisation of wheat bran	145
Table 6.8 ANOVA table for ferulic acid yield of mild alkaline treatment optimisation of wheat bran	145
Table 6.9 Treatment conditions and response from alkaline delignification treatment of wheat straw for production of cellulose-rich pulp and lignin extraction	146
Table 6.10 ANOVA table for residue cellulose content of alkaline delignification treatment optimisation of wheat straw	146
Table 6.11 ANOVA table for residue lignin content of alkaline delignification treatment optimisation of wheat straw	147
Table 6.12 ANOVA table for lignin yield of alkaline delignification treatment optimisation of wheat straw....	147
Table 6.13 Treatment conditions and response from alkaline delignification treatment of wheat bran for production of cellulose-rich pulp and lignin extraction	148
Table 6.14 ANOVA table for residue cellulose content of alkaline delignification treatment optimisation of wheat bran.....	148
Table 6.15 ANOVA table for residue lignin content of alkaline delignification treatment optimisation of wheat straw	149
Table 6.16 ANOVA table for lignin yield of alkaline delignification treatment optimisation of wheat straw....	149
Table 6.17 Treatment conditions and response factors for hydrochloric acid treatment of alkaline delignified wheat straw cellulose to produce nanocellulose.....	150

Table 6.18 ANOVA table for nanocellulose yield optimisation after hydrochloric acid treatment of wheat straw cellulose pulp	150
Table 6.19 ANOVA table for nanocellulose zeta potential optimisation after hydrochloric acid treatment of wheat straw cellulose pulp.....	151
Table 6.20 ANOVA table for nanocellulose polydispersity index optimisation after hydrochloric acid treatment of wheat straw cellulose pulp.....	151
Table 6.21 ANOVA table for nanocellulose length optimisation after hydrochloric acid treatment of wheat straw cellulose pulp	152
Table 6.22 Treatment conditions and response factors for enzymatic treatment of wheat straw cellulose to produce nanocellulose.....	152
Table 6.23 ANOVA table for nanocellulose glucose concentration optimisation after enzymatic treatment of wheat straw cellulose pulp.....	153
Table 6.24 ANOVA table for nanocellulose zeta potential optimisation after enzymatic treatment of wheat straw cellulose pulp	153
Table 6.25 ANOVA table for nanocellulose polydispersity optimisation after enzymatic treatment of wheat straw cellulose pulp	154
Table 6.26 ANOVA table for nanocellulose mean diameter optimisation after enzymatic treatment of wheat straw cellulose pulp	154
Table 6.27 Crystallinity measurement at various stages of two-stage alkaline treatment of wheat straw and bran	159
Table 6.28 Thermogravimetric analysis of mild and alkaline delignified wheat straw and wheat bran hemicelluloses.....	159
Table 6.29 Thermogravimetric analysis of mild alkaline and alkaline delignified wheat straw and wheat bran lignin	160
Table 6.30 Thermogravimetric analysis at various stages of two-stage alkaline treatment of wheat straw and wheat bran.....	160
Table 6.31 Crystallinity measurement for commercial and produced nanocellulose samples	161
Table 6.32 Thermogravimetric analysis of different nanocellulose samples.....	161

CHAPTER ONE

1.1 INTRODUCTION

It is estimated that the consumption of wheat worldwide is 718.13 million tonnes (USDA, 2015). Lee et al. (2007) also estimated that every 0.453 kg grain of wheat produced yields 0.590 – 0.635 kg of wheat straw on a dry matter basis whereas wheat bran makes approximately 14-19% of the dry weight of the white grain (Merali et al. 2013). Primarily wheat straw and bran are used in feeding of animals such as lambs and cattle (Brand et al. 1991).

In the biorefinery sector, both wheat straw and wheat bran have gained attention due to their chemical compositions. They have both being targets for extraction of hemicellulose and hydroxycinnamic acids (Bataillon et al., 1998; Pan et al., 1998; Peng and Wu, 2010; Vijayalaxmi et al., 2014). However, wheat straw has gained more attention in the extraction of lignin and cellulose for nanocellulose production (Liu, 2017; Sun et al., 2005). A possible reason for this is the low lignin (3-12%) and cellulose content (11-21%) of wheat bran as well as its complex cell wall structure which contains significant amount of both starch (11-39%) and protein (10-19%) thereby making it a less attractive choice in comparison to wheat straw. Moreover, cellulose fibers obtained from wheat bran have been known to have a low crystallinity (32%) in comparison to cellulose fibers from wheat straw (54%). Due to this reason, wheat bran has mainly being applied in bioethanol production (Palmarola-Adrados et al., 2005). Nevertheless, cellulose obtained from both wheat straw and commercial cellulose from wheat bran have shown potential to be used for nanocellulose production (Alemdar and Sain, 2008a; Nilsson, 2017).

Recent research have indicated that it is possible to extract hemicelluloses, lignin and hydroxycinnamic acids from agricultural residues by using an alkaline treatment albeit at different treatment conditions (Egüés et al., 2012; Hosseinian and Mazza, 2009). The use of alkaline treatment can be beneficial to the treatment process given that it results in minimal loss to cellulose content and improvement to crystallinity if well controlled (Karp et al., 2014). Alkaline treatment therefore presents a potential method of producing hemicellulose, hydroxycinnamic acid, lignin and a cellulose-rich fiber for nanocellulose production. It therefore makes alkaline treatment an interesting choice for developing a method for extracting these valuable products while obtaining a cellulose rich fiber for nanocellulose production. Furthermore, nanocellulose production has mainly employed the use of bleached cellulosic fibers or commercial cellulose fibers whereas, the use of other chemically produced cellulose fibers have received little attention albeit little differences (Alemdar and Sain, 2008a; Espinosa et al., 2017).

Nanocellulose production from the cellulose rich fibers have mainly being performed using sulfuric acid. Although, sulfuric acid results in a higher yield of nanocellulose, it results in a reduction of thermal properties of the produced nanocellulose. Due to this effect, the use of hydrochloric acid and enzymatic treatment as alternative nanocellulose production treatments of cellulose-rich fibers have recently received much attention (Cheng et al., 2017; Shibuya and Hayashi, 2008). However, a comparative

analysis of their yield and characteristics with each other as well as the traditionally produced nanocelluloses could provide a better understanding into the production methods and functionality of the produced nanocellulose.

This study therefore aims at developing a fractionation method to isolate hemicellulose, lignin, ferulic acid (from wheat bran), *p*-coumaric acid (from wheat straw) and obtaining cellulose rich fibers that can be used in nanocellulose production. Furthermore, the obtained cellulose-rich fibers obtained are used to produce nanocellulose by employing a sulfuric acid, hydrochloric acid and an enzymatic treatment and comparing the yield and properties of the produced nanocelluloses.

CHAPTER TWO

LITERATURE REVIEW

2.1 Composition of Wheat Straw and Bran

Wheat straw and bran contains components that need to be isolated before further processing to obtain nanocellulose. Although they are both residues from wheat, they contain different amounts of these components as can be seen from Table 2.1. The properties and characteristics of the components will be further discussed in the subsequent sections.

Table 2.1 Chemical composition of wheat straw and bran on dry matter (dm) basis.

Components	Wheat Straw (% dm)	Wheat Bran (% dm)	Reference
Cellulose	38.5 – 45.7	10.7 – 20.8	(Barman et al., 2012; Cripwell et al., 2015; Kaushik and Singh, 2011; Merali et al., 2013)
Hemicelluloses	24.0 – 38.2	33.5 – 58.2	(Favaro et al., 2012; Janker-obermeier et al., 2012; Lee et al., 2007; Merali et al., 2013)
Lignin	7.9 - 27.2	2.7 – 12.1	(Favaro et al., 2012; Jaisamut et al., 2013; Merali et al., 2013; Tutt et al., 2012)
Starch	2.7	11.0 – 38.9	(Barman et al., 2012; Cripwell et al., 2015; Onipe et al., 2015)
Protein	1.9 – 5.7	9.6 - 18.6	(Khan and Mubeen, 2012; Lee et al., 2007; Onipe et al., 2015)
Extractives	9.4	N/A	(Barman et al. 2012; Merali et al. 2013)
Ash	3.57 – 9.9	3.2 – 11.6	(Khan and Mubeen, 2012; Sánchez-Bastardo et al., 2013;

			Tahir et al., 2002; Tutt et al., 2012)
Ferulic Acid	0.11-0.25	0.40-1.5	(Boz, 2015; Buranov and Mazza, 2009; Sipponen et al., 2014; Sun et al., 1995)
<i>p</i> -Coumaric Acid	0.20-0.42	0.02-0.26	(Buranov and Mazza, 2009; Merali et al., 2013; Ou et al., 2012; Sipponen et al., 2014)

N/A represents not available

2.1.1 Cellulose

Cellulose is a polymer with a base unit of cellobiose which consists of two glucose monomers linked by β -1, 4-glucosidic bonds. The molecular formula of cellulose is $(C_6H_{10}O_5)_n$ and its density is 1.50 g/cm^3 . Cellulose is made up of both free secondary OH groups and primary OH group (Giri and Adhikari, 2013). Cellulose possesses a reducing end possessing a free hemi-acetyl, a non-reducing end with a free hydroxyl and internal rings anhydroglucose units (Kalia et al., 2011) (Figure 2.1).

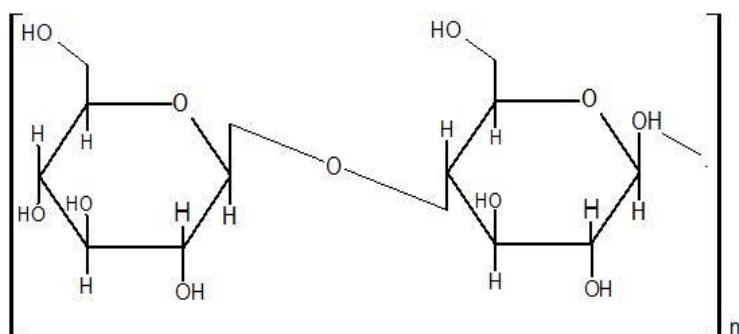


Figure 2.1 Structure of cellulose (Giri and Adhikari, 2013)

Cellulose forms linear chains that are stabilised by intramolecular hydrogen bonds, which assemble into microfibrils (Gardner and Blackwell, 1974). Microfibrils possess a diameter of 5-15 nm, which are formed when 36 cellulose chains with the same direction but with different starting and ending points, assemble. Intermolecular hydrogen bonds stabilise the microfibrils formed. It is due to this intra- and inter-molecular hydrogen bonds that cellulose possesses a level of resistance to degradation. Cellulose possesses a heterogeneous structure even though it is a homo-polysaccharide. In regions with less order, the intermolecular bonds are weaker and cellulose possesses an amorphous structure whereas in areas with more order there are stronger bonds, therefore, it possesses a crystalline structure (Krogh and Olsson, 2008).

Cellulose is either synthetically or naturally produced. In general, cellulose can possess one or more of these polymorphic forms: cellulose I, II, III and IV (Hu and Ragauskas, 2012). The unit structure of crystals of cellulose I are parallel. The unit structure in cellulose II are antiparallel and are the most thermodynamically stable form of the cellulose molecule. Cellulose II can be characterised as any cellulose that has undergone solubilisation and then re-precipitation. Cellulose I can be directly changed to cellulose II, however, II cannot be converted to cellulose I (Brown, 1999). Cellulose III is usually produced by reacting cellulose I and II with ammonia whereas cellulose IV is produced by heating cellulose III (Park et al. 2010). Cellulose I and II polymorphic forms are the basic types of cellulose present in most cellulose materials (Krogh and Olsson, 2008). Cellulose I exists as two crystalline sub allomorphs, cellulose I_{α} with a single chain triclinic structure and I_{β} with a double chain monoclinic structure (Hu and Ragauskas, 2012). The mechanical properties of nanofibers are attributes to these arrangements (Saxena, 2013). Most nanocellulose production concentrates on the I polymorphic forms because they are the most abundant (Mandal and Chakrabarty, 2011).

Most of the properties of cellulose are dependent on its degree of polymerisation (DP). DP is estimated to be the number of glucose units that comprises a single polymer molecule. Generally, the DP is estimated to be between 800-10000 units, however, it can extend to a value of 17000 units (Harmsen et al. 2010). Cellulose is able to absorb up to 14% water in the atmosphere causing it to easily swell in water (Krässig et al. 2012). However, at low temperatures cellulose is insoluble in water and dilute acid solutions (Harmsen et al. 2010). Elevated temperature can cause the breakage of the hydrogen bonds that holds the crystalline structure together. This is due to a build-up of energy due to an increase in temperature. This makes cellulose soluble in both water and dilute acid at elevated temperatures. Cellulose is soluble in concentrated acid although it has been shown that this can cause a severe degradation in the cellulose structure (Harmsen et al. 2010). The use of alkaline solutions can bring about a considerable amount of swelling in cellulose as well as the dissolution of the low molecular mass ($DP < 200$) portions of cellulose at temperatures above 150°C (Krässig et al. 2012). Cellulose is able to decompose at temperatures of 180°C and above (Thermowoodhandbook, 2003).

Wheat straw and wheat bran can be seen in Table 2.1 to possess cellulose contents of 39-46% and 11-21%, respectively. The cellulose content of the feedstock influences the crystallinity of the cellulose which is determined by using an x-ray diffraction method. The crystallinity is generally advantageous in the production of nanocellulose. The length of the crystalline portion can be between 100-250 nm with cross-sections (Alemdar and Sain, 2008b). Wheat straw has been reported to possess a crystallinity index of about 54%, which indicates that native wheat straw cellulose possess a relatively high amount of crystalline regions as compared to amorphous regions and with further treatment can be used to produce nanocellulose with a crystallinity of about 80% (Kaushik and Singh, 2011). On the other hand, commercial wheat bran cellulose was found to possess a crystallinity of 32%, which indicated that the cellulose was composed of less crystalline regions than amorphous regions. The cellulose when further

treated, resulted in nanocellulose with both cellulose I and II forms, which further reduced the crystallinity (Nilsson, 2017).

Wheat straw also possesses fiber bundles with a diameter in the range of 10-15 μ m and length of about 1410 μ m, which can be reduced to 30-40nm after treatment into nanocellulosic fibers (Giri and Adhikari, 2013). Whereas, wheat bran possess a fiber length of 1-1.5 μ m which when sulfuric acid treated resulted in nanocellulose of 80-100nm in diameter (Nilsson, 2017). Also, the degradation temperature of wheat straw cellulose has been reported to improve from 215 $^{\circ}$ C to 296 $^{\circ}$ C for its nanocellulose after undergoing treatment (Alemdar and Sain, 2008a), which makes it a viable source for production of composites.

The properties of wheat straw in comparison to other feedstock such as garlic straw Kallel et al. (2016) used for nanocellulose production indicates that it is a suitable feedstock choice to be considered for nanocellulose production. However, the properties of cellulose obtained from wheat bran as indicated by Nilsson (2017) presents a challenge with its low crystallinity and its ability to result in the production of both cellulose I and II polymorphs other than just cellulose I polymorphs which is seen in most nanocelluloses (Li et al., 2018).

2.1.1.1 Nanocellulose

Nanocellulose is a term used to refer to a cellulose crystal or fibril with at least one dimension within the nanometer range (Börjesson and Westman, 2015). Nanocellulose has recently received much interest in its application as a filler for biocomposites. Its application as a filler has been due to its high mechanical properties, high tensile strength, flexibility, and thermal properties among others (Börjesson and Westman, 2015; Deepa et al., 2011). Two main types of nanocelluloses are usually produced depending on the source and treatment approach; nanofibrillated celluloses and cellulose nanocrystals. They will be further discussed in the next sections.

2.1.1.2 Nanofibrillated cellulose (CNF)

They are long, threadlike bundles of cellulose fibers. CNFs are produced using mechanical treatment techniques sometimes in combination with chemical or enzymatic treatments. It involves the disintegration of the cellulose fibers along its long axis (Habibi, 2014). Some of the recent feedstocks that have been used for the production of CNFs are flax fibers, Kraft pulp, hemp fibers, cactus, soft and hard woods sugar beet pulp, wheat straw, potato and seaweed (Alain et al. 2000; Alemdar and Sain, 2008a; Chen et al. 2011; Dinand et al. 1999; Habibi, 2014; Thiripura Sundari and Ramesh, 2012).

In the mechanical treatment process, force is exerted on processed cellulose pulp to help peel the fibers, in turn, breaking the bonds that exist between the cellulose molecules, producing nanofibrils. The nanofibrils produced usually possess lengths of a few micrometres whereas the width ranges between 3-100 nm (Habibi, 2014).

There are several techniques of producing CNFs, which involves high pressure homogenization, microgrinding, and steam explosion. It is usually applied in fields such as the biocomposites materials for polymer matrix.

2.1.1.3 Cellulose Nanocrystals (CNC)

CNCs are generally crystalline rod-like particles in nature that are isolated after performing acid hydrolysis on the cellulosic fibers. They possess a width of about 3-50 nm and a length of 100-4000 nm (Bester, 2018). Throughout the years, hydrolysis for the production of CNCs has been done using cellulosic source materials such as hardwood pulp (Beck-Candanedo et al. 2005), softwood pulp (Orts et al. 2005), sisal (Garcia de Rodriguez et al. 2006) and cotton (Orts et al., 2005). Agricultural residues such as wheat straw (Dufresne et al., 1997), potato pulp (Alain et al. 2000), yellow pea (Dubief et al. 1999), waxy maize (Angellier et al. 2005), rice straw (El-Sakhawy and Hassan, 2007), banana fibers (Deepa et al. 2011) and algae (Strømme et al. 2002) have also been utilised to produce CNCs. The most common acids that have been used in this process are sulfuric acid, hydrochloric acid, hydrobromic acid and phosphoric acid among others (Wang et al. 2015).

Acid hydrolysis involves the diffusing of the acid into the glucosidic bonds of the amorphous parts of the processed cellulose pulp and hydrolysing it. After that, there is the hydrolysis of the easily accessible glucosidic bonds of the cellulose polymer and then the reducing end groups as well as the surface of the nanocrystal (Börjesson and Westman, 2015). The CNC produced is usually forms a stable colloidal dispersion when diluted with water or polar organic matter (Wang et al. 2015).

The properties of the formed nanocrystal depend on the cellulosic source, the reaction time and temperature (which are correlated to each other), the concentration and type of acid used (Börjesson and Westman, 2015). The crystallinity and fiber length as stated in Section 2.2 are usually the properties of the cellulosic source that affects the properties of the nanocrystal formed. It has been observed in most literature that a cellulosic source with a higher crystallinity and shorter fiber length has a high likelihood of producing nanocrystals with a high crystallinity and shorter nanocrystal length (Jonoobi et al., 2015). In addition, a higher reaction temperature means a shorter reaction time. A very short reaction time produces undispersed fibers. Whereas a longer reaction time means a complete hydrolysis of the nanocrystals. Also, the more difficult it is to hydrolyse the glucosidic bonds the longer the reaction takes (Beck-Candanedo et al. 2005). Depending on the type and concentration of the acid used, there could be the formation of charged groups. Liu et al. (2014) used 64 wt. % sulfuric acid solution to hydrolyse cellulosic fibers and noticed that it formed 0.5-2% charged sulfate groups which were attached to the surface of the nanocrystal. The charged sulfate groups influenced the stability of the nanocrystals in water by forming a stable colloidal suspension.

2.1.2 Hemicelluloses

Hemicelluloses are plant heteropolysaccharides whose chemical nature varies from plant to plant they are mainly made up of pentoses (xylose, rhamnose, arabinose), hexoses (glucose, mannose and galactose) and uronic acids (4-O-methyl-glucuronic and galacturonic acid). In hardwoods and agricultural plants (grasses and straws) the dominant hemicelluloses component is xylan, whereas the dominant hemicelluloses component in softwoods is glucomannans (Pu et al., 2008; Scheller and Ulvskov, 1871).

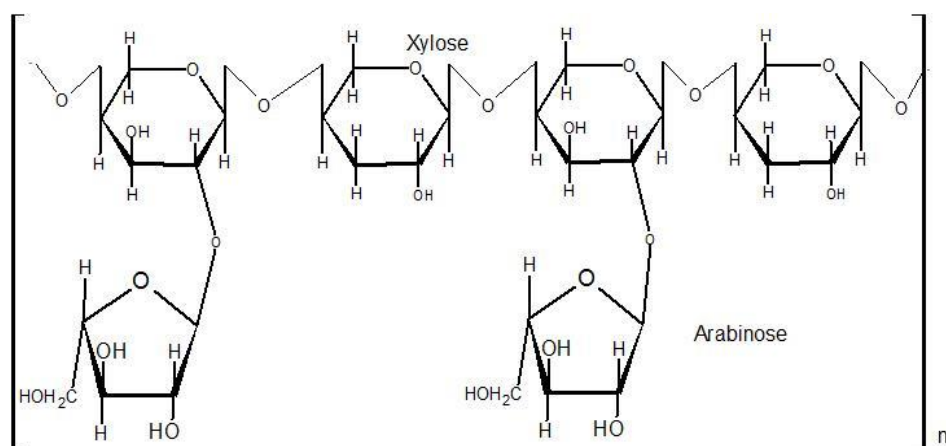


Figure 2.2 Structure of hemicelluloses (arabinoxylan) (Sinha et al., 2012)

Hemicelluloses are generally amorphous in nature due to their highly branched structure and the presence of connected acetyl groups (Kirk-Othmer, 2001). Hemicelluloses obtained from plants have DPs between 50-300 (Hu and Ragauskas, 2012). Hemicelluloses are generally insoluble in water at low temperature but at elevated temperatures (40-100⁰C) below that of cellulose, it begins to hydrolyse in water (Thermowoodhandbook, 2003). However, it is soluble in acid and alkaline solutions (Harmsen et al. 2010).

Xylans are the most abundant hemicelluloses in hardwoods and agricultural residues such as wheat straw and wheat bran (Saha, 2003). Xylan is a heteropolysaccharide with a homopolymeric backbone chain of 1,4-linked β -D-xylopyranosyl units (Sun and Sun, 2015). Different plants possess different xylan branches and composition. For example wheat arabinoxylan is mainly made up of 66% xylose and 34% arabinose, (Gruppen et al. 1992). Whereas, corn fiber xylan contains 48–54% xylose, 33–35% arabinose, 5–11% galactose, and 3–6% glucuronic acid (Doner and Hicks, 1997; Menon et al., 2010).

Monavari et al. (2009) stated that using dilute-acid pretreatment on biomass, from 70% up to 95% yield of hemicelluloses sugar could be recovered, although this process causes the degradation of the cellulose within the biomass due to high temperature (200⁰C) and also results in the production of monomers. Ballesteros et al. (2006) noticed that a hemicelluloses recovery of 45 – 69% can be obtained using steam explosion with the application of water as the impregnation agent, however with dilute H₂SO₄ (0.9%) as an impregnation agent, a yield of up to 85% was obtained with wheat straw. However,

the use of such a method was shown to result in the production of hemicellulosic monomers and oligomers. García et al. (2013) was also able to obtain yields of about 56% of the original hemicelluloses present within the biomass in a polymeric form with a cold alkaline extraction. Extraction of hemicelluloses are usually performed on the biomass after removing the lignin by either the use of a Soxhlet apparatus or by bleaching the biomass to produce a biomass made up of mostly hemicellulose and cellulose referred to as holocellulose (Peng et al., 2010a). However, the use of the Soxhlet apparatus has been less favoured due to its industrial limitation, time consuming nature and its low biomass capacity for the bleaching treatment (Rabetafika et al., 2014). However, the application of bleaching on the biomass has also been found to result in a loss of at least 20% of the hemicellulose as well as the hydroxycinnamic acid attached to the lignin within the biomass (K. Liu et al., 2016). However, this treatment can also result in the improving of the hemicellulose yield 9-93% of the bleached biomass with a purity up to 95% (Peng et al., 2010b; Xue et al., 2012).

Although both wheat straw and wheat bran contain hemicelluloses, it is evident from Table 2.1 that wheat bran (34-58%) generally contains more hemicelluloses as compared to wheat straw (24-38%). Due to the higher hemicelluloses content of wheat bran, it has received a lot of attention in the aspect of hemicellulose (arabinoxylan) extraction (Adams, 1955; Matavire, 2018; Sánchez-Bastardo et al., 2013). Alkaline extracted wheat bran hemicelluloses (arabinoxylan) with an arabinose to xylose ratio (A/X) of 0.50-0.56 have been used in bread making and the production of hydrogels among others (Koegelenberg, 2016; Matavire, 2018). Nevertheless, wheat straw hemicelluloses (arabinoxylan) with an A/X of 0.03-0.26 have also been noticed to be similarly applicable in papermaking industry as an additive to improve its mechanical properties among others (García et al., 2013; F Xu et al., 2006). Water extractable arabinoxylan from wheat bran has been used as emulsion stabilisers (Wrigley et al. 2016).

In the production of nanocellulose, hemicelluloses is one of the components that needs to be removed from the biomass, because it acts as a 'shield' for the cellulose making it difficult for both acid and enzymatic treatments to reach the cellulose for the production of nanocellulose (Kirk-Othmer, 2001). However an allowable amount of xylan (0.5-20%) is permitted in cellulose-rich pulp used for enzymatically produced nanocellulose (Teixeira et al. 2010; Penttilä et al. 2013). Penttilä et al. (2013) indicated that within this range the xylan has an insignificant effect on the inhibition of enzymes used for nanocellulose production. Furthermore, Espinosa et al. (2017) also showed that the maximum hemicellulose content of wheat pulp that can be used in the production of nanocelluloses was 23%. This therefore indicates that for both wheat straw and wheat bran considerable amounts of hemicelluloses (Table 2.1) need to be removed for the pulp obtained to be applied in nanocellulose production. Nevertheless, xylan from hemicelluloses can be used to reinforce nanocellulose in the production of xylan composite films (Saxena, 2013).

2.1.3 Lignin

Lignin is an amorphous, three-dimensional phenolic polymer (Hu and Ragauskas, 2012), which is made up of three cross linked phenylpropane units: guaiacyl, syringyl and *p*-hydroxyphenyl units (Harmsen et al. 2010) (Figure 2.3). The basic units are usually linked together by carbon-carbon or ether bond with an arylglyceryl- β -aryl ether linkage dominant in both hardwood and softwood lignin (Krogh and Olsson, 2008; Santos et al., 2015).

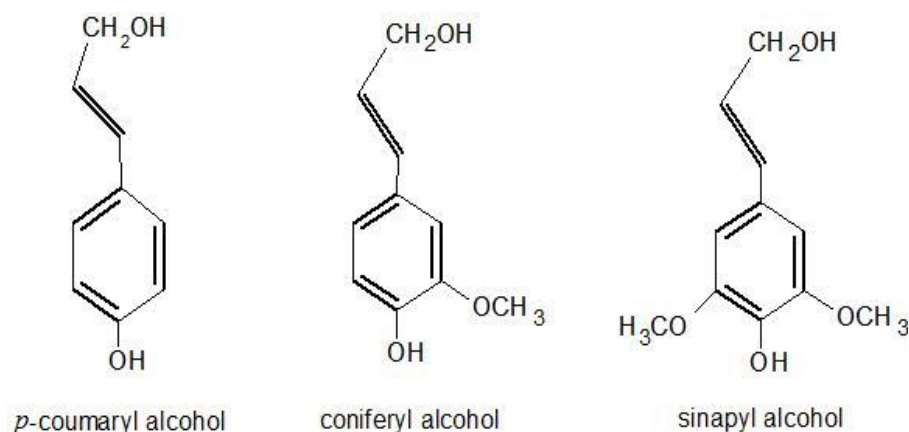


Figure 2.3 Structure of base unit alcohols (*p*-coumaryl alcohol, coniferyl alcohol and sinapyl alcohol) (Krogh and Olsson, 2008).

Softwood lignin is usually made up of guaiacyl units and a small number of *p*-hydroxyphenyl units whereas hardwood lignin is made up of guaiacyl and syringyl units with a small amount of *p*-hydroxyphenyl units (Sun and Sun, 2015). Agricultural residues such as wheat straw has been found to be made up of all three types of lignin with *p*-hydroxyphenyl units being the least (Wild et al., 2012). Wheat straw lignin has ratio of syringyl to guaiacyl to *p*-hydroxyphenyl units (S:G:H) being within the ranges 10:9:1 and 11:5:1 (Lourenço and Pereira, 2018). In addition, wheat straw lignin was found to contain both *p*-Coumaric acid (pCa) and ferulic acid (FA) in a ratio between 1.6 -1.7 (pCa/FA) (Santos et al., 2015; R. Sun et al., 2002). Whereas, wheat bran was found to possess a pCA to FA ratio between 0.13-0.18 (Kim et al., 2006).

Lignin is hydrophobic in nature (Hu and Ragauskas, 2012) and linked to hemicelluloses and cellulose in a complex cell wall matrix (Jonoobi et al., 2015). This helps to provide strength, stability and resistance to biological attacks for the plant (Adapa et al., 2009; Chabannes et al., 2001; Hu and Ragauskas, 2012). It also acts as a binding agent for the cellulose fibers. Degradation of lignin by the use of water can only occur at temperatures above 180°C without the presence of any strong acid (Harmsen et al. 2010).

Cansell et al. (1998) reported that the use of supercritical water ($T_{cr} = 647.1$ K, $P_{cr} = 22.1$ MPa) on lignin is able to enhance its degradation into the production of phenolic compounds Akgul and Kirci (2009) and Quesada-Medina et al. (2010) proposed the use of ethanol-water as the solvent. Ethanol can

improve the hydrothermal depolymerisation of lignin in the water to recoverable liquid products (Thring, 1994) and also help inhibit the repolymerisation of the products (Cheng et al. 2012). Nenkova et al. (2008) also depolymerised lignin using an aqueous alkaline solution of 5% NaOH at 180°C for 6 hours. In most nanocellulose productions, a bleaching step is used to remove all residual lignin and hemicelluloses from the biomass before further refinery of the cellulose is done (Abraham et al. 2011; Barana et al. 2016; Hassan et al. 2012; Johar et al. 2012; Kekäläinen et al. 2015; Moran et al. 2008; Rosa et al. 2012). Chemicals such as a mixture of sodium hypochlorite solution (El-Sakhawy and Hassan, 2007) and hydrogen peroxide (0.5% - 3%) (Moran et al. 2008) have been used to remove residual lignin.

Lignin can be used as a substitute for petroleum-derived phenol in the synthesis of phenol-formaldehyde resin (Cheng et al., 2012). Due to the nature of lignin, only about 2% of the total technical lignin produced is utilised in the production sector (Alekhina et al., 2015). It is used in producing stabilisers for plastics and rubbers (Kennedy et al., 1992), gels for separation of alcohol and other small organic molecules from fermentation broths (Griffith and Compere, 2008) and also the formulation of surfactants and dispersants (Glasser and Sarkanen, 1989).

In the production of nanocellulose, allowing the presence of a high amount of lignin will in turn result in a high amount of hemicellulose due to its complex cell wall matrix which is unrequired for nanocellulose production and must therefore be removed. The lignin-hemicellulose trend was observed by Teixeira et al. (2010). The study showed that a cellulose-rich pulp with a varying lignin content (0.4-16%) also resulted in hemicelluloses content (0.5-11%). However, Teixeira et al. (2010) indicated that with a maximum lignin content of 16% in the cellulose-rich pulp the maximum yield of nanocellulose was reduced from 65% to 52%. In addition, it was noticed in the study that cellulose-rich pulp with higher lignin content ($\geq 16\%$) resulted in production of nanocelluloses with longer length and diameter in comparison to those with lower lignin content (0.4-10%). It can therefore be summarised that given the wheat straw and wheat bran lignin content (Table 2.1), they need to be reduced to less than 10% to be applied in nanocellulose production.

2.1.4 Starch

Starch naturally occurs as granules which are used to store energy (Eriksson, 2012), composed of both amylose and amylopectin (Perez and Bertoft, 2010). Starch from different sources contain a variable composition; Liu & Ng (2015) reported 23–26% amylose and 74–77% amylopectin in wheat bran whereas waxy maize contains 100% amylopectin (Daniel et al. 2007). Amylose is a linear (1,4)- α -D-glycosidic linkages polymer with a molecular mass of 10^5 - 10^6 , whereas amylopectin is a bush-shaped (1,4)- α -D-glycosidic linkages and (1,6)- α -D-glycosidic linkages polymer with a molecular mass of one to several million (BeMiller and Huber, 2012) (Figure 2.4). Starch mainly differs from plant to plant with respect to their appearance, properties and particle size distribution (Daniel et al. 2007). Starch has

been reported to make up about 11.1- 39% of the dry weight of wheat bran depending on the debranning method used (Cripwell et al. 2015; Favaro et al. 2012; Liu and Ng, 2016; Tirpanalan et al. 2014) and 2.7% in wheat straw (Barman et al., 2012) . Starch present in biomass with more than 8% starch (Matawire, 2018) is generally isolated from the material before other fractionation methods are conducted (Brillouet and Mercier, 1981; Liu and Ng, 2016; Palmarola-Adrados et al., 2005).

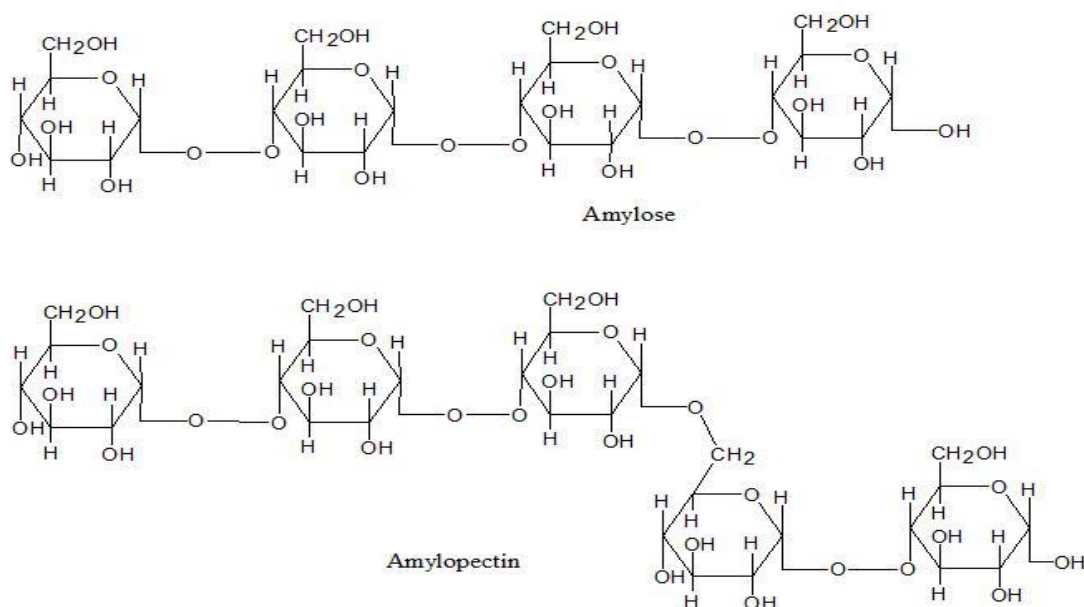


Figure 2.4 Structure of starch amylose (top) and amylopectin (bottom) (Visakh et al., 2014)

In general, starch is insoluble in cold water. As the temperature of the water begins to increase above 25°C there is strong vibration in the starch granule molecules causing a break in the intermolecular bonds bringing about absorption of water and swelling (BeMiller and Huber, 2012). Reacting β -amylase and glucoamylase on starch will produce maltose and D-glucose, respectively for both components of starch. However β -amylase can also produce β -limit-dextrins after its reaction with amylopectin (Daniel et al. 2007). Furthermore, due to the presence of a large amount of amylopectin (74-77%) in wheat bran starch it makes it susceptible to retrogradation due to exposed OH groups. Whereas, the presence of the amylose is the primary cause to the stiffening of wheat bran starch upon cooling due to the amylose molecules ‘zipping up’ together excluding the previously attached OH groups (Daniel et al. 2007).

Starch is used in industrial applications; to produce paper and paperboard products, as a sizing agent in textile products, in fermentation processes to produce ethanol and other products. Starch is also used in the processed food industry as a thickener or stabiliser, gelling agent, and a starting material for the production of sweeteners and polyols (BeMiller and Huber, 2012). Starch present in the lignocellulosic biomass must be removed before initiating the nanocellulose production process. If starch is not removed before the start of the production process, its degradation produces glucose which results in glucose inhibition in enzymatic treatment (Saha, 2004). Glucose is known to bind to the active sites of enzymes such as endoglucanases and exoglucanases used in enzymatic hydrolysis to produce

nanocellulose resulting in the accumulation of cellobiose which have a stronger inhibitory effect on these enzymes (Andersen, 2007; Zhai et al., 2018). Due to this effect of glucose on the nanocellulose production process, starch removal is a necessity in starch containing biomass for nanocellulose production.

2.1.5 Proteins

Proteins are made up of amino acid chains. Amino acids present in proteins are amphiprotic in nature (i.e. it possesses both acidic and basic functional groups). Amino acid possesses both an amino group and a carboxyl group, as well as a hydrogen atom (H) and a variable side chain (denoted as R in Figure 2.5) (Lehninger et al., 2004). The R group present in amino acid usually determines the characteristics of the amino acid.

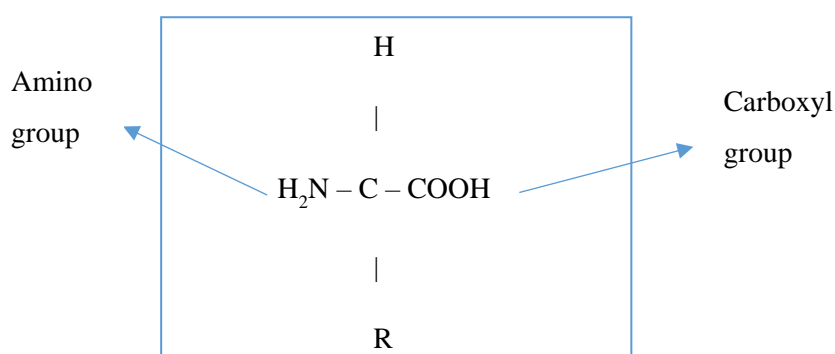


Figure 2.5 Structure of amino acid (basic unit of protein)

Proteins are generally soluble in water and insoluble in organic solvents like ether and benzene. They also possess low vapour pressure and melting temperatures above 200°C. The ability of protein to solubilize in a solvent is dependent on the salt concentration, organic solvent, solution pH and the presence of metal ions. At lower salt concentrations, the solubility of protein increases slightly but at higher salt concentrations the solubility of protein reduces drastically and thereby making it easier to precipitate the protein out of the solution. The solution pH influences the charge of the protein thereby influencing its precipitation properties. The charge possessed by a protein is influenced by the total charge of the amino acid groups present in the protein. A neutral point is said to have been reached at its isoelectric point. At this point, the protein can easily be precipitated out of the solution. Precipitation of protein is one of the most widely used method of protein recovery (Whitford, 1961).

As stated in Table 2.1, wheat bran contains 10-19% proteins whereas wheat straw contains 2-8% proteins making wheat bran a more viable source to target for protein extraction. It is widely known that wheat protein contains both gluten and prolamins which makes them extractable by both alkaline solutions and ethanol (Majzoobi and Abedi, 2014). The presence of proteins within wheat bran has been found to have no effect on the extraction of cell wall components such as hemicelluloses (arabinoxylan) (Beaugrand et al., 2004) however due to the starch protein matrix in wheat bran there is the removal of about half of the proteins during destarching of starch (Tirpanalan et al., 2014). Although wheat proteins

have been stated to have no effect on other cell wall components apart from starch it can however reduce the process efficiency per weight of substrate (Kim et al. 2013), thereby, causing a reduction in the cellulose content. However, an extraction of protein before the production of nanocellulose can be beneficial to the production process. The extraction process can lead to a partial disintegration of the material before further fractionation, as well as significantly improve biological treatment application on cellulose (Dale et al. 2009; Kim et al. 2013). Also if the protein can be extracted before the isolation of the nanocellulose, it is highly probable that the protein extracted will maintain their integrity, thereby making it easier to be used in other processes (Chiesa and Gnansounou, 2011). This can, in turn, improve the economic viability of the production process (Cookman and Glatz, 2009).

2.1.6 Hydroxycinnamic acids (*p*-coumaric and ferulic acid)

Hydroxycinnamic acids such as *p*-coumaric (4-hydroxycinnamic acid) and ferulic acid (4-hydroxy-3-methoxycinnamic acid) are the most abundant of phenolic acids found present in most agricultural residues (Figure 2.6). These hydroxycinnamic acids form lignin-phenolic-carbohydrate complexes within the cell wall of the residues. They are attached to both the lignin and carbohydrate by ether and ester bonds. Buranov and Mazza (2008) found that wheat straw contains 0.38% and 0.17% esterified and etherified *p*-coumaric acid, respectively, as well as, 0.10% and 0.22% esterified and etherified ferulic acid, respectively. The ether bonds are usually linked to lignin whereas the ester bonds to the carbohydrate. A cereal crop such as wheat has more ferulic acid present in the bran than in the straw, with more *p*-Coumaric acid present in the straw than in the bran (Boz, 2015; Ou et al., 2012).

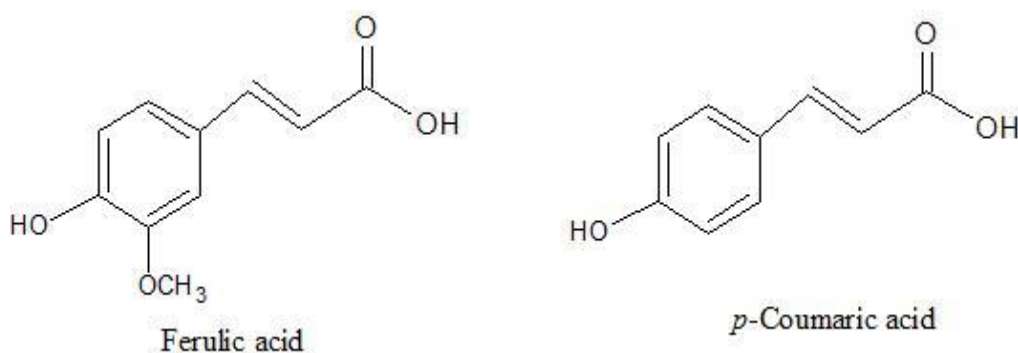


Figure 2.6 Structure of ferulic acid (right) and *p*-Coumaric acid (left) (Saad et al., 2019)

The hydroxycinnamic acids are usually extracted from natural sources by enzymatic and chemical treatments. Enzymes such as ferulic acid esterase used in the hydrolysis of ferulic acid are usually produced in very low quantities by microorganisms, also the hydrolysis of the hydroxycinnamic acid from these agricultural residues takes a very long time and results in low yields due to its inability to release bound acids (Ou et al., 2007). Due to these reasons, the option of using chemical hydrolysis to release these hydroxycinnamic acids has become the most favourable method. However, hot acid hydrolysis has been shown to cause degradation and result in lesser yield of hydroxycinnamic acids such as *p*-coumaric and ferulic acid in comparison to hot alkaline hydrolysis (Kim et al., 2006). The

ester linkages are hydrolysed using an alkali such as NaOH. These compounds found within the cell wall of biomass can also serve to induce swelling of the cell wall, thereby increasing solubility of the individual cell wall components such as lignin and hemicelluloses (Sun et al., 1995). Although, this is an advantage provided by the extraction of these hydroxycinnamic acids, it also results in an issue in terms of the purity of these acids. Due to this a number of purification methods have been investigated including the use of activated carbon, macro-porous resins and the use organic solvents such as ethanol (Buranov and Mazza, 2009; Couteau and Mathaly, 1997; Ou et al., 2007).

It is however interesting to note that, although these hydroxycinnamic acids make up a small percentage of the biomass composition, they have much commercial value. For example, 1 g ferulic acid is sold at ZAR 668 whereas 1 g *p*-Coumaric acid is sold at ZAR 710 by Sigma Aldrich. Furthermore, ferulic acid and *p*-Coumaric acid have been of interest due to their antioxidant properties. They have been applied as a high-value additive in both the pharmaceutical, food industry and cosmetic industries, among others. In the pharmaceutical industry ferulic acid is used as an additive to help reduce liver cholesterol and coronary diseases (Ou et al., 2007). Whereas, *p*-Coumaric acid is used as an additive to reduce the risk of stomach cancer (Max et al., 2009). In addition, ferulic acid has been found to be a precursor in the production of a value-added product such as vanillin (Tapin et al., 2006). Meanwhile, *p*-Coumaric acid has also been found to be a precursor in the production of *p*-hydroxybenzoic acid (K. Jiang et al., 2016).

2.2 Fractionation of Wheat Straw and Wheat Bran into Hemicellulose, Lignin, Cellulose and Hydroxycinnamic Acids

Due to the difference in their compositions (Table 2.1), treatments such as destarching, which can be conducted on wheat bran will not have any significant effect on wheat straw. Comparing the two biomass, wheat straw has received more research attention for fractionating processes, as well as the nanocellulose extraction (Barman et al. 2012; Curreli et al. 1997; Heikkinen et al. 2014; Kamel, 2007; Kaushik and Singh, 2011; Koti et al. 2012; Montane et al. 1998; Sun et al. 2004; Zimmermann et al. 2010). The focus of research utilising wheat bran has been more on the fractionation methods to produce arabinoxylan and ethanol because of its high starch and hemicelluloses contents (Brillouet and Mercier, 1981; Chotěborská et al. 2004; Favaro et al. 2012; Liu and Ng, 2016; Merali et al. 2013; Palmarola-Adrados et al. 2005; Sánchez-Bastardo et al. 2013; Tobergte and Curtis, 2013). To date, there has been limited research on the extraction of nanocellulose utilising wheat bran as raw material due to its high starch content and low crystallinity among others (Nilsson, 2017).

Therefore, components other than cellulose must first be extracted from the raw biomass material. Extraction of other cell wall components such as hemicellulose and lignin results in obtaining a cellulose-rich pulp that can be used for nanocellulose production. The minimum requirements stated in most literature for the cellulose-rich pulp for nanocellulose production are cellulose content $\geq 62\%$, crystallinity index $\geq 48\%$, hemicelluloses content $\leq 23\%$ and lignin $\leq 10\%$ (Espinosa et al., 2017; Kallel

et al., 2016; Teixeira et al., 2010). It is therefore necessary to reduce the hemicellulose and lignin contents while increasing the cellulose content and crystallinity before nanocellulose production from wheat straw and wheat bran. However, the process of reducing the hemicelluloses and lignin provides an opportunity to obtain additional value-added products in addition to nanocellulose. In addition removal of the two products would increase the purity of the nanocelluloses to be produced. It is therefore necessary to develop a method to extract lignin, hemicellulose, ferulic acid and *p*-Coumaric acid from the biomass while improving on its cellulose content and crystallinity to meet the minimum criteria for nanocellulose production.

2.2.1 Starch Removal from wheat bran

As stated in Section 2.1.4 the process of starch removal is an important step in nanocellulose production since it prevents the production of large amounts of monomeric sugars during the isolation steps. The process of starch removal from most grain residues is usually by using water or enzymes, which both affect the bonds and structure of starch. A number of studies have been conducted which have involved the removal of starch from residues such as wheat bran and triticale bran (Brillouet and Mercier, 1981; Favaro et al. 2012; García-Aparicio et al. 2011; Saunders and Walker, 1968; Tirpanalan et al. 2014). Starch is removed using only water or a bran water solution with enzymes.

Enzymes such as α -amylase, amyloglucosidase and Stargen™ 001 have been used to remove starch from bran materials. The use of enzymes has demonstrated a relatively high ability to remove a majority of the starch present in the material by converting them into glucose. Tirpanalan et al. (2014) treated wheat bran (with 9.1% starch content) mixed with deionized water at a ratio of 1:4, with 100L of α -amylase (at 85°C, pH 6.5 for 3h) from *Bacillus Licheniformis* and amyloglucosidase (at 55 °C, pH 5.5 for 18h) from *Aspergillus Niger* and obtained a free glucose yield of 107.6% based on the starch fraction. The excess glucose content was attributed to the presence of free glucose in wheat bran. Most recent works on wheat bran have used Termamyl SC and an amyloglucosidase obtained from Novozymes in a two-step starch liquefaction process (Anderson and Simsek, 2019). Several research papers have reported and proven that the treatment is able to remove almost or all the starch present in the wheat bran as well as a fraction of the soluble proteins within the wheat bran. This is usually achieved by sufficiently washing the wheat bran with water after destarching to wash off all solubilised components (Reisinger et al., 2014). This therefore indicates that an efficient enzymatic destarching of wheat bran cannot only lead to a removal of almost or all the starch present in the wheat bran but can also bring about a reduction in the protein content of the wheat bran. Such a process is very beneficial for the subsequent fractionation of the wheat bran by reducing the addition of additional treatment processes.

In addition, it is interesting to note that researches that have focused on solubilising protein from wheat bran by using protease in addition to other carbohydrate degrading enzymes have achieved only a 50-

58% protein removal (Arte et al., 2015; Neudoerffer and Smith, 1969). Moreover, addition of protease to the other carbohydrate degrading enzymes required the hydrolysis to be performed at a low temperature (30-35°C) which does not agree with the conditions for most starch degrading enzymes (55-85°C) (Arte et al., 2015; Tirpanalan et al., 2014). In addition, to ensure an almost total destarching (0.1%) and deproteinized (5.7%) wheat bran, the enzymatic destarching and deproteinizing step had to be repeated several times (Wang et al., 2014). Furthermore, this repetition of the enzymatic treatment is economically unfavourable due to high enzyme cost.

Starch removal by the use of only water have also been applied on wheat bran by Koegelenberg (2016) and Aguedo et al. (2014). The process is based on the principle of starch gelatinization and consequent removal by washing. At a lower initial starch content of 7%, Koegelenberg (2016) reduced the starch content to less than 1% by heating with water at 40°C for 15min. Aguedo et al. 2014 on the other hand, was able to reduce the starch content from an initial content of 20-22% to a final content of 5.4% by heating with water at 95°C for 10min. This indicated that to reduce the starch content of bran with a higher native starch content with the application of water it is necessary to increase the temperature sufficiently and wash the bran at an equally high temperature to prevent the gelatinised starch from easily accumulating back on the wheat bran particles. Although both processes (water and enzyme extraction) are meant to remove the starch present in the material, application of an enzyme breaks the starch into glucose whereas the application of water helps to retrieve the starch much more in their original nature through gelatinization and retrogradation (Goesaert et al., 2005). However, destarching of bran by the application of hot water can cause hydrolysis of hemicelluloses into oligomers and monomers. Similarly, the purity of the glucose product produced from the wheat bran starch after enzymatic treatment was also noticed to be within 45-55% (Tirpanalan et al. 2014). This is in support of the earlier statement that the process also extracts an amount of proteins thereby causing such purity levels.

2.2.2 Fractionation Methods for the Extraction of Hemicelluloses, Lignin and Producing Cellulose-Rich Pulp

Fractionation of the biomass is a key step in the production of nanocellulose. The three most commonly utilised pretreatment methods for nanocellulose fractionation are alkaline, acidic and steam explosion pretreatment (Gosselink et al. 2010; Johar et al. 2012; Moran et al. 2008; Šutka et al. 2013). These three techniques are usually performed after a mechanical size reduction has been performed on the biomass to help reduce the fiber dimension as well as improve the swelling capacity of the biomass (Zimmermann et al. 2010). The aim of this fractionation treatment is to increase the cellulose content ($\geq 62\%$) and crystallinity ($\geq 48\%$) of the fractionated cellulose pulp while preventing cellulose loss ($\leq 5\%$) (Espinosa et al., 2017; Kallel et al., 2016), the recovery of hemicelluloses and lignin from the biomass as by-products while avoiding structure disruption.

2.2.2.1 Alkaline Pretreatment (AP)

Alkaline pretreatment has become one of the essential pretreatment techniques being utilised in almost every single nanocellulose production process. It is meant to partially dissolve the lignin, hemicelluloses and pectin component of the biomass as well as the saponification of the ester bonds of the ferulic and *p*-Coumaric acid (Kim et al. 2016). This helps to free up the cellulose content, as well as reduce the amorphous regions of the biomass. The reagents usually used for this type of pretreatment are sodium hydroxide, sodium carbonate, potassium hydroxide, lime, and ammonia, with sodium hydroxide being extensively utilised in fractionation processes. Although most lignocellulosic materials contain cellulose, hemicelluloses, hydroxycinnamic acids and lignin, during alkaline treatment the degree to which the various components are affected by the treatment severity is not similar.

Generally, at alkali concentrations less than 4wt% and temperatures less than 100°C there are relatively insignificant structural changes to the cellulose component of the biomass (Table 2.2). This is because the β -1,4-glucosidic bonds in cellulose are alkali stable at these conditions (Knill and Kennedy, 2003). This was confirmed by Cui et al. (2012) when they treated corn stover with 2 wt.% NaOH for an extensive time (12 days) and obtained a cellulose degradation of about 5%. Above these conditions there is a high probability of the cellulose undergoing a higher amount of degradation. It can also be noted from Table 2.2 that although Barman et al. (2012) increased the temperature to 105°C, the amount of cellulose that was degraded did not exceed 4%. Modenbach (2013) proposed that another possible reason for this was that the addition of NaOH made the conditions unfavourable for microorganisms to feed on the cellulose, thereby protecting it from degradation to an extent.

Hemicelluloses on the hand experience a significant reduction of content due to susceptibility to alkaline solutions at alkali concentrations <4 wt.% and temperatures <100°C (Sun et al., 1996). Curreli et al. (1997) obtained over 74% of hemicelluloses removal from wheat straw under similar process conditions within a long time frame (Table 2.2). Barman et al. (2012) also experienced about 68% hemicelluloses reduction from wheat straw at a slightly higher temperature and a short amount of time which was because of an increase in the treatment severity due to an increase in concentration (Table 2.2). It can be noticed from Table 2.2 that a concentration of less than 4wt% and a temperature of less than 100°C, less than a 45% hemicelluloses removal at shorter residence time.

To further increase the amount of hemicelluloses removed, there is the need to increase the residence time to at least a 4-hour period or slightly increase the temperature above a 100°C, which in turn affects the severity of the treatment. The effects were noticed by Matavire (2018) when destarched wheat bran was treated with 1 M NaOH at 70°C for 4 hours which resulted in a yield of 55% hemicelluloses (arabinoxylan). However, recent hemicellulose extractions have been performed at conditions of 0.5–1.0 M alkaline solution, 10-18 h at 20–60 °C (Peng et al., 2010a; Xiao et al., 2001; F. Xu et al., 2006). Extractions at such mild alkaline conditions have resulted in a yield of 25-59% hemicellulose extraction from wheat straw (García et al., 2013; R. C. Sun et al., 2000). Nevertheless, the extension of the

treatment time also resulted in 11-59% lignin extraction (García et al., 2013; R. C. Sun et al., 2000). It is therefore necessary that the purpose of the treatment be determined before the increase in the process conditions is applied. Furthermore, Lee et al. (2014) proposed that extraction of hemicellulose first from the cell wall (cellulose, hemicellulose and lignin) benefits the feedstock to be used in nanocellulose production by creating a lignin ‘protection’ around the cellulose thereby reducing cellulose degradation into glucose.

Although most lignocellulosic materials possess lignin, the structure and amount present in various biomass differs. Also, the use of NaOH in alkaline treatment has been reported to cleave the ether and ester bonds in the lignin-carbohydrate complexes resulting in partial or total solubilisation of the lignin and the production of hydroxycinnamic acids (ferulic and *p*-coumaric acid) depending on the treatment condition (Lee et al., 2014; Modenbach, 2013). Due to these, the effect of NaOH on various biomass differs. From Table 2.2, although cotton stalk possessed the highest amount of lignin, the amount of lignin removed at very low severity is relatively high in comparison to others at such severity. Duguid et al. (2009) reported that pretreating ground maize stover with 0.8 wt.% NaOH for 2 hours at room temperature resulted in a less than 2% lignin reduction. Furthermore, it has been observed that increase in NaOH concentration is favourable for lignin removal from the lignocellulosic biomass. Wan et al. (2011) noticed that an increase in NaOH concentration from 4 wt. % to 40 wt. % resulted in an increase in lignin removal from 7% to 14.8%, respectively. However, the removal of lignin was also associated with an increase in hemicellulose removal from 5% to 55% at 4 wt. % and 40 wt. %, respectively. Li et al. (2014) also noticed that there was a 60% reduction of hemicelluloses when pretreating lignocellulosic material with 10% NaOH. The removal of hemicelluloses was attributed to the loss of acetyl and uronic ester groups of the hemicelluloses during the alkaline treatment (He et al., 2008). AP is known to influence the amorphous regions of the biomass. Since hemicelluloses and lignin are amorphous in nature most alkaline treatments have a strong effect on these components resulting in their solubilisation. This is can therefore bring about an increase in the crystallinity index of the biomass when measured using an x-ray diffraction method.

Alkaline pretreatment begins to have an effect on cellulose structure at alkali concentrations greater than 6 wt.% (Modenbach, 2013). AP at concentrations greater than 6 wt. % can cause swelling in the amorphous parts of cellulose. Whereas, further increase in the alkaline concentration causes swelling in the crystalline regions, breaking the hydrogen bonds to form amorphous regions resulting in a decrease in cellulose crystallinity (Modenbach, 2013). At 18% NaOH concentration, a 36% decrease was observed in the crystallinity index of cellulose of spruce pulp produced (Ciolacu and Popa, 2005). Moreover, the increase in NaOH concentration can lead to the conversion of crystalline portions from cellulose I to cellulose II (Olsson and Westman, 2013). The conversion of cellulose I to cellulose II has been found to begin at different alkali concentrations for different lignocellulose biomass. For example it was found that this transformation started at $\geq 7.5\%$, and $\geq 10\%$ for spruce pulp and cotton linter,

respectively (Ciolacu and Popa, 2005; Gupta et al., 2013). Furthermore, the amorphous regions produced during this conversion results in swelling of the cellulose, changing its physical appearance (Eronen et al., 2009).

Alkaline pretreatment at temperatures above 100°C has been shown to be advantageous to removal of high amounts of lignin (Table 2.2). It is due to this reason that alkaline delignification treatment method has been extensively investigated in literature for biomass such as wheat straw, rice husk, switchgrass and cotton stalks (Rosa et al., 2012; Silverstein et al., 2007; Xu et al., 2011; Zheng et al., 2018). Alkaline delignification is usually conducted at 1-5 wt.% NaOH concentration for 30-90 min at 121 °C using an autoclave (Chen et al., 2009; Xu et al., 2011). The main aim of this treatment is to remove as much lignin as possible from the biomass. Nevertheless, the alkaline delignification treatment also results in the removal of hemicellulose from the biomass as well as improving the cellulose content, accessibility and digestibility for enzymatic hydrolysis and chemical treatment (Han et al., 2012; Rosa et al., 2012). In addition, Han et al. (2012) indicated that the alkaline delignification treatment can introduce micropores onto the surface of the biomass which in turn improves enzyme accessibility to the cellulose during enzymatic hydrolysis. Alkaline delignification of various biomass has resulted in the extraction of 30-89% lignin within the biomass (Xu et al., 2011; Zheng et al., 2018). However, Silverstein et al. (2007) stated that with an increase of NaOH concentration to 10 wt.%, about 95% of lignin could be extracted from the biomass. Furthermore, it was observed that at NaOH concentration less than 2 wt.%, time had an insignificant effect on the lignin removal whereas NaOH concentration was only significant at longer residence times (90 mins). McIntosh and Vancov (2011) observed that 72% of lignin removal could be achieved at 2 wt. % NaOH at 90 min and 121°C in support of this assertion. In addition, to lignin removal and improving cellulose content of biomass during delignification treatment, the cellulose crystallinity of biomass is also improved for nanocellulose production (Rosa et al., 2012). Zheng et al. (2018) indicated an improvement in crystallinity index from 48% to 62% after delignification treatment which was advantageous for subsequent treatments.

Most AP conducted for nanocellulose production is performed at $\leq 100^{\circ}\text{C}$ and ≤ 12 wt.% NaOH) (Gosselink et al. 2010), however, the conditions may vary for different biomass materials. Montane et al. (1998) demonstrated this characteristic by pretreatment of wheat straw (which had been initially reduced to 40-mesh size) with variable NaOH loading (20-40 wt. %) at 95°C. They reported that about 6.5% of cellulose present was degraded at a loading of 40% and higher and that the maximum loading that could be applied for wheat straw was at 30% where there was no significant loss of the cellulose content. It can also be noticed that out of three conditions that influences the severity of the treatment (i.e. concentration, time, and temperature), concentration has the largest effect on the amount of cellulose recovered and hemicelluloses or lignin removal (Table 2.2).

Kim and Holtzaple (2006) reported that the crystallinity index of the alkaline pretreated biomass tends to increase after pretreatment. They also reported that this increase is not due to structural changes in the cellulose but rather due to the removal of lignin and hemicelluloses Johar et al. (2012), similarly noticed an increase from 47% to 50% in the crystallinity of grounded rice husk with 4 wt.% NaOH solution for 2 hours, repeated three times. The crystallinity index increased in these two studies because both lignin and hemicelluloses are made up of amorphous regions, which were removed by the alkaline treatment improving the biomass crystallinity.

Table 2.2 Effects of NaOH pretreatment conditions on various biomass and its effect on cellulose, hemicelluloses and lignin (continued on next page).

Feedstock	Conc., wt. %	Time, min	Temperature, °C	Severity Factor	Cellulose Recovery, %	Hemicelluloses Removal, %	Lignin Removal, %	References
Wheat straw	0.5	10	105	-0.03	98.6	18	32.1	(Barman et al., 2012)
	1	10	105	1.15	98.4	24.9	37.2	
	1.5	10	105	1.83	98.1	46.1	56.2	
	2	10	105	2.32	96.1	68.2	70.3	
					38.5	31.6	20.8	
Wheat Straw	4	10	100	3.35	99.6	44.9	64.9	(Montane et al., 1998)
	6	10	100	4.03	97.8	60.6	68	
	8	10	100	4.52	90.2	68.2	71.9	
					33.7	23.6	17.1	
Wheat straw	0.75	90	60	0.29	nr	nr	16	(McIntosh and Vancov, 2011)
	1	90	60	0.78	nr	nr	36	
	2	90	60	1.95	nr	nr	40	
	0.75	30	121	1.61	nr	20	33	
	1	30	121	2.1	nr	nr	51	
	2	30	121	3.27	nr	33	66	
					36	26	13.5	
Corn stover	1	60	120	2.37	69.2	65.9	91.4	(Eniko et al., 2002)
	5	60	120	5.09	58.1	79.2	93.7	
	10	60	120	6.27	46.7	88.2	95.9	
					41.3	27.9	22.1	

Table 2.2 continued

Feedstock	Conc., wt. %	Time, min	Temperature, °C	Severity Factor	Cellulose Recovery, %	Hemicelluloses Removal, %	Lignin Removal, %	References
Wheat straw	4	2d	35	3.89	96.8	24.2	64.1	(H. Jiang et al., 2016)
	4	5d	35	4.29	82.1	30.7	70.1	
	4	8d	35	4.5	73.3	45.9	71.3	
	6	2d	35	4.58	88	35.1	55.1	
	8	2d	35	5.07	85	35	80.2	
					34.1	23.1	16.7	
Wheat straw	1	1d	40	1.39	95.5	74.3	63.5	(Curreli et al., 1997)
					36	49	15	
Cotton stalks	0.5	30	90	0.01	82	37	37	(Silverstein et al., 2007)
	0.5	60	90	0.31	76	38	38	
	0.5	90	90	0.49	85	15	34	
	2	30	90	2.36	70	39	54	
	2	60	90	2.66	69.5	35	60	
	2	90	90	2.83	72	40	61	
	2	30	121	3.27	83	28	55	
	2	60	121	3.57	84	31	64	
	2	90	121	3.75	81	33	66	
					31.1	10.7	30.1	

Bold values represent initial biomass composition before NaOH pretreatment; *d represents day(s) and nr represents not recorded. Severity factor, $M_o = C^n \left(t \exp \left(\frac{T - T_{ref}}{14.75} \right) \right)$

Where; C is the chemical concentration (wt. %), n is an arbitrary constant, t is the pretreatment time (min), T is the pretreatment temperature (°C) and T_{ref} is 100°C.

AP can be used in combination with other treatments such as acidic treatments (Johar et al. 2012) or steam explosion (Abraham et al. 2011; Deepa et al. 2011). It is worth noting that AP is usually the first treatment step to be applied to the biomass before other treatments are performed. This is mainly due to the ability of the alkaline treatment to cause swelling and facilitate an effective surface modification (Abraham et al. 2011). A treatment that did not involve the use of a bleaching step was conducted on wheat straw and soy hulls by successive acid and alkaline treatments after an initial mild treatment of the biomass with NaOH loading (17.5% w/w for 2h) (Alemdar and Sain, 2008a). The treatments involved the use of HCl (1M at $80 \pm 5^\circ\text{C}$ for 2h) and then NaOH solution (2% w/w at $80 \pm 5^\circ\text{C}$ for 2h). This treatment produced an increase in cellulose content from 61.8% to 84.6%, mainly through the removal of hemicelluloses and lignin, reducing their content from 19.0% and 14.1% to 6.0% and 9.4%, respectively.

AP possesses the advantage over acid pretreatment due to the fact that they are mostly performed at low alkaline concentrations, do not require expensive and special materials due to corrosion and also there is the possibility of recovery and reuse of some of the reagents (Mosier et al. 2005). This treatment is mainly affected by type of alkaline used, the alkaline loading, reaction temperature and time (Modenbach, 2013).

2.2.2.2 Dilute Acid Pretreatment (DAP)

Pretreatment of lignocellulose materials using dilute acid is performed after alkaline treatment to increase its effectiveness on lignocellulosic materials (Alemdar and Sain, 2008a; Rosa et al., 2012). Its purpose is to dissolve the rest of the hemicelluloses into the liquid phase by converting them into monomers, as well as disruption of the lignin structure, which makes the cellulose easily accessible for downstream processing to nanocellulose. DAP occurs at low concentrations of the acid 2 wt.% and at high temperatures (120-210 °C) (Hu and Ragauskas, 2012). The elevated temperatures require a lesser time (5-60 minutes) for the pretreatment process (Yang et al. 2009). Sulfuric acid is commonly used at this pretreatment step due to its low cost, although nitric acid can also be used. Application of the acid pretreatment step has limited a requirement for special type acid-resistant reactors, as well as the neutralisation of acid step that is required to successfully utilise this method (Liu and Wyman, 2003).

Although DAP is meant to hydrolyse mostly the hemicelluloses portion of pretreated materials at harsher treatment conditions it can also hydrolyse the cellulose portion of the biomass (Hu and Ragauskas, 2012). The hydrolysis of cellulose occurs in two steps; rapid hydrolysis of the amorphous region which is more accessible to solvents, followed by the slower hydrolysis of the crystalline portion (Emsley et al., 1997; Foston and Ragauskas, 2010; Stephens et al., 2008). Since the pretreatment stages for nanocellulose production is centred on increasing the cellulose content and improving the cellulose crystallinity, it is therefore necessary to avoid extensive hydrolysis of the cellulose as much as possible.

The DAP process can only help disrupt the structure of lignin a little to promote accessibility to the cellulose present in the lignocellulosic material. Furthermore, this process does not lead to a significant delignification due to the acid insoluble nature of most lignin (Hu and Ragauskas, 2012). However, DAP above the melting temperature of lignin causes lignin to combine and move in and out of the cell wall and reforming as droplets on the surface of biomass cell wall (Pu et al. 2013).

2.2.2.3 Steam Explosion (SE)

SE is a pretreatment method applied to biomass to break the complex structure thereby making it easily accessible to both chemical and biological reactions. In this treatment process, the lignocellulosic material is exposed to highly pressured (0.69–4.83 MPa) saturated steam within the temperature range of 160-260°C for a few seconds to a few minutes. During this period, there is the release of acetic acid from the hydrolysis of hemicelluloses, with water itself acting as a weak acid to reduce pH and act as a DAP. Following this, the biomass is rapidly exposed to atmospheric pressure resulting in a sudden explosive decompression of the biomass (Hu and Ragauskas, 2012; Sun and Cheng, 2002).

This treatment is one of the few pretreatment techniques that has been used as both a pretreatment method and a cellulose defibrillation method in nanocellulose production due to the explosive decompression behaving in a similar way to mechanical treatments applied in nanocellulose production (Abraham et al. 2011; Cherian et al. 2010; Jacquet et al. 2015). This has been largely due to the fact that this treatment technique provides a means to improve cellulose accessibility at relatively low cost (low energy consumption compared to mechanical treatment), optimal solubilisation of hemicelluloses, depolymerisation of lignin, as well as low environmental impact compared with chemical treatments (Deepa et al. 2011; Saha, 2004).

SE is estimated to increase the crystallinity of the lignocellulose by 10-20%, by selectively removing the amorphous components (Cherian et al. 2010; Tanahashi et al. 1982; Wang et al. 2009). Furthermore, Asada et al. (2005) observed an increase in the degree of crystallinity from 36% to 45% at the optimum treatment condition (5 min) with a decrease to 42% at 10 min. They, therefore, proposed that a portion of the cellulose amorphous regions were crystallised as the steaming time increased but after a period the crystallised amorphous regions were transformed back into the amorphous state at a slower pace. In addition, SE can cause a decrease or increase in the properties of the lignocellulose material due to the increase in crystallinity. Sugar cane bagasse experienced a reduction in length, water absorption and its chemical reactivity whereas its tensile strength, density and Young's modulus increased (Asada et al., 2005).

Application of alkaline pretreatment followed by steam explosion has been shown to be advantageous during biomass pretreatment for nanocellulose production (Abraham et al., 2011; Cherian et al., 2010; Deepa et al., 2011; Kaushik and Singh, 2011). The treatment showed an increase in the lignocellulose crystallinity index; with banana leaf increasing from 11% to 54%, pineapple leaf from 11% to 36%,

jute from 9% to 53% and wheat straw increasing from 54% to 67%. The increase in the crystallinity index of pretreated lignocelluloses was reportedly due to the partial solubilisation of the hemicelluloses and removal of lignin. For example, the hemicelluloses and lignin fraction of pineapple leaf reduced from 12% and 4% to 4% and 2%, respectively (Cherian et al. 2010) whereas that of wheat straw reduced from 37% and 22% to 17% and 10%, respectively (Kaushik and Singh, 2011)..

Montane et al. (1998) reported a reduction of hemicelluloses content of wheat straw from 24% to 15% as the severity factor (M_0) was at 3.39, and a further reduction to 2% when the severity was increased to 4.13. However, the amount of lignin and cellulose were found not to behave in the same way as the hemicelluloses. Lignin was found to decrease from an initial value of 17% to 14% at a severity of 3.80 but then began to increase to a value of 18% as severity was increased to 4.13. This indicated that as severity increased there was the formation of pseudo-lignin within the lignocellulose material which increased the lignin content (Li et al. 2007). Cellulose, on the contrary, experienced a reduction in content from an initial at 34% to 32% when severity was 3.39 and a further decrease to 29% when severity was increased to 4.13. This indicated that at the high severity ($M_0 = 4.13$) cellulose degradation exceeded 5% cellulose loss stated in Section 2.2.2 which could have led to the production of 5-hydroxymethyl-2-furfural (HMF) (Hu and Ragauskas, 2012). It is, therefore, important to control SE treatment so that the severity factor does not cause a high cellulose loss ($\leq 5\%$) and an improvement in the lignocellulose crystallinity during the cellulose-pulp fractionation of lignocellulose and further production of nanocellulose. Moreover, steam explosion has been indicated to be insufficient in obtaining cellulose-rich pulp from wheat with cellulose content ($\geq 62\%$) and lignin ($\leq 10\%$) (Kaushik and Singh, 2011) and therefore the need to apply a bleaching treatment after the SE treatment to obtain cellulose rich pulp that can be used for nanocellulose production (Abraham et al., 2011; Cherian et al., 2010).

2.3 Nanocellulose Treatment Methods

The production of nanocellulose involves certain treatments to help refine and break down the processed cellulose pulp (cellulose content $\geq 62\%$, crystallinity index $\geq 48\%$, hemicelluloses content $\leq 23\%$ and lignin content $\leq 10\%$) into nano-sized particles. The treatment is only conducted after the fractionation of the biomass materials and the production of the cellulose-rich pulp. There are several methods applied in this conversion. These methods are divided into three main categories, which are mechanical, chemical, and biological. In most nanocellulose treatments, two of the major factors considered before the treatment were the pulp cellulose content and crystallinity. The cellulose content of the pulp used was 63-99% which directly influenced the crystallinity (48-75%) (Jonoobi et al., 2015; Teixeira et al., 2010). It was noticed that cellulosic pulp with a higher cellulose content tends to have a higher crystallinity index and vice versa.

2.3.1 Mechanical Methods

2.3.1.1 Microfluidization

In this process, the cellulose-rich pulp is mixed with water producing a slurry which is passed through different size z-shaped chambers at a high pressure and velocity (Rojas et al., 2015). The process results in defibrillation of the fibers due to the shear and impact forces experienced during their collision with the chamber walls and each other (Ferrer et al. 2012). The treatment is repeated several times to ensure maximum fibrillation of the cellulose-rich fibers. CNFs produced are in length of micrometres and diameters of 20-100 nm are produced by using a microfluidizer (Siro and Plackett, 2010). The microfluidizer is operated between pressures of 55-170 MPa (Ferrer et al. 2012; Lee et al. 2009; Paakko et al. 2007). During the operation of the microfluidizer, it is necessary to prevent the increase of temperature above 90°C to prevent pump cavitation within the microfluidizer (Ferrer et al. 2012). During application of the microfluidizer the fiber concentration is maintained between 0.5-6% w/w to prevent clogging in the fluidizer (Zimmermann et al. 2010).

2.3.1.2 Homogenizer

The production of CNFs using homogenizers is one of the oldest mechanical treatment techniques that has been used on cellulosic fibers (Siro and Plackett, 2010). This technique is based on the principle of passing a dilute cellulosic fiber suspension in through a valve of the homogenizer at a higher pressure (Stelte and Sanadi, 2009). The homogenizer undergoes a large rapid internal pressure reduction accompanied with shearing and impact forces after the introduction of the cellulose-rich fiber suspension thereby causing defibrillation of the cellulosic fibers producing CNFs. The homogenization treatment is usually carried out after a refining step has been carried out on the cellulosic material. The refining step is meant to peel off the external cell wall as well as loosen the internal cell wall making the homogenization process easier. In most treatment processes, the homogenization treatment is usually repeated several times to ensure a large degree of defibrillation. For example, softwood cellulosic fibers have been reported to produce nanofibers of 10-25 nm in diameter after 25 passes, whereas hardwood cellulosic fibers have been reported to produce nanofibers of that same range after about 75 passes (Stelte and Sanadi, 2009).

In the application of the homogenizer, the particle size of the materials is a factor to be considered, since it can bring about clogging of the homogenizer. Stelte and Sanadi (2009) noticed that hardwood cellulose fibers are more likely to clog within the homogenizer than softwood cellulose fibers. This is mainly due to the larger size of the hardwood cell wall fragments in comparison to the softwood cell wall fragments. It is therefore necessary to remove all particles that are larger than 250µm from the fiber suspension before introducing them into the homogenizer. Most cellulosic fibers that are treated by enzymatic hydrolysis are more likely to be easily homogenized than fibers treated by other methods due to cell wall swelling by endoglucanase making defibrillation easier (Henriksson et al. 2007). Also, the cellulosic fibers can undergo a refining step before the homogenization step to help reduce the

particle size (Siro and Plackett, 2010). The homogenizer has been applied on cellulosic fibers from biomass such as wheat straw, sugar beet pulp, bleached sulphite softwood pulp, banana rachis and potato pulp (Alain et al., 2000; Henriksson et al., 2007; Kaushik and Singh, 2011; Leitner et al., 2007; Zuluaga et al., 2007).

2.3.2 Chemical Methods

2.3.2.1 Oxidation

Oxidation is the most commonly used chemical method to convert cellulose to CNF (Kekäläinen et al., 2015; Nechyporchuk, 2015). The hydroxyl groups and the aldehyde end groups participate in the oxidation reactions of cellulose (Krässig et al. 2012). Oxidation treatment transforms only the primary cellulose hydroxyl groups into carboxyl or aldehyde groups (Anderson et al. 2014; Li et al. 2013). Extensively oxidised and degraded products are designated as oxycelluloses (Krässig et al. 2012).

In recent years, an effective oxidising agent known as 2,2,6,6-tetramethylpiperidinyl-1-oxyl (TEMPO), has been utilised as a catalyst in a process known as TEMPO-mediated oxidation (Bee et al. 2015). TEMPO-mediation is conducted at mild and aqueous conditions by introducing carboxyl and aldehyde functional groups into the cellulose-rich fiber (Zheng, 2014). The carboxyl and aldehyde functional groups generate inter-fibrillar repulsive forces between fibrils by resulting in surface modifications (Lee et al., 2014). The surface modification results in negatively charged surface which improves the fibrillation process by repelling the nanocellulosic fibers (Habibi and Vignon, 2008; Lasseguette et al., 2008; Lee et al., 2014; Saito et al., 2009).

A major challenge faced with using the TEMPO-mediated oxidation has been decolouration or depolymerisation of the nanofibers produced due to residual aldehyde groups during the alkaline treatment (Siro and Plackett, 2010). Saito et al. (2009) reported that the addition of NaClO₂ to the treatment system at a slightly acid condition resolved both the decolourisation and nanofiber depolymerisation issues. It was also reported that the treatment prevented the post-aggregation of nanoparticles during drying and therefore help maintain a uniform nanofiber distribution of about 5 nm in width (Siro and Plackett, 2010). In addition, Fukuzumi et al. (2009) noticed that films produced by TEMPO-mediation were transparent, flexible and have good oxygen barrier properties.

2.3.2.2 Acid hydrolysis

Acid hydrolysis is conducted by treating the cellulose-rich pulp with an acid under controlled treatment conditions to produce nanocellulose. In acid hydrolysis to produce nanocellulose the type of acid used, its concentration, the acid to pulp ratio, treatment time and temperature need to be controlled to result in effective hydrolysis (Rebouillat and Pla, 2013). During acid hydrolysis, the cellulosic pulp microfibrils undergoes crosswise division along the amorphous sections which results in a release of rod-like crystallite nanoparticles (Siro and Plackett, 2010). Acid hydrolysis can result in the production of either CNC or CNF.

Utilising acid hydrolysis in nanocellulose production requires the application of certain process steps to achieve the final product. The cellulose-rich pulp is first mixed with deionized water then an amount of concentrated acid. It is then diluted with an amount of water after the desired reaction time and temperature to a point where the reaction is brought to a stop. The acid hydrolysed mixture obtained is then separated by means of filtration or centrifugation. The colloidal suspension obtained is then washed and then dialysed against deionized water to remove any residual acid or salt present (Rebouillat and Pla, 2013). The dialysed nanoparticles are then dried by freeze drying or spray drying (Isogai, 2013; Lu and Hsieh, 2012).

Acids that have been reported for acid hydrolysis are hydrochloric acid (Lorenz et al., 2017), sulfuric acid (Li et al., 2018), phosphoric acid (Vanderfleet et al., 2017), phosphotungstic acid (Liu et al., 2014) and formic acid (Du et al., 2016) among others. Most acid hydrolysis treatment of cellulose to produce either CNC or CNF have utilised H_2SO_4 or HCl , or a combination of both (Correa et al., 2010) with H_2SO_4 being widely used to produce CNC (Helbert et al., 1996). Johar et al. (2012) performed acid hydrolysis treatment with sulfuric acid (10 M) on cellulosic pulp fibers from rice husk (fiber content 4-6 wt. %) after AP and bleaching. The mixture was heated at $50^\circ C$ for 40 min under continuous stirring which resulted in CNC with diameter of 10-15nm. The initial chemical treatments (AP and bleaching) resulted in an improvement of the rice husk cellulose content and crystallinity index from 31% to 96%, and 47% to 57%, respectively, with an improvement in the thermal stability of the resulting cellulose pulp. The sulfuric acid treatment produced CNC and resulted in a further increase in crystallinity index from 57 to 59%, however, it also resulted in a reduction of the thermal properties after drying due to an introduction of sulfate groups (Figure 2.7). However, sulfuric acid treatment remains a preferred treatment of choice over other acid treatment for production of CNC with a highly stable colloidal suspension (Mandal and Chakrabarty, 2011). Furthermore, a kind of CNC, which is known as cellulose nanowhiskers, due to their shorter length (80-400 nm), ultra- thin diameter (5-14 nm) and needle like structure have also been noticed to be formed by sulfuric acid treatment of cellulose pulp (Rosa et al., 2012; Teixeira et al., 2010). The CNC produced from sulfuric acid treatment have shown potential for applications in the fields of composites as a reinforcing phase, as well as pharmaceutical and optical industries as additives with thermal degradation temperatures between $220-335^\circ C$ (Li et al. 2009).

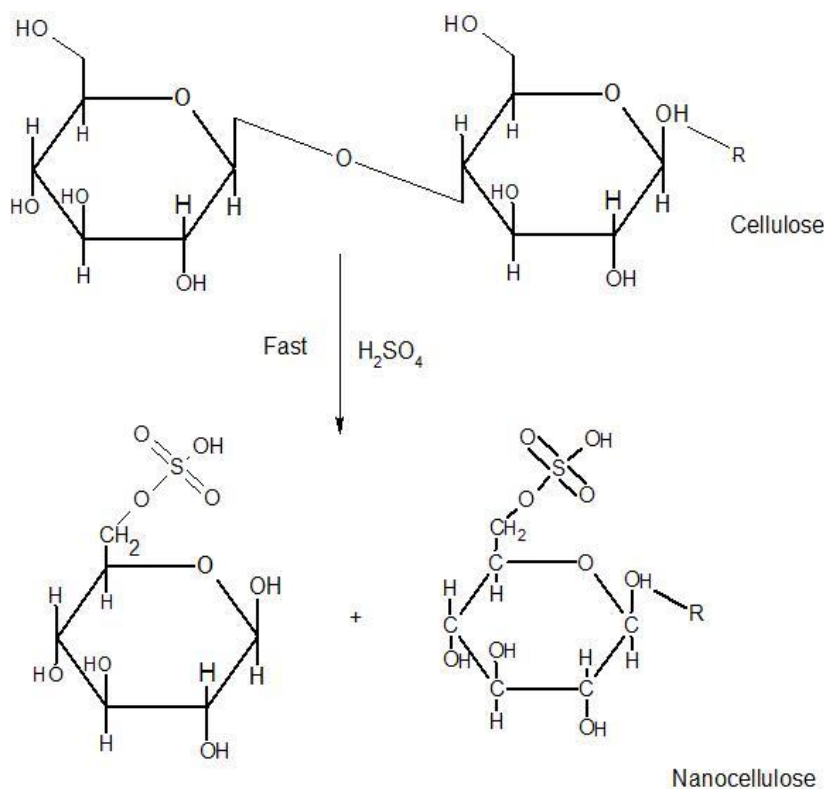


Figure 2.7 Mechanism of sulfuric acid treatment of cellulose to produce nanocellulose (Malladi et al., 2018)

Whereas, sulfuric acid hydrolysis of cellulose pulp have generally resulted in the production of CNC, hydrochloric acid hydrolysis of cellulose pulp have resulted in the production of CNF (Kaushik and Singh, 2011). However, the use of hydrochloric acid has been able to resolve the issue of the reduction the thermal degradation temperature of the CNF produced by the absence of sulfate groups from the sulfuric acid treatment (Tian et al., 2016) (Figure 2.8). Moreover, Kaushik and Singh (2011) noticed that after AP and bleaching to produce a wheat straw cellulose pulp (with cellulose content and crystallinity index of 75% and 71%, respectively), the use of hydrochloric acid resulted in an increase in both cellulose content (86%) and crystallinity (80%). Furthermore, Correa et al. (2010) noticed that CNF produced from hydrochloric acid treatment possessed higher crystallinity than CNF produced from sulfuric acid treatment in addition to its higher thermal degradation temperature. Nevertheless, Cheng et al. (2017) and Zeni et al. (2015) have shown that it is possible to produce CNC by using hydrochloric acid treatment on microcrystalline cellulose and commercial eucalyptus cellulose pulp. CNFs produced are usually applied in biocomposites materials as a reinforcing material due to their large surface to volume ratio and good mechanical properties as well as in for food packaging products among others (Giri and Adhikari, 2013; Kaushik and Singh, 2011).

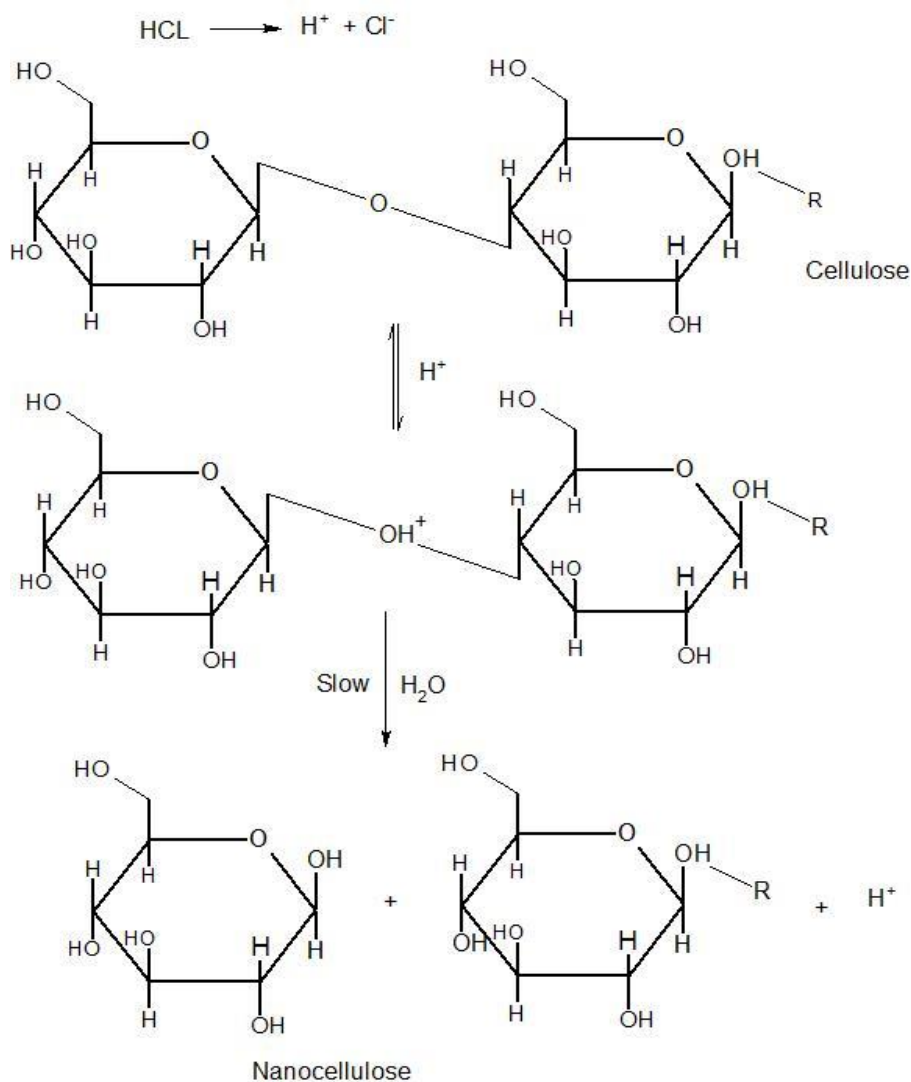


Figure 2.8 Mechanism of hydrochloric acid treatment of cellulose to produce nanocellulose (Islam et al., 2013)

Combination of sulfuric acid and hydrochloric acid have also been used to produce CNC and CNF. Correa et al. (2010) was able to produce CNF when a 2.1 (v/v) combination of sulfuric acid to hydrochloric acid was at 45°C for 75 min. However, Wang et al. (2007) found that a combination of hydrochloric acid (10% v/v) and sulfuric acid (30% v/v) for 10 hours at 68°C in an ultrasonicator resulted in the production of spherical nanocellulose a type of CNC. The production of this type of CNC could have been due to the acid combination ratio, extended treatment time as well as the ultrasonication used. In addition, combining hydrochloric acid with sulfuric acid produces CNCs with improved thermal stability due to fewer sulfate groups (Wang et al., 2007).

2.3.3 Biological Reaction

2.3.3.1 Enzymatic Treatment

The microbiological degradation of cellulose takes place by means of enzymatic hydrolysis of the β -glycosidic linkages and is of interest in connection with the use of plant biomass for nanocellulose production (Krässig et al. 2012). This form of treatment has been of interest due to its environmental

benefit and safe conditions. In comparison to chemical processes, enzymatic treatment for nanocellulose production presents the advantages of milder treatment conditions, higher cellulose selectivity thereby translating to higher yields of produced nanocellulose (Lee et al., 2014). The disadvantages of this treatment lies in the cost of cellulase enzyme and the extensive treatment time (up to 72 hours) required (Bee et al. 2015; Kalia et al. 2014; Rojas et al. 2015). However, the long treatment time required for nanocellulose production is influenced by the physical and chemical makeup of the biomass, amount of enzyme used, enzyme diffusion, accessibility and selectivity to the components of the cellulose fiber (Bee et al. 2015; Zhu et al. 2008).

The cellulose-rich fibers are usually hydrolysed by using cellulases. These cellulases are found in nature as a multicomponent enzyme system that permits selective hydrolysis of the cellulose in the cellulosic pulp (Bee et al. 2015). Exoglucanases and endoglucanases are the commonly used cellulase enzymes to hydrolyse cellulose to produce nanocellulose (Figure 2.9). Endoglucanases mainly act on the amorphous regions of cellulose whereas exoglucanases acts on the crystalline regions of cellulose in a controlled enzymatic hydrolysis (Siro and Plackett, 2010) Enzymatic hydrolysis to produce nanocellulose are usually performed at 45-50⁰C, pH 4-7 and 1-72 hours by using a buffer to maintain the enzyme activity (Filson et al., 2009; Janardhnan and Sain, 2011; Martelli-tosi et al., 2018). The choice of process conditions are dependent on the enzyme and its ability to break down the extensive cellulosic polymeric structure into shorter cellulose polymers (nanocellulose) (Ribeiro et al., 2019). The combination of these enzymes have been known to show synergistic effects in nanocellulose production (De Campos et al., 2013; Henriksson et al., 2007; Kostylev and Wilson, 2012) , resulting in the reduction of treatment time (6-24 hours) (Bester, 2018; Tibolla et al., 2014). Nevertheless, the use of only endoglucanase is preferred due to its ability to mainly hydrolyse the amorphous portions of the cellulose resulting in nanocellulose with higher crystallinity (Dai et al., 2018).

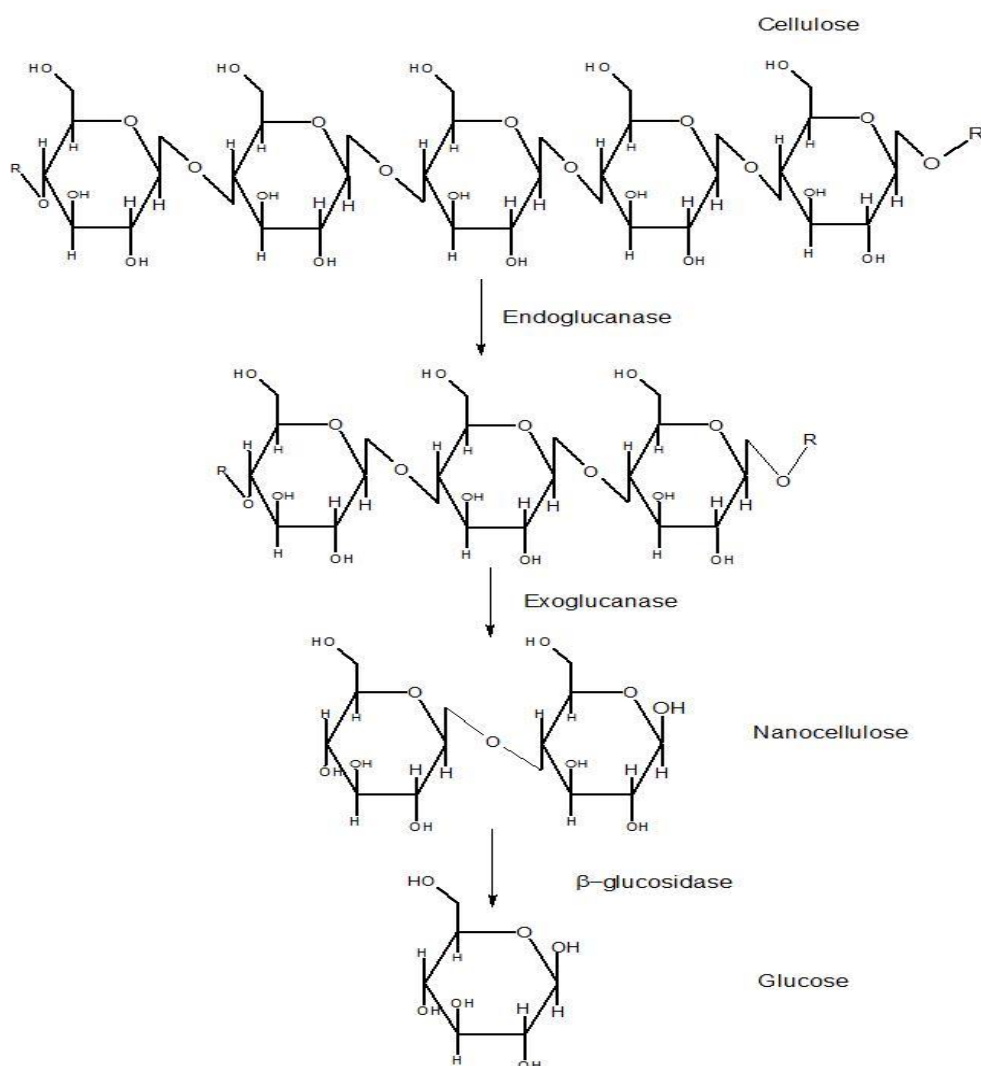


Figure 2.9 Mechanism of enzymatic treatment (with endoglucanase, exoglucanase and β -glucosidase) of cellulose (Pino et al., 2018)

The presence of lignin and hemicellulose within the cell wall structure of the cellulosic fiber can serve as barrier for effective enzymatic hydrolysis to produce nanocellulose. Due to this reason, several researchers have either used bleached cellulosic fibers, commercial recycled pulp or cellulose microcrystals to produce nanocellulose (Filson et al., 2009; Martelli-tosi et al., 2018; Samir et al., 2005). As stated in Section 2.1.3, lignin forms a lignin-carbohydrate matrix with the other cell wall components (hemicellulose and cellulose) thereby acting as a shield, preventing enzyme accessibility to cellulose. During enzymatic hydrolysis, the presence of lignin within the cellulosic pulp used have been known to result in high enzyme loadings (Kristensen et al., 2007) by binding with the enzymes through phenyl glucoside bonds (Karim et al., 2016). On the other hand, hemicelluloses with branched structures such as arabinoxylan are able to form covalent cross-link bonds with lignin producing lignin-carbohydrate complexes (LCC) (Karim et al., 2016). The LCCs formed in turn forms phenyl glucosidic bonds restricting enzyme access to the cellulose within the cellulosic fiber. Due to these reasons, removal of

hemicellulose and lignin from the cellulosic fiber before enzymatic treatment have become very vital for successful nanocellulose production.

Rojas et al. (2015) reported that pretreated fibers subjected to a 0.02% enzyme concentration are able to produce CNF when treated with exoglucanases and endoglucanases, while their molecular weight and fiber length are preserved. Also, there are enzymes produced from *Trichoderma reesei* and *Aspergillus xylinum* that are capable of reducing the size of microcrystalline cellulose to produce cellulose nanowhiskers (Rojas et al. 2015; Satyamurthy et al. 2011). Paakko et al. (2007) was able to perform enzymatic hydrolysis on bleached sulphite cellulose pulp by using a monocomponent endoglucanase (Novozym 476, Novozym A/S) without any further purification to produce CNFs. Filson et al. (2009) also reported on the use of microwave heating (at 50°C and 60 minutes) on recycled pulp, hydrolysed with endoglucanase enzyme. They were able to produce CNCs (widths of 30-80 nm and lengths of 100 nm-1.8µm) using endoglucanase enzyme (84 EGU per 200mg of recycled pulp) with a higher yield of cellulose by applying microwave heating (38.2%) than using conventional heating methods (29%).

2.4 Production of Nanocellulose

Nanocellulose production as already stated, involves different treatment methods, such as those described in Section 2.3. However, these combination of treatment methods can be grouped under a combination of chemical treatments (CC), a chemical and mechanical/physical combination (CM) and a combination of chemical, mechanical/physical and biological treatments (CMB) (Moran et al. 2008; Paakko et al. 2007; Šutka et al. 2013). These treatment combinations are usually performed on the cellulose-rich pulp after the biomass has been reduced in size to improve treatment efficiency. CC method is usually used in the production of the CNC (Moran et al. 2008), whereas CM is used in the production of CNF (Kaushik and Singh, 2011). CMB on the other hand can be used in the production of both CNF and CNC (Anderson et al. 2014; Satyamurthy et al. 2011).

The CC method has been applied by researchers such as Johar et al. (2012) to produce CNC from materials such as rice husk. The general treatment process is thus represented in the Figure. 2.10 with the inclusion of a starch removal from the raw material before nanocellulose production. The first step after starch removal (if biomass contains large amount of starch) is to use an alkaline treatment step to partially dissolve the hemicelluloses, lignin, and other components such as pectin and ash to make the cellulose content easily accessible. Although the alkaline treatment performed has no extreme effect on the lignin, it can cause a minor reduction in the lignin content. This characteristic was observed by Johar et al.(2012) on rice husk when the lignin content reduced from 23% to 21%. This step is followed by an acid treatment step to help in hydrolysing a large amount of the hemicelluloses present within the material. Researchers such as Moran et al. (2008) and Costa et al. (2015) did not use the acid treatment step and went on to a bleaching step. The direct use of the bleaching step was due to the fact that the

alkaline treatment step can be used to remove over 68% of the hemicelluloses content present in the biomass if performed at a higher temperature and alkaline concentration (Barman et al. 2012). In addition, it can help successfully extract a larger part of the hemicelluloses fraction from the biomass before further processing. Bleaching the material after alkaline treatment has been shown to have a significant effect on both the hemicelluloses and lignin contents of the material. For example, bleaching alkaline treated rice husk can remove almost all the hemicelluloses, lignin and ash content of the rice husk, producing a cellulose content of 96% (Johar et al. 2012). This method does not present an effective means of fractionation of the individual content of the material.

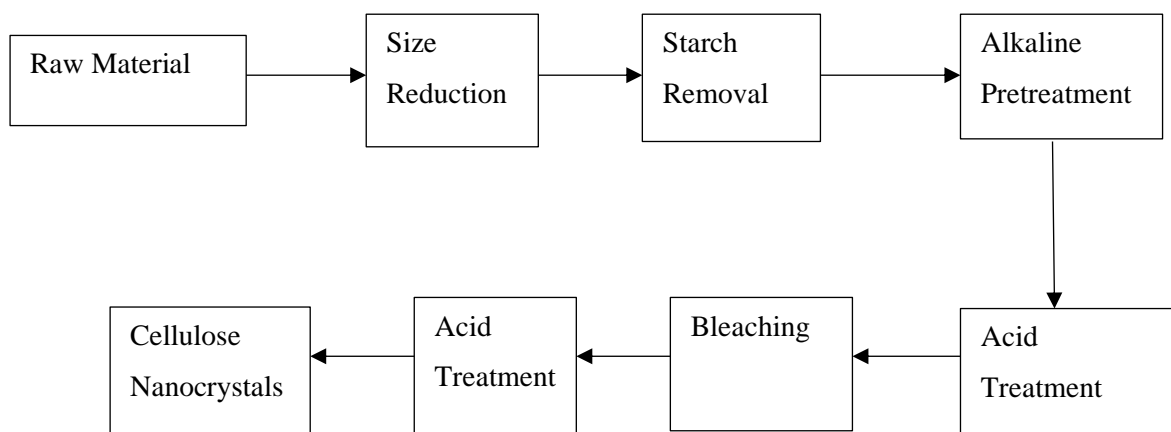


Figure 2.10 Chemical Treatment Combination (CC) for the production of CNC (adapted from Johar et al. (2012))

The main aim of the CC method combination is the production of the cellulosic fibers with low impurity contents (lignin, hemicelluloses, ash, pectin), without regards for the by-products produced from the raw material without degrading the cellulose to the point where it is no more suitable for nanocellulose production. The removal of the hemicelluloses and lignin contents of the material leads to an increase in its crystallinity (Costa et al. 2015). Although chlorite solution is the most widely used bleaching agent in most nanocellulose treatments, hydrogen peroxide has been shown to present a greener approach as well as performs just as well as the chlorite solution (Moran et al. 2008). In addition, the acid hydrolysis step performed in producing CNCs have mostly centred on the application of sulfuric acid, H_2SO_4 . The use of sulfuric acid in the hydrolysis of cellulosic fibers has been reported by Liu et al. (2014) to produce charged groups on the surface of the CNC. Aside all the disadvantages mentioned earlier, Roman and Winter, (2004) also reported that these charged groups formed are capable of diminishing the thermostability of the crystals and therefore the use of hydrochloric acid will be much more preferable to produce similar products.

Out of the three nanocellulose production approaches, the CM approach is the one with many variations. The variation depicted by Figure 2.11 is one that includes starch removal, with the treatment steps that follow derived from Kaushik and Singh (2011) to produce CNFs from wheat straw. The CM approach is usually centred on a combination of chemical and mechanical treatment approaches to reduce energy and chemical usage (Bharimalla et al. 2015). Other variations of this method includes that from

Abraham et al. (2011), Cherian et al. (2010) and Deepa et al. (2011), which utilised a second steam explosion treatment with similar process conditions as the first one after the acid treatment of the bleached material. Alemdar and Sain (2008) also utilised a different variation, which did not utilise both steam explosion and bleaching. The alkaline treatment was followed by an acid treatment and then another alkaline treatment before two mechanical treatments were performed on the wheat straw to produce the CNF.

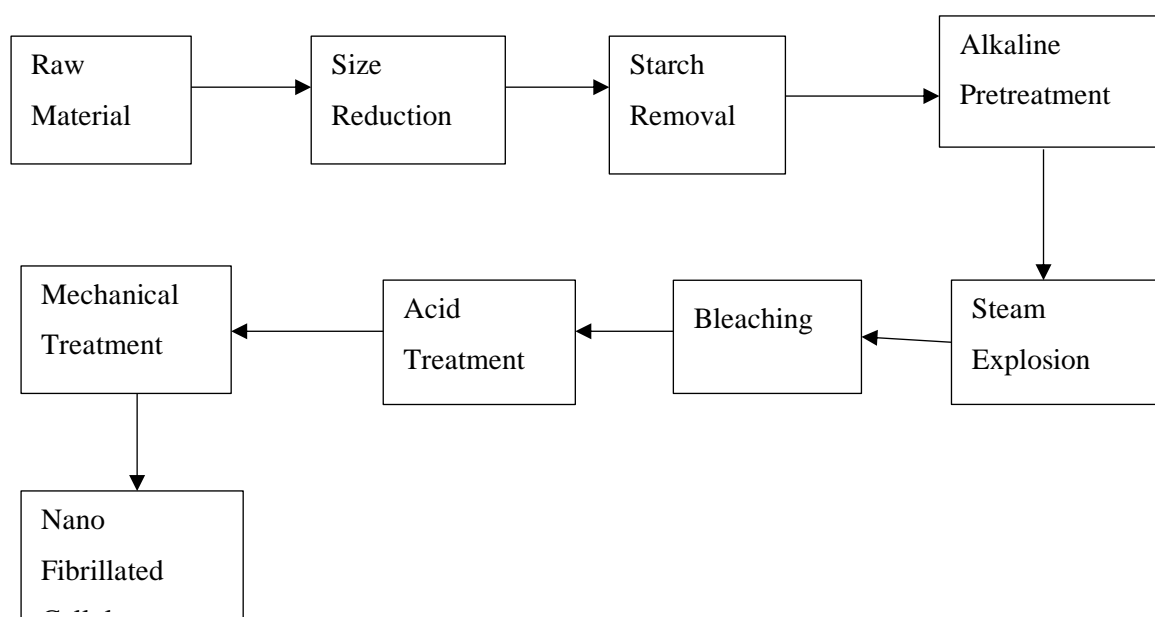


Figure 2.11 Chemical-Mechanical combination (CM) method for the production of CNF (adapted from Kaushik and Singh, (2011))

Each of these variations to the selected treatment combinations possess their own merits. The variation presented by Alemdar and Sain (2008) prevents the usage of a bleach treatment on the material thereby helping to keep the integrity of the components of the material during the fractionation and prevent the degradation of the cellulose-rich pulp obtained for subsequent production of nanocellulose (Sun et al., 2004). However, this variation also allows the presence of a larger amount of the hemicelluloses and lignin content as compared to the other variations that utilised a bleaching step. Furthermore, the variation presented by Abraham et al. (2011), Cherian et al. (2010) and Deepa et al. (2011) produces CNFs that are shorter in length in comparison to those produced by Alemdar and Sain (2008). In addition, it requires a higher energy consumption in comparison to the other two variations. Although the variation presented by Kaushik and Singh (2011) contains a bleaching step, the conditions for the bleaching step are milder as compared to that presented by Abraham et al. (2011), Cherian et al. (2010) and Deepa et al. (2011). The milder conditions therefore affected the amount of lignin and hemicelluloses that was removed. The latter were able to remove almost all the hemicelluloses and lignin content present as compared to the former that was able to remove a little over half of the lignin and hemicelluloses present in the material.

In addition, the type of mechanical treatment that is performed on the treated fibers have been shown to influence the particle size range of the CNF produced. For example, CNFs produced from cryocrushed fibers by Alemdar and Sain (2008) possessed a size range of 10-80 nm with most falling between 30-40 nm range whereas that produced from homogenization by Cherian et al. 2010 possessed a size range of 5-60 nm with most falling between 5-25 nm. This indicates that the type of mechanical treatment selected has a direct effect on the size range of majority of the fibers produced.

Among the three nanocellulose combination methods, the one that has been least investigated is the CMB method. De Campos et al. (2013) is among the few who have applied this method in the production of nanofibers. This method has been applied on materials such as curauá, sugarcane bagasse, bleached Kraft fiber and bleached sulphite softwood pulp (reference). Figure 2.12 depicts the most common variations of this method utilised in the production of CNFs with the addition of a starch removal steps. In most research works that utilise the CMB method, the fiber that undergoes the enzymatic hydrolysis is usually obtained from pulping industries as already bleached materials feedstocks (Henriksson et al., 2007; Siddiqui et al., 2011; Svagan et al., 2007). However, these cellulose pulps can also be alternatively produced by utilising lignocellulose fractionation methods albeit with different cellulose properties which are not detrimental to nanocellulose production (De Campos et al. 2013).

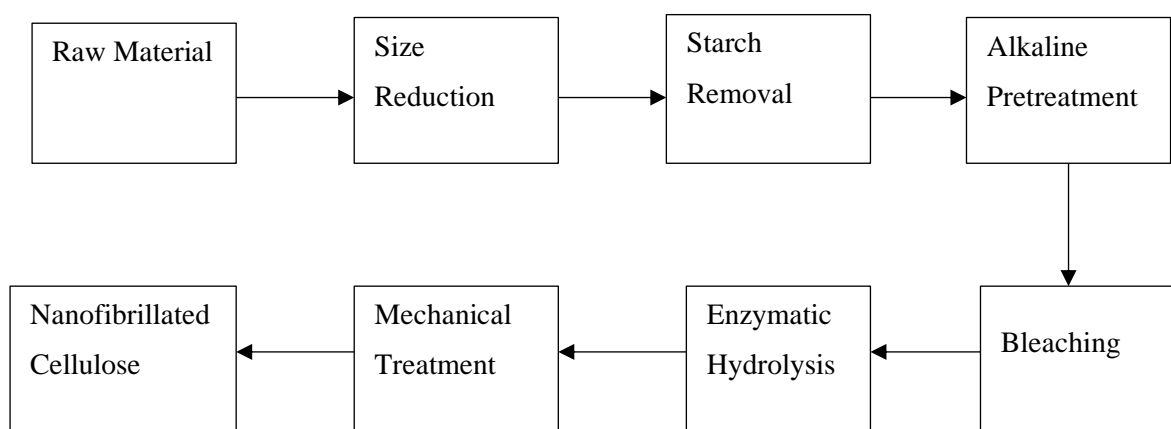


Figure 2.12 Chemical-Mechanical-Biological combination (CMB) method for the production of CNF(adapted from de Campos et al. (2013))

The only variation to this method (Figure 2.12) is the introduction of another mechanical treatment step before the enzymatic hydrolysis step. This variation has been utilised by researchers such as López-rubio et al. (2007) among others. The inclusion of an addition mechanical treatment step before the enzymatic hydrolysis step is mainly for the purpose of increasing the accessibility of the cell wall to enzymatic action (López-rubio et al. 2007). Although this method in general helps to prevent the use of excessive amount of chemicals and is therefore more environmentally friendly than the other two methods, it presents the disadvantage of taking a longer processing time in comparison with the other two methods (Bharimalla et al. 2015).

For the enzymatic hydrolysis step, although the same enzyme can be applied on different feedstocks the enzyme concentrations may differ due to the cellulose and hemicelluloses contents of the feedstock. This behaviour was reported by de Campos et al. (2013), when they noticed that curauá (cellulose 90.91% and hemicelluloses 2.41%) required a higher enzyme concentration than sugarcane bagasse (40.04% cellulose and 25.15% hemicelluloses). The lesser enzyme concentration made it easier to attack the hemicelluloses and cellulose bonds resulting in defibrillation. Although more nanofibers were produced after this treatment with nanofiber length of 55 nm for sugarcane bagasse and 30 nm for curauá, the crystallinity of the fibers was reduced, i.e. from 84% to 77% for curauá and from 73% to 70% for sugarcane bagasse. This result indicated that the enzymes used resulted in a degree of depolymerisation of the cellulose chains affecting both the cellulose portions and the amorphous portions. Although the crystallinity reduced after enzymatic hydrolysis, it increased again after the application of the mechanical treatment. The final mechanical treatment performed on the enzymatic hydrolysed fibers is either homogenization or microfluidization to help in dispersing the fibers and produce more uniform fiber distribution (Henriksson and Berglund, 2007; Tanpichai et al. 2012).

The production of nanocellulose from WS and WB can be made to undergo any of the three-combination method to produce nanocellulose. Although all three nanocellulose production methods for wheat straw and bran may be feasible, they all present their respective advantages and disadvantages. To make the best out of these three processing combinations a few modifications can be made to each combination and incorporated together to produce a suitable combination method. Furthermore, to ensure that the method combination is industrially and economically feasible, it is necessary to ensure that it possesses:

- less processing steps with respect to those used for processing most agricultural residues in literature
- no bleaching step that can affect the structure of the hemicellulose, lignin, hydroxycinnamic acids and cause cellulose degradation
- fractionation of the other cell wall components (hemicellulose, lignin and hydroxycinnamic acid) thereby producing value-added products in addition to cellulose-rich fiber with high crystallinity for nanocellulose production
- Preventing the use of concentrated acid (sulfuric acid) and extensive treatment times (24-72 hours of enzymatic treatment) however ensuring that the produced nanocellulose has thermal properties that is feasible for biocomposites production.

2.5 Research Gaps

Research has been conducted on cellulose-rich fibers from various agricultural residues such as wheat straw, and wheat bran among others for nanocellulose production. In addition to the cellulose-rich fibers that can be obtained from both wheat straw and wheat bran (Nilsson, 2017; Oun and Rhim, 2016a),

wheat straw and bran have been shown to be a rich source of other cell wall components such as hemicellulose, lignin, *p*-Coumaric acid and ferulic acid (Buranov and Mazza, 2009, 2008; Pan et al., 1998). Alkaline treatment has been used to extract hemicellulose, *p*-Coumaric acid and ferulic acid at mild alkaline treatment conditions whereas alkaline delignification treatment has been used in delignifying wheat for extraction of lignin and production of cellulose-rich fibers for nanocellulose production (Espinosa et al., 2017). Extracting hemicellulose, lignin, *p*-Coumaric acid and ferulic acid can add extra value to the nanocellulose treatment process. However, till date a suitable treatment method has not been developed to achieve this aim. Furthermore, given the effects of alkaline treatments on the cell wall components it provides a possible solution by combining both the mild and alkaline delignification treatments to obtain all these products in addition to producing cellulose-rich fibers from wheat straw and wheat bran for nanocellulose production. This treatment approach could result in cellulose rich fibers with a high crystallinity (Tibolla et al., 2017) and cellulose content (Espinosa et al., 2017) as well as improved swelling capabilities (Cherian et al., 2010) of the cellulose pulp that will facilitate easier chemical or enzymatic treatment of the fibers to produce nanocellulose.

Furthermore, cellulose-rich fibers used for nanocellulose production have been mainly bleached cellulose fibers (Martelli-tosi et al., 2018), recycled pulp (Zeni et al., 2015) or commercial microcrystalline cellulose (Cheng et al., 2017). It is interesting to note that, processes that have produced cellulose rich fibers from wheat residue without bleaching have had to use at least three pretreatment steps to increase the cellulose content above 73% (Alemdar and Sain, 2008a). Further reduction in pretreatment steps for wheat residues have resulted in a maximum of about 62% cellulose content (Espinosa et al., 2017). Therefore, it is necessary to develop a method of obtaining cellulose-rich fibers from wheat with as minimum pretreatment steps as possible for nanocellulose treatment.

Moreover, the traditional method of producing nanocellulose from cellulose rich fibers have been mainly through sulfuric acid hydrolysis. The use of sulfuric acid is known to result in low thermal degradation temperatures of the produced nanocellulose (Johar et al., 2012). Therefore, other treatment methods such as hydrochloric acid and enzymatic treatment have been used to resolve this issue. However, a comparative analysis of a sulfuric acid treatment to a hydrochloric acid treatment and an enzymatic treatment using a two-stage alkaline treated cellulose-rich pulp have not yet been investigated. A comparative analysis of the treatment approaches could share more light on the similarities of the treatment approaches on the properties of the nanocellulose produced (Jonoobi et al., 2015). Such a comparative analysis could help in determining which treatment method is most suitable for production of nanocellulose for a particular application.

2.6 Aims and Objectives of the Study

The goal of this study is to develop a process to produce cellulose-rich fibers for production of nanocellulose while co-extracting hemicelluloses and lignin from wheat straw and wheat bran as well as ferulic acid (from wheat bran) and *p*-coumaric acid (from wheat straw) with the least process routes.

- Identify fractionation processes from literature and develop a fractionation process for the isolation of cellulose and the co-extraction of hemicelluloses, lignin, ferulic acid and *p*-coumaric acid from wheat bran and straw, respectively.
- Experimental validation and optimisation of the developed process route by determining appropriate conditions for fractionation of wheat straw and bran into cellulose with the aim of the producing nanocellulose while extracting hemicelluloses, lignin, ferulic acid and *p*-coumaric acid where applicable as co-products and or by-products.
- Determine the yield, purity, and thermal property of the developed treatment route on the cellulose, hemicellulose and lignin extracted. Whereas determining the antioxidant activity in substitution of thermal property for ferulic acid and *p*-coumaric acid extracted.
- Determine optimum conditions required for isolation of nanocellulose from two-stage alkaline treated wheat straw and bran by using response surface methodology and comparing an enzymatic treatment, a hydrochloric acid treatment with a conventional sulfuric acid hydrolysis treatment. In determination of the optimised conditions the process parameters to be considered are the yield, surface charge, polydispersity index and fiber size, whereas at the optimised conditions the effect of the treatments on the produced nanocellulose should be determined by FTIR, XRD and TGA to determine its potential application.

CHAPTER THREE

EXPERIMENTAL PROCEDURES

3.1 Materials and Chemicals

The wheat straw (WS) used in this work was obtained from NK Feeds in Paarl whereas the wheat bran (WB) was obtained from Eureka Mills, South Africa. They were extensively washed with distilled water under room temperature several times with rigorous stirring to remove any dust and impurity and then air dried. This experiment made use of 5L beakers, stirrers, water baths, starch assay kit, seamless cellulose tube (99.99% retention, MWCO 12400) and an autoclave.

The reagents that were used in this work were analytical reagent sodium hydroxide, hydrochloric acid, 2,2-diphenyl-1-picrylhydrazyl (DPPH) and acetic acid obtained from Scienceworld South Africa whereas Viscozyme L (enzyme activity 100 FBG/g) and Fibercare R (enzyme activity 4500 ECU/g) were obtained from Novozyme. Commercial CNC and CNF produced from bleached southern pine pulp and softwood Kraft pulp, respectively were obtained from the University of Maine Nanofiber Plant, USA.

3.2 Statistical analysis

Statistica software (TIBICO Software Incorporation, version 13.2) was used for analysis of variance (ANOVA) and optimisation (central composite design) of the experiments. The ANOVA function helped to determine the significance of the independent variables to the responses obtained at $p < 0.05$, as well as how well the experimental responses correlated with the predicted responses by the model. The ANOVA analysis was also used to determine if the treatment conditions (independent variables) were able to reach the optimum treatment condition for the various responses which was referred to as a quadratic term. Similarly, the ANOVA analysis determined if the responses directly increased or decreased with the increase in the independent variable referred to as the linear term.

The central composite design (CCD) for modelling of all experiments were conducted by using the design of experiment function in the Statistica software at each treatment stage. A predictive model of a mathematical generated equation given a set of independent variables to predict a given dependent response was generated. The predictive model was further used to predict the response surface methodology (RSM) of interaction of the selected independent variables (process conditions such as time, sodium hydroxide concentration and time) with the responses or dependant variables (such as purity, yield, zeta potential and length). The Statistica software was further used to determine the desirability plots and optimised conditions for the independent variables with respect to the responses from the experiment. The desirability plot was obtained by means of assigning a desirability value to the responses or dependant variables with 0 being the minimum and 1 being the highest. Statistica combined these desirability values and generates the desirability plots and conditions for the independent variables.

Means and standard deviations for measurements were determined from replicate measurements by using Microsoft Excel, 2013.

3.3 Fractionation of Wheat Straw and Bran

3.3.1 Milling

Wheat straw was cut into smaller pieces and milled to reduce the fiber length to enhance its swelling ability in water. This was achieved by using a Drotsky S1 hammer mill to reduce the size to about 0.8 mm in length. Wheat bran was also milled with the Retsch SM 100 cutting mill to reduce the size to about 0.8 mm in length.

3.3.2 Starch Removal

Since wheat bran contains a large amount of starch and this starch is interlinked with the other cell wall components, removal of the starch was necessary to ensure an effective separation of the other cell wall components. Also, considering the commercial value of starch relative to the other cell wall components it was easier and best to remove this starch by means of enzymatic hydrolysis.

The WB starch was therefore hydrolysed with a two-step enzymatic treatment at a bran/water ratio of 1:5. It underwent liquefaction by a thermostable α -amylase (150 mL of Termamyl SC DS/ ton starch) at 85°C and pH 5.5 for 2 hours. In the saccharification step, amyloglucosidase (400 ml Saczyme Plus/ ton starch) was added at 55°C and pH 4.5 for 4 hours to make certain that total starch hydrolysis was achieved. The slurry was then filtered through a Munktell filter paper with a quality 5 before being washed with deionised water. This resulted in a solid residue which was then termed as destarched wheat bran (DWB).

The starch content was determined for the destarched wheat bran by using the Megazyme starch assay kit. The DWB was then analysed for its protein content using the Kjeldahl method, after which the cellulose, hemicelluloses, lignin, extractives and ash contents were also determined.

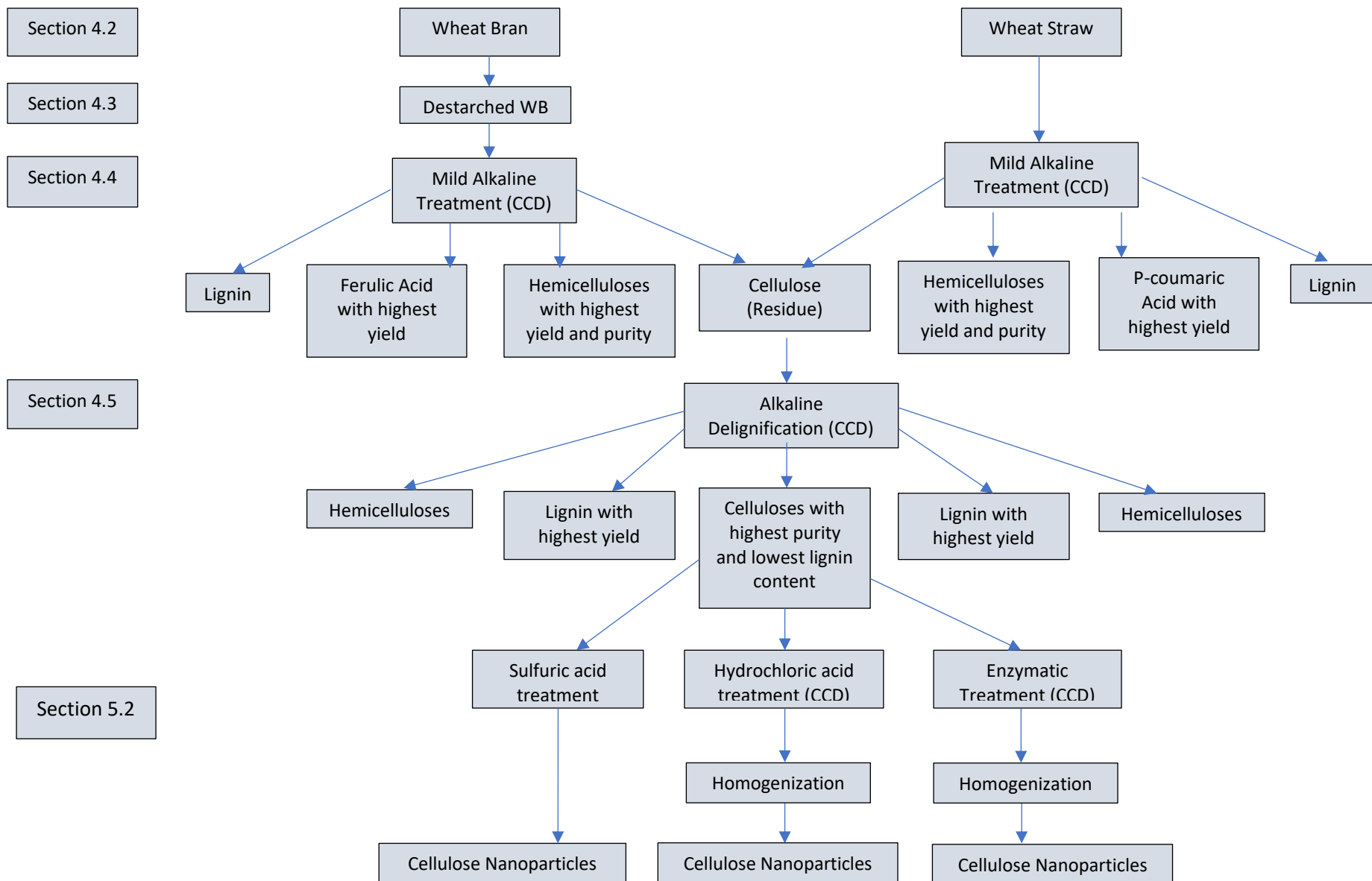


Figure 3.1 Process flow diagram for comparative analysis of methods for producing nanocellulose from wheat straw and bran, with co-extraction of valuable products

3.3.3 Mild Alkaline Treatment for Extraction of Hemicelluloses and Hydroxycinnamic Acids (Ferulic and *p*-Coumaric Acids)

The first alkaline treatment step termed the mild alkaline treatment step was conducted with the aim of hemicelluloses and hydroxycinnamic acid extraction (ferulic acid for wheat bran and *p*-coumaric acid for wheat straw and wheat bran (Figure 3.1). The treatment was performed by combining the treatment conditions stated by Peng et al. 2010 and Xu et al. 2006 (0.5-1M NaOH, 20-60°C and 10-16 hours) that favoured hemicellulose extraction and Buranov and Mazza (2009) (0.1-0.5 M NaOH and 50-70°C) that favoured hydroxycinnamic acid (ferulic and *p*-coumaric acid) extraction and making a compromise of yield for both extracts. However, due to the presence of lignin during alkaline extractions as stated in 2.2.2.1, the purity of the hemicelluloses obtained was considered as a response factor.

For both wheat straw and wheat bran, the concentration was varied at 1.5-2.5 wt. % NaOH aqueous solution for 16 hours at 20-60°C (Table 3.1). 10 g of the dried sample (DWB or WS) was placed in 100 ml of the NaOH solution (fiber to liquid ratio of 1:10) in a 250 mL schott bottle. This experiment was performed using a central composite design (CCD) with the variables in Table 3.1. After the treatment, the samples were centrifuged at 8000 rpm for 15 mins, the solids separated, washed until neutral and dried at 40°C in an oven. The liquid recovered after centrifuging was neutralized with 6 M HCl to pH 5.5 and the hemicelluloses precipitated with 3 vol. of 95% ethanol at room temperature. The precipitated hemicelluloses were then decanted, washed with 70% ethanol and dried using an oven at 40°C. The liquid filtrate was then vacuum evaporated to an ethanol concentration of 30% to obtain ferulic and *p*-coumaric acid since they are soluble at that ethanol concentration (Buranov and Mazza, 2009). The ferulic and *p*-coumaric acid were separated by centrifuging at 8000 rpm for 15 min as the supernatant. Ethanol was again added to the residue obtained after centrifuging till an ethanol concentration of 30% was achieved and centrifuged again to separate the ferulic and *p*-coumaric acid. Finally, the residue obtained was concentrated by using a rotary evaporator to recover the ethanol and the residue dried at 40°C in an oven to obtain the crude lignin.

Table 3.1 Parameters used for optimisation of mild alkaline treatment of wheat straw and wheat bran for the extraction of hemicelluloses and hydroxycinnamic acids (*p*-coumaric and ferulic acid).

Variables	Optimisation Parameters		
	Low Value	Centre Value	High Value
NaOH conc./ wt.%	1.5	2.0	2.5
Temperature	20	40	60

To determine the concentration of the ferulic and *p*-coumaric acid, 1ml of the acid extract was diluted in 1ml of 95% anhydrous ethanol, filtered through a 0.45 µm nylon syringe filter and analysed by high-

performance liquid chromatography (HPLC) for phenolic compounds. The dried residues as well as the dried hemicelluloses were then analysed for simple sugars and lignin. After which the dried solid WS and WB residues underwent an x-ray diffraction (XRD) to help determine the crystallinity, a Fourier Transform Infrared Spectroscopy (FTIR) analysis to determine chemical changes in the fiber structure, a Scanning Electron Microscopy (SEM) imaging to determine the fiber morphology as well as Thermogravimetric Analysis (TGA). The extracted hemicelluloses and lignin also underwent FTIR analysis, TGA and compositional analysis.

3.3.4 Alkaline Delignification Treatment for Producing Cellulose-rich Fiber with Minimal Lignin Content and Extraction of Lignin

The second stage alkaline treatment was termed as the alkaline delignification (SA) step. The alkaline delignification was aimed at obtaining cellulose-rich residues with high cellulose content and low lignin content while extracting a high lignin yield as possible (Figure 3.1). The delignification treatment was conducted by using the methodology by Rosa et al. (2012). A screening step was first conducted to determine the sodium hydroxide concentration and time to be used for the optimisation in the delignification step based on conditions used in alkaline delignification treatments stated in Section 2.2.2.1 with respect to effects on the mid alkaline residues used. The selected conditions used for the optimisation are presented in Table 3.2 and 3.3.

Mild alkaline treated wheat straw and wheat bran dried residues were placed in an aqueous sodium hydroxide solution at a fiber to liquid ratio of 1:10. The concentration of NaOH was varied from 8–12 wt.% NaOH for wheat straw and 6-10 wt.% NaOH concentration for wheat bran at a residence time of 30-90 min at 121°C in an autoclave (Table 3.2 and 3.3).

Table 3.2 Parameters used for optimisation of severe treatment of mild alkaline treated wheat straw solid residues

Variables	Optimization Parameter		
	Low Value	Centre Value	High Value
NaOH conc./ wt.%	8	10	12
Time/min	30	60	90

Table 3.3 Parameters used for optimisation of severe treatment of mild alkaline treated wheat bran solid residues

Variables	Optimization Parameter		
	Low Value	Centre Value	High Value
NaOH conc./ wt.%	6	8	10
Time/min	30	60	90

After the treatment, the samples were centrifuged at 8000 rpm for 15 mins, the solid residue washed until neutral and dried at 40°C. The solid residues were then analysed by FTIR, SEM, TGA, XRD and

compositional analysis. The pH of the filtrate containing the alkali lignin was adjusted to 5.5 by using 6 M HCl and 3 vol. of 95% ethanol at room temperature to precipitate the hemicelluloses present. The precipitated hemicelluloses were centrifuged out, washed, and dried at 40°C in an oven. The supernatant which contained the lignin was vacuum evaporated to recover the ethanol after which it was centrifuged, and then oven dried. The extracted crude lignin and hemicellulose were then analysed by FTIR, TGA and compositional analysis.

3.4 Nanocellulose Production with Cellulose-Rich Fibers

The nanocellulose production step was done using three different methods; the traditional sulfuric acid treatment, and two alternative approaches being a hydrochloric acid treatment and an enzymatic treatment approach. The treatments were performed on the two-stage alkaline cellulose-rich residues. The alternative treatments were aimed at producing cellulose nanoparticles and comparing their yield and characteristics with each other as well as the traditionally produced nanocelluloses using the delignified cellulose-rich residues.

3.4.1 Sulfuric Acid Hydrolysis of Cellulose-Rich Fibers

The cellulose rich fibers obtained after the alkaline delignification treatment was treated in 64% sulfuric acid solution. The treatment was performed according to the procedure illustrated by Liu et al. (2016). The cellulose-rich fibers were mixed in a fiber to acid solution ratio of 1:20 in a three neck-flask at 45°C for 60 min.

The resulting mixture after the treatment was diluted with 10 parts distilled water and centrifuged at 3000×g for 10mins. The precipitate produced was dialysed against distilled water for 3 days with four water changes each day. The resulting solution was then neutralized with 0.1 M NaOH to pH 5, dialysed for a day then centrifuged and dried to obtain the cellulose nanoparticles. The nanoparticles were then analysed by FTIR, TGA, SEM, surface charge (zeta potential), polydispersity index (PdI) and an XRD (for crystallinity).

$$Yield(\%) = \frac{m \times 100}{M} \quad \text{Eqn. 1}$$

Where m is the mass of the freeze dried nanocellulose produced; M is the mass of starting cellulose-rich fiber

3.4.2 Hydrochloric Acid Hydrolysis of Cellulose-Rich Fibers

The hydrochloric acid treatment was performed as an alternative treatment to the traditional sulfuric acid treatment. The hydrochloric acid treatment was performed similarly to what was performed by Cheng et al. (2017) with a few changes. A screening was performed to determine the optimisation treatment temperature and time for using 4 M HCl. The treatment conditions obtained for the optimisation are presented in Table 3.4. The cellulose rich fibers from alkaline delignification treatment were treated with 4 M HCl at a fiber to acid ratio of 1:20 (Cheng et al., 2017) at varied time and

temperature with agitation (Table 3.4). The resulting mixture was washed until pH above pH 5 with distilled water by centrifuging at 3000×g for 10 mins. The precipitate produced was re-suspended in distilled water and neutralized with 0.1 M NaOH. The treated nanoparticle produced was then diluted to produce a 2-3% fiber suspension, which was subjected to a high-speed homogenizer for 20 mins. The resulting mixture was then freeze dried to obtain the cellulose nanoparticle. The nanoparticles produced were then analysed by FTIR, TGA, SEM, surface charge (zeta potential), polydispersity index (PdI) and an XRD (for crystallinity). The yield for the nanocellulose was calculated as stated in Eqn.1.

Table 3.4 Parameters to be considered for hydrochloric acid hydrolysis nanocellulose production of wheat straw and bran cellulose.

Variables	Optimization Parameters		
	Low Value	Centre Value	High Value
Temperature/ ^o C	80	100	120
Time/hrs	4	6	8

3.4.3 Enzymatic Treatment of Cellulose-Rich Fibers

An enzymatic treatment was also performed as another alternative treatment to the sulfuric acid treatment. The cellulose rich fibers obtained from the alkaline delignification treatment were subjected to an enzymatic hydrolysis as illustrated by Bester (2018). A screening step was first conducted to determine the enzyme dosages as well as the time to produce nanoparticles with the minimum glucose formation. The obtained conditions were then used for the optimisation of enzymatic treatment (Table 3.5). A 5 wt. % cellulose pulp suspension of the cellulose rich fibers in a 50 mM acetate buffer solution (pH 5) was used with constant shaking at 150 rpm. The samples were treated at 50°C using an incubator (MRC Orbital shaker TS600) at different treatment times and enzyme dosages at pH 5. The enzymatic hydrolysis optimisation was performed using variable dosages of FiberCare R and Viscozyme L solution from Novozyme as well as at variable time (Table 3.5).

Table 3.5 Parameters to be considered for enzymatic hydrolysis nanocellulose production of wheat straw and bran cellulose.

Variables	Optimization Parameters		
	Low Value	Centre Value	High Value
Time/hrs	6	8	10
FiberCare R Dosage/ ECU/g	50	75	100
Viscozyme L Dosage/ FBG/g	10	15	20

After each enzymatic treatment, the sample in the reactor flask was heated to about 80°C for 30 min to stop enzyme activity. After which the samples were washed twice by centrifugation at 6000 rpm for 10 mins and vacuum filtered through a 1.6 µm glass membrane fitted to a Buchner funnel. The enzymatic treated fiber produced was then diluted to produce a 2-3% fiber suspension, which was subjected to a high-speed homogenizer for 20 mins. This resulted in shearing and impact forces that produces cellulose nanoparticles. The cellulose nanoparticles produced were then freeze-dried. The yield for the nanocellulose was calculated using Eqn 1.

3.5 Characterization

Characterization of the products and residues is an important part of experimentation because it helps to obtain both quantitative and qualitative information of the products and residues. Due to this reason characterization methods were performed on the products obtained after the two-stage alkaline treatment and the nanocellulose production stage. These characterization methods have been briefly explained in the subsequent sections below.

3.5.1 Sample Preparation

A representative sample of both wheat straw and bran was obtained using the coning and quartering method. The samples were further milled using a Retch ZM200 equipped with a 2mm circular blade to mill to a sample size of about 250-425µm. The milled samples were further screened in a Retch AS200 shaker to obtain samples within the specified size range to be used for compositional analysis. The samples are first conditioned in a conditioning room at 25°C for 48 hours before compositional analysis was conducted.

3.5.2 Compositional Analysis

Raw material and treated material composition were determined by employing the National Renewable Energy Laboratory (NREL) Laboratory Analytical Procedure (LAP) methods for biomass. The NREL methods were used to determine the moisture, ash, hemicellulose, lignin and cellulose content of the biomass. Analysis were performed in triplicates.

3.5.2.1 Determination of moisture content

The moisture content of the biomass, also referred to as the dry weight of the biomass was determined by drying approximately 2.0 g of the biomass in a convection oven at $105 \pm 3^\circ\text{C}$ overnight and weighing to obtain the final weight of the biomass. The difference between the final weight and the initial weight of the biomass resulted in the moisture content of the biomass (Sluiter et al., 2008a). The moisture content was determined by the equation:

$$\% \text{ Moisture content} = \frac{M_W - M_D}{M_D} \times 100 \quad \text{Eqn. 2}$$

Where M_W and M_D are initial and oven dried mass of sample, respectively.

3.5.2.2 Determination of ash content

The ash content of the various samples was determined by weighing a crucible, placing 3 g of the sample in a crucible, and placed in a furnace at 575°C for 5 hours. The sample was then removed cooled to room temperature in a desiccator and weighed to obtain the ash content of the sample (Sluiter et al., 2008b). The ash content was determined by the equation:

$$\% \text{ Ash content} = \frac{M_{AC} - M_C}{M_W} \times 100 \quad \text{Eqn. 3}$$

Where M_{AC} , M_C and M_W are mass of ash and crucible, mass of crucible and mass of sample, respectively.

3.5.2.3 Determination of extractives

The extractives in the sample were determined in a two-step process involving a water extractive step and an ethanol extractive step. 5g of the individual samples were placed in a thimble and placed in a Soxhlet tube of a Soxhlet apparatus. Then 190 mL of water was placed in a pre-weighed 250 ml round bottom flask, attached to the Soxhlet apparatus, and placed on a heating mantle to reflux for 24 hours. After the time limit, the water was evaporated, and the round bottom flask dried in an oven at 105°C overnight after which it was cooled to room temperature in a desiccator and weighed again to obtain the difference in weight which was the water extractives in the samples. The ethanol extractives was also obtained by using the sample in the thimble after the water extractives and repeating the same steps (Sluiter et al., 2008c). The water extractives and ethanol extractives were determined separately by the equation below and summed up to obtain the total extractives in this study:

$$\% \text{ Extractive (X)} = \frac{M_{FE(X)} - M_F}{M_W} \times 100 \quad \text{Eqn. 4}$$

Where (X), M_{FE} , M_F , M_W represents water or ethanol, mass of oven dried flask with extractives, mass of flask and mass of sample, respectively.

3.5.2.4 Determination of structural carbohydrates and lignin.

The lignin, hemicelluloses and cellulose contents were determined after performing a two-step acid hydrolysis on the extractive free samples (Sluiter et al., 2012). In the first acid hydrolysis step, 3 ml of 72% (w/w) H_2SO_4 was added to 0.3 g of the sample and placed in a water bath at 30°C for 60 min while stirring with a glass stirring rod after every 10 min interval. After which, it was diluted to 4% H_2SO_4 adding 84 mL deionized water and autoclaved for 1 h at 121°C for the second hydrolysis. The sample produced after this treatment was then vacuum filtered and through a pre-weighed crucible. The collected residue in the crucible was then dried in an oven at 105°C overnight, weighed and transferred into a muffle furnace at 575°C for 5 hours after which it was cooled in a desiccator and weighed again to determine the acid insoluble lignin (Eqn. 5). An aliquot of the filtrate after the vacuum filtrate was taken and the absorbance determined at 240 nm between six hours of the hydrolysis to determine the acid soluble lignin (Eqn. 6). The total lignin content used in this study was determined as the sum of

the acid soluble and acid insoluble lignin. 10 ml of the filtrate collected after vacuum filtering was then reduced to pH 7 by using 7 N KOH, filtered through a 0.22 μm syringe filter and analysed by using HPLC for the presence of xylose, arabinose, cellulose, furfural and HMF. The HPLC system used had an Aminex HPX-87H ion exclusion column with a 65°C column temperature and a flowrate of 0.6 ml/min. The HPLC system also had Shodex R 101 refractive index which was operated at 45°C. The hemicelluloses content was determined as the combination of the xylose and arabinose content (Eqn. 7), whereas the cellulose content on the other hand was determined from the glucose content (Eqn.8) of the samples. In addition, Eqn. 9 was used to calculate the arabinose to xylose ratio (A/X) for the hemicelluloses used in this study.

$$AIL = \frac{(M_{CR}-M_C)-(M_{CA}-M_C)-M_P}{M_D} \quad \text{Eqn. 5}$$

Where AIL, M_{CR} , M_C , M_{CA} , M_P and M_D are acid insoluble lignin, mass of crucible and oven dried hydrolysis residue, mass of crucible, mass of crucible and ash, mass of protein in sample and mass of oven dried sample, respectively.

$$ASL = \frac{UV_{wav} \times V_f \times Dilution}{\epsilon \times M_D} \times 100 \quad \text{Eqn. 6}$$

Where ASL, UV_{wav} , V_f , Dilution, ϵ and M_D are acid soluble lignin, sample absorbance at 240 nm, volume of filtrate, biomass absorptivity (25 L/gcm) and mass of oven dried sample, respectively.

$$Hemicellulose \text{ content} = 0.88 \times (arabinose + xylose) \quad \text{Eqn. 7}$$

$$Cellulose \text{ content} = 0.9 \times (glucose \text{ content}) \quad \text{Eqn. 8}$$

$$AX = \frac{arabinose \text{ content of hemicellulose}}{xylose \text{ content of hemicellulose}} \quad \text{Eqn. 9}$$

3.5.2.5 Determination of protein content

The protein content of the samples was determined by using a protein analyser from VELP Scientifica, Italy fitted with both a digester and automated distillation column. 1 g of oven dried powdered sample was placed into the digestion column provided with another set of digestion column left empty (as blank). After which, two cubes of antifoaming agents (provided by VELP Scientifica) and 12 ml of 98% sulfuric acid were added to each test tube. The digestion of the sample was performed in two steps. The first being a digestion at 300°C for 40 min after which it was immediately followed by the second digestion at 420°C for 90 min. The digestion columns were then allowed to cool to 50°C and transferred into the automated distillation column where 5 ml of sodium hydroxide and 10 ml of boric acid were added. The resulting solution was the titrated against 0.2 N hydrochloric acid and the crude protein content of the sample estimated from the Kjeldahl method using a nitrogen factor of 6.25 (Hames et al., 2008). The protein content was determined by the equation:

$$\text{Protein content} = \frac{(V_{ts}-V_b) \times 1.4007 \times 0.2 \times 6.25}{M_D} \quad \text{Eqn. 10}$$

Where V_{ts} , V_b and M_D are volume of titrated sample, volume of titrated blank and oven dried mass of sample (1.0 g), respectively.

3.5.2.6 Determination of starch content

The starch content of the samples is determined using a starch assay kit (KSTA 09/14) from Megazyme. A sample weighing 0.1 g was placed in a test tube where 0.2 mL of aqueous ethanol (80% v/v) was used to wet the sample and vigorously mixed. Thermostable α -amylase (3 ml) was added, and the solution placed in boiling water for 6 min. The tube was placed in a water bath at 50°C for 10 min to reduce its temperature to 50°C after which 0.1 ml of amyloglucosidase enzyme provided was added and allowed to incubate for 30 min. All the contents of the test tube were transferred to a 100 ml volumetric flask and topped up to the 100 ml mark and vigorously mixed. An aliquot of the solution was centrifuged at 2000×g for 10 min and the clear filtrate used for the assay. 0.1 ml of the clear filtrate were transferred in triplicates to a glass test tube and 3 ml of GOPOD reagents (provided by Megazyme) added to each test tube and incubated for 20 min. A control and blank were performed using a glucose standard and water respectively in place of the samples following the same steps. The incubated samples and glucose standard were read against water at an absorbance of 510 nm to obtain the starch content (Megazyme, 2016).

3.5.2.7 Determination of antioxidant DPPH free radical scavenging activity

The DPPH free radical scavenging activity of ferulic acid (from wheat bran) and *p*-Coumaric acid (from wheat straw) was determined by using the method described by Phongthai et al. (2016). A 0.25 mL aliquot of the sample (ferulic or *p*-coumaric acid) was mixed with 1 mL of 0.1 mM DPPH in 95% ethanol. A similar mixture is made but with ethanol (as blank) instead of ferulic or *p*-Coumaric acid. The mixtures were homogeneously mixed with a vortex mixer and left to stand in a dark room for 30 min. The absorbance of the various mixtures was determined by using a spectrophotometer (Cecil 2021, 2000 Series, Lasec SA) at 517 nm against the blank. The scavenging activity for DPPH (S) was determined by using the equation below

$$\%S = \frac{\text{Absorbance}_{\text{blank}} - \text{Absorbance}_{\text{sample}}}{\text{Absorbance}_{\text{blank}}} \times 100 \quad \text{Eqn. 11}$$

3.5.3 Fourier Transform Infrared Spectroscopy (FTIR)

FTIR was used to analyse the untreated samples and the samples at each stage of treatment to directly determine any chemical changes in the structure of the fibers after treatment by identifying the functional groups present. An analysis in the range of 400 – 4000 cm^{-1} with a resolution of 4 cm^{-1} using a Thermo Nicolet Nexus 670 spectrometer. This was conducted by powdering dried samples into ultra-thin pellets and measured with the attenuated total reflectance mode of the spectrometer of which 32

scans were taken. The peaks of the spectra obtained were compared with literature to assist in peak assignments.

3.5.4 X-Ray Diffraction and Crystallinity

X-ray diffraction was performed on both the wheat straw and bran after each treatment stage using a Bruker D2 Phaser x-ray diffractometer with a monochromatic CuK α radiation source ($\lambda=1.54184 \text{ \AA}$, 30 kV) with a 2θ angle range from 5° to 50° ($1^\circ/\text{min}$) at room temperature. Each coin sized sample was grounded into powder and levelled on a sample holder. This helped to promote total uniform and complete exposure to the x-ray (Johar et al. 2012).

The Crystallinity Index (CI) of both wheat straw and bran were calculated using the Segal method (Eqn. 11) (Rosa et al. 2012). This involved using the height of 2 0 0 peak (I_{200} , $2\theta = 22.5^\circ$) and the minimum between the 2 0 0 and 1 1 0 peaks (I_{am} , $2\theta = 18^\circ$) for the calculation:

$$CI = \frac{I_{200} - I_{am}}{I_{200}} \times 100\% \quad \text{Eqn. 12}$$

3.5.5 Scanning Electron Microscopy

The characterization of the fiber morphology of each treated fiber was performed using scanning electron microscopy at the Central Analytical Facility (CAF) in the Chamber of Mines Building, Stellenbosch University. SEM micrographs of the treated fibers were taken in quadruplets using a MERLIN, Zeiss scanning electron microscope operated at 3 kV and higher, in which the fiber samples were coated with gold to eliminate the electron charging effects (Rezanezhad et al. 2013). The morphological changes of the fractionated fibers were observed from micrographs obtained, however for the produced nanocelluloses additional information of the fiber length and diameter were determined by using image j software in conjunction with the micrographs. The software possesses inbuilt tools that help with quantitative image analysis. An average of 50 measurements were taken for each image for the four SEM images for the nanocelluloses of which an average was estimated and used as the sample length and diameter.

3.5.6 Thermogravimetric Analysis (TGA)

TGA was done to compare the degradation of the treated fibers with the untreated ones, as well as help to determine the effects of the treatment on the products. The thermal stability of the samples were determined using a Mettler Toledo TGA, Thermogravimetric analyser (TGA500) with a heating rate of $10^\circ\text{C}/\text{min}$ within a temperature range of $25 - 600^\circ\text{C}$ in a nitrogen atmosphere in order to prevent any thermoxidative degradation (Moran et al. 2008).

3.5.7 Particle Morphology and Surface Charge

Particle size, polydispersity index (PdI) and zeta potential (ZP) of the cellulose nanoparticles were determined by using a Nano-ZS90 size analyser (Malvern Instruments) Zetasizer. The analysis of the samples by the instrument was done by a dynamic light scattering method after a dilution of the sample

to less than 0.01% (w/w). Analysis by the equipment occurred after 120 seconds equilibrating time at a scattering angle of 90° at 25°C. The measurements were taken in triplicate and the intensity-weighted mean hydrodynamic diameter was calculated by the instrument by using a cumulant method. This resulted in obtaining a mean particle size with most of the intensity peak.

Polydispersity index is a dimensionless number (ranging from 0 to 1) calculated from the cumulant number from the sample analysis by the equipment. It helps to determine the extent to which a sample is either monodispersed or polydispersed. Samples with a PdI < 0.08 are said to be very monodispersed and are rarely seen except from monodispersed standards, whereas samples with a PdI > 0.7 can be said to possess a broad size distribution (International Standards Organization, 2008).

CHAPTER FOUR

Two-stage alkaline treatment of wheat straw and wheat bran to extract hemicellulose, lignin, *p*-coumaric acid (from wheat straw), ferulic acid (from wheat bran) and produce cellulose-rich fibers for nanocellulose production

4.1 Introduction

Waste valorisation, a means of adding value to waste by converting or producing other products from them, has recently received much attention from most researchers. Agricultural residues have become a target for most waste valorisation research (Luzi et al., 2019; Menon et al., 2010). Wheat straw and wheat bran generated from the harvesting and processing of wheat, respectively are agricultural wastes that have also been targeted for waste valorisation research due to their chemical composition.

Wheat straw has been found to contain 38-45% cellulose, 24-38% hemicelluloses, 8-27% lignin and about 0.42% *p*-coumaric acid which has caused it to receive in the field of producing cellulose-rich fibers for nanocellulose production, hemicelluloses, lignin and *p*-coumaric acid extraction (Alemdar and Sain, 2008a; Pan et al., 1998; Peng and Wu, 2010; Watkins et al., 2015). On the other hand, wheat bran has also been found to contain 11-21% cellulose, 36-58% hemicelluloses, 3-12% lignin and up to 1.5% ferulic acid which has mainly made it a target for the extraction of hemicelluloses and ferulic acid (Aguedo et al., 2014; Wu et al., 2017). Extraction of these value-added products from both wheat straw and wheat bran can be accomplished by employing treatment methods such as an alkaline treatment.

Alkaline treatment has been found to be an effective means of extracting hemicelluloses, lignin, ferulic and *p*-coumaric acid from most agricultural residues. However, the treatment has been found to have minimal effects on the cellulose content of the biomass when the treatment conditions are well regulated, which could potentially result in the production of cellulose-rich fibers for nanocellulose production. The main issue with using an alkaline treatment in the extraction of these products is the issue of conflicting treatment conditions for the extraction of hemicellulose, lignin, ferulic and *p*-coumaric acid as well as interference of these cell wall components during the extraction of others. It therefore makes it necessary to determine optimised treatment conditions that can be employed in extracting these products.

Due to this reason, this research aims to use and optimise a two-stage alkaline treatment by employing a central composite design and response surface methodology to determine optimum process conditions for the extraction of hemicellulose, lignin, ferulic and *p*-coumaric acid from wheat bran and wheat straw. The first stage involves the optimisation of a mild alkaline treatment to extract hemicellulose, *p*-

coumaric acid (from wheat straw), ferulic acid (from wheat bran) and lignin as a by-product of the treatment (Figure 3.1). The residues obtained from the mild alkaline treatment is then optimised for an alkaline delignification treatment to improve the cellulose content of the residue whereas reducing and extracting lignin from the residue with the extracting of hemicelluloses as a by-product (Figure 3.1). The two-stage alkaline treatment suitability in the production of cellulose-rich fibers for nanocellulose production is determined by characterising the residue and comparing it to the criteria stated in Section 2.3 (cellulose content $\geq 62\%$, crystallinity index $\geq 48\%$, hemicelluloses content $\leq 23\%$ and lignin $\leq 10\%$).

4.1.1 Outline of two-stage alkaline treatment of wheat and wheat bran to extract hemicellulose, lignin, *p*-Coumaric acid (from wheat straw), ferulic acid (from wheat bran) and produce cellulose-rich fibers for nanocellulose production

Wheat straw and wheat bran are both rich sources of cell wall components such as hemicellulose, lignin, hydroxycinnamic acids (ferulic and *p*-coumaric acids) as well as possible source of cellulose-rich biomass which can be used for nanocellulose production. Chapter Four, focused on using a two-step alkaline treatment (Figure 3.1) which was the developed pretreatment method combination for the extraction of hemicellulose, lignin, ferulic acid and *p*-Coumaric acid as well as obtaining a cellulose-rich pulp that meets the criteria stated in Section 4.1 (cellulose content $\geq 62\%$, crystallinity index $\geq 48\%$, hemicelluloses content $\leq 23\%$ and lignin $\leq 10\%$) for nanocellulose production. An overview of the treatments and objectives of each treatment have been provided below

- Section 4.2 of the study focused on the composition of the wheat straw and wheat bran with the end goal of fractionation and nanocellulose production while predicting the suitability of the biomass to the two-step alkaline treatment process to obtain a cellulose-rich pulp and value-added products.
- The next treatment, a destarching treatment (Figure 3.1, Section 4.3) was only performed on the wheat bran given its high starch content (11–39%) as stated in Section 2.1. A two-step enzymatic treatment was performed as stated in Section 3.2.2 to remove as much starch as possible. The destarched wheat bran (DWB) obtained was then analysed to determine its composition and how the destarching affected other cell wall components such as cellulose, lignin, hemicellulose, and protein as well as the starch content itself.
- The first alkaline treatment performed on the wheat straw and wheat bran was referred to as the mild alkaline treatment step (Figure 3.1, Section 4.4) due to the treatment conditions (1.5-2.5 wt.% NaOH conc., 20-40°C at 16 hours) applied. The optimisation at the mild alkaline treatment step focused on extracting hemicellulose with a high yield and purity while co-extracting ferulic acid (for wheat bran) and *p*-coumaric acid (for wheat straw) with high yields.

Moreover, at the optimum conditions obtained, the lignin extracted, and composition of the residue obtained were also characterised (Figure 3.1, Section 4.4 and 4.6).

- The second alkaline treatment performed termed as the alkaline delignification treatment was performed on the wheat straw and wheat bran residues obtained after the mild alkaline treatment (Figure 3.1, Section 4.5). The alkaline delignification optimisation was aimed at obtaining cellulose-rich residues with high cellulose content and low lignin content that can be used in nanocellulose production, while co-extracting lignin from the mild alkaline treated wheat straw and wheat bran residues. Furthermore, the hemicellulose extracted during the treatment at the optimised conditions was also characterised (Figure 3.1, Section 4.5). The characterisation of the delignified wheat straw and wheat bran cellulose-rich pulp obtained after the treatment was further discussed in Section 4.6.
- Section 4.6 referred to as cellulose isolation focused on how the destarching (for wheat bran only) and the two-stage alkaline treatment affected the cellulose-rich pulp obtained. Furthermore, this section aimed at determining whether the cellulose-rich pulp obtained could be directly applied for nanocellulose production based on the criteria stated in Section 2.3.
- Section 4.7 focused on conclusions from the two-step alkaline treatment applied on both the wheat straw and wheat bran with relation to the aims and objectives of the study.

4.2 Chemical Composition of Wheat Straw and Wheat Bran

The chemical compositions of both wheat straw and wheat bran are shown in Table 4.1. From the values obtained for wheat straw, it can be noticed that most of the values obtained were within range or remarkably close to that cited by various literature works as represented in Table 2.1. However, the value for the hemicelluloses composition (19%) of the wheat straw was relatively lower in comparison to that in Table 2.1 (24-38%) which might be due to cultivar type, region of cultivation, and soil used in cultivation (Barman et al., 2012). Also, its arabinose to xylose ratio (A/X) was found to be 0.12 which indicated that the hemicelluloses within the wheat straw has a more linear structure (Sun et al., 2005). Similar hypothesis can be drawn for the high extractives (14%) in the untreated wheat straw. The composition of the wheat straw indicated that the wheat straw acquired did not require any additional treatments before the fractionation process. The cellulose content of the wheat straw (36%) albeit low was in close agreement to the cellulose content of wheat straw (39%) reported by Espinosa et al. (2017) pretreated for the production of nanocellulose. The lignin (19%) and *p*-coumaric acid (0.25%) content of wheat straw were similar to reported data in literature and indicates potential to be extracted (Mussatto et al., 2007; Peng and Wu, 2010; Sun et al., 2005).

The hemicelluloses content of untreated wheat bran (22%) was found to be slightly less than ranges cited in most literature (Table 2.1) (34-58%) which could have been due to cultivar type and region of cultivation of the wheat bran (Barman et al., 2012). The A/X for the untreated wheat bran was found to be 0.67 which indicated a more branched structure of the hemicelluloses which is in agreement with

hemicelluloses from wheat bran (F. Xu et al., 2006). In addition, the starch (30%) and protein (15%) present in the wheat bran indicated that milling process used in separating the bran from the wheat was not very effective (Chotěborská et al., 2004). The ineffective milling process could have resulted in unseparated starchy endosperm of the grain attaching to bran, thereby increasing the starch and protein contents of the wheat bran (Liu and Ng, 2016), and resulting in a reduction to the process efficiency per weight of substrate (Kim et al., 2013).

Table 4.1 Chemical composition of untreated wheat straw, untreated wheat bran and destarched wheat bran.

Composition	Untreated WS	Untreated WB	Destarched WB
Cellulose, %	35.7 ± 2.4	10.3 ± 0.6	16.7 ± 0.4
Hemicelluloses, %	18.8 ± 1.4	22.0 ± 0.8	33.7 ± 0.7
Lignin, %	19.3 ± 3.2	11.2 ± 0.5	18.6 ± 0.7
Starch, %	3.9 ± 0.2	30.0 ± 0.3	0.4 ± 0.2
Protein, %	1.3 ± 0.3	14.9 ± 2.5	15.4 ± 4.8
Ash, %	3.6 ± 0.1	3.7 ± 0.1	2.4 ± 0.2
Extractives, %	13.9 ± 0.4	9.8 ± 0.8	8.4 ± 0.5
Ferulic Acid, %	0.17 ± 0.04	0.28 ± 0.05	0.34 ± 0.03
<i>p</i> -Coumaric Acid, %	0.24 ± 0.03	-	0.07 ± 0.01
Total, %	96.8	102.2	100.8

Where WS and WB are wheat straw and wheat bran, respectively. The standard deviations were calculated from replicate measurements.

Finally, the cellulose content (10%) of the wheat bran obtained was relatively low to that of most biomass used in the preparation of nanocellulose (Khalil et al., 2012). Based on the cellulose content of the wheat bran it can be inferred that after the two-stage alkaline treatment and partial hydrolysis, less than 10% nanocellulose can be produced from the wheat bran. Whereas, a complete hydrolysis of the wheat bran into ethanol might be a suitable application for the wheat bran given its total carbohydrate content of 62% (Table 4.1). Similar, carbohydrate contents (cellulose (12%), hemicellulose (34%) and starch (26%)) were obtained by Favaro et al. (2012) to produce ethanol. Furthermore, the crystallinity of the wheat bran cellulose (discussed in Section 4.6.2) which was negligible for the untreated wheat bran indicated that it was made up of more amorphous regions than crystalline regions and might not be suitable for nanocellulose production after the two-step alkaline treatment.

4.3 Destarching of wheat bran

The two-step enzymatic destarching of wheat bran resulted in the reduction of the starch content of the wheat bran to less than 1% (Table 4.1). The starch reduction accounted for the removal of almost 100% of the wheat bran starch indicating the effectiveness of the enzymes as well as the treatment step. The efficiency was comparable to what was obtained (100%) by Tirpanalan et al. (2014). Also, the destarching step can be noticed (Table 4.2) to have had a significant effect on the protein (37%

reduction) within the wheat bran. As stated in section 2.9.1, starch extraction has been noticed to partially solubilise the protein content resulting in the removal of part of the protein (Tirpanalan et al., 2014). Brillouet and Mercier (1981) stated that the hot water used in the gelatinization step of the destarching process was the main cause of the partial removal of proteins from wheat bran.

In comparison to other feedstocks such as wheat straw that have been used for production of nanocellulose, such low levels of starch (0.3%) have been shown to be acceptable in the production process resulting in insignificant inhibition to enzymatic hydrolysis to produce nanocelluloses due to their amorphous nature (Tibolla et al., 2017). Also, the destarching of the wheat bran resulted in an overall increase in the composition of the other components of the wheat bran. The results obtained (Table 4.1) are in close agreement to those cited by Sánchez-Bastardo et al. (2013) for destarched wheat bran. The results indicated that to obtain wheat bran with high cell wall (cellulose, hemicelluloses, lignin and ferulic acid) composition, it was necessary to obtain wheat bran with a low starch content or improve on the debranning process. These will in turn serve to improve the economics of the process by eliminating the enzymatic destarching step.

Table 4.2 Mass balance for destarching of wheat bran

Composition	Untreated WB	Hydrolysate	Destarched WB	Recovery, %
Cellulose, g/100g	10.3 ± 0.6	n/r	10.1 ± 0.2	97.4
Hemicelluloses, g/100g	22.0 ± 0.8	1.4 ± 0.2	20.3 ± 0.4	98.4
Lignin, g/100g	11.2 ± 0.5	n/r	11.2 ± 0.4	99.9
Starch, g/100g	30.0 ± 0.3	29.5 ± 0.5	0.3 ± 0.1	99.3
Protein, g/100g	14.9 ± 2.5	5.5 ± 0.3	9.3 ± 2.9	99.4
Ash, g/100g	3.7 ± 0.1	n/r	1.4 ± 0.1	39.2
Extractives, g/100g	9.8 ± 0.8	n/r	5.1 ± 0.3	52.0
Total, g/100g	101.9	36.4	57.6	92.3

Where WB and n/r are wheat bran and not recorded, respectively. The standard deviations were calculated from replicate measurements.

$$\text{Recovery } X, \% = \frac{\text{Hydrolysate } X + \text{Destarched WB } X}{\text{Untreated WB } X} \times 100, \text{ where } X \text{ represents component.}$$

4.4 Mild Alkaline Treatment of Untreated Wheat Straw and Destarched Wheat Bran for Hemicellulose, *p*-Coumaric Acid and Ferulic Acid Extraction

The mild alkaline treatment optimisation was performed on both the untreated wheat straw and the destarched wheat bran at 1.5-2.5 wt.% NaOH concentration, 20-60°C for 16 h to target the extraction of hemicelluloses, *p*-coumaric acid (for wheat straw) and ferulic acid (for wheat bran) (Figure 3.1). The results obtained for wheat straw indicated that at a 95% confidence level both NaOH conc. and temperature were significant both in the linear and quadratic terms for both the extracted hemicelluloses and the *p*-coumaric acid (Figure 4.1a, b and c) indicating that in all three responses the optimum treatment conditions were reached. Furthermore, the hemicellulose yield and purity had R-squared values of 0.90 and 0.94, respectively whereas the *p*-coumaric acid yield had an R-squared value of 0.70 indicating that the latter there was a larger significant difference between the experimental and predicted values than the former responses.

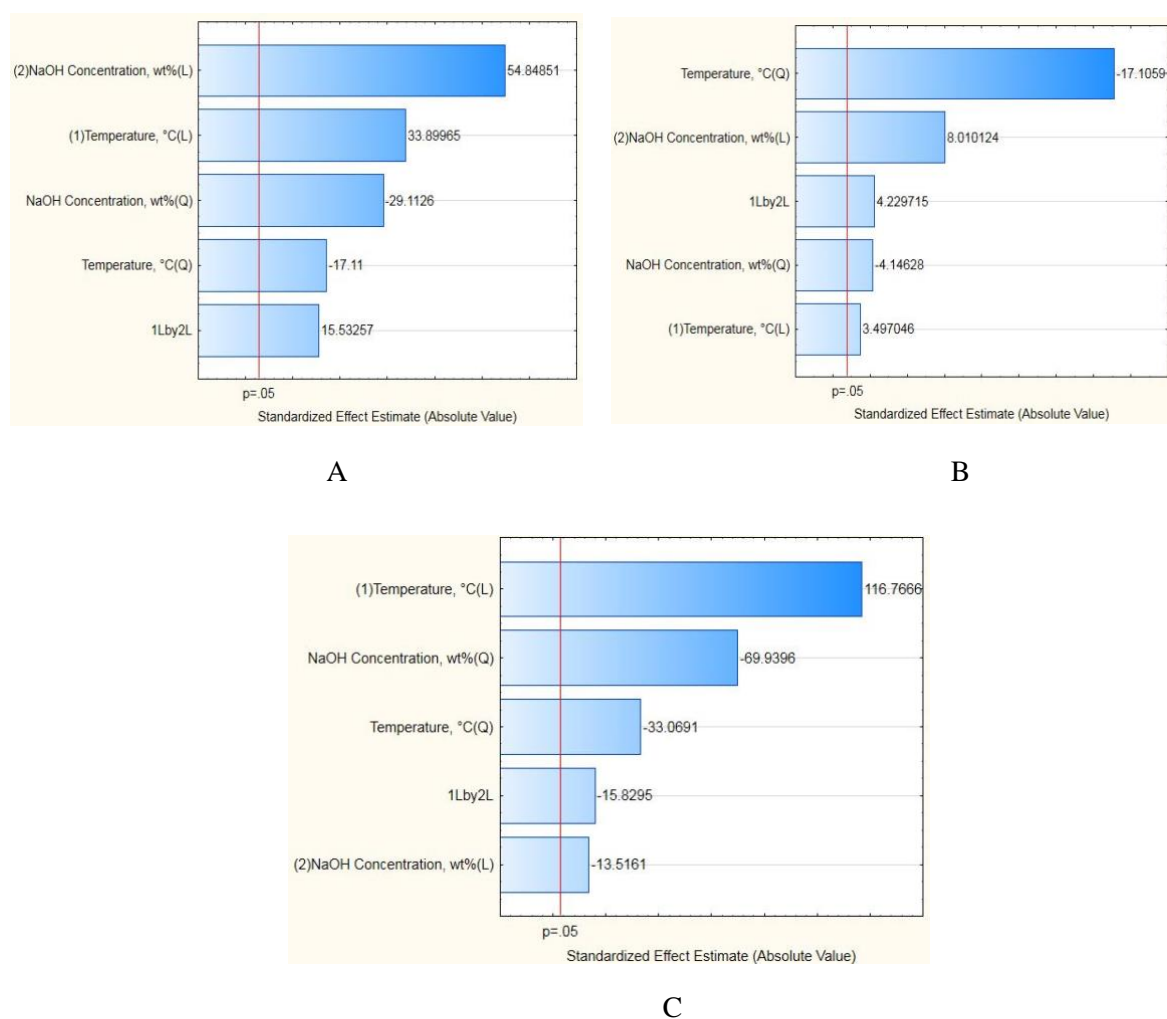


Figure 4.1 Pareto charts for mild alkaline treatment of wheat straw for hemicelluloses and *p*-coumaric acid extraction A) Hemicelluloses yield B) Hemicelluloses purity C) *p*-Coumaric acid yield

From Table 4.3, as the treatment conditions increased, the yield and purity of the mild alkaline extracted wheat straw hemicelluloses (MAWS Hemis) was found to increase. The quadratic effect of the MAWS Hemis yield was observed as the yield increased from 11.6% to an optimum of 33.6% and a final reduction as the treatment conditions was increased (above 60°C and 2.0 wt.%) to a yield of 32.6%. Similarly, the quadratic effect of the MAWS Hemis purity was observed as an initial increase in purity till the treatment conditions reached 40°C and 2.0 wt.% obtaining an optimum purity of 40.21% after which any further increase in treatment conditions resulted in a reduction of the MAWS Hemis purity (Table 4.3). However, the hemicelluloses purity was found to be mainly influenced by temperature (Figure 4.1b) which resulted in a reduction in purity of the hemicelluloses obtained (37.9%) at the optimum conditions (54.14 °C, 2.35 wt.% NaOH). The results obtained at the optimum conditions were comparable to the hemicellulose yield of 35.4% obtained by Bian et al. (2010) after extracting hemicelluloses from holocellulose at room temperature with an alkaline concentration of 10 wt.% for 16 hours.

Table 4.3 Treatment conditions and response from mild alkaline treatment of wheat straw for hemicellulose and *p*-Coumaric acid extraction

Temperature, °C	NaOH Concentration, wt.%	Hemicelluloses Yield/ Original Hemicelluloses, %	Hemicelluloses Purity, %	<i>Lignin Content in Hemicelluloses, %</i>	<i>p</i> -Coumaric Acid, %	<i>p</i> -Coumaric Acid Purity, %
40.00	1.29	11.64	31.22	<i>24.94</i>	60.78	<i>57.27</i>
40.00	2.71	31.43	40.21	<i>21.89</i>	35.29	<i>66.58</i>
40.00	2.00	29.03	39.07	<i>27.92</i>	83.82	<i>64.50</i>
40.00	2.00	29.02	39.86	<i>27.36</i>	83.82	<i>63.77</i>
40.00	2.00	29.26	37.46	<i>28.26</i>	83.33	<i>63.45</i>
40.00	2.00	29.76	39.12	<i>26.69</i>	83.82	<i>64.05</i>
40.00	2.00	29.41	38.34	<i>27.67</i>	84.31	<i>63.74</i>
60.00	1.50	19.11	27.61	<i>24.77</i>	92.16	<i>63.89</i>
60.00	2.50	33.68	35.44	<i>22.13</i>	94.61	<i>63.74</i>
20.00	1.50	20.88	31.65	<i>26.12</i>	55.39	<i>64.35</i>
20.00	2.50	25.92	31.76	<i>21.89</i>	71.57	<i>56.18</i>
68.28	2.00	32.61	30.07	<i>18.53</i>	91.67	<i>61.21</i>
11.72	2.00	16.05	23.44	<i>14.78</i>	29.41	<i>61.87</i>

Italicised values not included in model as response

The compositional analysis of the MAWS Hemis indicated that the main contaminant was lignin. The lignin composition was found to increase till the temperature reached 40°C (Table 4.3). The result indicates that temperatures above 40°C were also favourable for the extraction of lignin. The presence

of lignin within all the MAWS Hemis could have been as a result of incomplete cleavage of the α -benzyl ether linkages which exist between lignin and hemicelluloses (Xu et al. 2006). Furthermore, the increase in the lignin extraction was as a result of higher temperatures favouring the alkaline extraction of lignin as stated by McIntosh and Vancov (2011). A bleach treatment to produce holocellulose, could have improved both the MAWS hemicellulose purity and yield (Bian et al., 2010). However, the bleach treatment would have resulted in the loss of 20% of the hemicellulose present within the wheat straw as well as the *p*-coumaric acid present within the wheat straw (K. Liu et al., 2016).

The hemicellulose yield and purity of mild alkaline treated destarched wheat bran had R^2 values of 0.90 and 0.92, respectively, whereas the ferulic acid yield had an R^2 value of 0.72 indicating that ferulic acid yield presented a lesser correlation between the experimental and predicted values than the former two responses. From Table 4.4, the yield of hemicelluloses recovered for the mild alkaline treatment of the destarched wheat bran was 6.6-32.7% with purity of 29.4-47.1% as treatment conditions increased. The increase of both hemicellulose yield and purity was found to be significantly affected by the extraction temperature at a 95% confidence level (Figure 4.2a and b). Similarly, the yield of ferulic acid was affected by the extraction temperature at 95% confidence level (Figure 4.2c). In all these three cases, the NaOH concentration also influenced the yield and purity albeit not as significant as the temperature (Figure 4.2a, b and c). The results indicated that for wheat bran hemicelluloses and ferulic acid extraction the treatment temperature could have either a positive or negative influence on the yield and purity of hemicelluloses and ferulic acid.

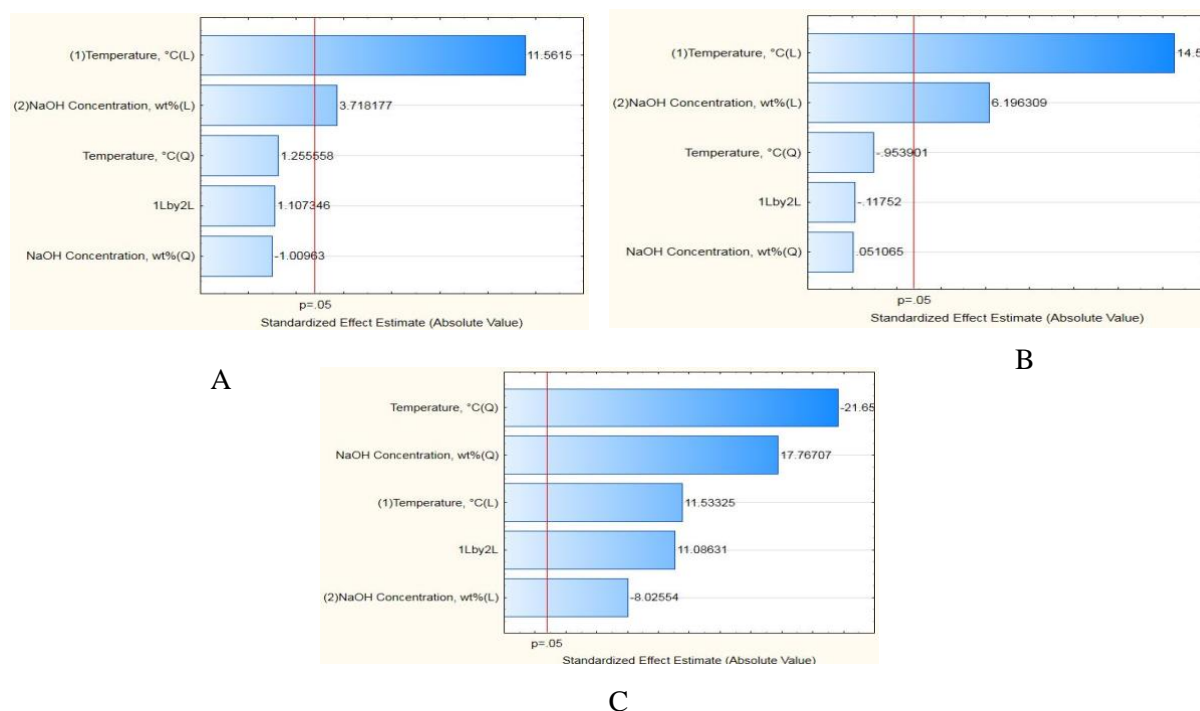


Figure 4.2 Pareto charts for mild alkaline treatment of wheat bran for hemicelluloses and ferulic acid extraction
 A) Hemicelluloses yield B) Hemicelluloses purity C) Ferulic acid yield

Table 4.4 Treatment conditions and response from mild alkaline treatment of destarched wheat bran for hemicellulose and ferulic acid extraction

Temperature, °C	NaOH Concentration, wt. %	Hemicelluloses Yield/ Original Hemicelluloses, %	Hemicelluloses Purity, %	<i>Lignin Content in Hemicelluloses, %</i>	Ferulic Acid, Yield, %	<i>Ferulic Acid Purity, %</i>
40.000	1.293	15.21	36.69	<i>21.18</i>	75.63	<i>88.96</i>
40.000	2.707	17.65	41.27	<i>18.52</i>	65.19	<i>93.82</i>
40.000	2.000	15.80	37.18	<i>21.37</i>	75.94	<i>94.02</i>
40.000	2.000	14.53	37.58	<i>21.63</i>	75.64	<i>93.92</i>
40.000	2.000	18.67	39.19	<i>19.42</i>	76.92	<i>93.89</i>
40.000	2.000	16.65	38.56	<i>21.44</i>	77.47	<i>93.95</i>
40.000	2.000	18.92	39.43	<i>19.61</i>	77.12	<i>93.70</i>
60.000	1.500	17.16	38.68	<i>22.50</i>	69.08	<i>93.57</i>
60.000	2.500	27.38	43.94	<i>20.12</i>	76.07	<i>94.08</i>
20.000	1.500	6.97	30.94	<i>21.75</i>	73.87	<i>93.67</i>
20.000	2.500	13.03	36.43	<i>15.43</i>	66.72	<i>93.62</i>
68.280	2.000	32.67	47.11	<i>19.10</i>	58.10	<i>94.11</i>
11.720	2.000	6.63	29.35	<i>19.54</i>	31.52	<i>95.06</i>

Italicised values not included in model as response

4.4.1 Extraction of Recovered Alkali Soluble Hemicelluloses and Lignin at the Optimum Mild Alkaline Conditions

4.4.1.1 Yield and Composition of Recovered Hemicelluloses and Lignin at the Optimum Mild Alkaline Conditions

At the optimum multiple response conditions obtained for hemicelluloses extraction from the wheat straw, a yield of 34.7% of the original hemicellulose was recovered (Table 4.5). Similar results (39%) have been obtained by García et al. (2013) when performing an alkaline treatment on wheat straw. Furthermore, it can be noticed from Figure 4.3 that since the optimum treatment temperature (54⁰C) exceeded 40⁰C, it resulted in a minimal reduction in the purity of the hemicelluloses from 40.2 to 37.9% (Table 4.5). Lignin as the main impurity in the hemicelluloses accounted for 28.7% which was found to be higher than 17.5% obtained by Koegelenberg (2016). Such high lignin content was likely due to incomplete cleavage of lignin-hemicellulose bonds (Rabetafika et al., 2014). In addition, ash (16.2%) was also found to be present within the wheat straw hemicelluloses extracted. The presence of ash could have been due to both the ash extracted from the wheat straw as well as the neutralised salts from the hemicellulose precipitation (K. Liu et al., 2016; Xiao et al., 2001). The results indicated that during mild alkaline treatment of wheat straw, whereas hemicelluloses yield was favoured by an increase in temperature above 40⁰C, hemicelluloses purity was reduced at the same condition due to an increase in lignin and ash content.

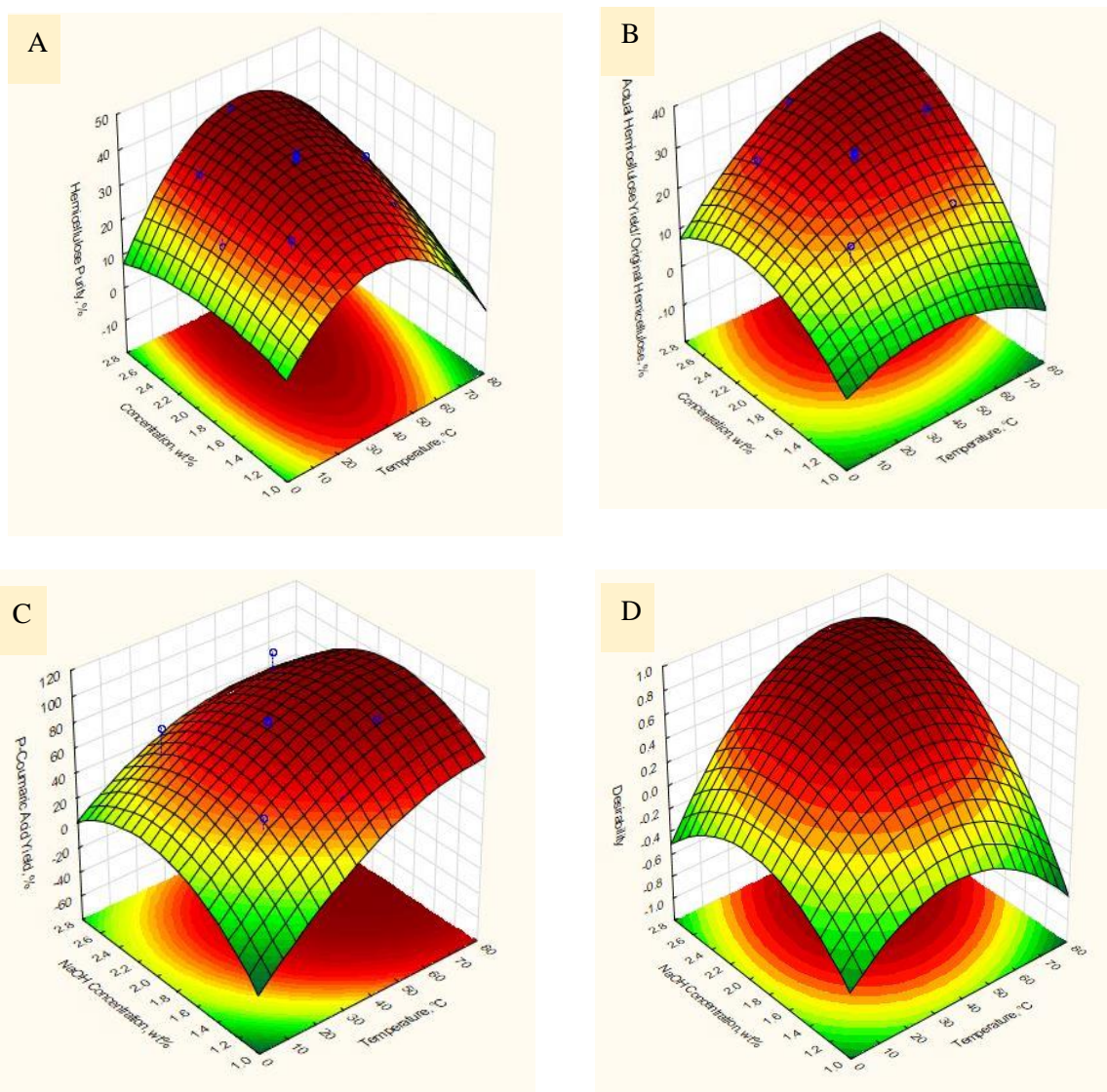


Figure 4.3 Surface plot of optimisation of wheat straw mild alkaline extracted A) Hemicelluloses purity B) Hemicelluloses yield/ original hemicelluloses C) *p*-Coumaric acid yield D) Desirability (54.14 °C, 2.35 wt.% NaOH) with NaOH concentration and temperature as independent variables

Table 4.5 Predicted and experimental values at optimised conditions for mild alkaline treated wheat straw for hemicellulose and *p*-coumaric acid extraction

Optimised Conditions MA WS (54.14 °C, 2.35 wt.% NaOH)			
	Hemicelluloses Purity, %	Actual Hemicelluloses Yield/Raw WS Hemicelluloses, %	<i>p</i> -Coumaric Acid Yield, %
Predicted Values	38.68 ± 1.29	34.60 ± 0.49	84.80 ± 2.04
Experimental Values	37.85 ± 0.19	34.73 ± 0.31	85.29 ± 2.84

Even though, the mild alkaline treatment of wheat straw was targeted at extracting hemicelluloses and *p*-coumaric acids, significant yields of the crude lignin were obtained from wheat straw (44.8%) (Figure 4.4). Similar results were obtained by R. C. Sun et al. (2002) when wheat straw was treated with 0.5 M NaOH where they noticed that with a 32.3% yield of hemicellulose, there was an associated 61.0% yield of lignin extracted. Furthermore, Sun and Tomkinson (2002) stated that about 50% of the total lignin in wheat straw was extracted at 0.5 M alkali concentration at 35⁰C. Moreover, results from Table 4.5 indicated that the recovered wheat straw lignin had a purity of 84.4%. In addition, there were two main impurities, ash (9.6%) and hemicelluloses (4.9%). The ash content could be attributed to both the ash within the wheat straw used in the extraction as well as the neutralised salts that dissolved in the ethanol used in separation of the hemicelluloses and lignin (K. Liu et al., 2016). The results obtained from the recovered hemicelluloses and lignin from the mild alkaline treatment of the wheat straw indicated that the treatment was not selective enough. Rabetafika et al. (2014) stated that without performing a bleaching treatment on the biomass, the likelihood of having a large contamination of lignin in alkaline extracted hemicelluloses is present. In addition, although this bleaching step could improve the purity and yield of the extracted hemicelluloses, it could also result in at least a 20% loss of the original hemicelluloses in the biomass before alkaline extraction (K. Liu et al., 2016).

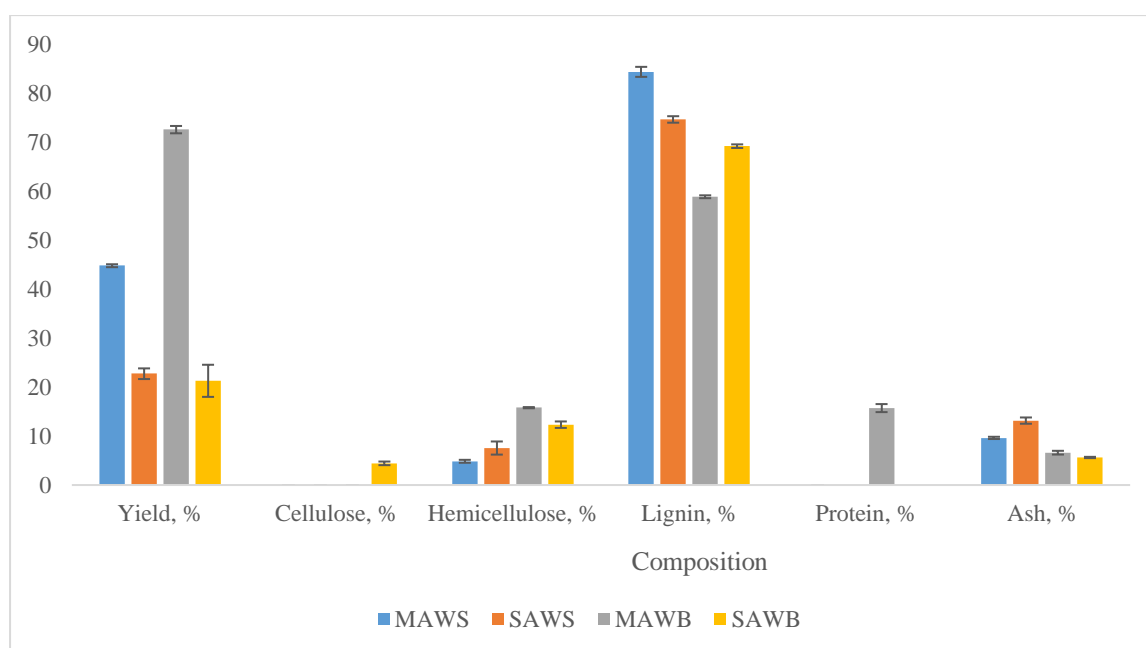


Figure 4.4 Yield and chemical composition of recovered lignin for mild alkaline wheat straw (MAWS), alkaline delignified wheat straw (SAWS), mild alkaline wheat bran (MAWB) and alkaline delignified wheat bran (SAWSB) at optimum conditions

The linear effect of the MAWB yield and purity (Figure 4.5) resulted in optimum condition of 68.28 °C and 2.71 wt.% NaOH for the mild alkaline treatment of the destarched wheat bran giving a yield of 36.98% of the hemicellulose in the destarched wheat bran (Table 4.6) which was also comparable to yield of hemicellulose obtained by (García et al., 2013). Furthermore, the results obtained at the optimum conditions indicated that the hemicellulose produced had a purity of 47.6% which was close to the 49% obtained by Koegelenberg (2016). Similarly, the lignin content (19.5%) of the wheat bran hemicelluloses obtained (Figure 4.4) in this study was close to the lignin content (17.5%) obtained by Koegelenberg (2016) for hemicelluloses extraction from destarched wheat bran. Furthermore, due to the fact that wheat bran protein contains gliutins which are alkaline soluble (Arte et al., 2015), 26.6% of the wheat bran recovered hemicellulose was found to be made up of proteins. R. C. Sun et al. (2002) indicated that the presence of proteins in hemicellulose could help improve dough gas retention as well as thermal properties. The results obtained for the mild alkaline treated destarched wheat bran indicated that at the optimum conditions (68.28 °C, 2.71 wt. % NaOH) both hemicelluloses yield (36.98%) and purity (47.56%) were improved.

Table 4.6 Predicted and experimental values at optimised conditions for mild alkaline treated wheat bran for hemicellulose and ferulic acid extraction

Optimised Conditions MA WB (68.28 °C, 2.71 wt.% NaOH)			
	Hemicelluloses Purity, %	Actual Hemicelluloses Yield/Raw WB Hemicelluloses, %	Ferulic Acid, Yield, %
Predicted Values	47.78 ± 3.51	33.67 ± 7.27	64.32 ± 3.5
Experimental Values	47.56 ± 0.30	36.98 ± 1.18	65.63 ± 1.0

At the optimum mild alkaline treatment conditions, the yield of recovered lignin was 72.64% of the destarched wheat bran lignin with a purity of 59% (Figure 4.4). The main impurities that were present within the MAWB lignin were hemicelluloses, proteins, and ash with 16%, 16% and 7%, respectively (Figure 4.6). The presence of proteins (16%) within the lignin could be due to the fact that wheat bran proteins are made up of both alkaline soluble portions (glutelin) and ethanol soluble portions (gliadins) (Waga, 2004). The mild alkaline treatment could have resulted in the extraction of these proteins which could have been further deposited in the lignin during the ethanol precipitation and washing step of the hemicelluloses. It is interesting to note that due to the absence of a bleach treatment before the mild alkaline treatment of both wheat straw and wheat bran, a higher yield and purity of lignin was recovered than for the hemicelluloses extracted. The results indicated that the selectivity of the mild alkaline

treatment in the extraction of hemicelluloses with a high yield and purity was significantly reduced by the absence of a preliminary bleach treatment as well as a comprehensive purification step.

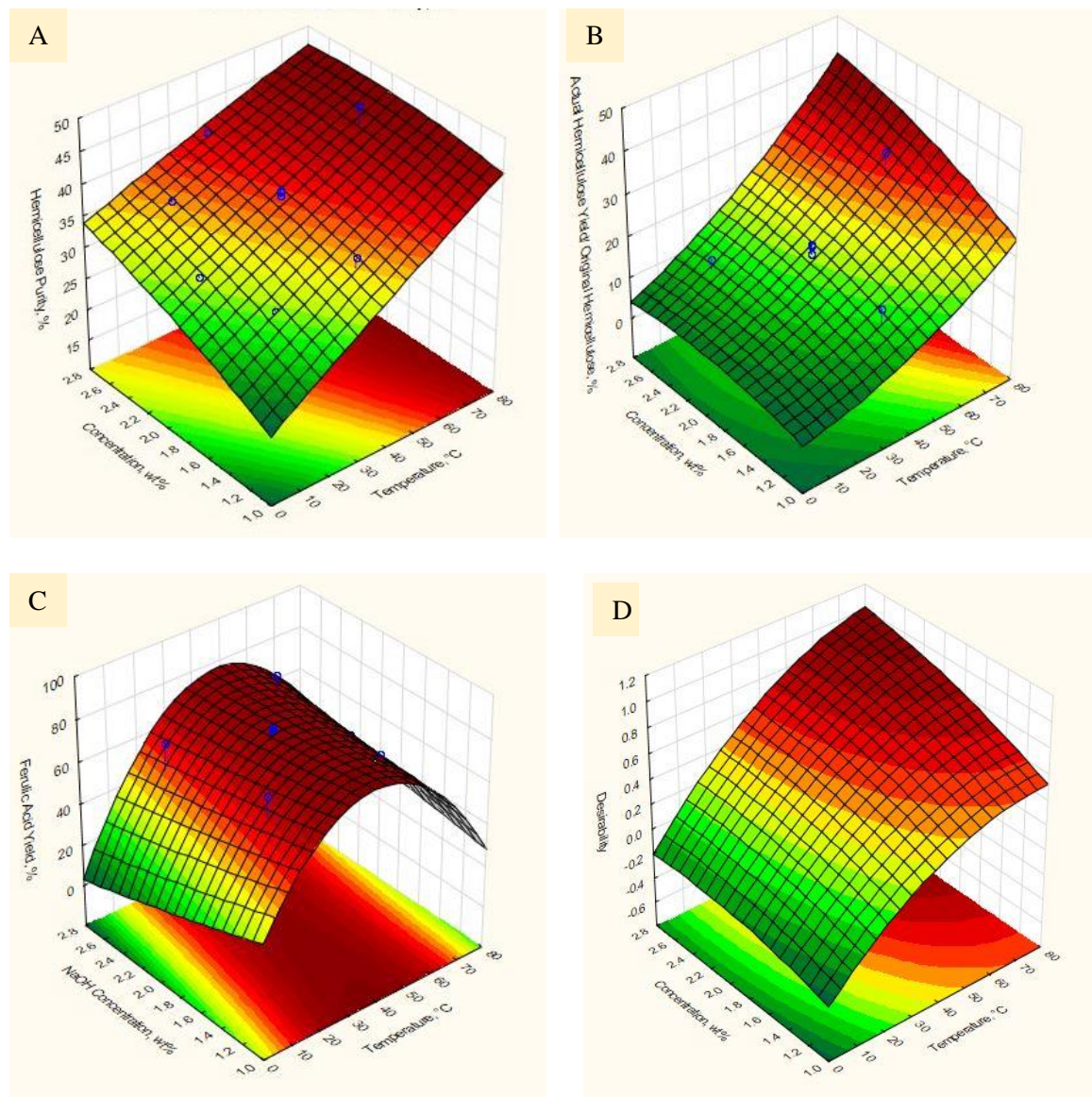


Figure 4.5 Surface plot of optimisation of wheat bran mild alkaline extracted A) Hemicelluloses purity B) Hemicelluloses yield/ original hemicelluloses C) Ferulic acid yield D) Desirability (68.28°C, 2.71 wt. % NaOH) with NaOH concentration and temperature as independent variables.

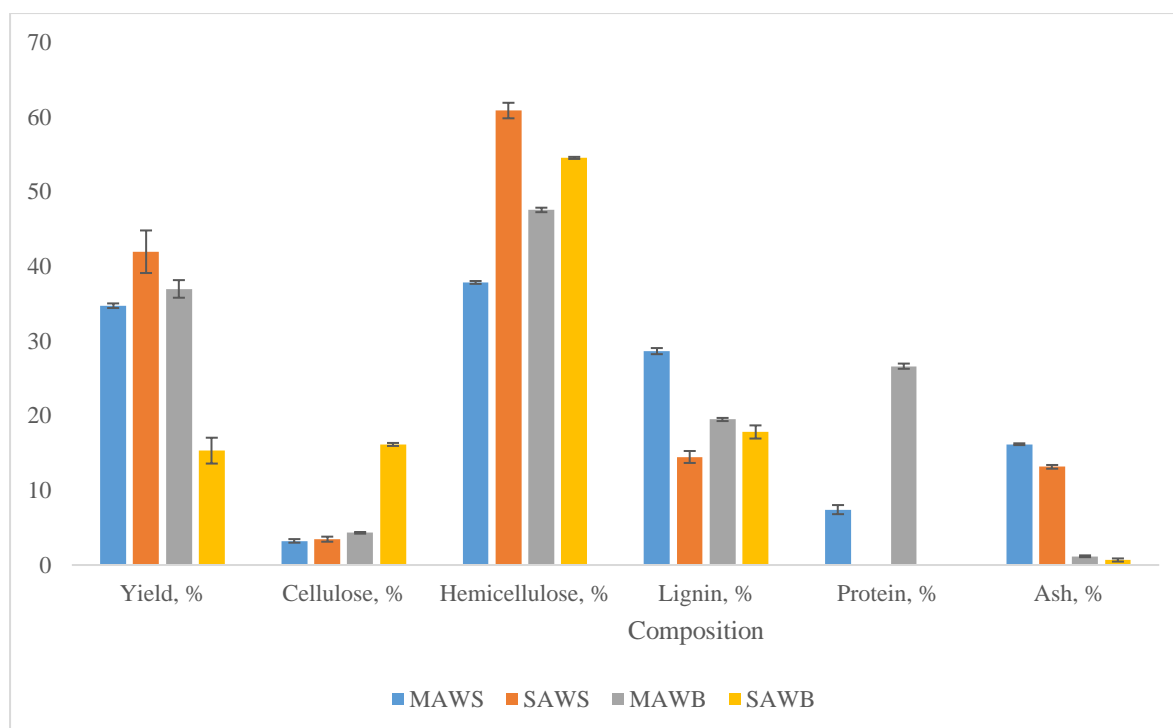


Figure 4.6 Yield and chemical composition of recovered hemicelluloses for mild alkaline wheat straw (MAWS), alkaline delignified wheat straw (SAWS), mild alkaline wheat bran (MAWB) and alkaline delignified wheat bran (SAWSB) at optimum conditions.

4.4.1.2 Fourier Transform Infrared Spectroscopy (FTIR) of Recovered Alkali Soluble Hemicelluloses and Lignin at the Optimum Alkaline Delignification Conditions

The FTIR spectra for both the MAWS Hemis and the MAWB Hemis was represented in Figure 4.7. Both MAWS Hemis and MAWB Hemis showed peaks at 3316, 2919, 985 cm^{-1} and 896 cm^{-1} that can be attributed to the presence of O-H stretching vibrations of hemicelluloses (Buranov and Mazza, 2010), C-H stretching of hemicelluloses (Farhat et al., 2017), C-O stretching of arabinose side chains of hemicelluloses (Sun et al., 2005) and β -glycosidic linkages of hemicelluloses (Sabiha-Hanim and Aziatul-Akma, 2016), respectively. The C-O-C stretch of the hydroxyl group of xylan peak (1034 cm^{-1}) for hemicelluloses and the aromatic ring peak (1595 cm^{-1}) of lignin were present for both MAWS Hemis and MAWB Hemis. However, MAWS Hemis showed a higher intensity for both the xylan (1034 cm^{-1}) and lignin (1595 cm^{-1}) peak than that for the MAWB Hemis which was consistent with the results from the compositional analysis. Finally the presence of proteins were noticed in the MAWB Hemis based on a peak at 1640 cm^{-1} , which has been found to be related to the C-N stretch of Amide I in protein (Warren et al., 2015). In addition, Hou et al. (2017) stated that during alkaline treatment there is a transformation of agricultural residue protein through denaturing which causes a shift of peaks from 1540 cm^{-1} to 1640 cm^{-1} when it forms an α -helix structure. It is likely the wheat bran protein experienced this peak shift since the peak for the protein (1540 cm^{-1}) of destarched wheat bran (Figure 4.16) was found to be absent from the mild alkaline treated wheat bran residues, however the protein peak (1640

cm^{-1}) was found to be present in MAWB Hemis. In summary, the FTIR results agreed with the compositional analysis results obtained.

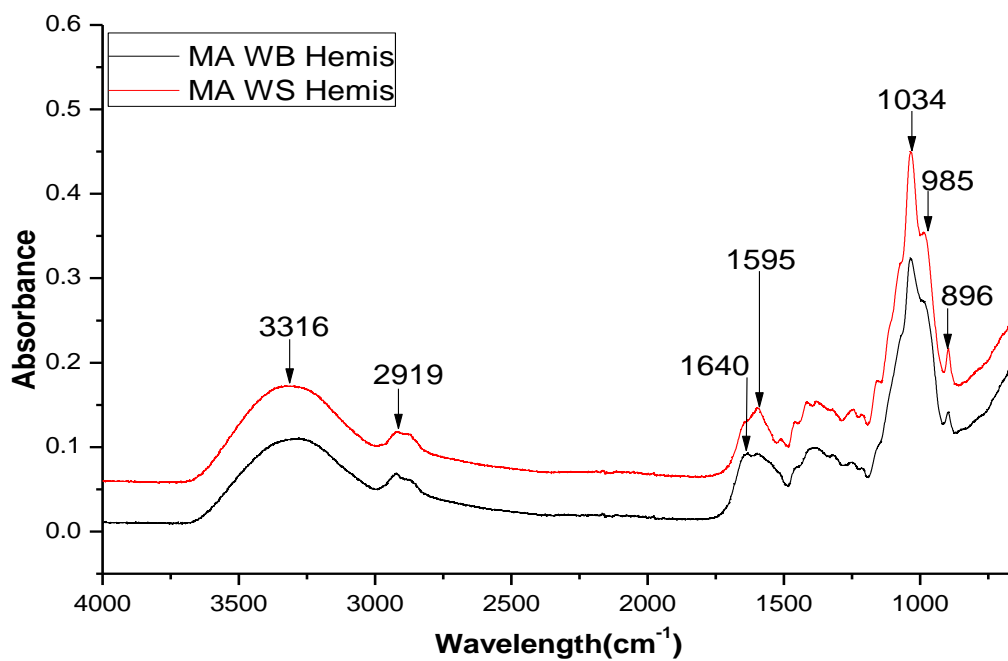


Figure 4.7 FTIR spectra of functional group changes of mild alkaline wheat straw extracted hemicelluloses (MA WS Hemis) and mild alkaline wheat bran hemicelluloses (MA WB Hemis)

The FTIR spectra for both MAWB lignin and MAWS lignin was shown in Figure 4.8. Similar peaks at 3258, 2918 and 1034 cm^{-1} which indicated the presence O–H, C–H₂ and C–O stretch in the both lignin extracts. The presence of peaks at 897 cm^{-1} within both MAWB lignin and MAWS lignin indicated the presence of sugar units of hemicelluloses within the lignin extracts. The presence of these peaks agreed with the result obtained from its quantitative analysis. Similar, to MAWB Hemis, the peak at 1648 cm^{-1} can be attributed to C–N stretch of Amide I in protein of wheat bran lignin (Warren et al., 2015). MAWS lignin and MAWB lignin were noticed to possess prominent peaks at 1593, 1516 and 1251 cm^{-1} which indicated the high presence of lignin in them. Furthermore, peaks for syringyl units, guaiacyl units and p- hydroxyphenyl units where noticed at 1327-1330 cm^{-1} , 1259-1271 cm^{-1} and 834-837 cm^{-1} for both MAWS lignin and MAWB lignin (Lisperguer et al., 2009; R. Sun et al., 2000; Yang et al., 2016). However, for MAWB lignin the peak intensities increased in the order guaiacyl units>syringyl units> p-hydroxyphenyl units whereas in MAWS lignin the peak intensities were in the order syringyl units >guaiacyl units> p-hydroxyphenyl units. The FTIR spectra indicated that MAWB lignin was made up of more guaiacyl units than syringyl units whereas the opposite was true for the MAWS lignin

(Lourenço and Pereira, 2018). In general, the FTIR results agreed with the compositional analysis performed on both MAWS lignin and MAWB lignin.

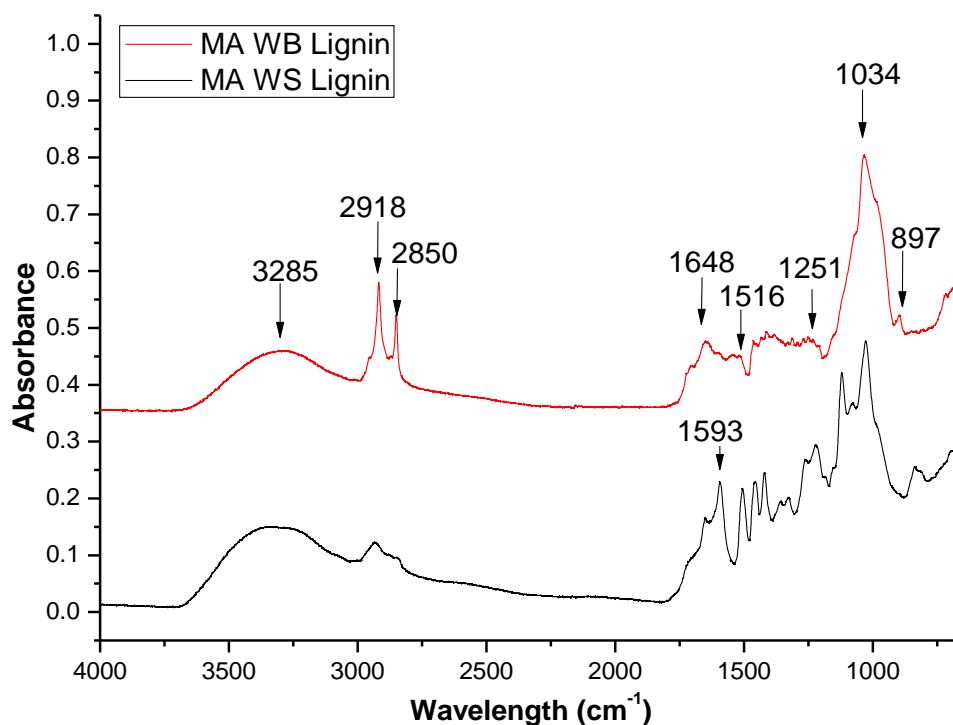


Figure 4.8 FTIR spectra of functional group changes of mild alkaline wheat straw extracted lignin (MAWS Lignin) and mild alkaline wheat bran lignin (MAWB Lignin).

4.4.1.3 Thermal Stability of Recovered Alkali Soluble Hemicelluloses and Lignin at the Optimum Mild Alkaline Conditions

The thermal stability of MAWS Hemis and MAWB Hemis were represented in Figure 4.9. The thermogram of the hemicelluloses indicated a two-step weight change for both MAWS Hemis and MAWB Hemis (Figure 4.9). The first step occurred between temperature ranges of 25–110°C for both MAWS Hemis and MAWB Hemis. This weight loss can be attributed to loss of water within the hemicellulose samples. The results obtained by analysing the MAWS Hemis and MAWB Hemis indicated that the loss of water or moisture from both were close (10% and 9%, respectively). It could therefore be said that there is not much difference between the ability of both the MAWS Hemis and the MAWB Hemis to absorb moisture from the atmosphere.

The second weight loss step, had thermal decomposition temperature range for both hemicelluloses between 205–380°C (Figure 4.9) which was found to be similar to the temperature decomposition ranges (200–380°C) cited by Werner et al. (2014) when determining the thermal characteristics of various hemicellulose samples. Furthermore, both the onset and maximum decomposition temperature (T_{onset} and T_{max} , respectively) for MAWS Hemis was about 22°C less than that of the MAWB Hemis (Figure

4.9). Werner et al. (2014) indicated that hemicelluloses with a more branched structure had higher thermal decomposition temperatures in comparison to hemicelluloses with a linear structure which could have been a result for MAWB Hemis having higher T_{onset} and T_{max} values in comparison to MAWS Hemis. The T_{onset} and T_{max} values obtained indicated that mild alkaline treated destarched wheat bran hemicelluloses had higher thermal properties than wheat straw hemicelluloses. Moreover, the higher char content of MAWS Hemis (26%) in comparison to MAWB Hemis (15%) could be attributed to the higher lignin content of MAWS Hemis (28.7%) in comparison to the lignin content of the MAWB Hemis (19.5%) (Jiang et al., 2014). The results indicated that although mild alkaline treatment resulted in hemicelluloses with 19.5-28.7% of lignin, the thermal properties of the lignin were still comparable to results obtained by other researchers such as Jiang et al. (2014). It can therefore be concluded that with a 10-29% lignin content in alkaline recovered hemicelluloses, the thermal decomposition temperatures of hemicelluloses falls within 200-400⁰C. The compositional analysis and thermal properties of the hemicelluloses obtained indicated potential for application in hydrogels and papermaking industries (Farhat et al., 2017; Matavire, 2018).

MAWS lignin and MAWB lignin underwent a three-step weight loss which was indicative by their broader thermal decomposition range (Figure 4.10) in comparison to the hemicelluloses (Figure 4.10). The first weight loss was attributed to moisture loss which occurred at 40-100⁰C. The moisture loss was 7% and 5% for MAWS lignin and MAWB lignin, respectively. The results indicated that there was a slight difference between the ability of both MAWS lignin and MAWB lignin to absorb moisture from the atmosphere. The second weight loss began at T_{onset} which occurred at 171⁰C and 147⁰C for MAWS lignin and MAWB lignin, respectively. T_{onset} was mainly attributed to the decomposition of hemicellulose. This indicated a faster oxidisation of the lignin as compared to that of hemicelluloses resulting in a T_{max} of 276⁰C and 295⁰C for MAWB lignin and MAWS lignin, respectively (Mao et al., 2012). The difference in the T_{onset} and T_{max} values of MAWS lignin and MAWB lignin could be attributed to the larger hemicelluloses content of MAWB lignin (15.8%) than that of MAWS lignin (4.9%) (Wild et al., 2012). Moreover, the higher lignin content of MAWS lignin (84.4%) resulted in a higher T_{comp} (448⁰C) in comparison with the 338⁰C obtained by MAWB lignin with a lower lignin content (58.9%). The thermogram for both the MAWB lignin and MAWS lignin can be seen to level off at a relatively higher weight percentages in comparison to the corresponding hemicelluloses (Figure 4.9). This resulted in char at 600⁰C been almost double that obtained for MAWS and MAWB hemicelluloses. The char obtained for MAWS and MAWB lignin are 49% and 29%, respectively which were similar to lignin char obtained by other researchers (Watkins et al., 2015; Wild et al., 2012). Based on the lignin composition and thermal decomposition temperature obtained for both MAWS lignin and MAWB lignin, it indicated their potential application in polymer composite materials (Li and Mcdonald, 2014)

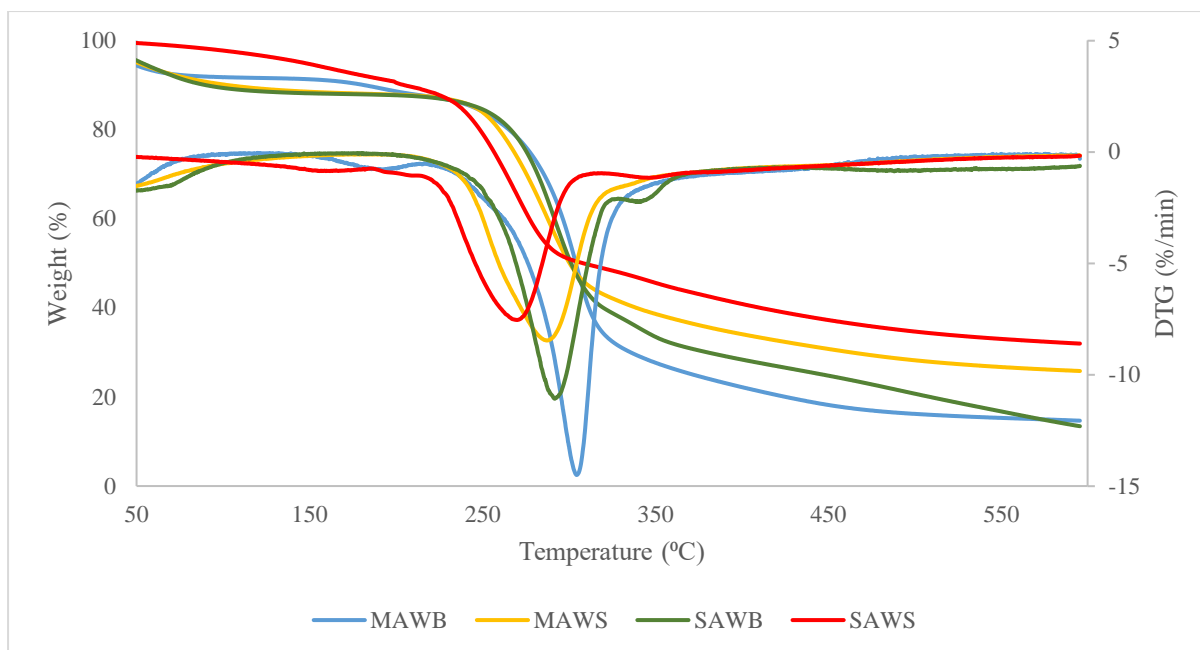


Figure 4.9 Thermal stability of mild alkaline wheat bran hemicelluloses (MAWB); mild alkaline wheat straw hemicelluloses (MAWS); alkaline delignified wheat bran hemicelluloses (SAWB); alkaline delignified wheat straw hemicelluloses (SAWS)

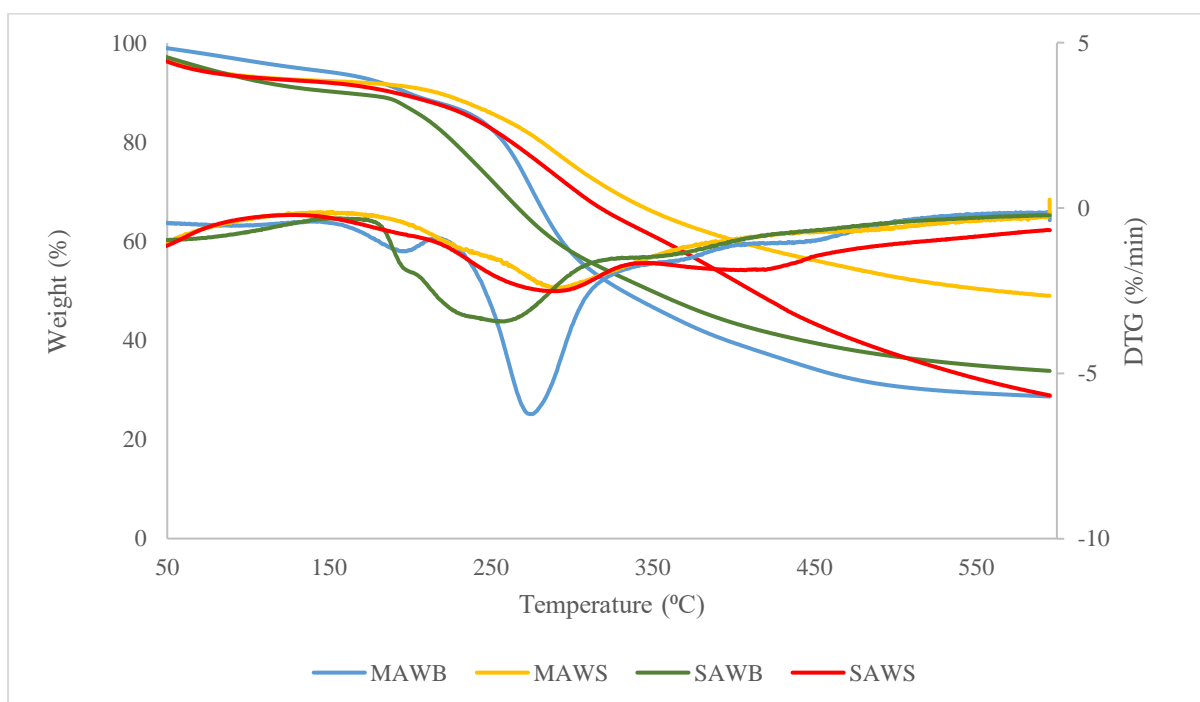


Figure 4.10 Thermal stability of mild alkaline wheat straw extracted lignin (MAWS); mild alkaline wheat bran extracted lignin (MAWB); alkaline delignified wheat straw extracted lignin (SAWS); alkaline delignified wheat bran extracted lignin (SAWB)

4.4.2 Mild Alkaline Extraction of *p*-coumaric Acid (from Wheat Straw) and Ferulic Acid (from Wheat Bran)

Alkaline hydrolysis of both wheat straw and bran resulted in the release of ferulic and *p*-Coumaric acid (Figure 3.1). Ferulic and *p*-coumaric acid occurred by breaking the ester bonds in the lignin-carbohydrate complexes (K. Liu et al., 2016). From Figure 4.3 and 4.4 that, the NaOH treatment performed on both the wheat straw and wheat bran resulted in the release of considerable amount of *p*-coumaric acid and ferulic acid, respectively. The results obtained from the mild alkaline treatment indicated that at temperatures above ambient temperatures there was a release of more than half of the phenolics available in both the wheat straw and bran (Buranov and Mazza, 2008).

4.4.2.1 Yield of Alkali Soluble *p*-Coumaric and Ferulic Acid

The surface plot for wheat straw extracted *p*-coumaric acid (Figure 4.3c), indicated that temperature has a larger significant effect on the yield of *p*-coumaric acid extracted from the wheat straw than the NaOH concentration. Nevertheless, a combination of both factors causing an increase in severity of the treatment conditions resulted in an increase in the yield of *p*-coumaric acid. However, an increase in NaOH concentration above 2 wt.% resulted in the reduction of the yield of *p*-coumaric acid from the wheat straw (Figure 4.3c) (Sun et al., 1995). At the optimum condition, the yield obtained for the *p*-coumaric acid was 85% with a 45% antioxidant activity obtained by using 2, 2-diphenyl-1-picrylhydrazyl (DPPH) as a control.

On the other hand, the yield of ferulic acid (Figure 4.4c) was the best at mid temperature treatment conditions (40⁰C) (Figure 4.4c). The initial high yield of ferulic acid can be attributed to the free ferulic acid present within the wheat bran that were readily released with the alkaline treatment. The reduction in the ferulic acid content as the severity of the treatment increased could be attributed to the release of other hydroxycinnamic compounds such as vanillin which could be produced from ferulic acid conversion (Buranov and Mazza, 2009). The results obtained indicated that higher alkaline extraction conditions did not favour the higher yield of ferulic acid extracted from wheat bran due to the release of bound ferulic acid content. Similar results were observed by Hasyierah et al. (2011). Finally, at the optimum condition, the yield of ferulic acid recorded was 66% with an antioxidant activity of 15%. The antioxidant activity was similar to the antioxidant activity (15%) obtained by Phongthai et al. (2016) for rice bran phenolics. Furthermore Phongthai et al. (2016) stated that such DPPH antioxidant activity promotes foaming abilities and applications in emulsions.

4.4.2.2 *p*-Coumaric Acid and Ferulic Acid Composition

Alkaline treatment results in the extraction of both *p*-coumaric acid and ferulic acid in wheat straw and wheat bran, which are bound to the lignin-carbohydrate complex. However, due to the nature of wheat straw and wheat bran, they contain varying amounts of these phenolic. Since both *p*-coumaric and ferulic acid are present within wheat straw and wheat bran, the treatment results in the release of both phenolic acids, which are both further soluble in 30% and above ethanol concentration as used in this

work. Wheat straw extracted *p*-coumaric acid had a purity of between 56–67% with the main contaminant being ferulic acid, which made up between 20–36% of the total extracted phenolics. Whereas, wheat bran extracted wheat bran extracted ferulic acid had a purity between 89–95% with the main impurity being *p*-coumaric acid, which made up between 3–5% of the total extracted phenolics. At the optimum condition for wheat straw extraction, the *p*-coumaric acid extracted had a purity of 64% with a ferulic acid contamination of 29% where at the optimum value for wheat bran extraction, the ferulic acid purity was 95% with a 2% *p*-coumaric acid contamination. The high contamination of *p*-coumaric acid in wheat straw is mainly due to the high amount of ferulic acid present within the wheat straw as compared to the *p*-coumaric acid present within the wheat bran.

4.5 Alkaline Delignification Treatment of Mild Alkaline Treated Residues for Lignin Extraction and Production of Cellulose-Rich Pulp

Although, alkaline treatment is known to affect the lignin and hemicelluloses portions of the cell wall of agricultural residues, alkaline treatments as stated in section 2.2.2.1 can also affect the cellulose content. Alkaline delignification treatment (Figure 3.1) performed at 8–12 wt.% NaOH concentration and 6–10 wt.% NaOH concentration for wheat straw and bran, respectively for 30–90 mins at 121°C in an autoclave indicated its effectiveness in improving the cellulose content of the residues obtained while reducing the lignin content of the cellulose-rich pulp obtained (Figure 4.11 and 4.12). As the preceding treatment to the nanocellulose treatment step, it was necessary to take the cellulose and lignin content of the residue into consideration, therefore it was made the primary factor to be considered in this treatment step.

The alkaline delignification treatment performed on wheat straw indicated that selected NaOH concentration range (8-12 wt.%) was significant in both the linear and quadratic terms whereas time was only significant in the quadratic term for both cellulose and lignin content of the residue (Figure 4.13a and b). Furthermore, an R-squared value of 0.88 and 0.93 were obtained at a 95% confidence level indicating a good correlation between the predictive model and the experiment performed for both residue cellulose and lignin content, respectively. The result was in agreement with the claim made by Silverstein et al. (2007) that in alkaline delignification, the NaOH concentration had the most significant effect on the cellulose content of the residue whereas at NaOH concentrations greater than 4wt.% time had the most significant effect on the amount of lignin removed. As the treatment conditions increased, it resulted in the reduction of both the lignin and hemicelluloses content thereby contributing to an increase in the cellulose content of the residues after treatment (Figure 4.11). However, the reduction of cellulose content after the optimum treatment conditions (10 wt.% NaOH and 60 min) was a result of cellulose degradation (Figure 4.11a). Modenbach (2013) stated that this effect was because of breaking of the intermolecular hydrogen bonds of cellulose which results in alteration of their chain conformations producing more amorphous regions which are further degraded as the treatment continues.

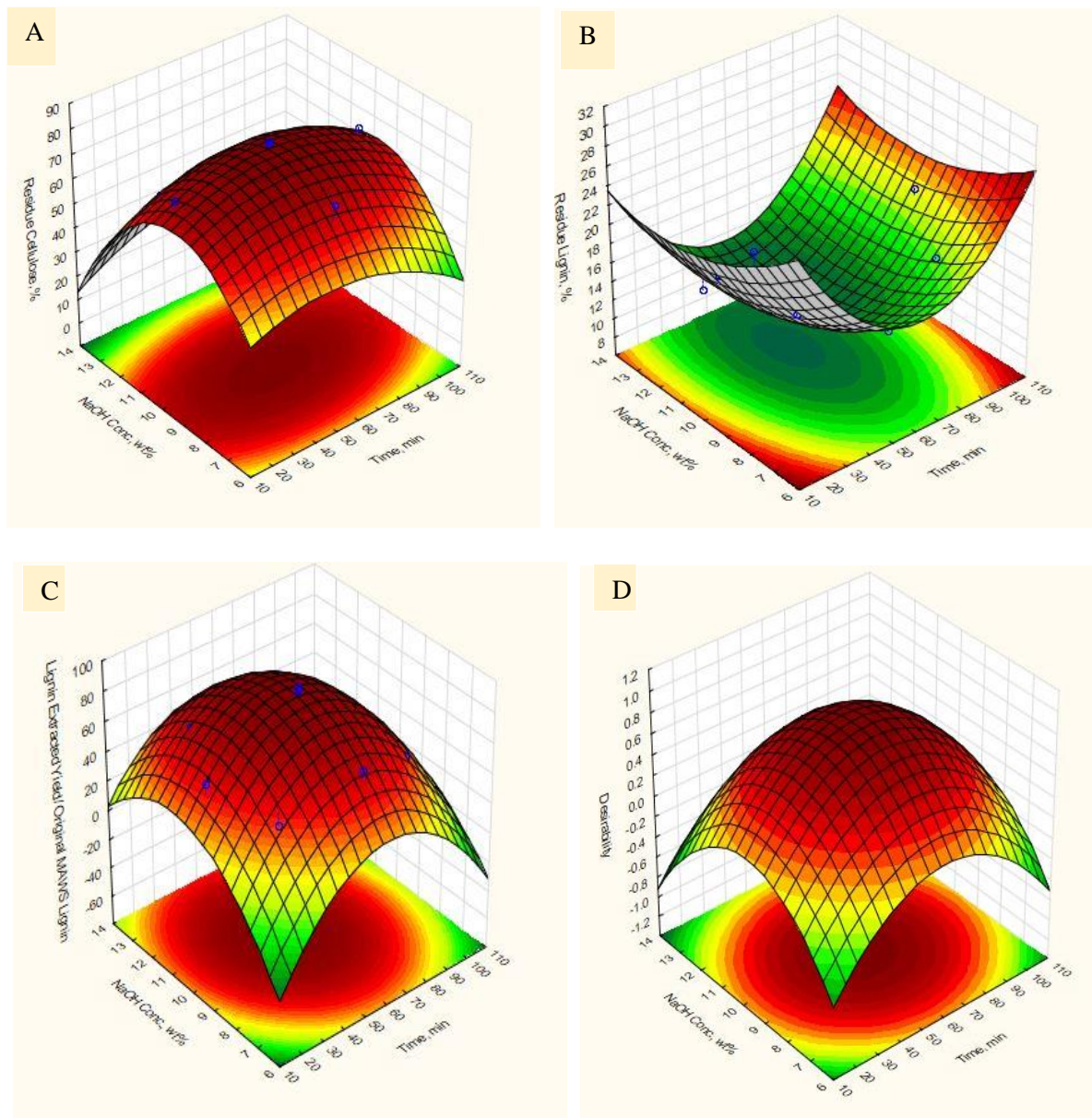


Figure 4.11 Surface plot of optimisation of alkaline delignified (SA) wheat straw A) Cellulose content in residue after SA treatment B) Lignin content in residue after SA treatment C) Extracted lignin yield/ lignin in mild alkaline wheat straw (MAWS) residue D) Desirability (10 wt.% NaOH, 60 min) with NaOH concentration and time as independent variables

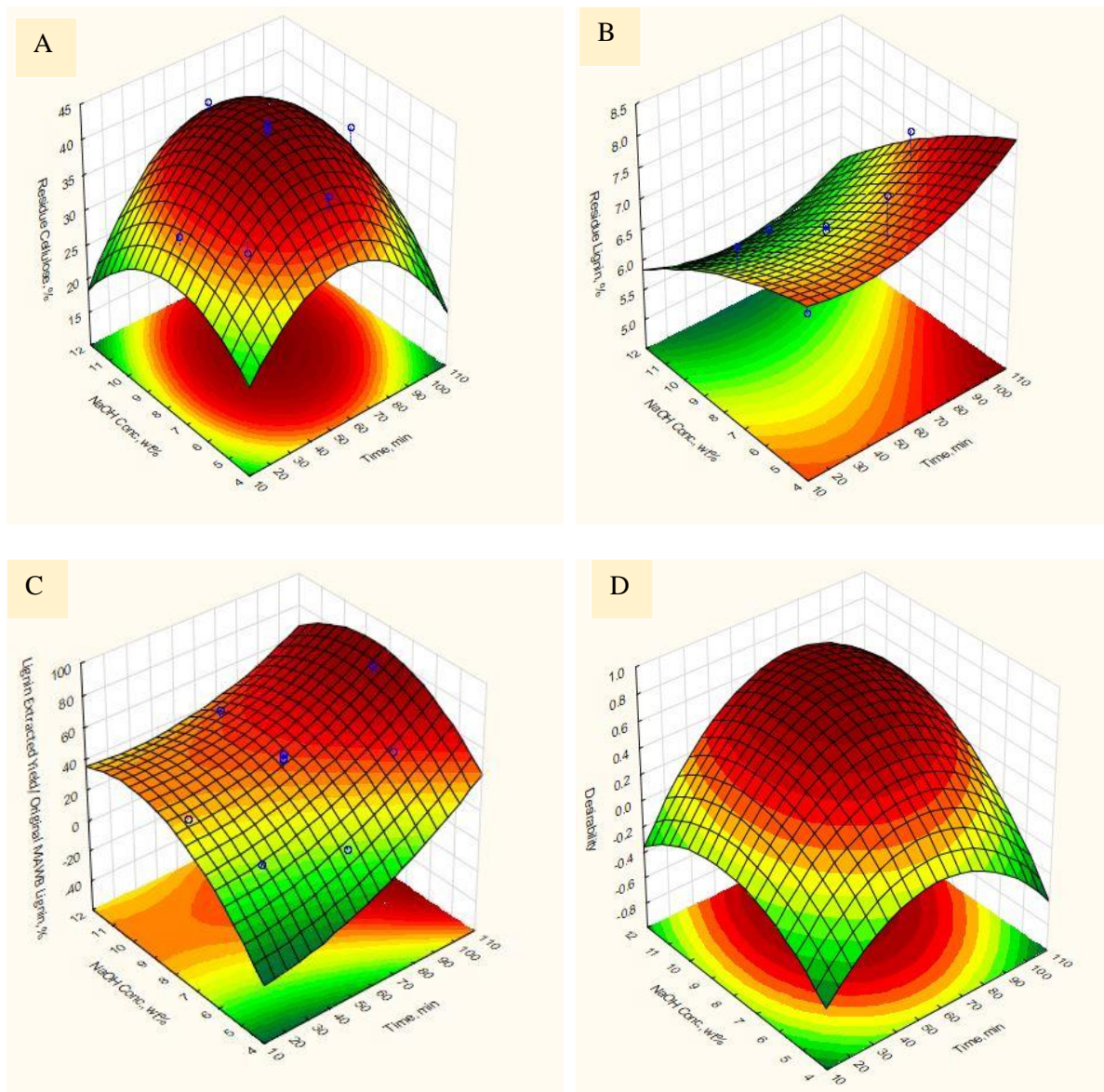


Figure 4.12 Surface plot of optimisation of alkaline delignified (SA) wheat bran A) Cellulose content in residue after SA treatment B) Lignin content in residue after SA treatment C) Extracted lignin yield/ lignin in mild alkaline treated wheat bran (MAWB) residue D) Desirability(9.41 wt.% NaOH, 81.2 min) with NaOH concentration and time as independent variables

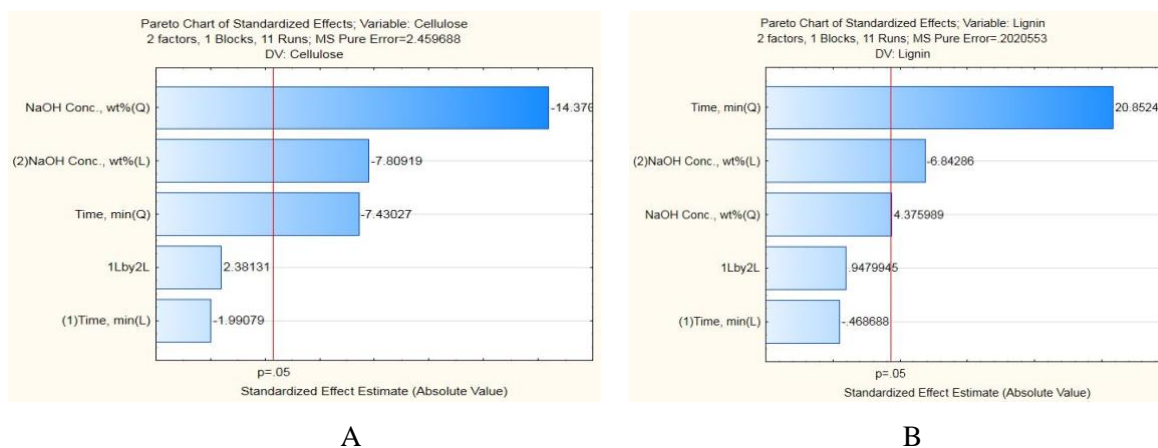


Figure 4.13 Pareto Charts A) Cellulose in residue B) Lignin in residue after alkaline delignification of mild alkaline treated wheat straw

The increase in the lignin content after the optimum treatment conditions was attributed to recondensation of lignin when treated at very severe conditions (Figure 4.11b). The effect occurs at very severe conditions when lignin broken from the cell wall of the wheat straw joined back together to form insoluble lignin fragments (Lee et al., 2014). The hemicelluloses content of the wheat straw reduced with an increase in NaOH concentration indicating that the hemicelluloses present within the straw became easier to remove at higher alkaline concentration (10-12wt.%) resulting in depletion as process conditions became more severe. From the results obtained from the desirability profile it showed that the optimum conditions needed to obtain a high cellulose content whereas having a low lignin content in the wheat straw residues can be obtained at a treatment condition of 10 wt. % NaOH concentration for 60 mins in an autoclave at 121°C (Figure 4.11d). The experimental values obtained for the treated wheat straw residues indicated that the results were within the range of the predicted values (Table 4.7) from the desirability profile for the cellulose content and a lignin content of the wheat straw residues. It can be summarised that the two-stage alkaline treatment on the wheat straw resulted in a cellulose-rich pulp that meets the criteria stated in Section 4.1 (cellulose content $\geq 62\%$, crystallinity index $\geq 48\%$, hemicelluloses content $\leq 23\%$ and lignin content $\leq 10\%$) such that it can be directly applied in nanocellulose production.

Table 4.7 Predicted and experimental values from optimised conditions for alkaline delignification treatment of wheat straw for production of cellulose-rich pulp and lignin extraction

Optimised Conditions Alkaline Delignified Wheat Straw (60 min, 10 wt.% NaOH)			
	Residue Cellulose, %	Residue Lignin, %	Lignin Extracted Yield/ Original MA WS Lignin, %
Predicted Values	77.46 ± 3.71	4.95 ± 1.12	62.78 ± 3.04
Experimental Values	76.25 ± 0.66	5.17 ± 0.16	60.12 ± 1.09

Unlike wheat straw, the factors considered for wheat bran (6-10 wt.% NaOH concentration and 30-90 min) were both significant in the quadratic terms for the residue cellulose content with an R-squared value of 0.80 at a 95% confidence level indicating a good prediction of the model by the experiment (Figure 4.14a). The Pareto charts indicated that for the wheat bran the NaOH concentration was high enough (6-10 wt. %) that increase in the NaOH concentration had a lesser effect on the residue cellulose content. On the other hand, due to the high NaOH concentration (6-10 wt.%), the reaction time began having a more significant effect on the cellulose content which was in agreement with the assertion made by Silverstein et al. (2007) for NaOH concentrations greater than 4wt.%. The cellulose content of the wheat bran residue was noticed to increase from an initial value (after mild alkaline treatment) of about 36% to 48% after the alkaline delignification treatment (Table 4.8). The results obtained indicated that the treatment was unable to increase the cellulose content of the wheat bran to a level ($\geq 62\%$) at which it could be applied in nanocellulose production. Whereas, after the optimum treatment conditions (81.2 min, 9.41 wt.% NaOH), the cellulose within the wheat bran began degrading resulting in the reduction of the cellulose content (Figure 4.12a).

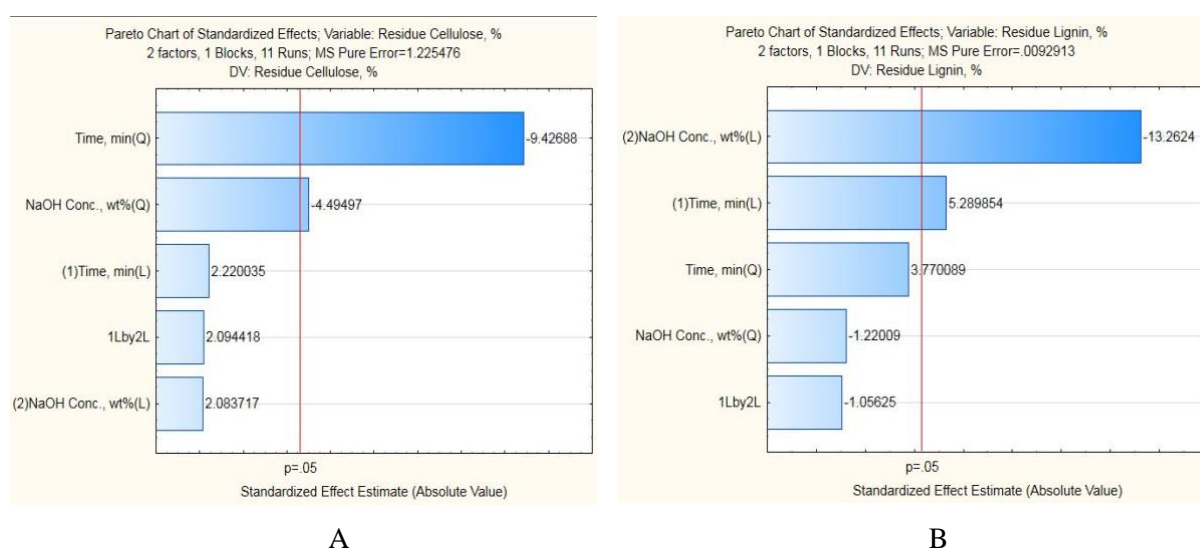


Figure 4.14 Pareto Charts A) Cellulose in residue B) Lignin in residue after alkaline delignification of mild alkaline treated wheat bran

Table 4.8 Predicted and experimental values from optimised conditions for alkaline delignification treatment of wheat bran for production of cellulose-rich pulp and lignin extraction

Optimised Conditions SA WB (81.2 min, 9.41 wt% NaOH)			
	Residue Cellulose, %	Residue Lignin, %	Lignin Extracted Yield/ Original MA WB Lignin, %
Predicted Values	47.10 ± 2.26	6.47 ± 0.23	62.35 ± 4.25
Experimental Values	48.10 ± 0.04	6.29 ± 0.86	61.51 ± 3.28

The lignin content of the alkaline delignified wheat bran indicated that as the treatment conditions became more severe the lignin content of the treated wheat bran residues experienced continuous reduction (Figure 4.12b). At the optimum condition (81.2 min, 9.41 wt.% NaOH), there was a significant reduction in the lignin content and then a slight reduction of the cellulose content due to the production of more degradation products. However, after the optimum condition the wheat bran residue lignin content experienced a slight increase which can be attributed to lignin re-condensation as stated earlier (Figure 4.12b). It can be concluded from the results after the two-stage alkaline treatment that focusing wheat bran treatment on optimisation for the extraction of only lignin, ferulic acid and hemicelluloses will be more favourable for the wheat bran. Furthermore, both the initial (10%) and final wheat bran celluloses (48%) contents, crystallinity (which will be discussed in Section 4.6.2) and hemicelluloses content (31%) indicated that the two-stage alkaline treated wheat bran will require further treatment to be applied in nanocellulose production.

4.5.1 Extraction of Recovered Alkali Soluble Hemicelluloses and Lignin at the Optimum Alkaline Delignification Conditions

4.5.1.1 Yield and Composition of Recovered Alkali Soluble Hemicelluloses and Lignin at the Optimum Alkaline Delignification Conditions

The alkaline delignification performed on the mild alkaline residues of wheat straw and wheat bran also resulted in the extraction of hemicelluloses (Figure 3.1). The yield of hemicellulose extracted at the optimum alkaline delignification conditions with respect to the original hemicelluloses present within the untreated wheat straw was 41.96% (Figure 4.6). The increase in hemicelluloses yield at the optimum alkaline delignification treatment condition of the wheat straw in comparison to the yield of hemicellulose extracted at the optimum of the mild alkaline treatment (37.85%) can be attributed to both the treatment conditions and the partial release of the cell wall structure during the mild alkaline treatment step. The partial loosening of the cell wall matrix after the mild alkaline treatment was evident in the SEM images (discussed in section 4.6.3), which could have resulted in improvement in the hemicellulose extraction (Rosa et al., 2012).

The improvement in the hemicellulose extraction translated to hemicelluloses with a purity of 60.87% (Figure 4.6). However, the alkaline delignified wheat straw hemicelluloses purity indicated the presence of other cell wall components such as lignin, ash, and cellulose, which made up 14.47%, 13.15% and 3.46%, respectively (Figure 4.6). The lignin content of the hemicelluloses could be due to ineffective separation of the lignin during the hemicelluloses precipitation step with ethanol (Section 3.2.4) resulting in the dissolving of both the polymeric hemicellulose and macromolecules of lignin (H. Li et al., 2015). Whereas, the ash content could have been as a result of the initial ash present within the MAWS which was found to reduce in Section 4.6 after the delignification treatment as well as the salt from the neutralization process (K. Liu et al., 2016). The presence of the cellulose in the hemicellulose could have been as a result of the treatment conditions, which is usual with most alkaline delignification treatments (Zheng et al., 2018). The results obtained for the alkaline delignification of the wheat straw indicated that the treatment was favourable for the extraction of hemicelluloses, lignin, and cellulose-rich wheat straw for nanocellulose production.

At the optimum alkaline delignification conditions for wheat straw, 60.12% (Table 4.7) of the lignin present within the MAWS residue was extracted which translated to 22.74% of the lignin present within the untreated wheat straw (Figure 4.4). The yield of the lignin extracted (60.12%) at the alkaline delignification step was within the range of 30-89% of the feedstock indicated by most researchers (Xu et al., 2011; Zheng et al., 2018). Also, the lignin extracted had a purity of 74.7% with ash making up most of the impurities (13.16%) and hemicelluloses making up 7.56% (Figure 4.4). The high presence of ash in the alkaline delignified wheat straw lignin (SAWS lignin) can be mainly attributed to the presence of salts within the extract after neutralising the alkaline solution (K. Liu et al., 2016). Furthermore, the minimal quantity of lignin in the alkaline delignified wheat straw residues (5.17%), indicates that the treatment achieved its aim of extracting lignin while reducing the lignin content of the resulting cellulose-rich pulp for nanocellulose production.

The yield of the hemicelluloses extracted after the alkaline delignification with respect to the hemicellulose in the destarched wheat bran was 15.32% (Figure 4.6). The hemicellulose yield obtained indicated that the treatment conditions used for the alkaline delignification were unfavourable for the extraction of hemicelluloses within the wheat bran as they were for the lignin. Xu et al. (2011) stated at higher alkaline loadings (≥ 3 wt.%), although alkaline delignification treatment could result in significant lignin removal, there is the likelihood of higher solid loss at the conditions which can result in extracting lower amounts of polymeric hemicelluloses. In this study, it was noticed that the optimum alkaline delignification conditions (81.2 min, 9.41 wt.% NaOH) resulted in a 17% loss of the mild alkaline treated wheat bran which could have explained the low hemicellulose yield. The results indicated that the optimum alkaline delignification conditions were too severe for the extraction of the hemicelluloses in the destarched wheat bran.

The effects of the optimum treatment condition for the delignified wheat bran was further seen in the purity of the extracted hemicelluloses. The purity of the delignified wheat bran hemicelluloses was 54.53% with cellulose, lignin, and ash contents of 16.15%, 17.82% and 0.67% (Figure 4.6). Furthermore, it was found that the hemicelluloses extracted was mainly made up of xylose (48.96%) whereas the arabinose made up 13.01%, which was unexpected for wheat bran hemicelluloses indicating a significant loss of hemicelluloses. In addition, the high cellulose content (16.15%) in the extracted hemicelluloses from the alkaline delignified treatment further attests to the fact that the optimum treatment conditions were severe to cause the significant loss of solids and carbohydrates from the wheat bran. The presence of lignin within the hemicellulose extract was due to the same reason as that in the hemicelluloses of the alkaline delignified wheat straw. In summary, the alkaline delignification treatment of the wheat bran was an effective means of extracting lignin from the wheat bran. Furthermore, the alkaline delignification treatment was not an effective means of obtaining a cellulose-rich wheat bran residue as well as extracting hemicelluloses.

At the optimum treatment condition for the alkaline delignification of wheat bran, a yield of 61.51% of the lignin in the mild alkaline treated wheat bran was extracted (Table 4.8) which translated to 21.29% of the lignin present within the destarched wheat bran (Figure 4.4). The lignin extracted (61.51%) was similarly within the range stated by researchers for alkaline delignification treatments (Xu et al., 2011; Zheng et al., 2018). Furthermore, the purity of the alkaline delignified wheat bran lignin (SAWB lignin) was 69.2% (Figure 4.4). In addition, the effects of the treatment conditions on the hemicelluloses and celluloses of the mild alkaline treated wheat bran residues at the optimum delignification conditions were observed again with 12.33% hemicelluloses and 4.43% celluloses in the SAWB lignin (Figure 4.4). The hemicelluloses and celluloses present within the SAWB lignin could have been due to the delignification treatment conditions resulting in monomeric sugars which were deposited in the SAWB lignin during fractionation which likely occurred in this study (McIntosh and Vancov, 2011). The results obtained for the delignification treatment of the wheat bran indicated that the delignification treatment conditions were unsuitable for the carbohydrates (cellulose and hemicelluloses) in the destarched wheat bran.

4.5.1.2 Fourier Transform Infrared Spectroscopy (FTIR) of Recovered Alkali Soluble Hemicelluloses and Lignin at the Optimum Alkaline Delignification Conditions

The FTIR spectra for the extracted hemicelluloses from the alkaline delignification treatment at the optimum conditions was shown in Figure 4.16. Spectra of both alkaline delignified wheat bran hemicelluloses (SAWB Hemis) and alkaline delignified wheat straw hemicelluloses (SAWS Hemis) possessed a peak at 1640 cm^{-1} which indicated the presence of absorbed water in the extracted hemicelluloses (R. C. Sun et al., 2000). Whereas, the presence of lignin within the extracted hemicelluloses was noticed by the presence of a peak at 1278 cm^{-1} (Xiao et al., 2001). Both SAWB Hemis and SAWS Hemis possessed spectra peaks at 3333 cm^{-1} and 2901 cm^{-1} which indicated bands

for OH and CH₂ stretching (Yuan et al., 2010). However, due to the large amount of glucose in the SAWB Hemis, it presented a more prominent peak at 3333 cm⁻¹ than that of SAWS Hemis. The presence of xylan within both hemicelluloses was noticed by the presence of a peak at 1031 cm⁻¹ (Buranov and Mazza, 2010). Furthermore, the peak for SAWB Hemis xylan was very prominent which is in support of the result obtained from the compositional analysis of the SAWB Hemis indicating structural changes to the SAWB Hemis (Zheng et al., 2018). In conclusion, the FTIR spectra obtained for SAWS Hemis and SAWB Hemis agreed with the compositional analysis results obtained.

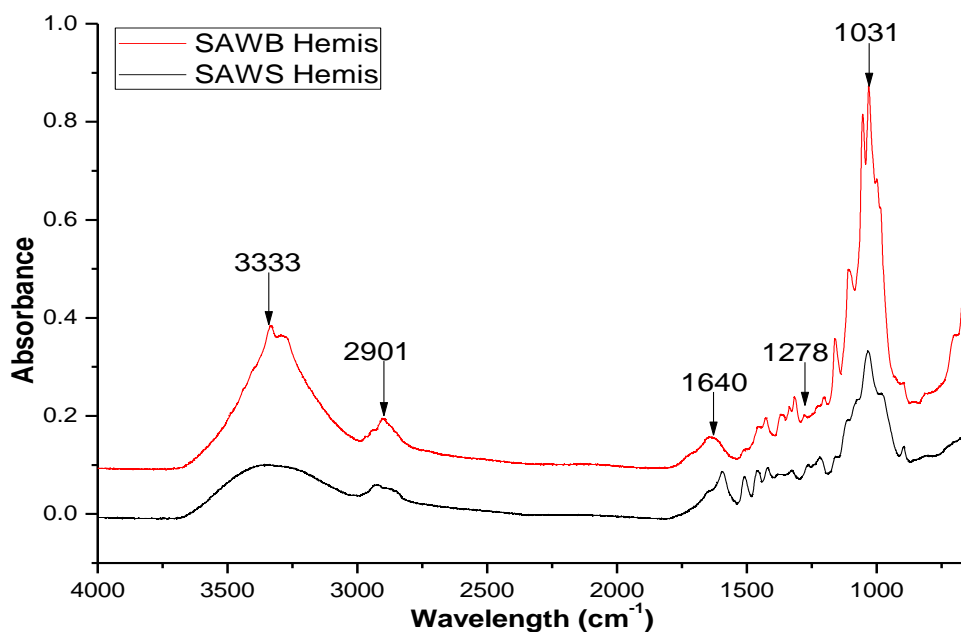


Figure 4.15 FTIR spectra of functional group changes of alkaline delignified wheat straw extracted hemicelluloses (SAWS Hemis) and alkaline delignified wheat bran hemicelluloses (SAWB Hemis)

The FTIR spectra for both alkaline delignified wheat straw lignin (SAWS lignin) and the alkaline delignified wheat bran lignin (SAWB lignin) was depicted in Figure 4.17. Both SAWS lignin and SAWB lignin possess the characteristic peak at 3200 cm⁻¹ and 2922 cm⁻¹, which can be attributed to O-H and C-H₂ stretching, respectively. Whereas, peaks at 1709, 1590 and 1270 cm⁻¹ can be attributed to aromatic vibration of lignin. The peak at 1270 cm⁻¹ can be attributed to the guaiacyl ring breathing of lignin which was very prominent in the SAWB lignin in comparison to the SAWS lignin (R. Sun et al., 2000). The syringyl ring breathing of lignin was noticed to also be more prominent in SAWS lignin at the peak of 1327 cm⁻¹ (Lisperguer et al., 2009) than for SAWB lignin. Also, SAWB Lignin possess a peak at 837 cm⁻¹ which can be attributed to the C-H of p-hydroxyphenyl units of lignin which was not present within SAWS lignin which could have probably degraded during the alkaline delignification step (Yang et al., 2016). In conclusion, both wheat straw and wheat bran lignin possess an S-G-H lignin

substructure with wheat bran lignin having more guaiacyl units than syringyl units with the opposite also being true for wheat straw lignin (Lourenço and Pereira, 2018).

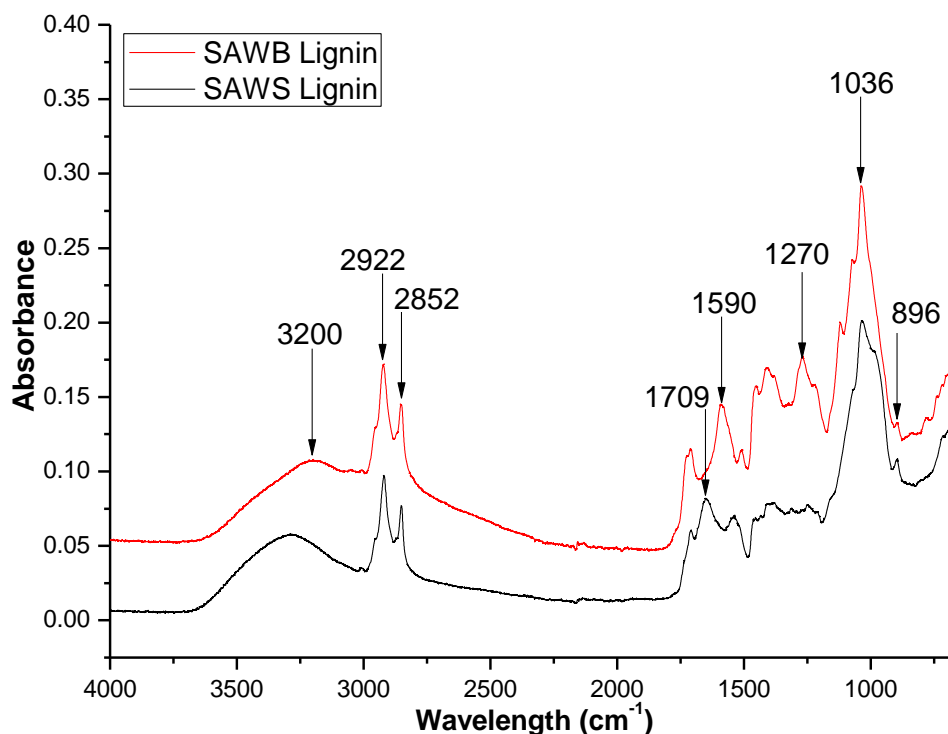


Figure 4.16 FTIR spectra of functional group changes of alkaline delignified wheat straw extracted lignin (SAWS Lignin) and alkaline delignified wheat bran lignin (SAWB Lignin)

4.5.1.3 Thermal Stability of Recovered Alkali Soluble Hemicelluloses and Lignin at the Optimum Alkaline Delignification Conditions

Alkaline delignified treatment of wheat straw and bran resulted in a similar two-step weight loss trend as observed in the mild alkaline extracted hemicelluloses. Unlike the mild alkaline extracted hemicelluloses, the SAWB Hemis experienced a higher moisture loss (11%) as compared to that of the SAWS Hemis (2%). The observation was corroborated by the prominence of the absorbed water peak in the SAWB hemicelluloses as compared to that in the SAWS Hemis (Figure 4.9).

Apart from the moisture content, the other values for the SA hemicelluloses reflected a similar trend as what was observed at the mild alkaline stage (Figure 4.9). SAWS Hemis were also observed to have T_{onset} and T_{max} values that were similarly about 20°C less than that observed for SAWB Hemis (Figure 4.9). The observation can be similarly explained as was for the MA treated hemicelluloses (Section 4.4.1.3). Similarly, as with the mild alkaline hemicelluloses, the SAWS Hemis had a high char content (32%) than that of the SAWB Hemis (13%). The reason for such results could be similarly related to the ash content as explained in Section 4.3.1.3. In conclusion, the alkaline delignification treatment resulted in loss of hemicelluloses as well as hemicelluloses with high cellulose content (16.15%), which

negatively affected that the thermal properties of SAWB Hemis. The composition and thermal properties of the extracted hemicelluloses indicated potential to be applied as in the making of hydrogels and paper additives (Yuan et al., 2016).

Alkaline delignified extracted lignin also underwent a three-step weight loss. The loss of moisture present within the alkaline delignified lignin was the first weight loss experienced at 50-110°C. The moisture content of the SAWS lignin and the SAWB lignin were similar, with the latter having a 1% increase over the former (Figure 4.10). Due to the presence of hemicellulose and cellulose within the lignin extracts, the second stage of the weight loss (T_{onset}) began between 140-180°C (Figure 4.10). In the second stage of the thermogravimetric analysis of lignin, T_{max} was observed to be higher in SAWS lignin (291°C) than in SAWB lignin (256°C). This could have been due to higher lignin content of SAWS lignin (74.7%) than SAWB lignin (69.2%) or the faster oxidation of the lignin present within SAWB lignin than in the SAWS lignin (Mao et al., 2012). From Figure 4.10 that both lignin possessed a wide degradation temperature range. However, the higher lignin content in SAWS lignin (74.7%) resulted in it possessing a higher T_{comp} than that of SAWB lignin (69.2%). Finally, the results obtained indicated that there was a high char content from both SAWS lignin (29%) and SAWB lignin (34%) (Watkins et al., 2015). Based on the lignin composition and high char content obtained for both SAWS lignin and SAWB lignin, it indicated their potential application as partial replacements in phenolic resins due to their fire resistant properties (Watkins et al., 2015).

4.6 Cellulose Isolation

Cellulose is the main component that can be used in the successful production of nanocellulose. It is therefore essential to increase the cellulose content of the biomass to a reasonable high value as possible with minimal cellulose degradation before the production of nanocellulose. Due to this, the effectiveness of the two-stage alkaline treatment in improving the cellulose content was considered for nanocellulose production. The results for the mild alkaline and alkaline delignification treatments are shown in Figure 4.17 and 4.18.

From the results shown in Figure 4.17 and 4.18 it can be summarized that the initial cellulose content of the untreated wheat straw and wheat bran influenced the final cellulose content of the residues (SAWS and SAWB) after the two-stage treatment. The successive alkaline treatments performed on the wheat straw indicated an increase for mild alkaline (57%) and alkaline delignification (57%) after each subsequent treatment. This showed that both treatments contributed similarly to improving the cellulose content of the wheat straw for nanocellulose production. Furthermore, this assertion was supported by the crystallinity results (discussed in Section 4.6.2), which indicated a similar increase (25%) in the crystallinity of the wheat straw cellulose after each alkaline treatment. In addition, the cellulose content of the wheat straw (76%) obtained after the delignification treatment of the wheat straw was comparably to cellulose content of cotton linter (77%) used in nanocellulose production (Espinosa et al., 2017;

Morais et al., 2013). The hemicelluloses (3%) and lignin content (5%) were both within the range of 0.5-23% (Espinosa et al., 2017; Teixeira et al., 2010) and 0.4-10% (Teixeira et al., 2010), respectively stated in Section 2.12 and 2.13 to be required for nanocellulose production. Finally, the two-stage alkaline treatment resulted in the recovery of 97% of the wheat straw cellulose, which indicated that the two-stage alkaline treatment caused minimal losses (3%) to the wheat straw cellulose while improving its crystallinity for nanocellulose treatment.

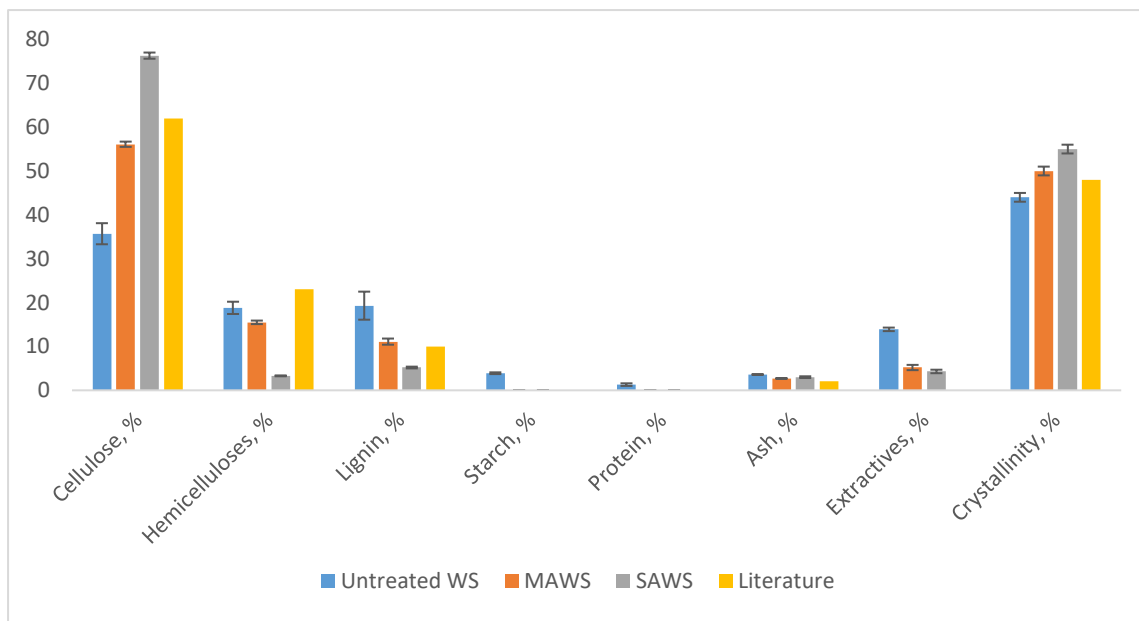


Figure 4.17 Chemical composition and crystallinity of wheat straw at different treatment stages with comparison with the set literature parameters.

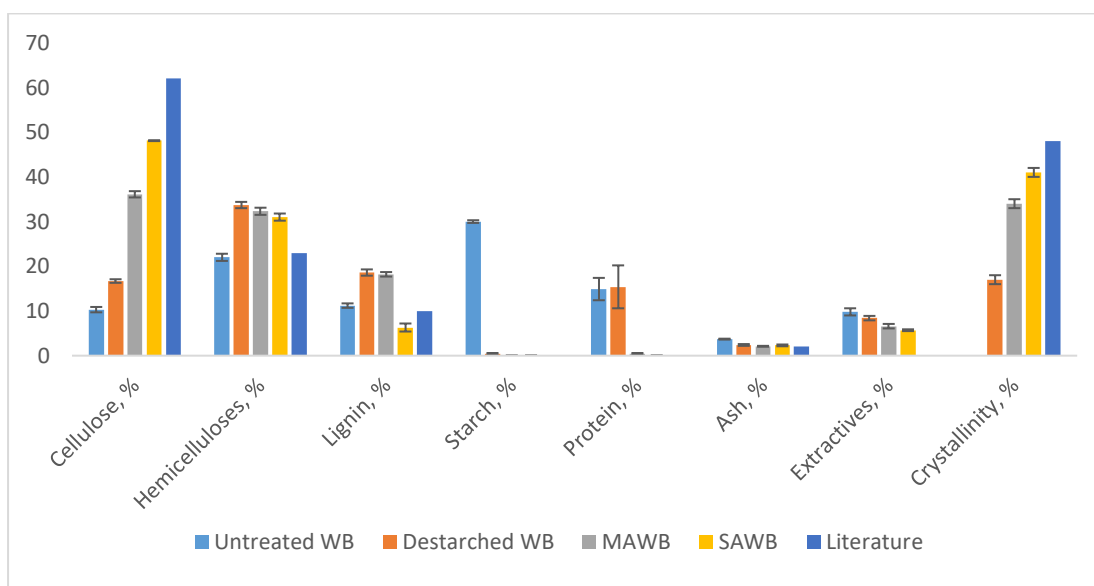


Figure 4.18 Chemical composition and crystallinity of wheat bran at different treatment stages with comparison with the set literature parameters.

The results (Figure 4.18) indicated that the two-stage treatment was an ineffective method for cellulose isolation for nanocellulose production from destarched wheat bran. Nevertheless, the two-stage alkaline treatment resulted in an increase of cellulose content of about 188% after destarching the wheat bran. Whereas, the mild alkaline treatment of the wheat bran resulted in about a 116% increase in the cellulose content after destarching, the alkaline delignification treatment contributed the other 72% increase in the cellulose content (Figure 4.18). In summary, the mild alkaline treatment performed on the wheat bran was much more effective in improving the cellulose content than the alkaline delignified treatment. The assertion was similarly supported by the crystallinity of the wheat bran (discussed in Section 4.6.2), where the mild alkaline treatment resulted in a higher increase (100%) of wheat bran cellulose crystallinity than the alkaline delignification treatment (22%).

The cellulose (48%), hemicellulose (31%) and crystallinity (41%) of the SAWB obtained after the two-stage alkaline treatment in this study were not within the ranges of cellulose-rich pulp stated in Section 4.1 used in nanocellulose production. A cellulose content (48%) indicated a larger presence (52%) of other cell wall components (hemicellulose, lignin, ash, and extractives) within the wheat bran which need to be removed before the cellulose-pulp can be used in nanocellulose treatment. Furthermore, the hemicellulose content (31%) was far above the allowable 20% stated by Penttilä et al. (2013) in cellulose pulp for nanocellulose production that will not inhibit enzymatic hydrolysis to produce nanocellulose. Whereas, the crystallinity (41%) was found to be less than the minimum of 47% stated by Kallel et al. (2016) for successful production of nanocellulose. Therefore, further nanocellulose treatments were focused on the alkaline delignified wheat straw.

4.6.1 Fourier Transform Infrared Spectroscopy of Wheat Straw and Wheat Bran Treated and Untreated Samples

The FTIR spectra for untreated WS and WS residues from both the mild and alkaline delignification extractions were shown in Figure 4.19. The peaks within the band range of 3200-3345 cm^{-1} were assigned to the OH stretching vibration of cellulose within the untreated and alkaline treated wheat straw residues (Rosa et al., 2012). An increase in the intensity of this peak indicated an increase in the cellulose content of the samples (Zheng et al., 2018). The increase in the OH stretching vibration of cellulose peak as subsequent treatments were performed are consistent with the increase in cellulose from compositional analysis (Figure 4.17). In addition, the peak at 1731 cm^{-1} present within the untreated WS attributed to the ester linkage of carboxylic group of the ferulic and *p*-coumaric acids of lignin (Kumar et al., 2014). The peak at 1731 cm^{-1} was absent from the MAWS and SAWS residues which was due to the mild alkaline treatment resulting in the breaking of those linkages and removal of the ferulic and *p*-coumaric acid groups from the untreated WS. It can also be noticed that the peak at 1242–1275 cm^{-1} showed a decrease in the peak height for untreated WS, MAWS and SAWS residues consecutively (Luzi et al., 2019). The decrease in this peak was attributed to hemicelluloses and lignin reduction, which was consistent with the hemicelluloses and lignin values present within the untreated,

MAWS, and the SAWS residues in the compositional analysis in Figure 4.17. Furthermore, the lignin reduction was noticed by the presence of a peak at 2919 cm^{-1} which was attributed to CH_2 stretching of lignin for untreated WS which was absent from MAWS and SAWS due to the mild alkaline treatment (Zheng et al., 2018). The FTIR spectra (Figure 4.19) for the wheat straw agreed with the compositional analysis (Figure 4.17) and indicated the effectiveness of the treatment route taken on improving the cellulose content and reduction of the lignin and hemicellulose contents of the wheat straw.

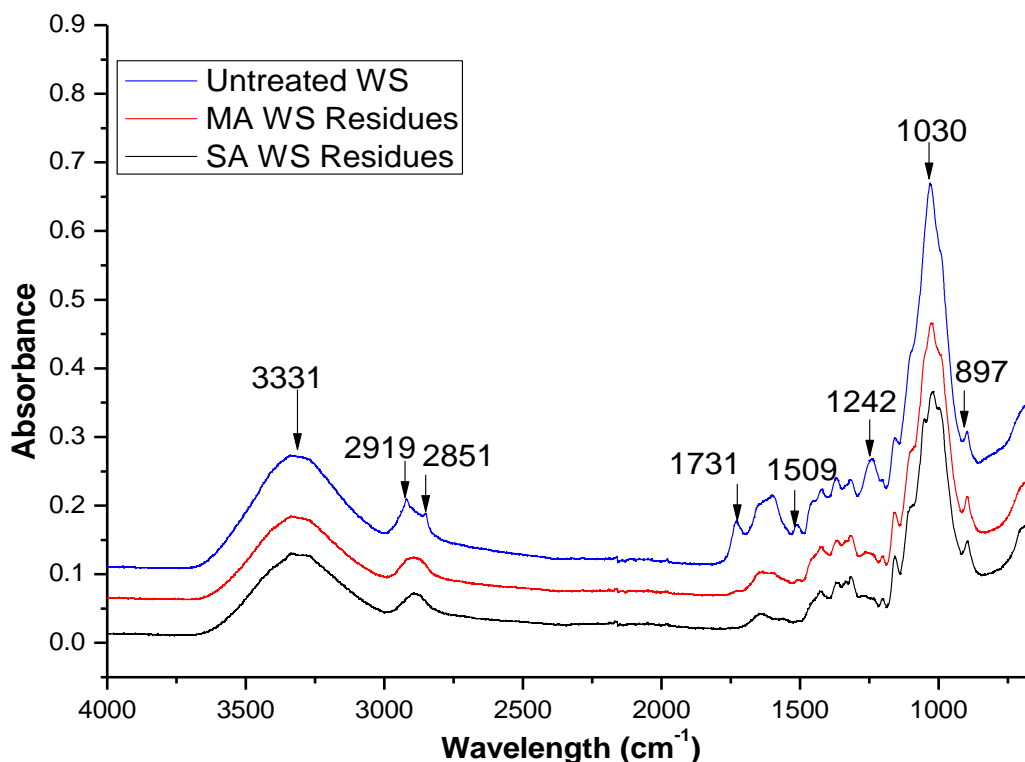


Figure 4.19 FTIR spectra of functional group changes of untreated wheat straw (WS), mild alkaline wheat straw (MAWS) residues and alkaline delignified wheat straw (SAWS) residues

The FTIR spectra for untreated wheat bran (WB), mild alkaline treated wheat bran (MAWB) residues and alkaline delignified wheat bran (SAWB) residues was shown in Figure 4.20. Both the untreated WB and MAWB residue can be seen to possess a peak at 2854 cm^{-1} which was not prominent in SAWB residue. The peak at 2854 cm^{-1} was assigned to the CH stretching of lignin (Zheng et al., 2018) which indicated the effectiveness of the delignification treatment in partially removing the lignin within the mild alkaline treated wheat bran as could be observed in Figure 4.18. The result was supported by the prominence of this peak in the alkaline delignified extracted lignin (Figure 4.16). The peak at 1732 cm^{-1} assigned to the presence of ester linkage of ferulic and *p*-coumaric acid were not very prominent in all the samples indicating the low content of ferulic acid and *p*-coumaric acid as seen in Figure 4.18 (Kumar et al., 2014). However, this peak was only present in the untreated WB and absent from the MAWB and SAWB residue indicating that the mild alkaline extraction was able to totally remove all the ferulic

and *p*-coumaric acid at the optimised condition as indicated by Figure 4.20. Also, the peak representing the protein within the untreated wheat bran (1540 cm^{-1}) was seen to be absent from both the MAWB residue and the SAWB residue indicating the effectiveness of the mild alkaline treatment in extraction of the protein present within the wheat bran (Adapa et al., 2011). The usual peak for CO stretching of cellulose and that of the β -glucosidic linkage of hemicelluloses can be seen at 1031 and 897 cm^{-1} , respectively (Rosa et al., 2010). Nevertheless, all three wheat bran samples possessed peaks at 3333 - 3281 and 2924 - 2920 cm^{-1} representing OH stretching of cellulose and CH_2 stretching of lignin, respectively (Rosa et al., 2010). Moreover, there was an increase in peak intensities of the cellulose between 3333 - 3281 cm^{-1} from subsequent treatments after destarching. In addition, the ability of all three samples to absorb water can be seen by the presence of a peak at 1636 cm^{-1} whereas the aromatic vibration of lignin is represented by the peak at 1506 cm^{-1} (Liu et al., 2017). In summary, the FTIR spectra (Figure 4.20) obtained for wheat bran agreed with the results obtained in the compositional analysis (Figure 4.18).

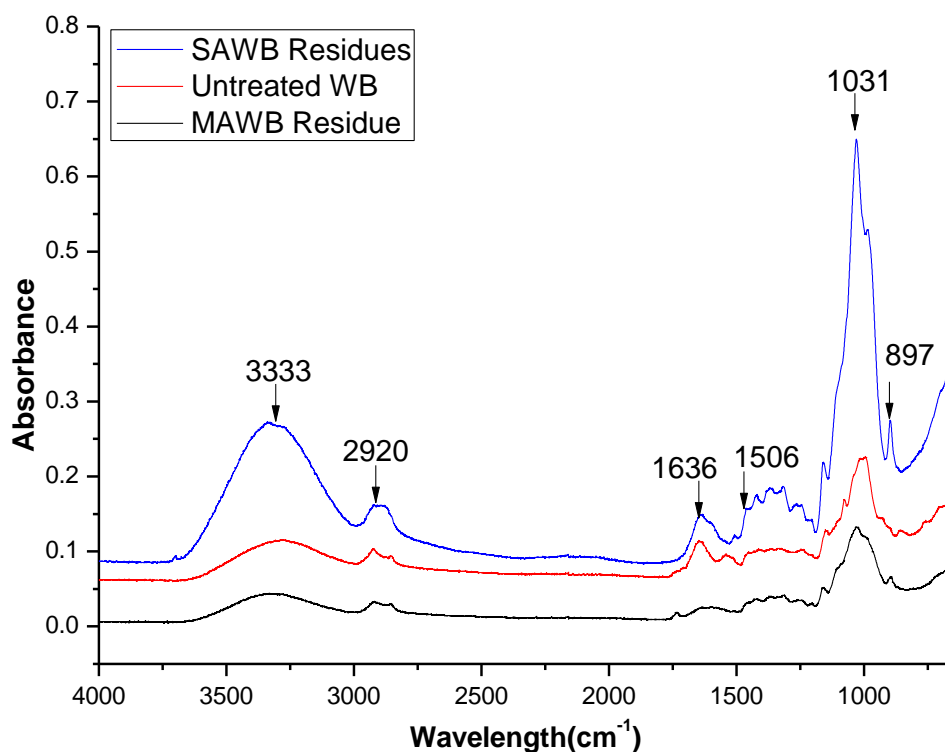


Figure 4.20 FTIR spectra of functional group changes for untreated wheat bran (WB), mild alkaline wheat bran (MAWB) residues and alkaline delignified wheat bran (SAWB) residues.

4.6.2 X-Ray Diffraction and Crystallinity of Wheat Straw and Wheat Bran Treated and Untreated Samples

Cellulose is made up of both crystalline and amorphous regions. These crystalline regions are formed due to the hydrogen bonds between the cellulose molecules arranged in an ordered pattern whereas the

amorphous regions exist in a complete disordered state (Alemdar and Sain, 2008a). Crystallinity of the samples was determined based on the crystalline portions and the amorphous portions within the sample.

The XRD test performed for the untreated and the treated samples for both wheat straw and wheat bran showed an increase in the crystallinity index after successive treatments (Figure 4.17 and 4.18). The peak for the crystalline intensity for wheat straw increased slightly from $2\theta=21.8^\circ$ to 22.4° to 22.6° for untreated, MAWS and SAWS, respectively. This slight changes in the peak intensity were attributed to the effect of the alkaline treatment on the wheat straw samples (Kallel et al., 2016). Also, the wheat straw cellulose obtained about a 25% increase in its crystallinity index after the two-step alkaline treatment which indicated the effectiveness of the alkaline treatments on the amorphous regions of the cell wall components (hemicelluloses and lignin). The crystallinity obtained for SAWS was relatively comparable to others obtained for straw cellulose used in nanocellulose production such as wheat, rice and barley straw (Oun and Rhim, 2016a). The observed alkaline delignified wheat straw crystallinity in addition to the cellulose content (76%) indicated that the SAWS residues could be directly applied in the nanocellulose production stage.

Unlike wheat straw, the crystalline intensity for untreated and destarched wheat bran were not prominently visible. This was due to the low cellulose content of both the untreated (10%) and destarched (17%) wheat bran as can be seen in Figure 4.18. The low cellulose content influenced the crystallinity index observed for the untreated wheat bran especially. The observation was because cellulose is the only cell wall component that possessed crystalline regions whereas both lignin and hemicelluloses were made up of amorphous regions. Due to the cell wall composition the crystallinity index for the untreated wheat bran was not able to the calculated (Figure 4.18). Unlike wheat straw, the spectra for wheat bran showed the prominent peaks at the height of 2 0 0 peak (I_{200} , $2\theta = 22.5^\circ$) and the minimum between the 2 0 0 and 1 1 0 peaks (I_{am} , $2\theta = 18^\circ$) after the mild alkaline treatment. The prominence of the peaks after mid alkaline treatment indicated the effectiveness of the mild alkaline treatment by resulting in about a 100% increase in the crystallinity index of the destarched wheat bran. In addition, an increase in crystallinity index of about 22% was observed in the SAWB indicating that there was an improvement in crystallinity due to the alkaline delignification treatment as was corroborated by the increase in cellulose content from the compositional analysis (Figure 4.18).

In conclusion, the XRD results obtained for the wheat bran indicated that it was necessary to obtain wheat bran with a higher initial crystallinity to improve its crystallinity to a minimum of 48% (Kallel et al., 2016) with the use of the two-stage alkaline treatment. Furthermore, the WB XRD results indicated that further treatment of the wheat bran could result in a further increase in its crystallinity to be applied for nanocellulose production. However, Nilsson (2017) stated that further treatment of the

wheat bran cellulose pulp could rather result in the conversion of cellulose I into cellulose II through a solubilisation and reprecipitation process, which results in the reduction of the wheat bran crystallinity.

4.6.3 Structural Changes of Wheat Straw and Wheat Bran Treated and Untreated Samples

The structural morphology of both the untreated and treated fibers of wheat straw and bran were investigated by using SEM analysis and the images were shown in Figure 4.21. From Figure 4.21 a and d both untreated wheat straw and wheat bran, respectively had most of their fibers arranged and clustered in bundle forms indicating a more compact structure. In wheat straw micrographs, the mild alkaline treatment resulted in breaking up the compact fiber-bundle structure a little whereas the alkaline delignification treatment broke up more of the bundle structure resulting in the release of more individual structures, ash, hemicelluloses and lignin (Figure 4.21 b and c) (Liu et al., 2017; Rosa et al., 2010). This can be attributed to the partial removal and extraction of the other cell wall components such as lignin, hemicelluloses and ash holding the fiber structure together after the successive chemical treatments (Figure 4.17) (Alemdar and Sain, 2008b).

The destarching performed on wheat bran resulted in the removal of most of the starch granules resulting in the reduction of starch content and exposing other cell wall components to further treatments (Figure 4.21 e) (Leticia et al., 2017). Although, mild alkaline and alkaline delignified treatment of wheat bran improved the cellulose content of the residues, the compact fiber-bundle structure was only partially released (Figure 4.21 f and g) due to the hemicelluloses and lignin contents of both residues (Figure 4.18). This is in support of the results obtained after the compositional analysis indicating that to use the alkaline delignified treated wheat bran fiber for nanocellulose production, the fibers will have to undergo further treatments to break their bundle structure and improve the cellulose content and crystallinity by releasing the hemicelluloses and lignin present.

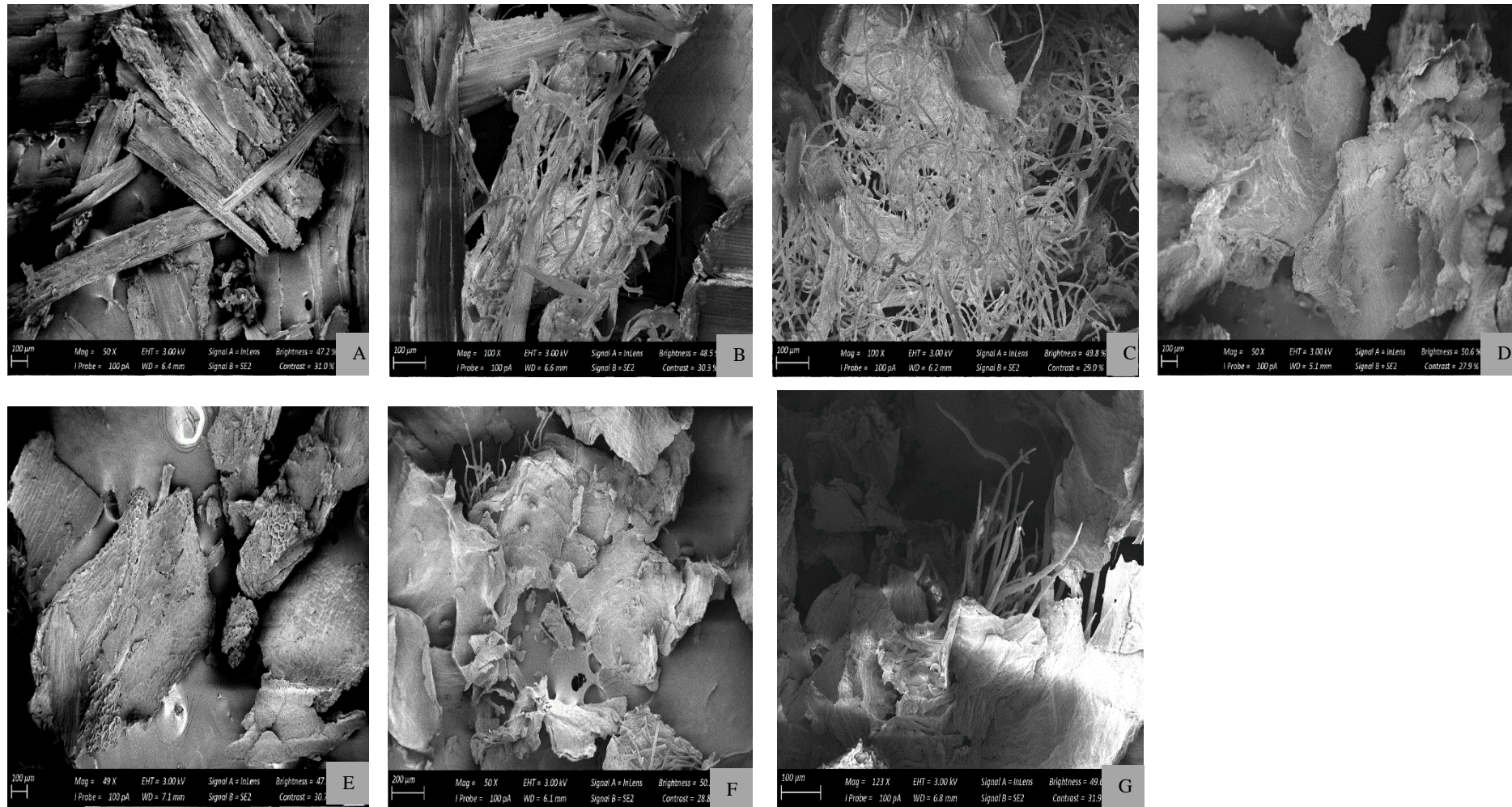


Figure 4.21 Scanning electron micrographs for a) untreated wheat straw b) mild alkaline treated wheat straw c) alkaline delignified wheat straw d) untreated wheat bran e) destarched wheat bran f) mild alkaline treated wheat bran g) alkaline delignified wheat bran

4.6.4 Thermal Stability of Wheat Straw and Wheat Bran Treated and Untreated Samples

Generally, cellulosic materials experience two steps in weight loss. The first step is attributed to the loss of weight due to evaporation of absorbed water from the fibers (Oun and Rhim, 2016b). The weight loss was observed between 100–120°C for both wheat straw and bran (Figure 4.22 and 4.23). All three wheat straw samples (untreated wheat straw, MAWS and SAWS), experienced about a 6% weight loss although it slightly decreased after every treatment step (Figure 4.22). Similarly, untreated, destarched, MA and SA wheat bran samples experienced a weight loss of about 8%, albeit a slight increase from destarched WB to SAWB (Figure 4.23). The results indicated that between wheat straw and wheat bran, wheat bran had a higher capacity to retain moisture due to their more fibrous nature.

In the second phase of the weight loss for both biomass, wheat straw samples experienced a major weight loss between 270–450 °C whereas that for wheat bran was between 224-430 °C (Figure 4.22 and 4.23). The weight loss was mainly due to thermal degradation of cellulosic components within the samples, beginning with hemicelluloses to the cellulose and then finally to lignin (Costa et al., 2015). From Figure 4.22 and 4.23 the onset decomposition temperature (T_{onset}) of the various samples increased after every treatment indicating that the amorphous regions were being removed improving their thermal stabilities. However, the thermal stability of alkaline delignified wheat bran showed a reduction in the onset temperature (from 252°C to 242°C), which could have been due to the degradation of some of the cellulose resulting in a reduction of the thermal properties. The assertion is supported by the cellulose recovery of 83% obtained from the two-stage alkaline treatment of the wheat bran (Figure 4.18).

The residues remaining (char) after thermal degradation at 600 °C, was estimated in the both wheat straw and bran at various stages (Figure 4.22 and 4.23). After each treatment both wheat straw and bran had a relative reduction in the char left. The reduction was mainly attributed to the reduction of hemicelluloses and lignin within the samples as well as an increase in cellulose crystallinity after every treatment stage (Oun and Rhim, 2016a). Whereas, the increased observed for SAWB could be related to the loss of cellulose after the treatment.

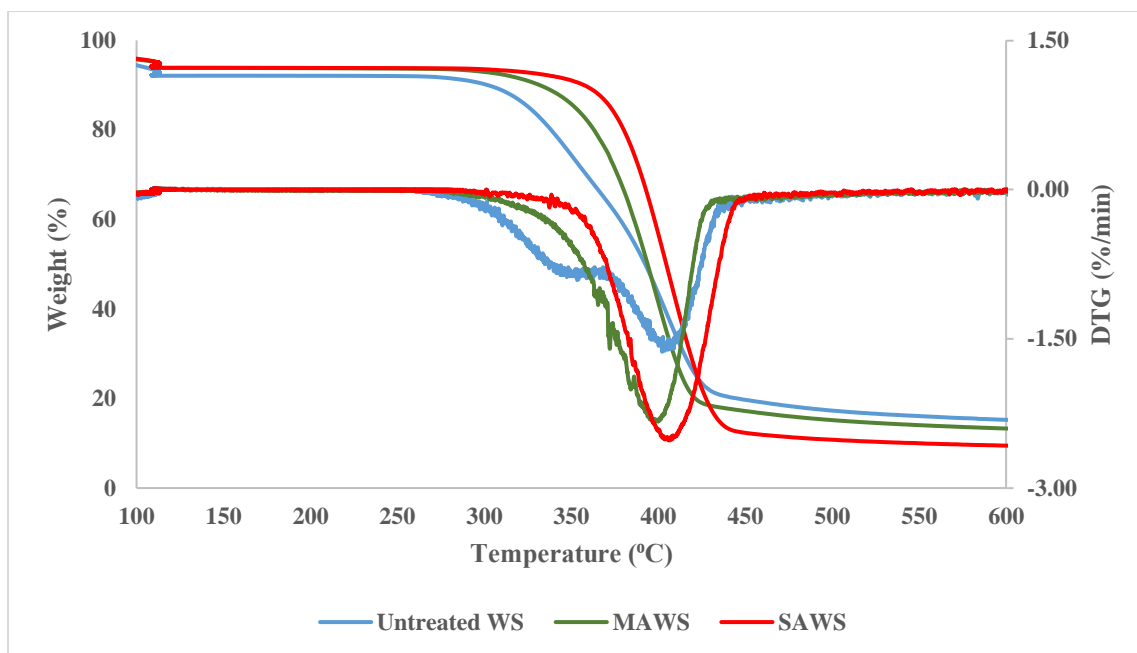


Figure 4.22 Thermal stability of untreated wheat straw (WS), mild alkaline wheat straw (MAWS) and alkaline delignified wheat straw (SAWS)

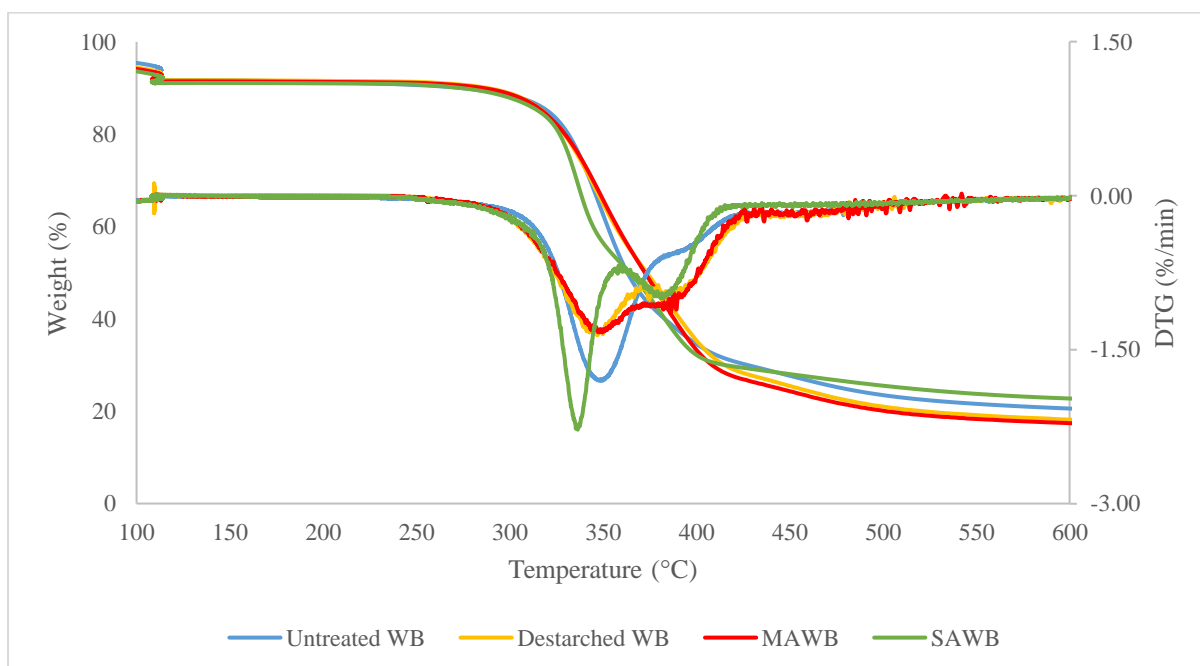


Figure 4.23 Thermal stability of untreated wheat bran (WB), destarched wheat bran (WB), mild alkaline wheat bran (MAWB) and alkaline delignified wheat bran (SAWB)

4.7 Summary of Results

The two-stage alkaline treatment performed on both wheat straw and wheat bran resulted in the extraction of hemicelluloses, lignin, ferulic acid and *p*-Coumaric acid. The process condition selected for both mild and alkaline delignified treatments were significant for both wheat straw and wheat bran.

The results obtained for the two-stage alkaline treatment of wheat straw indicated the effectiveness of the treatment in the fractionation of the wheat straw and production of high value products. At the optimised mild alkaline treatment conditions (54.14⁰C, 2.35 wt.% NaOH concentration and 16 h) for wheat straw, yields of 35% and 45% were obtained for hemicelluloses and lignin, respectively. Whereas, the yield of the co-extracted *p*-coumaric acid at the mild alkaline stage was found to be 85% with a 45% antioxidant activity. Furthermore, the optimised treatment conditions (60 min, 10 wt.% NaOH, 121⁰C) for the alkaline delignification of wheat straw resulted in yield of 42% and 23% for the hemicelluloses and the lignin, respectively. The total yield of the hemicelluloses and lignin were 77% and 68% of hemicelluloses and lignin, respectively. The hemicelluloses obtained can be applied in the papermaking industry as an additive to improve its mechanical properties (García et al., 2013; F Xu et al., 2006) whereas the lignin can be applied in polymer composite application (Li and McDonald, 2014). In conclusion, the two-stage alkaline treatment achieved the aim of the experiment by extracting majority of the hemicellulose, lignin and *p*-coumaric acid from the wheat straw.

Moreover, the two-stage alkaline treatment was advantageous to the wheat straw for nanocellulose production. A total cellulose recovery of 97% was obtained indicating that the treatment resulted in minimal losses (3%) of the wheat straw cellulose. In addition, the cellulose content of the wheat straw cellulose pulp obtained showed an increase from an initial 36% to 76% after the two-stage alkaline treatment which was optimal for nanocellulose production. The increase in cellulose content translated to an increase in cellulose crystallinity from 44% to 55% which was above the minimum crystallinity (48%) observed in literature for nanocellulose production. The improvement of the cellulose crystallinity had a positive effect on the wheat straw thermal degradation temperature by improving the onset degradation temperature from 264⁰C to 288⁰C and the maximum degradation temperature from 402⁰C to 406⁰C. In summary, the two-stage alkaline treatment of the wheat straw achieved its aim of producing cellulose-rich wheat straw pulp for nanocellulose production.

The two-stage alkaline treatment was shown to be effective in the fractionation of some of the components of the wheat bran in comparison to others. The yield obtained for hemicelluloses and lignin was 37% and 73%, respectively at the optimised mild alkaline conditions (68.28⁰C, 2.71 wt.% NaOH concentration, 16 h) for wheat bran. Whereas, the yield of ferulic acid was 66% with a 15% antioxidant activity at the optimised mild alkaline treatment conditions. In addition, the optimised alkaline delignification treatment (121⁰C, 9.41 wt% NaOH concentration and 81 min) resulted in a 15% and 21% yield of hemicelluloses and lignin, respectively. The two-stage alkaline treatment of the wheat

bran resulted in the extraction of 52% hemicelluloses and 92% lignin. The hemicelluloses obtained from the two-stage alkaline treatment of the wheat bran can be applied in making of hydrogels (Jiang et al., 2014; Matavire, 2018), whereas the lignin can be applied in polymer composite application (Li and McDonald, 2014). The results from the two-stage alkaline treatment indicated that the treatment approach was beneficial for the extraction of lignin and ferulic acid whereas the treatment approach could not extract a considerable amount of the hemicelluloses (48%) present within the wheat bran.

Furthermore, the two-stage alkaline treatment resulted in 83% recovery of the cellulose present within the wheat bran. The cellulose recovery indicated that the treatment approach resulted in a significant loss (17%) of cellulose. The reduction of the both the onset and the maximum thermal degradation temperatures (from 252°C to 242°C and 350°C to 336°C, respectively) after the alkaline delignification treatment indicated that the cellulose loss experienced was mainly due to the alkaline delignification treatment on the mild alkaline treated wheat bran. Nevertheless, the delignification treatment conditions resulted in an increase in crystallinity from 34% to 41% for MAWB and SAWB, respectively. However, the crystallinity obtained was not high (41%) enough to be applied in nanocellulose production ($\geq 48\%$ crystallinity). Moreover, the wheat bran cellulose pulp obtained was made up of 31% hemicelluloses which exceeded the maximum of 20% stated by Penttilä et al. (2013) beyond which hemicelluloses affected enzymatic hydrolysis to produce nanocellulose. In summary, the two-stage alkaline treatment approach taken for the wheat bran was not a favourable treatment method to produce cellulose-rich fibers for nanocellulose production.

CHAPTER FIVE

Nanocellulose Production

Introduction

Recent interest in environmental sustainability has influenced research into the use of both biodegradable and environmentally friendly methods in the processing industry. In light of this, the use of plant waste biomass as the precursor in the production of nanocellulose has become the main focus of most nanocellulose research due to their high cellulose content.

Plant biomass used in nanocellulose production usually undergoes three treatment steps; pretreatment, purification and hydrolysis. The pretreatment step usually focuses on removing hemicellulose, lignin and ash, leaving the cellulose fiber by breaking the lignin-carbohydrate complex bonds. A secondary treatment, the purification treatment is usually performed to improve the cellulose content within the residue to levels for application in nanocellulose treatment. This is usually done by bleaching the biomass, resulting in removal of the residual hemicellulose, lignin, and ash. The purified cellulose from the plant biomass is then hydrolysed by using either a chemical or enzymatic treatment. The chemical hydrolysis treatment can be done alone or be combined with mechanical treatment. Whereas, the enzymatic treatment is usually combined with mechanical treatment to produce nanocellulose.

Sulfuric acid (50–65 wt.%) treatment is the commonest applied nanocellulose production method. Furthermore, when applied at the right treatment conditions, it results in a high yield of nanocellulose as well as producing a stable colloidal suspension in water (Helbert et al., 1996; Pereira et al., 2017). The stable colloidal suspension in water is as a result of the esterification of the hydroxyl groups of the cellulose by the sulfate groups (Phanthong et al., 2018). However, the presence of these sulfate groups also result in a reduction of thermal properties of the produced nanocellulose affecting its application in high temperature processes (Wang et al., 2007). Due to this, recent acid hydrolysis treatments have focused on using hydrochloric acid in the production of nanocellulose as an alternative approach. Kaushik and Singh (2011) used 1 M HCl in conjunction with a mechanical treatment to obtain nanocellulose of 10–50nm in diameters. Similarly, Du et al. (2016) obtained less than a 2% yield of nanocellulose from treating bleached softwood Kraft pulp with 2 M HCl. However, Cheng et al. (2017) was able to obtain a nanocellulose yield of 89% using commercial microcrystalline cellulose by using 4 M HCl. Whereas, using 6 M HCl was able to obtain a 94% yield that was comparable to that from sulfuric acid treatment but with improved thermal degradation (Yu et al., 2013). In general, acid hydrolysis results in the corrosion of treatment vessels, production of chemical waste and waste of water from dialysis (B. Li et al., 2015).

Enzymatic treatment presents an alternative solution to these problems by presenting milder hydrolysis condition, low or no chemical waste which are more environmentally friendly. The function of enzymes

on cellulose are based on their selectivity. The presence of an endoglucanase enzyme is required to produce nanocellulose. Due to this most enzymatic treatment research have used a mono-component endoglucanase such as FiberCare R whereas multicomponent endoglucanase such as Viscozyme L which hydrolyses hemicelluloses and cellulose have also been used (De Campos et al., 2013; Nechyporchuk, 2015). Enzymatic treatment presents the disadvantage of treatment times up to 72 hours in comparison to acid hydrolysis. However, Tibolla et al. (2014) and Bester (2018) have indicated that it is possible to produce nanofibers at 24 and 6 hours, respectively.

The nonuniform nature, yield and nanoparticle aggregation have restricted hydrochloric acid and enzymatic treatment nanoparticle application in favour of sulfuric acid produced nanocellulose (Vanderfleet et al., 2017). The nanocellulose production stage was aimed at optimising nanocellulose production from two-stage alkaline treated wheat straw cellulose by using a hydrochloric acid treatment and an enzymatic treatment as alternative approaches to the traditional sulfuric acid treatment. The yield, uniform particle size (polydispersity), surface charge (zeta potential), thermal stability and crystallinity of the obtained nanocellulose were determined at the optimised conditions for the alternative approaches and compared to the traditional treatment as well as commercial nanocelluloses.

5.1 Yield, Particle Morphology and Surface Charge for Nanocellulose Production

5.1.1 Commercial Cellulose Nanocrystals (CNC) and Cellulose Nanofibers (CNF)

The commercial CNC and CNF obtained from University of Maine were used in this study as control samples. The CNC was produced by means of an acid treatment whereas the CNF was produced by a mechanical size reduction treatment. The control samples were analysed in triplicates.

The resulting mean particle size, polydispersity index and surface charge are represented in Table 5.1. The length obtained from the measurement was 173 ± 5 nm for CNC whereas that for the CNF was greater than $1 \mu\text{m}$. The diameters obtained from the measurement were 27 ± 6 nm for CNC and 24 ± 8 nm for CNF. The observed values were within the range of declared values for both the CNC (length 150-200 nm, diameter 5-20 nm) and CNF (length up to several 100 μm and diameter up to 50 nm) provided by the University of Maine Nanofiber Plant, USA. The results indicated the effectiveness and accuracy of particle morphology analysis.

Table 5.1 Dimension, zeta potential (ZP) and polydispersity index (PDI) of produced commercial and sulfuric acid cellulose nanocrystal from wheat straw

Sample	ZP, mV	PdI	Length, nm	Diameter, nm
Commercial CNC	-45 ± 8	0.47 ± 0.01	173 ± 5	27 ± 6
Commercial CNF	-14.5 ± 1	1 ± 0.03	$>1\mu\text{m}$	27 ± 8

Furthermore, the zeta potential (ZP) of the commercial CNC was -40 ± 8 mV, indicating a high stability in water whereas that of commercial CNF was -14.5 ± 1 mV indicating a relative stability in water (Patel and Agrawal, 2011). Also, the polydispersity index (PdI) of CNC was 0.47 ± 0.01 which indicated it was slightly monodispersed whereas that of the commercial CNF was 1 ± 0.03 indicating its highly polydispersed nature.

5.1.2 Sulfuric Acid Hydrolysis of Cellulose-Rich Fibers from Two-step Alkaline Treatment of Wheat Straw

A 33.8% yield of sulfuric acid produced cellulose nanoparticles (SCN) was obtained from the treatment of SAWS. The result was close to the yield (34.5%) obtained from treating bleached corncob residue at similar treatment conditions by Liu et al. (2016). The yield indicated that the treatment conditions used were not too severe to result in the loss of the SCN produced (Liu, 2017). The SCN produced had a diameter of 17 ± 4 , length of 235 ± 14 nm with 0.55 ± 0.04 PdI which indicated a slightly polydispersed fiber length. However, the fiber length was in the range of CNC (100-4000 nm), whereas the SCN PdI was slightly above that of the commercial CNC (0.47 ± 0.01). Nevertheless, the ZP of the produced SCN (-35 ± 3 mV) was within the range of the commercial CNC (-45 ± 8 mV) obtained indicating its high stability in water (Patel and Agrawal, 2011).

5.1.3 Optimisation of Hydrochloric Acid Hydrolysis of Cellulose-Rich Fibers from Two-step Alkaline Treatment of Wheat Straw

The optimization of process conditions was done to maximise yield, maximise zeta potential, minimise polydispersity index and obtain smaller fiber length of the produced hydrochloric acid treated cellulose nanofibers (HCN). The process conditions chosen for hydrochloric acid treatment of SAWS were significant at a 95% confidence level in both the linear and quadratic terms for both temperature and time for yield (Figure 5.1a) meaning that optimum treatment conditions were reached for both variables. The R-squared obtained for the yield of HCN was 0.97 indicating a good relation between the treatment model and the experiments performed.

Hydrochloric acid treatment of SAWS resulted in 8–24% yield of cellulose nanoparticles (Figure 5.2a). The results indicated an increase in HCN yield from 80°C to about 100°C before experiencing a reduction at temperatures above 100°C (Figure 5.2a). The reduction in the yield (20.31 ± 1.24) was noticed at the optimum multiple response treatment conditions (7.41 h, 114.14 °C), which was mainly due to the increase in temperature above 110°C, which could have resulted in the deformation of HCN. Furthermore, it was found that the increase in temperature (above 110°C) at the optimum conditions was favourable to the zeta potential, particle length and the polydispersity index of the produced HCN (Figure 5.2). In addition, an increase in temperature to 120°C and above resulted in ‘burning’ of samples as observed by Vanderfleet et al. (2017) when treating cotton pulp with 85 wt.% phosphoric acid.

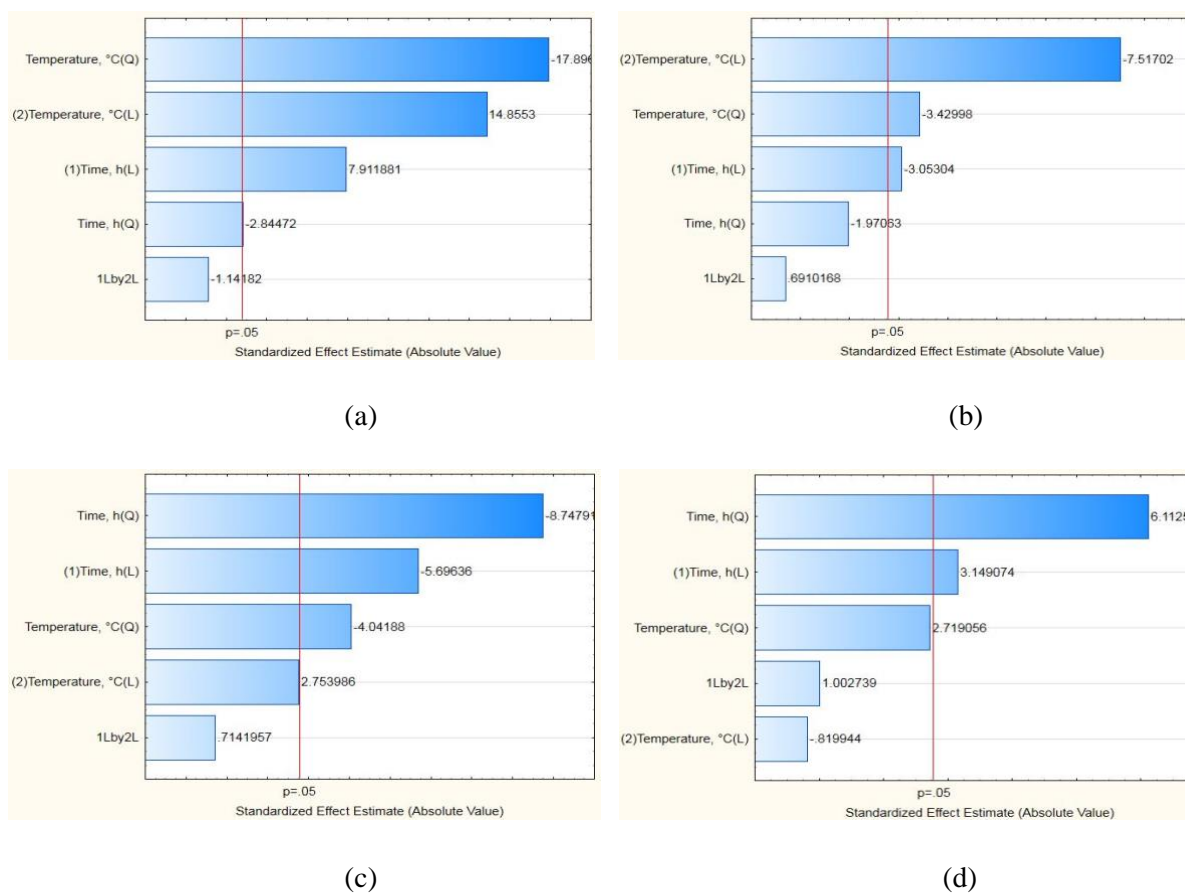


Figure 5.1 Pareto chart of optimisation of hydrochloric acid produced nanocellulose (a) yield (b) zeta potential (c) polydispersity index (d) particle length

In general, zeta potential (ZP) of HCN was lower (-13.1 to -21.3 mV) than that of SCN (-35 ± 3). The reason for this observation was mainly due to the presence of sulfate ions in SCN which esterified the hydroxyl groups of the cellulose creating a higher surface negative charge as compared to that of HCN (Bondeson et al., 2006). HCN ZP increased as treatment conditions became more severe from 4 h and 80°C to 6 h and 128.28°C (Figure 5.2b). Whereas, it was found to decrease from 4 h and 80°C to 6 h and 71.72°C (-12.0 mV). The result indicated that reaction temperature had a major effect on the ZP as compared to the time (Figure 5.1b) (Vanderfleet et al., 2017). Based on the nanoparticle colloidal stability values stated by Patel and Agrawal (2011), most of the samples could be termed as relatively stable (± 10 – 20 mV), whereas, at 6 h and 128.28°C the HCN could be termed as moderately stable (± 20 – 30 mV). The results obtained for HCN ZP were within -10.5 mV and -21.6 mV obtained by Correa et al. (2010) and Tian et al. (2016), respectively when working with 37 wt.% HCl. Finally, the HCN produced at the optimum condition was noticed to be relatively stable with a ZP of -16.3 mV (Table 5.4).

The reaction time was found to be the major factor affecting both the particle length and the PdI (Figure 5.1c and d). An increase in time from 4 h to 6 h was noticed to result in a reduction in particle length and an increase in PdI (Figure 5.2c and d). Whereas, the opposite was found to occur when the time increased from 6 h to 8 h. The high PdI (0.92) observed at 6 h and 100°C could be due to the sample having a broad size distribution (B. Li et al., 2015). In addition, the high PdI (0.92) could be due to sample aggregation which most likely occurred due to the low ZP (-13.2 mV) observed. At the optimum conditions, the PdI (0.53) was found to be slightly polydispersed (Table 5.2) supporting the earlier claim that the polydispersity improved as the treatment conditions increased. Finally, the HCN produced was found to have a length (541 nm) and diameter (17 nm) with a threadlike structure which indicated that the produced HCN were CNFs.

Table 5.2 Optimised conditions for hydrochloric acid treated wheat straw cellulose nanoparticles (HCN)

Optimised Conditions for HCN (7.41 h, 114.14 °C)				
	Yield, %	ZP, mV	PdI	Length, nm
Predicted Values	22.57 ± 0.99	-18.1 ± 1.70	0.64 ± 0.10	541 ± 62
Experimental Values	20.31 ± 1.24	-16.3 ± 1.50	0.53 ± 0.20	514 ± 50

Where ZP is zeta potential; PdI is polydispersity index; HCN is hydrochloric acid produced cellulose nanoparticles

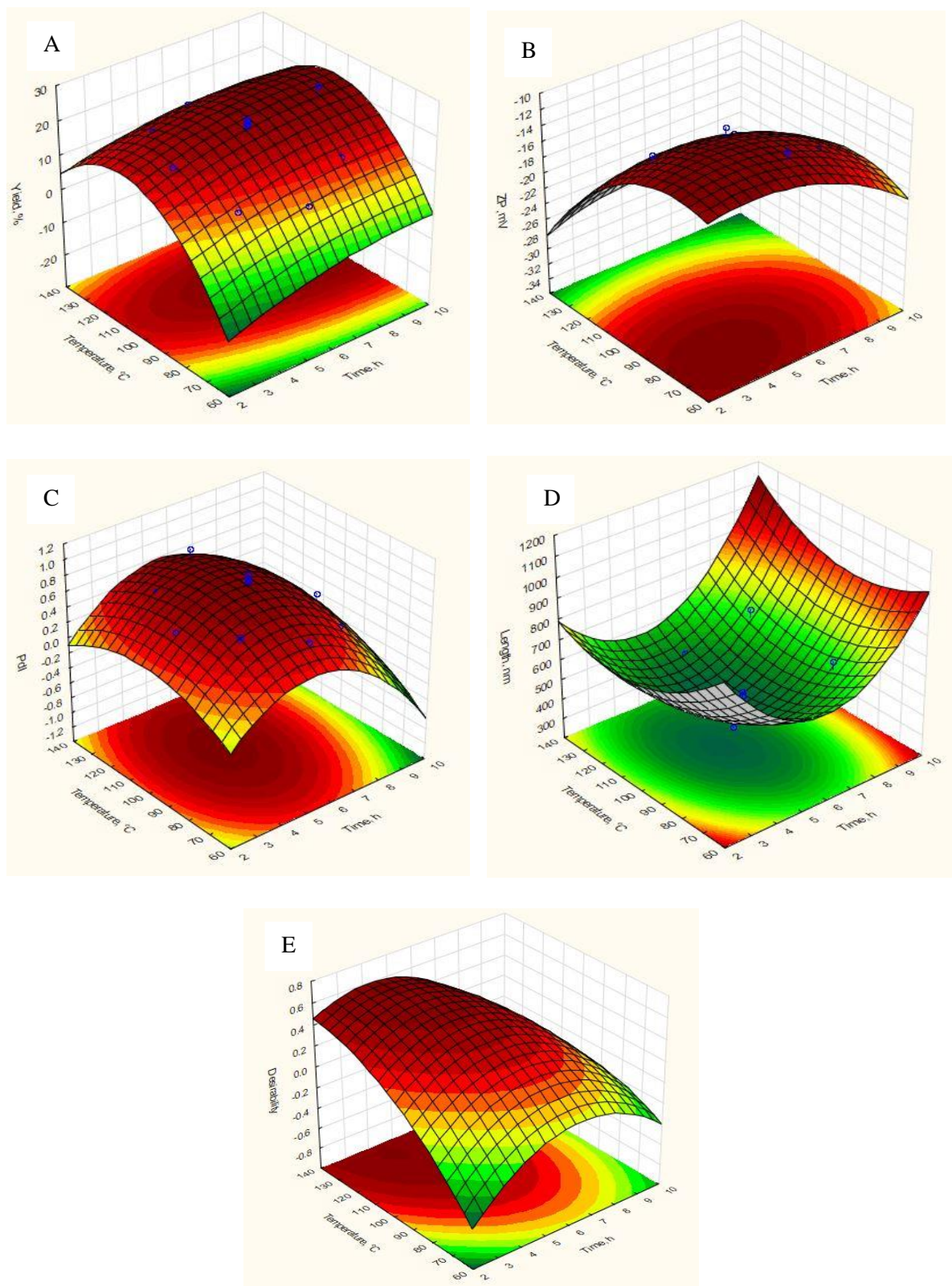


Figure 5.2 Surface plot of optimisation of HCN process conditions A) Yield B) Zeta Potential (ZP) C) Polydispersity Index (PdI) D) Nanocellulose Length E) Desirability with time (7.41 hours) and temperature (114.14⁰C) as dependent variables

5.1.4 Optimisation of Enzymatic Hydrolysis of Cellulose-Rich Fibers from Two-step Alkaline Treatment of Wheat Straw

The process conditions investigated for enzymatic treatment were targeted at minimising glucose formation and obtaining shorter diameters (less than 50 nm) for the produced enzymatically hydrolysed cellulose nanoparticles (ECN). The R-squared obtained for the glucose formation was 0.96, which indicated a good fit between the predicted and experimental model values. From Figure 5.3a, it was noticed that the multicomponent enzyme, Viscozyme L had the largest significant effect on the glucose concentration. The linear increase was due to the multicomponent structure of Viscozyme L comprising of an endoglucanases, exoglucanases and a β -glucosidase that functioned synergistically resulting in the increase of glucose production as the hydrolysis continues (Bester, 2018). Furthermore, an increase in the mono-component enzyme, FiberCare R resulted in slight increases in glucose concentration (14 to 18 g/L). The increase was mainly attributed to the synergistic behaviour of FiberCare R in the presence of an enzyme such as Viscozyme L which enhanced cellulase performance resulting in an increase in glucose concentration (Kostylev and Wilson, 2012). At the optimum treatment conditions (4.64 h, 75 ECU/g Fibercare R dosage and 10.80 FBG/g Viscozyme L dosage) the glucose concentration of the produced ECN was 14.28 g/L with an ECN yield of $17.16 \pm 2.30\%$ achieving the aim of treatment (Figure 5.4). The yield of ECN obtained was higher than 11% yield obtained by both Anderson et al. (2014) and Bester (2018) when enzymatically hydrolysing bleached kraft pulp and paper sludge, respectively to produce cellulose nanoparticles. Moreover, the ECN yield ($17.16 \pm 2.30\%$) obtained at the optimum conditions was comparable to the yield obtained by the HCN ($20.31 \pm 1.24\%$) (Figure 5.4). The comparable yields between ECN and HCN indicated that both treatments performed almost equally in producing cellulose nanoparticles. In summary, the short residence time (4.64 h) enzymatic treatment performed as well as the 7.41 h hydrochloric acid treatment at the enzyme dosages and acid concentrations used. The yield of nanoparticles obtained implied that combination of the mono-component enzyme (FiberCare R) and multicomponent enzyme (Viscozyme L) could help substantially reduce the time required to produce nanocellulose with enzymatic treatment thereby making the enzymatic treatment a more attractive nanocellulose production method.

The statistical model fitted to the mean diameter of the ECN produced indicated a poor fit with an R-squared value of 0.44 and a lack of fit F and P value of 6.21 and 0.507, respectively (Appendix B, Table 6.25). The result indicated that although there was some lack of correlation between the predicted and experimental values obtained by the model through ANOVA analysis, the lack of fit was statistically insignificant. Also, the mean particle diameter was found to be 12–22 nm, therefore the model was used in the optimisation process (Figure 5.5f, g and h). Previous studies by Bester (2018) and Bondeson et al. (2006) also noticed similar trends when optimising the particle size of nanoparticles produced by using an enzymatic approach and an acid approach, respectively. The short mean particle diameter of the various nanocellulose samples was due to the synergistic effect of the combination of FiberCare R

and Viscozyme L which cleaved the bonds of the micro and nanofibers of the wheat straw as similarly observed by De Campos et al. (2013). The length obtained for the various ECN produced at various treatment conditions were greater than 1 μm making it not suitable to be used in the optimisation. Similarly, at the optimum treatment condition the length was greater than 1 μm with a diameter of 17 nm indicating that the produced ECN were CNFs (Figure 5.4).

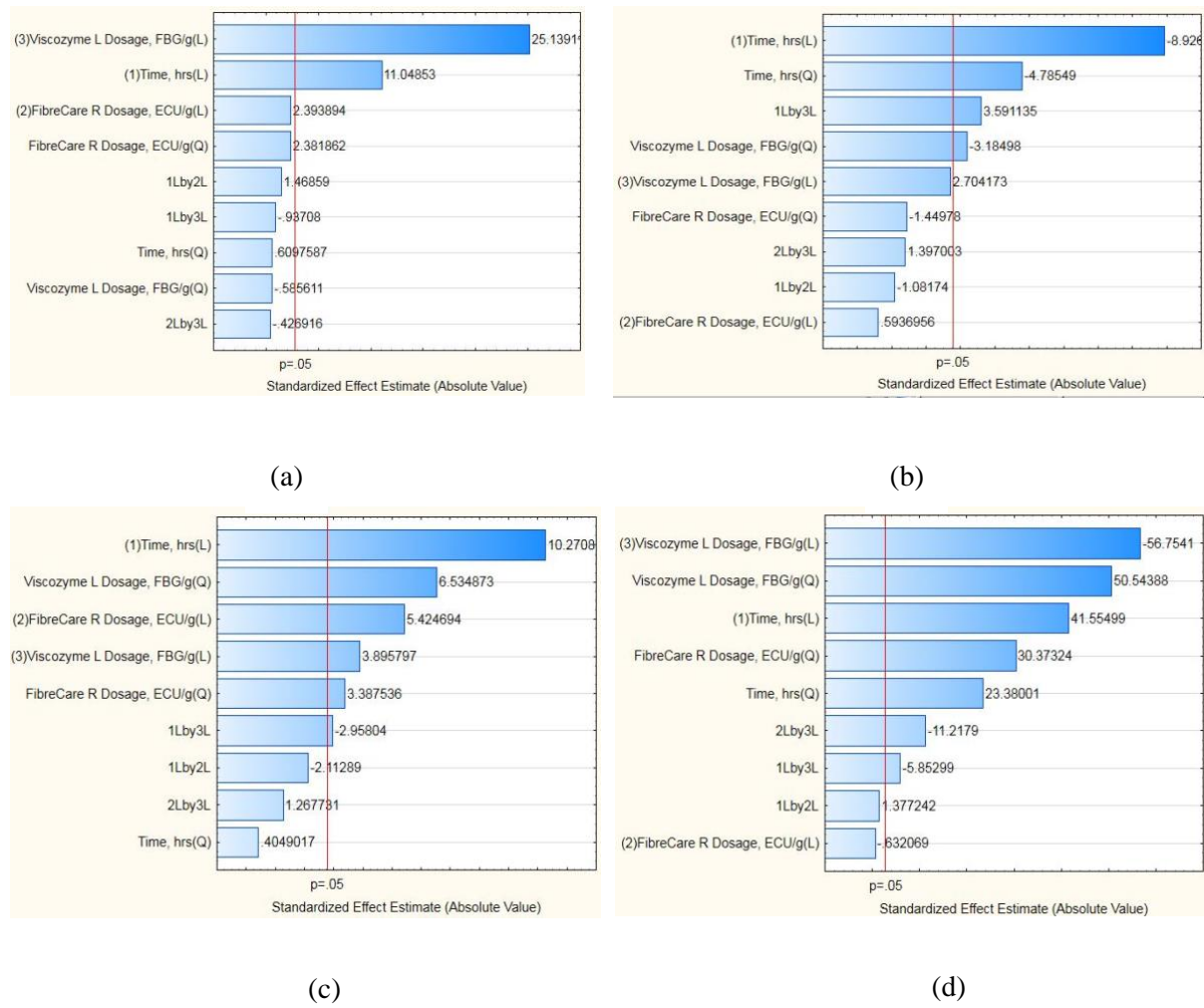


Figure 5.3 Pareto chart of optimisation of enzymatic treatment produced nanocellulose (a) glucose concentration (b) zeta potential (c) polydispersity index (d) particle diameter

For the enzymatic treatment, the treatment time and Viscozyme dosage were found to have a significant effect on the zeta potential with both having a quadratic and linear effect on the zeta potential with an R-squared of 0.85. The significance of both effects means that the optimum treatment conditions were reached with both treatment conditions. An increase in time from 4 to 6 hours and an increase in Viscozyme dosage from 10 to 15 FBG/g resulted in an increase in the zeta potential. On the other hand, a further increase in time and Viscozyme dosage resulted in a reduction in zeta potential. The zeta potential of the optimised ECN was -15.2 ± 0.6 mV, which indicated that the produced nanocellulose had a relative stability in water (Patel and Agrawal, 2011). Furthermore, the obtained ECN ZP was comparable to that obtained for HCN (-16.3 ± 1.5 mV), indicating that with enzymatic treatment

coupled with mechanical treatment almost equal stability of the nanocellulose can be obtained as that of a mild acid approach (Figure 5.4).

The polydispersity index (PdI) for all the ECN samples indicated a more polydispersed nature of all the samples with PdI values between 0.9-1.0. However, the model resulted in an R-squared value of 0.91 which indicated a good correlation between the model and experimental values. The PdI was found to increase with an increase in treatment time, which was attributed to the linear effect observed in Figure 5.3c. Furthermore, it was found that both enzymes had a linear and quadratic effect on the PdI observed (Figure 5.3c). The PdI was found to reduce as the Viscozyme and FiberCare dosages were increased from 10 to 15 FBG/g and 50 to 60 ECU/g, respectively. However, a further increase in the dosage of either enzyme resulted in an increase of ECN PdI (Figure 5.6). At the optimum conditions a PdI of 0.92 ± 0.13 which was comparable to that of commercial CNF with a PdI of 1 ± 0.03 was observed (Figure 5.6). Thus, indicating the high polydispersity nature of most nanofibers due to their structure (Espinosa et al., 2017).

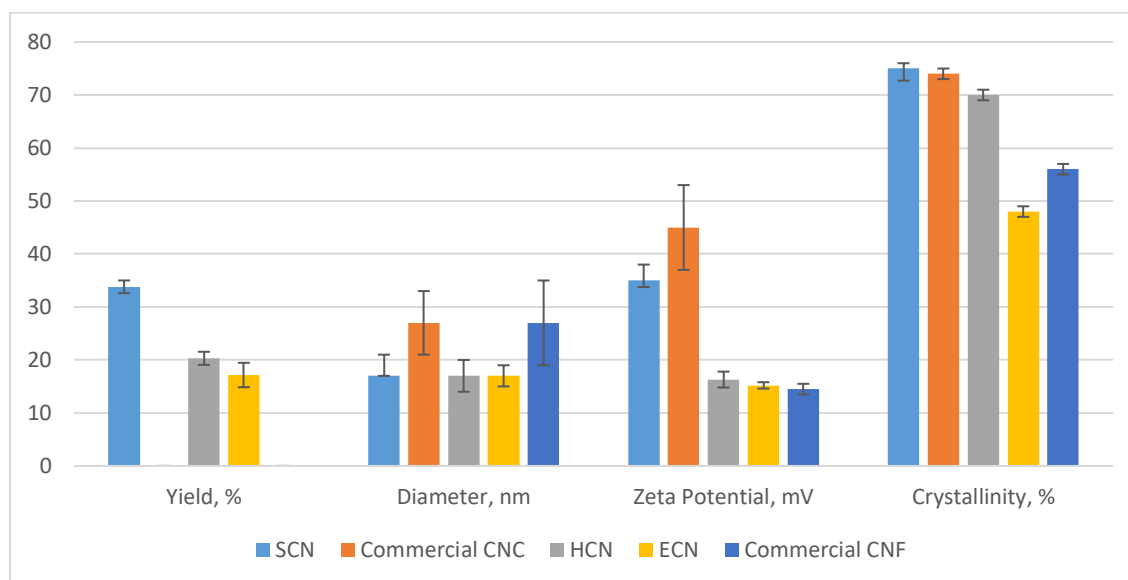


Figure 5.4 Yield, diameter, zeta potential and crystallinity for commercial nanocelluloses, sulphuric acid produced nanocelluloses (SCN), hydrochloric acid produced nanocelluloses (HCN), and enzymatic treatment produced nanocelluloses (ECN)

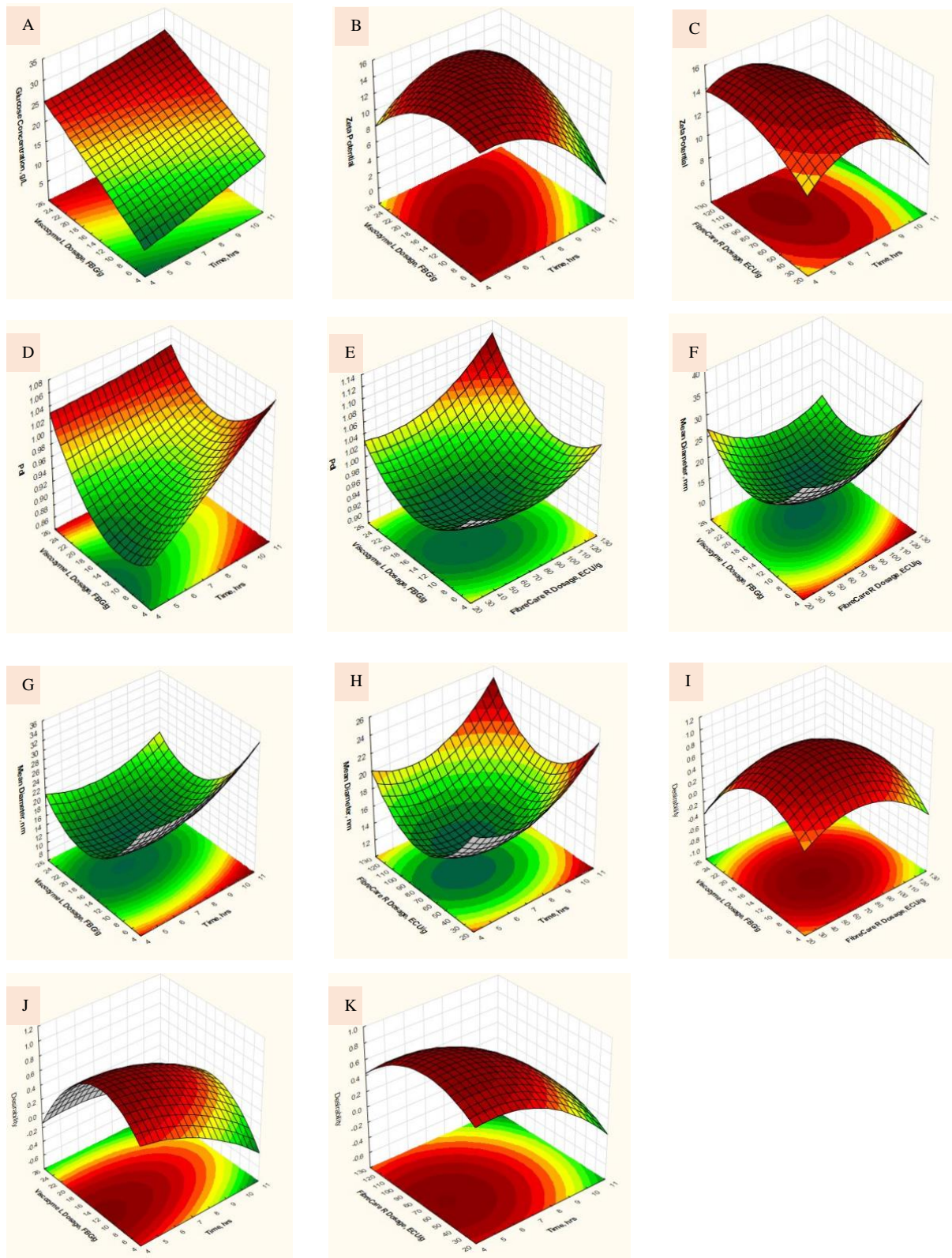


Figure 5.5 Surface plot of optimisation of ECN (A) Glucose Concentration (B-C) Zeta Potential (ZP) (D-E) Polydispersity Index (PdI) (F-H) Nanocellulose Diameter (I-K) Desirability with time (4.64 h), FiberCare Dosage (75 ECU/g) and Viscozyme Dosage (10.8 FBG/g) as dependent variables

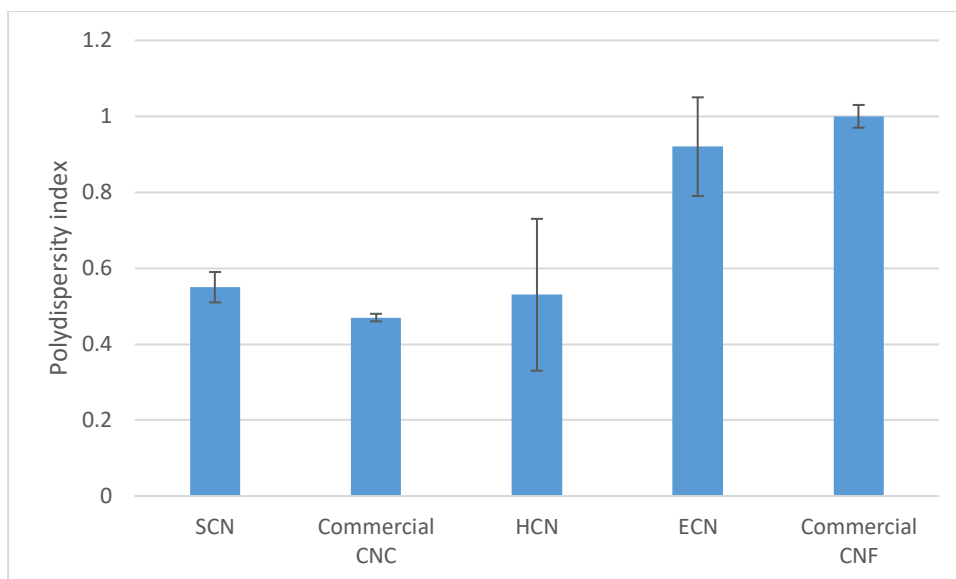


Figure 5.6 Polydispersity index of commercial nanocelluloses, sulphuric acid produced nanocelluloses (SCN), hydrochloric acid produced nanocelluloses (HCN), and enzymatic treatment produced nanocelluloses (ECN)

5.2 Fourier Transform Infrared Spectroscopy of Functional Group Changes of Produced Nanocelluloses and Commercial Nanocelluloses

The FTIR peaks of both the produced nanocelluloses (SCN, ECN and HCN) and the commercial CNC and CNF are represented in Figure 5.7. The various nanocellulose samples possessed the OH stretching peak at 3333cm^{-1} for cellulose (Maiti et al., 2013). Similarly, the β -glucosidic linkage between sugar units in cellulose, CO stretch of cellulose and the asymmetric stretch of cellulose were noticed by the presence of peaks at 896 , 1030 and 1160cm^{-1} , respectively (Oun and Rhim, 2016a). In addition, the characteristic peak of absorbed water at 1644cm^{-1} was observed in all produced nanocellulose samples (Li et al., 2018).

HCN, ECN and commercial CNC were noticed to possess significant peaks at 2900cm^{-1} and 1427cm^{-1} which indicated the presence of CH_2 stretching and the CH deformation of cellulose, respectively. The presence of these two peaks in HCN, commercial CNC and ECN and its absence from the commercial CNF and SCN could be attributed to the harshness of the treatment performed on the cellulose. Although the hydrochloric acid used in the production of HCN was milder than the sulfuric acid used, it was noticed from the Figure 5.2 that as process conditions exceeded 100°C , it resulted in reduction of yield from deformation and loss of cellulose. Similarly, the production of ECN resulted in the increase in glucose concentration from the deformation of cellulose. In addition, due to the presence of a peak at 1226cm^{-1} indicating the OH deformation of cellulose in the commercial CNC, it can be summarised that the commercial CNC was also produced using a harsh treatment. Finally, the presence of a peak at 1315cm^{-1} attributed to CH_2 wagging of cellulose was noticed in the commercial CNC, SCN, HCN and ECN during the nanocellulose production process. The results obtained from the FTIR spectra agreed

with the results obtained from sulfuric acid hydrolysis, optimisations of the hydrochloric acid and the enzymatic produced nanoparticles.

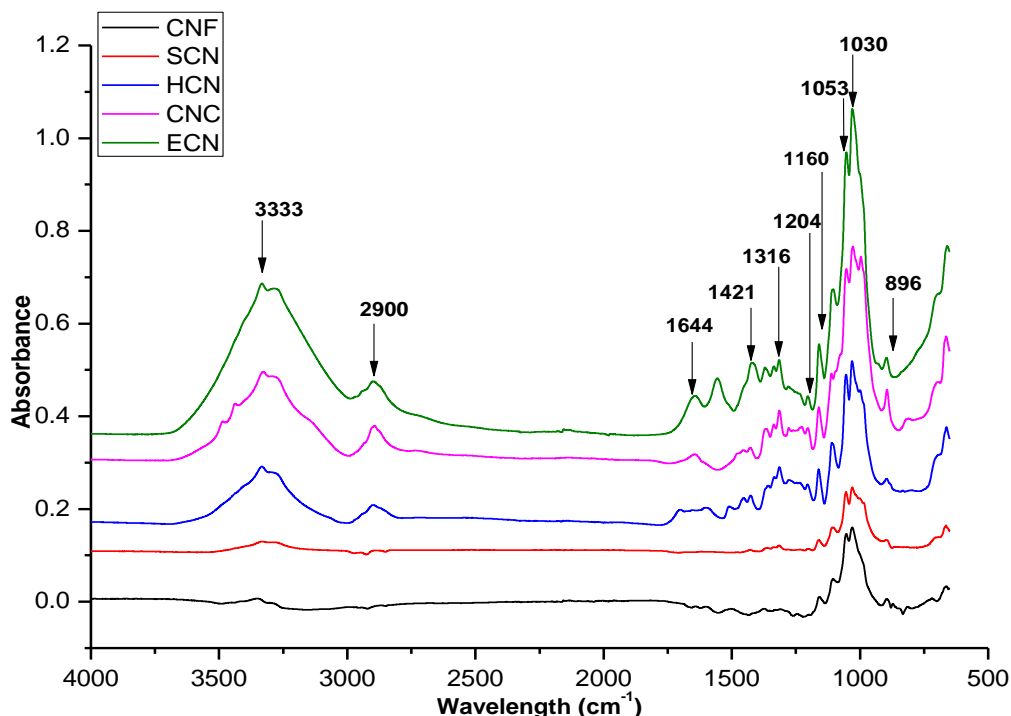


Figure 5.7 FTIR spectra of chemical group changes of nanofibrillated cellulose (CNF), cellulose nanocrystals (CNC), sulfuric acid nanoparticles (SCN), hydrochloric acid nanoparticles (HCN) and enzymatic cellulose nanoparticles (ECN).

5.3 X-Ray Diffraction and Crystallinity of Produced Nanocelluloses and Commercial Nanocelluloses

The results for the XRD test performed on the various nanocellulose samples indicating their crystallinity were presented in Figure 5.4. SCN had the highest crystallinity of both the treated and the commercially obtained samples. SCN and HCN resulted in a 36% and 27% increase, respectively in the crystallinity of SAWS (55%), whereas ECN resulted in a 13% reduction in the crystallinity of SAWS. In addition, SCN had a slightly higher crystallinity (75%) than that of the commercial CNC (74%). The results indicated that the sulfuric acid treatment performed was not too harsh to destroy some of the crystalline portions of the SCN produced as supported by the lack of deformation of the cellulose groups from the FTIR spectra and the high yield (34%) of SCN obtained (Liu, 2017).

The results also indicated that, although hydrochloric acid treatment resulted in an increase in the crystallinity of the produced HCN from the SAWS, the crystallinity was 5% less than that of SCN. The observation could have been due to the elevated temperature (114⁰C) at the optimised conditions of

HCN as indicated by both Figure 5.2 and the FTIR spectra obtained (Figure 5.7). However, this result was in conformity with most literature, which indicated that sulfuric acid treatment performed at the right treatment conditions resulted in nanocellulose with higher crystallinity than hydrochloric acid produced nanocellulose (Zeni et al., 2015). Finally, the decrease in the crystallinity (13%) of ECN as compared with that of SAWS crystallinity was mainly due to the combination of the enzymatic and mechanical treatment used in the production of ECN. The reduction in crystallinity from the application of mechanical treatment was mainly due to the breaking of some of the crystalline regions of the nanocellulose produced, as well as depolymerisation of the nanocellulose resulting in the reduction of the crystallinity observed (De Campos et al., 2013). Furthermore, the presence of exoglucanases in Viscozyme L could have also attributed to the reduction in crystallinity since the exoglucanases mainly attacks crystalline regions (Siro and Plackett, 2010). The result obtained was in conformity with the FTIR spectra obtained in Figure 5.7 which also indicated the deformation of some cellulosic functional groups present in both HCN and ECN.

5.4 Thermal Stability of Produced Nanocelluloses and Commercial Nanocelluloses

Thermal stability of nanocellulosic materials is a principal factor to be considered in their use in nanocomposite materials for various applications, where temperature is an essential. Nanocellulosic materials, just as their precursor cellulose undergo two weight loss steps (Kunaver et al., 2016). The first weight loss attributed to evaporation of absorbed water from the nanocellulose was observed between 50–110°C for all nanocellulosic samples. Both commercial and produced nanocellulose experienced weight loss between 2-3%, indicating that most nanocellulose had low water retaining capacity (Figure 5.8).

A major weight loss was experienced between 180-420°C for all nanocellulose samples during the second phase weight loss (Figure 5.8). SCN, HCN and ECN experienced a reduction in their thermal properties in comparison to the SAWS (Figure 4.22) used in their production. The reduction in thermal properties could have been mainly due to their nano-fiber dimensions which led to a larger surface area, promoting effective heating and thermal degradation in comparison with the macroscopic structure of SAWS fibers (Jiang and Hsieh, 2013). ECN had the lowest T_{onset} value (174°C) which could have been as a result of the combination of the mechanical and enzymatic treatment which was performed (De Campos et al., 2013). SCN had a low T_{onset} (180°C) just slightly higher than that of ECN and the lowest T_{max} value (309°C). The result was mainly due to the presence of sulfate groups on the surface of SCN which substituted the OH groups of the nanocellulose, resulting in the reduction of the degradation activation energy (Teixeira et al., 2010).

HCN had the highest T_{max} value (380°C) among the produced nanocelluloses (SCN, HCN and ECN) which is characteristic of hydrochloric acid produced nanocellulose due to the absence of surface sulfate and carboxyl groups (Du et al., 2016). Furthermore, it was observed from Figure 5.8 that, although HCN had the highest T_{max} value (380°C) among the three produced nanocellulose samples, the T_{max} recorded for ECN was just slightly lower (378°C). The observation indicated that although two different methods were used in the production of HCN and ECN, by virtue of both being CNFs they had a relatively high T_{max} as compared to that of the CNC from SCN (Jonoobi et al., 2015). Moreover, the closeness in the T_{max} values of HCN and ECN could also be attributed to the insignificant difference between their zeta potential values ($-16.3 \pm 1.5 \text{ mV}$ and $-15.2 \pm 0.6 \text{ mV}$, respectively) (Kargarzadeh et al., 2012).

After pyrolysis at 600°C , the char obtained was estimated for both commercial and produced nanocellulose samples (Figure 5.8). The results indicated that all nanocellulose samples had a high char content (17-25%) as compared to SAWS (10%). However, the increase in char content observed was less than three times that of SAWS, which was less than the four to seven times reported by Jiang and Hsieh 2013. The char content observed for SCN was similar to that observed for sulfuric acid treated cotton linter (24.1%) (Kunaver et al., 2016). In addition, the char content observed for HCN was comparative to that observed for hydrochloric acid treated bleached softwood kraft pulp (30%) (Du et al., 2016). Furthermore, the high char remaining could be attributed to the favoured dehydration reaction of the nanocellulose at lower thermal temperatures. Finally, it was noticed that ECN had the lowest char content with respect to HCN, SCN and the commercial CNC, which was expected as most enzymatic produced nanoparticles have a relatively lower char content as compared to chemically produced ones (Espinosa et al., 2017).

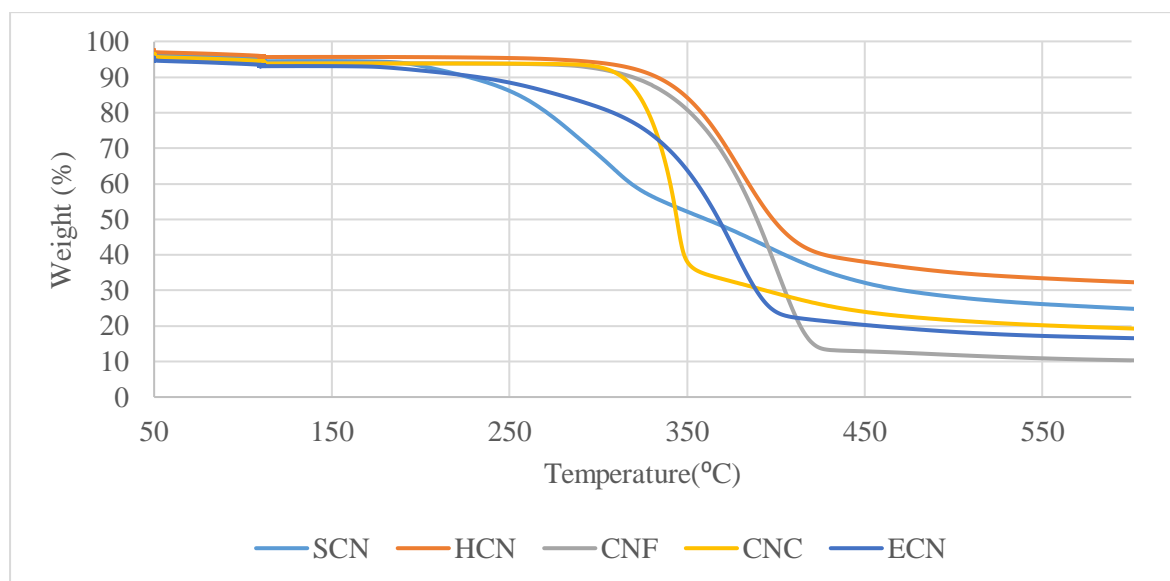


Figure 5.8 Thermogravimetric analysis of sulfuric acid nanoparticles (SCN), hydrochloric acid nanoparticles (HCN), nanofibrillated cellulose (CNF), cellulose nanocrystals (CNC), enzymatic cellulose nanoparticles (ECN)

In summary, the alternative treatment methods, hydrochloric acid, and enzymatic treatment resulted in improved thermal degradation temperatures in comparison to the traditional sulfuric acid treatment. Furthermore, hydrochloric acid and enzymatic treatment resulted in almost similar yields and zeta potentials albeit lower than that of the sulfuric acid treatment.

5.5 Conclusions

The alternative treatments (hydrochloric acid and enzymatic treatment) performed, resulted in similar yields, zeta potential and maximum thermal degradation temperatures. In addition, although the values were not statistically different, the hydrochloric acid treatment performed slightly better than the enzymatic treatment. Moreover, the hydrochloric acid treatment resulted in nanoparticles with improved crystallinity in comparison to the cellulose-rich fibers used whereas the enzymatic treatment resulted in a reduction in crystallinity of its nanoparticles in comparison to the cellulose-rich fibers. However, the treatment resulted in the production of ECN with the lowest char content.

On the other hand, the sulfuric acid treatment resulted in a higher yield, zeta potential and crystallinity in comparison to the alternative approaches. These results indicated that sulfuric acid treatment conditions carefully selected can result in the production of nanoparticles with high yields and less cellulose deformations. However, the maximum thermal degradation temperature of the sulfuric acid nanoparticles was found to be the least in comparison to the alternative approaches. This was mainly due to the sulfate groups attached to the sulfuric acid hydrolysed cellulose nanoparticles.

In conclusion, both enzymatic and hydrochloric acid treatment performed similarly in terms of yield and zeta potential with higher maximum thermal degradation temperature than the traditional sulfuric acid treatment. In addition, the yield of nanoparticles obtained from enzymatic treatment were obtained at a relatively shorter treatment time (4.64 h) with respect to the yield of the hydrochloric acid produced nanoparticles (7.41 h) making it a more attractive treatment approach when considering yield of nanoparticles produced. Nevertheless, the PDI recorded at the optimum condition for the hydrochloric acid treatment (0.53 ± 0.20) was within the ranges of that recorded for the sulfuric acid treatment (0.55 ± 0.04). The hydrochloric acid treatment also resulted in a crystallinity index (70%) that was the closest to that of the sulfuric acid treatment (75%). In conclusion, the hydrochloric acid treatment conditions improved the nanoparticle polydispersity index and fiber morphology as compared to enzymatic hydrolysis.

The nanocelluloses produced (SCN, HCN and ECN) presents the potential to be applied in aerogels, hydrogels and wastewater treatment (France et al., 2017; Shak et al., 2018). Due to the increased surface area and crystalline nature of the nanocelluloses, it makes them a suitable for application as adsorbent in wastewater treatment. The ECN and HCN can be applied in the treatment of industrial or aquaculture wastewater containing residual antibiotics (Shak et al., 2018). The presence of the surface hydroxyl

groups provides hydrophilic sites that promotes the self-assemble and growth of inorganic particles into a new structure by nucleation. The SCN can also be applied in industrial and mining wastewater streams containing metals (Shak et al., 2018). The presence of the surface sulphate groups, serves to attract the metal particles resulting in the removal of the metals from the wastewater.

CHAPTER SIX

CONCLUSIONS AND RECOMMENDATION

This research was aimed at producing nanocellulose from wheat straw and wheat bran while co-extracting valuable products in the process. To achieve this a two-stage alkaline treatment was chosen to help fractionate the complex cell wall matrix to release lignin, hemicelluloses, ferulic and *p*-Coumaric acid. The mild alkaline treatment was optimised for extraction of hemicelluloses and *p*-Coumaric acid or ferulic acid for wheat straw and wheat bran, respectively. Whereas, the alkaline delignified treatment was optimised for improving the cellulose content of the residue whereas reducing its lignin content for nanocellulose production. The cellulose-rich pulp obtained after the alkaline delignification treatment was then treated with sulfuric acid, hydrochloric acid as well as with enzymes combined with a mechanical treatment to produce nanocellulose.

6.1 Conclusions

A few conclusions could be drawn from the results obtained at various stages of treatment

The destarching performed on the wheat bran resulted in an almost 100% starch extraction as well as a reduction of the protein content by almost 34%. The results from the destarching treatment indicated that an efficient destarching would not only lead to the removal of starch but would also lead to partial removal of protein thereby increasing cell wall components content with respect to the destarched wheat bran residue, improving cellulose crystallinity and loosening of cell wall matrix for subsequent extractions.

The two-stage alkaline treatments of wheat straw resulted in a *p*-coumaric acid, lignin, and hemicellulose yield of 85%, 68% and 77%, respectively. The results are comparable to results obtained by researchers who have extracted *p*-coumaric acid, hemicellulose, and lignin from wheat straw. However, the treatment methodology resulted in hemicelluloses with significant lignin contaminations. Although, the lignin contamination could have been reduced by applying a delignification (bleaching) step before the mild alkaline treatment, it would have also resulted in a significant loss (at least 20%) of hemicellulose and *p*-coumaric acid (K. Liu et al., 2016). In conclusion, the two-stage alkaline treatment was able to achieve the aims of the research by extracting hemicellulose, lignin and *p*-coumaric acid from the wheat straw.

Furthermore, the two-stage alkaline treatment improved the cellulose content while reducing the lignin content of the residues for nanocellulose production. The cellulose content and lignin content of the residues were 76% and 5%, respectively. This resulted in an increase in crystallinity from an initial 44% to 55%. The cellulose rich pulp was found to meet the criteria for application in nanocellulose production. In summary, the two-stage alkaline treatment was an effective treatment method to produce cellulose-rich fibers from wheat straw for nanocellulose production.

The two-stage alkaline treatment of wheat bran resulted in a ferulic acid, lignin and hemicellulose yield of 66%, 94% and 52%, respectively. Similar to the wheat straw hemicelluloses, wheat bran hemicelluloses had lignin as its main contaminant. However, the lower hemicelluloses yield was attributed to the process conditions for the delignification treatment. The delignification treatment led to significant loss (10%) of hemicelluloses and cellulose (17%) within the mild alkaline treated wheat bran, which indicated that the delignification treatment was unfavourable choice for the wheat bran.

Although, the delignification treatment was unfavourable for the destarched wheat bran, it still led to the improvement of both the cellulose content (from 17% to 48%) and crystallinity (from 17% to 41%) whereas reducing the lignin content (from 19% to 6%) of the obtained residues. However, the significant loss of cellulose resulted in a reduction in the thermal stability temperatures for delignified wheat bran residues. Moreover, the hemicellulose content (31%), cellulose content and crystallinity of the cellulose pulp obtained after the two-stage alkaline treatment of the wheat bran indicated that cellulose-rich pulp obtained did not meet the criteria to be directly applied in nanocellulose production.

Nanocellulose production from delignified wheat straw using sulfuric acid, hydrochloric acid and enzymatic treatment presented certain interesting results. The results indicated that although sulfuric acid produced cellulose nanoparticles presented a higher yield (34%) and crystallinity (75%), it presented lower thermal properties as compared to both hydrochloric acid and enzymatic treatment. In addition, the yield, zeta potential and maximum thermal decomposition temperature for nanoparticles produced by enzymatic treatment were similar to that of hydrochloric acid treatment. Furthermore, enzymatic treatment performed at a shorter treatment time (4.64 h) resulted in a yield comparable with the hydrochloric acid treatment performed at a longer time (7.41 h). The crystallinity obtained for hydrochloric acid produced nanocellulose presented values (70%), which were close to that of sulfuric acid produced nanoparticles and higher than both commercial CNF (56%) and enzymatic hydrolysis produced nanoparticles (48%). Moreover, hydrochloric acid produced cellulose nanoparticles resulted in improved polydispersity index (0.53 ± 0.20) and fiber morphology (514 ± 50 nm length) as compared to both enzymatic treatment and commercial CNF. In summary, between enzymatic and hydrochloric acid treatments, the latter resulted in nanoparticles with improved properties than the former.

Furthermore, the properties and characteristics of the products obtained at various stages of the treatment indicates potential to be applied and not limited to the outlined field

Table 6.1 Potential applications of various treatment products based on analysed characteristics

Product	Potential applications	References
Hemicelluloses	Hydrogels and additive in paper making industries	Farhat et al., (2017); Matavire, (2018); Yuan et al., (2016)
Lignin	Polymer composite materials and partial replacement in phenolic resins	Li and McDonald, (2014); Watkins et al., (2015)
Ferulic acid	As precursor in vanillin production, pharmaceutical industry	Ou et al., (2007); Tapin et al., (2006)
<i>p</i> -Coumaric acid	As precursor in <i>p</i> -hydroxybenzoic acid production, enhancing foaming abilities and applications in emulsions	K. Jiang et al., (2016); Phongthai et al., (2016)
SCN, HCN and ECN	Aerogels, hydrogels, and waste-water treatment	(France et al., 2017; Shak et al., 2018)

6.2 Recommendations and future work

The purity of the hemicelluloses and lignin could have been improved by dialysing the ethanol precipitated products before drying. The dialysis of the product before drying would have resulted in reduction of the neutralised salts in the products thereby reducing the ash content to negligible levels serving to improve the purity of both lignin and hemicelluloses (Rabetafika et al., 2014).

Nanocellulose production treatments involving the production of cellulose-rich fiber from wheat bran could use wheat bran with a cellulose content and crystallinity above 20% and 30%, respectively as the starting material. It has been shown in this study that wheat bran with cellulose content <20% and crystallinity <20% could not meet criteria for cellulose-rich fibers for nanocellulose production after the two-step alkaline treatment. Therefore, the need to obtain a starting material with higher cellulose content and crystallinity.

The yield of both hydrochloric acid and enzymatic treated nanocellulose could be improved by using a high-pressure homogeniser after the treatments rather than using a high shear homogeniser as seen in most literature works (Kaushik & Singh 2011; Leitner et al. 2007). The use of a high-pressure homogeniser is known to improve the treatment efficiency by producing a higher yield of cellulose nanoparticles.

The polydispersity index of the nanocellulose samples could also be further improved by spray drying the nanocellulose samples instead of using the freeze drying method employed in this study. Bester

(2018) stated that employing spray drying instead of freeze drying could reduce nanoparticle agglomeration thereby improving further analysis of the nanoparticles.

Finally, the entire treatment process can be further improved by combining the nanocellulose treatment process with a bioethanol production as a co-product (Dai et al., 2018). A nanocellulose treatment such as the enzymatic treatment could make use of the hydrolysed glucose at the optimum treatment condition (14.28 g/l) to generate a theoretical yield of 7.3 g/l bioethanol. Production of the bioethanol will improve the process economics by increasing the number of products that can be obtained from the process.

Furthermore, technoeconomic analysis can be performed to determine the potential economic impact of the proposed treatment approach with respect to traditional treatment approaches. The maximising of the product profile with limited treatment steps should help improve the process economics. Converting a cheap agricultural residue such as wheat straw into cellulose (ZAR 537) then to nanocellulose (ZAR 8778) tends to increase the price of traditional product (cellulose) by about 16 times. Moreover, further improving the purity of products such as hemicelluloses, lignin, ferulic acid and *p*-coumaric acid could improve their market price thereby influencing the technoeconomic analysis of the process. Market prices such as ZAR 2439/3 g, ZAR 1250/100 g, ZAR 668/1 g, ZAR 710/1 g can be obtained for purified hemicelluloses, lignin, ferulic acid and *p*-coumaric acid, respectively.

REFERENCES

- Abraham, E., Deepa, B., Pothan, L.A., Jacob, M., Thomas, S., Cvelbar, U., Anandjiwala, R., 2011. Extraction of nanocellulose fibrils from lignocellulosic fibres: A novel approach. *Carbohydr. Polym.* 86, 1468–1475. doi:10.1016/j.carbpol.2011.06.034
- Adams, G.A., 1955. Constitution Of A Hemicellulose From Wheat Bran. *Can. J. Chem.* 33, 56–67. doi:10.1139/v55-009
- Adapa, P., Karunakaran, C., Tabil, L., Schoenau, G., 2009. Potential Applications of Infrared and Raman Spectromicroscopy for Agricultural Biomass, in: *Agricultural Engineering International: The CIGR Ejournal*. pp. 1–25.
- Adapa, P.K., Tabil, L.G., Schoenau, G.J., Canam, T., Dumonceaux, T., 2011. Quantitative Analysis of Lignocellulosic Components of Non-Treated and Steam Exploded Barley , Canola , Oat and Wheat Straw Using Fourier Transform Infrared Spectroscopy. *J. Agric. Sci. Technol.* 178–188.
- Aguedo, M., Fournies, C., Dermience, M., Richel, A., 2014. Extraction by three processes of arabinoxylans from wheat bran and characterization of the fractions obtained. *Carbohydr. Polym.* 105, 317–324. doi:10.1016/j.carbpol.2014.01.096
- Akgul, M., Kirci, H., 2009. An environmentally friendly organosolv (ethanol-water) pulping of poplar wood. *J. Environ. Biol.* 30, 735–740.
- Alain, D., Danièle, D., Michel, R.V., 2000. Cellulose microfibrils from potato tuber cells: Processing and characterization of starch-cellulose microfibril composites. *J. Appl. Polym. Sci.* 76, 2080–2092. doi:10.1002/(SICI)1097-4628(20000628)76:143.0.CO;2-U
- Alekhina, M., Ershova, O., Ebert, A., Heikkinen, S., Sixta, H., 2015. Softwood kraft lignin for value-added applications : Fractionation and structural characterization. *Ind. Crop. Prod.* 66, 220–228. doi:10.1016/j.indcrop.2014.12.021
- Alemdar, A., Sain, M., 2008a. Isolation and characterization of nanofibers from agricultural residues - Wheat straw and soy hulls. *Bioresour. Technol.* 99, 1664–1671. doi:10.1016/j.biortech.2007.04.029
- Alemdar, A., Sain, M., 2008b. Biocomposites from wheat straw nanofibers: Morphology, thermal and mechanical properties. *Compos. Sci. Technol.* 68, 557–565. doi:10.1016/j.compscitech.2007.05.044
- Andersen, N., 2007. *Enzymatic Hydrolysis of Cellulose*. Technical University of Denmark.
- Anderson, C., Simsek, S., 2019. Mechanical profiles and topographical properties of films made from alkaline extracted arabinoxylans from wheat bran , maize bran , or dried distillers grain. *Food*

Hydrocoll. 86, 78–86. doi:10.1016/j.foodhyd.2018.02.016

- Anderson, S.R., Esposito, D., Gillette, W., Zhu, J.Y., Baxa, U., Mcneil, S.E., 2014. Enzymatic preparation of nanocrystalline and microcrystalline cellulose. *Tappi J.* 13, 35–42.
- Angellier, H., Molina-Boisseau, S., Dufresne, A., 2005. Mechanical properties of waxy maize starch nanocrystal reinforced natural rubber. *Macromolecules* 38, 9161–9170. doi:10.1021/ma0512399
- Arte, E., Katina, K., Holopainen-mantila, U., Nordlund, E., 2015. Effect of hydrolyzing enzymes on wheat bran cell wall integrity and protein solubility. *Cereal Chem.* 93, 162–171. doi:10.1094/CCHEM-03-15-0060-R
- Asada, C., Nakamura, Y., Kobayashi, F., 2005. Chemical characteristics and ethanol fermentation of the cellulose component in autohydrolyzed bagasse. *Biotechnol. Bioprocess Eng.* 10, 346–352. doi:10.1007/BF02931853
- Ballesteros, I., Negro, M.J., Oliva, J.M., Cabanas, A., Manzanares, P., Ballesteros, M., 2006. Ethanol production from steam-explosion pretreated wheat straw. *Appl. Biochem. Biotechnol.* 129–132, 496–508.
- Barana, D., Salanti, A., Orlandi, M., Ali, D.S., Zoia, L., 2016. Biorefinery process for the simultaneous recovery of lignin, hemicelluloses, cellulose nanocrystals and silica from rice husk and *Arundo donax*. *Ind. Crops Prod.* 86, 31–39. doi:10.1016/j.indcrop.2016.03.029
- Barman, D.N., Haque, M.A., Kang, T.H., Kim, M.K., Kim, J., Kim, H., Yun, H.D., 2012. Alkali Pretreatment of Wheat Straw (*Triticum aestivum*) at Boiling Temperature for Producing a Bioethanol Precursor. *Biosci. Biotechnol. Biochem.* 76, 2201–2207. doi:10.1271/bbb.120480
- Bataillon, M., Mathaly, P., Cardinali, A.N., Duchiron, F., 1998. Extraction and purification of arabinoxylan from destarched wheat bran in a pilot scale. *Ind. Crops Prod.* 8, 37–43.
- Beaugrand, J., Crônier, D., Debeire, P., Chabbert, B., 2004. Arabinoxylan and hydroxycinnamate content of wheat bran in relation to endoxylanase susceptibility. *J. Cereal Sci.* 40, 223–230. doi:10.1016/j.jcs.2004.05.003
- Beck-Candanedo, S., Roman, M., Gray, D., 2005. Effect of conditions on the properties behavior of wood cellulose nanocrystals suspensions. *Biomacromolecules* 6, 1048–1054.
- BeMiller, J.N., Huber, K.C., 2012. Starch. *Ullmann's Encycl. Ind. Chem.* 34, 431–505. doi:10.1002/14356007.a25
- Bester, L.M., 2018. Development and optimisation of a process for cellulose nanoparticle production from waste paper sludge with enzymatic hydrolysis as an integral part. Stellenbosch University.

- Bharimalla, A.K., Deshmukh, S.P., Patil, P.G., Vigneshwaran, N., 2015. Energy Efficient Manufacturing of Nanocellulose by Chemo- and Bio-Mechanical Processes : A Review. *World J. Nano Sci. Eng.* 5, 204–212.
- Bian, J., Peng, F., Peng, P., Xu, F., Sun, R., 2010. Isolation and fractionation of hemicelluloses by graded ethanol precipitation from *Caragana korshinskii*. *Carbohydr. Res.* 345, 802–809. doi:10.1016/j.carres.2010.01.014
- Bondeson, D., Mathew, A., Oksman, K., 2006. Optimization of the isolation of nanocrystals from microcrystalline cellulose by acid hydrolysis. *Cellulose* 13, 171–180. doi:10.1007/s10570-006-9061-4
- Börjesson, M., Westman, G., 2015. Crystalline Nanocellulose - Preparation , Modification , and Properties, in: *Intech*. pp. 159–191.
- Boz, H., 2015. Ferulic acid in cereals - A review. *Czech J. Food Sci.* 33, 1–7. doi:10.17221/401/2014-CJFS
- Brand, T.S., Cloe, S.W.P., Franck, F., 1991. Wheat-straw as roughage component in finishing diets of growing lambs. *S. Afr. J. Anim. Sci.* 21, 184–188.
- Brillouet, J.-M., Mercier, C., 1981. Fractionation of Wheat Bran Carbohydrates. *J. Sci. Food Agric* 32, 243–251. doi:10.1002/jsfa.2740320307
- Brown, R.M., 1999. Cellulose structure and biosynthesis. *Pure Appl. Chem.* 71, 767–775. doi:10.1351/pac199971050767
- Buranov, A.U., Mazza, G., 2010. Extraction and characterization of hemicelluloses from flax shives by different methods. *Carbohydr. Polym.* 79, 17–25. doi:10.1016/j.carbpol.2009.06.014
- Buranov, A.U., Mazza, G., 2009. Extraction and purification of ferulic acid from flax shives , wheat and corn bran by alkaline hydrolysis and pressurised solvents. *Food Chem.* 115, 1542–1548. doi:10.1016/j.foodchem.2009.01.059
- Buranov, A.U., Mazza, G., 2008. Lignin in straw of herbaceous crops. *Ind. Crops Prod.* 8, 237–259. doi:10.1016/j.indcrop.2008.03.008
- Cansell, F., Rey, S., Beslin, P., 1998. Thermodynamic Aspects of Supercritical Fluids Processing: Applications of Polymers and Wastes Treatment. *Oil Gas Sci. Technol.* 53, 71–98. doi:10.2516/ogst:1998010
- Chabannes, M., Barakate, A., Lapierre, C., Marita, J.M., Ralph, J., Pean, M., Danoun, S., Halpin, C., Grima-Pettenati, J., Boudet, A.M., 2001. Strong decrease in lignin content without significant

- alteration of plant development is induced by simultaneous down-regulation of cinnamoyl CoA reductase (CCR) and cinnamyl alcohol dehydrogenase (CAD) in tobacco plants. *Plant J.* 28, 257–270. doi:10.1046/j.1365-313X.2001.01140.x
- Chen, M., Zhao, J., Xia, L., 2009. Comparison of four different chemical pretreatments of corn stover for enhancing enzymatic digestibility. *Biomass and Bioenergy* 33, 1381–1385. doi:10.1016/j.biombioe.2009.05.025
- Chen, W., Yu, H., Liu, Y., Chen, P., Zhang, M., Hai, Y., 2011. Individualization of cellulose nanofibers from wood using high-intensity ultrasonication combined with chemical pretreatments. *Carbohydr. Polym.* 83, 1804–1811. doi:10.1016/j.carbpol.2010.10.040
- Cheng, M., Qin, Z., Chen, Y., Hu, S., Ren, Z., Zhu, M., 2017. Efficient Extraction of Cellulose Nanocrystals through Hydrochloric Acid Hydrolysis Catalyzed by Inorganic Chlorides under Hydrothermal Conditions. *ACS Sustain. Chem. Eng.* 5, 4656–4664. doi:10.1021/acssuschemeng.6b03194
- Cheng, S., Wilks, C., Yuan, Z., Leitch, M., Charles, C., 2012. Hydrothermal degradation of alkali lignin to bio-phenolic compounds in sub / supercritical ethanol and water e ethanol co-solvent. *Polym. Degrad. Stab.* 97, 839–848. doi:10.1016/j.polymdegradstab.2012.03.044
- Cherian, B.M., Leao, A.L., de Souza, S.F., Thomas, S., Pothan, L.A., Kottaisamy, M., 2010. Isolation of nanocellulose from pineapple leaf fibres by steam explosion. *Carbohydr. Polym.* 81, 720–725. doi:10.1016/j.carbpol.2010.03.046
- Chiesa, S., Gnansounou, E., 2011. Protein extraction from biomass in a bioethanol refinery - Possible dietary applications: Use as animal feed and potential extension to human consumption. *Bioresour. Technol.* 102, 427–436. doi:10.1016/j.biortech.2010.07.125
- Chotěborská, P., Palmarola-Adrados, B., Galbe, M., Zacchi, G., Melzoch, K., Rychtera, M., 2004. Processing of wheat bran to sugar solution. *J. Food Eng.* 61, 561–565. doi:10.1016/S0260-8774(03)00216-4
- Ciolacu, D., Popa, V.I., 2005. Structural changes of cellulose determined by dissolution in aqueous alkali solution. *Cellul. Chem. Technol.* 39, 179–188.
- Cookman, D.J., Glatz, C.E., 2009. Extraction of protein from distiller's grain. *Bioresour. Technol.* 100, 2012–2017. doi:10.1016/j.biortech.2008.09.059
- Correa, A.C., Eliangela de Morais, T., Luiz, A.P., Mattoso, L.H.C., 2010. Cellulose nanofibers from curaua fibers. *Cellulose* 17, 1183–1192. doi:10.1007/s10570-010-9453-3
- Costa, L.A.S., Assis, D.D.J., Gomes, G.V.P., Jania, B.A., Fonsêca, A.F., Druzian, J.I., 2015. Extraction

- and characterization of nanocellulose from corn stover. *Mater. Today Proc.* 2, 287–294. doi:10.1016/j.matpr.2015.04.045
- Couteau, D., Mathaly, P., 1997. Purification of ferulic acid by adsorption after enzymic release from a sugar-beet pulp extract. *Ind. Crops Prod.* 6, 237–252.
- Cripwell, R., Favaro, L., Rose, S.H., Basaglia, M., Cagnin, L., Casella, S., van Zyl, W., 2015. Utilisation of wheat bran as a substrate for bioethanol production using recombinant cellulases and amylolytic yeast. *Appl. Energy* 160, 610–617. doi:10.1016/j.apenergy.2015.09.062
- Cui, Z., Shi, J., Wan, C., Li, Y., 2012. Comparison of alkaline- and fungi-assisted wet-storage of corn stover. *Bioresour. Technol.* 109, 98–104. doi:10.1016/j.biortech.2012.01.037
- Curreli, N., Fadda, M.B., Rescigno, A., Rinaldi, A.C.A., Soddu, G., Sollai, F., Vaccargiu, S., Sanjust, E., Rinaldi, A.C.A., Benedetta, F.M., Rescigno, A., Rinaldi, C.A., Soddu, G., Sollai, F., Vaccargiu, S., Sanjust, E., Rinaldi, A.C.A., 1997. Mild alkaline/oxidative pretreatment of wheat straw. *Process Biochem.* 32, 665–670. doi:10.1016/S0032-9592(97)00020-4
- Dai, J., Chae, M., Beyene, D., Danumah, C., Tosto, F., Bressler, D.C., 2018. Co-Production of Cellulose Nanocrystals and Fermentable Sugars Assisted by Endoglucanase Treatment of Wood Pulp. *Materials (Basel)*. 11, 1645. doi:10.3390/ma11091645
- Dale, B.E., Allen, M.S., Laser, M., Lynd, L.R., 2009. Protein feeds coproduction in biomass conversion to fuels and chemicals. *Biofuels, Bioprod. Biorefining* 6, 246–256. doi:10.1002/bbb
- Daniel, J.R., Whistler, R.L., Roper, H., Elvers, B., 2007. Starch, *Ullmann's Encyclopedia of Industrial Chemistry*. Wiley-VCH Verlag GmbH & Co. KGaA, Weinheim.
- De Campos, A., Correa, A.C., Cannella, D., de M Teixeira, E., Marconcini, J.M., Dufresne, A., Mattoso, L.H.C., Cassland, P., Sanadi, A.R., 2013. Obtaining nanofibers from curaua and and sugarcane bagasse fibers using enzymatic hydrolysis followed by sonication. *Cellulose* 20, 1491–1500. doi:10.1007/s10570-013-9909-3
- Deepa, B., Abraham, E., Cherian, B.M., Bismarck, A., Blaker, J.J., Pothan, L.A., Leao, A.L., de Souza, S.F., Kottaisamy, M., 2011. Structure, morphology and thermal characteristics of banana nano fibers obtained by steam explosion. *Bioresour. Technol.* 102, 1988–1997. doi:10.1016/j.biortech.2010.09.030
- Dinand, E., Chanzy, H., Vignon, M.R., 1999. Suspensions of cellulose microfibrils from sugar beet pulp. *Food Hydrocoll.* 13, 275–283.
- Doner, L.W., Hicks, K.B., 1997. Isolation of hemicellulose from corn fiber by alkaline hydrogen peroxide extraction. *Cereal Chem.* 74, 176–181. doi:10.1094/CCHEM.1997.74.2.176

- Du, H., Liu, C., Zhang, Y., Yu, G., Si, C., Li, B., 2016. Preparation and characterization of functional cellulose nanofibrils via formic acid hydrolysis pretreatment and the followed high-pressure homogenization. *Ind. Crop. Prod.* 94, 736–745. doi:10.1016/j.indcrop.2016.09.059
- Dubief, D., Samain, E., Dufresne, A., 1999. Polysaccharide microcrystals reinforced amorphous poly(3-hydroxyoctanoate) nanocomposite materials. *Macromolecules* 32, 5765–5771. doi:10.1021/ma990274a
- Dufresne, A., Cavallé, J.-Y., Helbert, W., 1997. Thermoplastic nanocomposites filled with wheat straw cellulose whiskers. Part II: Effect of processing and modeling. *Polym. Compos.* 18, 198–210. doi:10.1002/pc.10274
- Duguid, K.B., Montross, M.D., Radtke, C.W., Crofcheck, C.L., Wendt, L.M., Shearer, S.A., 2009. Effect of anatomical fractionation on the enzymatic hydrolysis of acid and alkaline pretreated corn stover. *Bioresour. Technol.* 100, 5189–5195. doi:10.1016/j.biortech.2009.03.082
- Egüés, I., Sanchez, C., Mondragon, I., Labidi, J., 2012. Effect of alkaline and autohydrolysis processes on the purity of obtained hemicelluloses from corn stalks. *Bioresour. Technol.* 103, 239–248. doi:10.1016/j.biortech.2011.09.139
- El-Sakhawy, M., Hassan, M.L., 2007. Physical and mechanical properties of microcrystalline cellulose prepared from agricultural residues. *Carbohydr. Polym.* 67, 1–10. doi:10.1016/j.carbpol.2006.04.009
- Emsley, A., Heywood, R., Ali, M., Eley, C., 1997. On the kinetics of degradation of cellulose. *Cellulose* 4, 1–5. doi:10.1023/A:1018408515574
- Eniko, V., Zsolt, S., Kati, R., 2002. Chemical Pretreatments of Corn Stover for Enhancing Enzymatic Digestibility. *Appl. Biochem. Biotechnol.* 02, 98–100.
- Eriksson, J., 2012. Barley starch, structure and properties. Swedish University of Agricultural Sciences.
- Eronen, P., Österberg, M., Jääskeläinen, A.S., 2009. Effect of alkaline treatment on cellulose supramolecular structure studied with combined confocal Raman spectroscopy and atomic force microscopy. *Cellulose* 16, 167–178. doi:10.1007/s10570-008-9259-8
- Espinosa, E., Sánchez, R., Otero, R., Domínguez-robles, J., Rodríguez, A., 2017. A comparative study of the suitability of different cereal straws for lignocellulose nanofibers isolation. *Int. J. Biol. Macromol.* 103, 990–999. doi:10.1016/j.ijbiomac.2017.05.156
- Farhat, W., Venditti, R., Quick, A., Taha, M., Mignard, N., Becquart, F., Ayoub, A., 2017. Hemicellulose extraction and characterization for applications in paper coatings and adhesives. *Ind. Crop. Prod.* 107, 370–377. doi:10.1016/j.indcrop.2017.05.055

- Favaro, L., Basaglia, M., Casella, S., 2012. Processing wheat bran into ethanol using mild treatments and highly fermentative yeasts. *Biomass and Bioenergy* 46, 605–617. doi:10.1016/j.biombioe.2012.07.001
- Ferrer, A., Filpponen, I., Rodríguez, A., Laine, J., Rojas, O.J., 2012. Valorization of residual Empty Palm Fruit Bunch Fibers (EPFBF) by microfluidization : Production of nanofibrillated cellulose and EPFBF nanopaper. *Bioresour. Technol.* 125, 249–255. doi:10.1016/j.biortech.2012.08.108
- Filson, P.B., Dawson-Andoh, B.E., Schwegler-Berry, D., 2009. Enzymatic-mediated production of cellulose nanocrystals from recycled pulp. *Green Chem.* 11, 1808. doi:10.1039/b915746h
- Foston, M., Ragauskas, A.J., 2010. Changes in lignocellulosic supramolecular and ultrastructure during dilute acid pretreatment of Populus and switchgrass. *Biomass and Bioenergy* 34, 1885–1895. doi:10.1016/j.biombioe.2010.07.023
- France, K.J. De, Hoare, T., Cranston, E.D., 2017. Review of Hydrogels and Aerogels Containing Nanocellulose. *Chem. Mater.* 29, 4609–4631. doi:10.1021/acs.chemmater.7b00531
- Fukuzumi, H., Saito, T., Iwata, T., Kumamoto, Y., Isogai, A., 2009. Transparent and High Gas Barrier Films of Cellulose Nanofibers Prepared by TEMPO-Mediated Oxidation Transparent and High Gas Barrier Films of Cellulose Nanofibers Prepared by TEMPO-Mediated Oxidation. *Biomacromolecules* 10, 162–165. doi:10.1021/bm801065u
- García-Aparicio, M., Trollope, K., Tyhoda, L., Diedericks, D., Görgens, J., 2011. Evaluation of triticale bran as raw material for bioethanol production. *Fuel* 90, 1638–1644. doi:10.1016/j.fuel.2010.10.049
- Garcia de Rodriguez, N.L., Thielemans, W., Dufresne, A., 2006. Sisal cellulose whiskers reinforced polyvinyl acetate nanocomposites. *Cellulose* 13, 261–270. doi:10.1007/s10570-005-9039-7
- García, J.C., Díaz, M.J., Garcia, M.T., Feria, M.J., Gómez, D.M., López, F., 2013. Search for optimum conditions of wheat straw hemicelluloses cold alkaline extraction process. *Biochem. Eng. J.* 71, 127–133. doi:10.1016/j.bej.2012.12.008
- Gardner, K.H., Blackwell, J., 1974. The hydrogen bonding in native cellulose. *BBA - Gen. Subj.* 343, 232–237. doi:10.1016/0304-4165(74)90256-6
- Garidel, P., Schott, H., 2006. Fourier-Transform Midinfrared Spectroscopy for Analysis and Screening of Liquid Protein Formulations Part 2: Detailed Analysis and Applications. *Bioprocess Int.* 1, 48–55.
- Giri, J., Adhikari, R., 2013. A Brief review on extraction of nanocellulose and its application. *Bibechana* 9, 81–87.

- Glasser, G.W., Sarkanen, S., 1989. Lignin Structure and Reactions. *Am. Chem. Soc.* 59, 1–21. doi:10.1021/ba-1966-0059
- Goesaert, H., Brijs, K., Veraverbeke, W.S., Courtin, C.M., Gebruers, K., Delcour, J.A., 2005. Wheat flour constituents: How they impact bread quality, and how to impact their functionality. *Trends Food Sci. Technol.* 16, 12–30. doi:10.1016/j.tifs.2004.02.011
- Gosselink, R., Kolk, H. Van Der, Harmsen, P., Bakker, R., 2010. Alkaline pretreatment of wheat straw, in: *Food and Biobased Research*. pp. 1–31.
- Griffith, W.L., Compere, A.L., 2008. Separation of Alcohols from Solution by Lignin Gels. *Sep. Sci. Technol.* 43, 2396–2405. doi:10.1080/01496390802148571
- Gruppen, H., Hamer, R.J., Voragen, A.G.J., 1992. Water-unextractable cell wall material from wheat flour. 1. Extraction of polymers with alkali. *J. Cereal Sci.* 16, 41–51. doi:10.1016/S0733-5210(09)80078-7
- Gupta, P.K., Uniyal, V., Naithani, S., 2013. Polymorphic transformation of cellulose I to cellulose II by alkali pretreatment and urea as an additive. *Carbohydr. Polym.* 94, 843–849. doi:10.1016/j.carbpol.2013.02.012
- Habibi, Y., 2014. Key advances in the chemical modification of nanocelluloses. *R. Soc. Chem.* 1519–1542. doi:10.1039/c3cs60204d
- Habibi, Y., Vignon, M.R., 2008. Optimization of cellouronic acid synthesis by TEMPO-mediated oxidation of cellulose III from sugar beet pulp. *Cellulose* 15, 177–185. doi:10.1007/s10570-007-9179-z
- Hames, B., Scarlata, C., Sluiter, A., 2008. Determination of Protein Content in Biomass. *Natl. Renew. Energy Lab.* 1–5. doi:Report No.TP-510-42625
- Han, L., Feng, J., Zhang, S., Ma, Z., Wang, Y., Zhang, X., 2012. Alkali pretreated of wheat straw and its enzymatic hydrolysis. *Brazilian J. Microbiol.* 43, 53–61. doi:10.1590/S1517-83822012000100006
- Harmsen, P., Huijgen, W., Bermudez, L., Bakker, R., López, L., Bakker, R., 2010. Literature Review of Physical and Chemical Pretreatment Processes for Lignocellulosic Biomass. *Food Biobased Res.* 1–49.
- Hassan, M.L., Mathew, A.P., Hassan, E.A., El-Wakil, N.A., Oksman, K., 2012. Nanofibers from bagasse and rice straw: Process optimization and properties. *Wood Sci. Technol.* 46, 193–205. doi:10.1007/s00226-010-0373-z

- Hasyierah, N., Salleh, M., Zulkali, M., Daud, M., Arbain, D., Ahmad, M.S., Syahidah, K., Ismail, K., 2011. Optimization of alkaline hydrolysis of paddy straw for ferulic acid extraction. *Ind. Crop. Prod.* 34, 1635–1640. doi:10.1016/j.indcrop.2011.06.010
- He, Y., Pang, Y., Liu, Y., Li, X., Wang, K., 2008. Physicochemical characterization of rice straw pretreated with sodium hydroxide in the solid state for enhancing biogas production. *Energy and Fuels* 22, 2775–2781. doi:10.1021/ef8000967
- Heikkinen, H., Elder, T., Maaheimo, H., Rovio, S., Rahikainen, J., Kruus, K., Tamminen, T., 2014. Impact of steam explosion on the wheat straw lignin structure studied by solution-state nuclear magnetic resonance and density functional methods. *J. Agric. Food Chem.* 62, 10437–10444. doi:10.1021/jf504622j
- Helbert, W., Cavaille, J.Y., Dufresne, A., 1996. Straw Cellulose Whiskers . Part I: Processing and mechanical behavior. *Polym. Compos.* 17, 604–611.
- Henriksson, M., Berglund, L.A., 2007. Structure and Properties of Cellulose Nanocomposite Films Containing Melamine Formaldehyde. *J. Appl. Polym. Sci.* 106, 2817–2824. doi:10.1002/app
- Henriksson, M., Henriksson, G., Berglund, L.A., Lindstro, T., 2007. An environmentally friendly method for enzyme-assisted preparation of microfibrillated cellulose (MFC) nanofibers. *Eur. Polym. J.* 43, 3434–3441. doi:10.1016/j.eurpolymj.2007.05.038
- Hosseinian, F.S., Mazza, G., 2009. Triticale bran and straw: Potential new sources of phenolic acids, proanthocyanidins, and lignans. *J. Funct. Foods* 1, 57–64. doi:10.1016/j.jff.2008.09.009
- Hou, F., Ding, W., Qu, W., Olayemi, A., Xiong, F., Zhang, W., 2017. Alkali solution extraction of rice residue protein isolates : Influence of alkali concentration on protein functional , structural properties and lysinoalanine formation. *Food Chem.* 218, 207–215. doi:10.1016/j.foodchem.2016.09.064
- Hu, F., Ragauskas, A., 2012. Pretreatment and Lignocellulosic Chemistry. *Bioenergy Res.* doi:10.1007/s12155-012-9208-0
- Islam, M.T., Alam, M.M., Zoccola, M., 2013. Review on modification of nanocelluloses for application in composites. *Int. J. Innov. Res. Technol. Sci.* 2, 5444–5451.
- Isogai, A., 2013. Wood nanocelluloses : fundamentals and applications as new bio-based nanomaterials. *J. Wood Sci* 59, 449–459. doi:10.1007/s10086-013-1365-z
- Jacquet, N., Maniet, G., Vanderghem, C., Delvigne, F., Richel, A., 2015. Application of Steam Explosion as Pretreatment on Lignocellulosic Material: A Review. *Ind. Eng. Chem. Res.* 54, 2593–2598. doi:10.1021/ie503151g

- Jaisamut, K., Paulová, L., Patáková, P., Rychtera, M., Melzoch, K., 2013. Optimization of alkali pretreatment of wheat straw to be used as substrate for biofuels production. *Plant, Soil Environ.* 59, 537–542.
- Janardhnan, S., Sain, M., 2011. Bio-Treatment of Natural Fibers in Isolation of Cellulose Nanofibres : Impact of Pre-Refining of Fibers on Bio-Treatment Efficiency and Nanofiber Yield. *J. Polymwe Env.* 19, 615–621. doi:10.1007/s10924-011-0312-6
- Janker-obermeier, I., Sieber, V., Faulstich, M., Schieder, D., 2012. Solubilization of hemicellulose and lignin from wheat straw through microwave-assisted alkali treatment. *Ind. Crop. Prod.* 39, 198–203. doi:10.1016/j.indcrop.2012.02.022
- Jiang, F., Hsieh, Y., 2013. Chemically and mechanically isolated nanocellulose and their self-assembled structures. *Carbohydr. Polym.* 95, 32–40. doi:10.1016/j.carbpol.2013.02.022
- Jiang, H., Chen, Q., Ge, J., Zhang, Y., 2014. Efficient extraction and characterization of polymeric hemicelluloses from hybrid poplar. *Carbohydr. Polym.* 101, 1005–1012. doi:10.1016/j.carbpol.2013.10.030
- Jiang, H., Zeng, Y., Nie, H., Li, Y., Ding, J., Zhou, H., 2016. NaOH Pretreatment of Wheat Straw at a Mesophilic Temperature: Effect on Hydrolysis and Loss of Organic Carbon. *Polish J. Environ. Stud.* 25, 1541–1548. doi:10.15244/pjoes/62647
- Jiang, K., Li, L., Long, L., Ding, S., 2016. Comparison of alkali treatments for efficient release of p - coumaric acid and enzymatic saccharification of sorghum pith. *Bioresour. Technol.* 207, 1–10. doi:10.1016/j.biortech.2016.01.116
- Johar, N., Ahmad, I., Dufresne, A., 2012. Extraction, preparation and characterization of cellulose fibres and nanocrystals from rice husk. *Ind. Crops Prod.* 37, 93–99. doi:10.1016/j.indcrop.2011.12.016
- Jonoobi, M., Oladi, R., Davoudpour, Y., 2015. Different preparation methods and properties of nanostructured cellulose from various natural resources and residues : a review. *Cellulose* 22, 935–969. doi:10.1007/s10570-015-0551-0
- Kalia, S., Boufi, S., Celli, A., Kango, S., 2014. Nanofibrillated cellulose: Surface modification and potential applications. *Colloid Polym. Sci.* 292, 5–31. doi:10.1007/s00396-013-3112-9
- Kalia, S., Dufresne, A., Cherian, B.M., Kaith, B.S., Avérous, L., Njuguna, J., Nassiopoulos, E., 2011. Cellulose-based bio- and nanocomposites: A review. *Int. J. Polym. Sci.* 2011, 1–35. doi:10.1155/2011/837875
- Kallel, F., Bettaieb, F., Khiari, R., García, A., Bras, J., Chaabouni, S.E., 2016. Isolation and structural characterization of cellulose nanocrystals extracted from garlic straw residues. *Ind. Crops Prod.*

87, 287–296. doi:10.1016/j.indcrop.2016.04.060

- Kamel, S., 2007. Nanotechnology and its applications in lignocellulosic composites, a mini review. *Express Polym. Lett.* 1, 546–575. doi:10.3144/expresspolymlett.2007.78
- Kargarzadeh, H., Ahmad, I., Abdullah, I., Dufresne, A., Zainudin, S.Y., Sheltami, R.M., 2012. Effects of hydrolysis conditions on the morphology, crystallinity, and thermal stability of cellulose nanocrystals extracted from kenaf bast fibers. *Cellulose* 19, 855–866. doi:10.1007/s10570-012-9684-6
- Karim, Z., Afrin, S., Husain, Q., Danish, R., 2016. Necessity of enzymatic hydrolysis for production and functionalization of nanocelluloses. *Crit. Rev. Biotechnol.* 1–16. doi:10.3109/07388551.2016.1163322
- Karp, E.M., Donohoe, B.S., O'Brien, M.H., Ciesielski, P.N., Mittal, A., Bidy, M.J., Beckham, G.T., 2014. Alkaline pretreatment of corn stover: Bench-scale fractionation and stream characterization. *ACS Sustain. Chem. Eng.* 2, 1481–1491. doi:10.1021/sc500126u
- Kaushik, A., Singh, M., 2011. Isolation and characterization of cellulose nanofibrils from wheat straw using steam explosion coupled with high shear homogenization. *Carbohydr. Res.* 346, 76–85. doi:10.1016/j.carres.2010.10.020
- Kekäläinen, K., Liimatainen, H., Biale, F., Niinimäki, J., 2015. Nanofibrillation of TEMPO-oxidized bleached hardwood kraft cellulose at high solids content. *Holzforschung* 69, 1077–1088. doi:10.1515/hf-2014-0269
- Kennedy, P.M., McSweeney, C.S., Welch, J.G., 1992. Influence of dietary particle size on intake, digestion, and passage rate of digesta in goats and sheep fed wheaten (*Triticum aestivum*) hay. *Small Rumin. Res.* 9, 125–138. doi:10.1016/0921-4488(92)90191-6
- Khalil, H.P.S.A., Bhat, A.H., Yusra, A.F.I., 2012. Green composites from sustainable cellulose nanofibrils: A review. *Carbohydr. Polym.* 87, 963–979. doi:10.1016/j.carbpol.2011.08.078
- Khan, T.S., Mubeen, U., 2012. Wheat Straw: A Pragmatic Overview 4, 673–675.
- Kim, J.S., Lee, Y.Y., Kim, T.H., 2016. A review on alkaline pretreatment technology for bioconversion of lignocellulosic biomass. *Bioresour. Technol.* 199, 42–48. doi:10.1016/j.biortech.2015.08.085
- Kim, K., Tsao, R., Yang, R., Cui, S.W., 2006. Phenolic acid profiles and antioxidant activities of wheat bran extracts and the effect of hydrolysis conditions. *Food Chem.* 95, 466–473. doi:10.1016/j.foodchem.2005.01.032
- Kim, S., Holtzapfle, M.T., 2006. Delignification kinetics of corn stover in lime pretreatment. *Bioresour.*

- Technol. 97, 778–785. doi:10.1016/j.biortech.2005.04.002
- Kim, T.H., Yoo, C.G., Lamsal, B.P., 2013. Front-end recovery of protein from lignocellulosic biomass and its effects on chemical pretreatment and enzymatic saccharification. *Bioprocess Biosyst. Eng.* 36, 687–694. doi:10.1007/s00449-013-0892-8
- Kirk-Othmer, 2001. *Kirk-Othmer Encyclopedia of Chemical Technology*, 4th, vol.20. ed, Encyclopedia of Chemical Technology. Wiley.
- Knill, C.J., Kennedy, J.F., 2003. Degradation of cellulose under alkaline conditions. *Carbohydr. Polym.* 51, 281–300. doi:10.1016/S0144-8617(02)00183-2
- Koegelenberg, D., 2016. Arabinoxylan as partial flour replacer : The effect on bread properties and economics of bread making by. Stellenbosch University. doi:10.1016/j.foodchem.2016.10.130
- Kostylev, M., Wilson, D., 2012. Synergistic interactions in cellulose hydrolysis. *Biofuels* 3, 61–70. doi:10.4155/bfs.11.150
- Koti, S., Prashanti, S., Gentela, J., Kothagauni, S., Jagavati, S., Rao, V., 2012. Optimization of Pretreatment of Wheat Straw Using Alkali and Biphasic Acid Hydrolysis. *Dyn. Biochem. Process Biotechnol. Mol. Biol.* 6, 91–94.
- Krässig, H., Schurz, J., Steadman, R.G., Schliefer, K., Albrecht, W., Mohring, M., Schlosser, H., 2012. Cellulose. *Ullmann's Encycl. Ind. Chem. Vol.6* 565–582. doi:10.1002/14356007.a05
- Kristensen, J.B., Borjesson, J., Bruun, M.H., Tjerneld, F., Jorgensen, H., 2007. Use of surface active additives in enzymatic hydrolysis of wheat straw lignocellulose. *Enzyme Microb. Technol.* 40, 888–895. doi:10.1016/j.enzmictec.2006.07.014
- Krogh, K., Olsson, L., 2008. Biomass degrading enzymes from *Penicillium* – cloning and characterization. Technical University of Denmark.
- Kumar, A., Negi, Y.S., Choudhary, V., Bhardwaj, N.K., 2014. Characterization of Cellulose Nanocrystals Produced by Acid-Hydrolysis from Sugarcane Bagasse as Agro-Waste. *J. Mater. Chem.* 2, 1–8. doi:10.12691/jmpc-2-1-1
- Kunaver, M., Anžlovar, A., Žagar, E., 2016. The fast and effective isolation of nanocellulose from selected cellulosic feedstocks. *Carbohydr. Polym.* 148, 251–258. doi:10.1016/j.carbpol.2016.04.076
- Lasseguette, E., Roux, D., Nishiyama, Y., 2008. Rheological properties of microfibrillar suspension of TEMPO-oxidized pulp. *Cellulose* 15, 425–433. doi:10.1007/s10570-007-9184-2
- Lee, D., Owens, V.N., Boe, A., Jeranyama, P., 2007. Composition of Herbaceous Biomass Feedstocks.

South Dakota.

- Lee, S., Chun, S., Kang, I., Park, J., 2009. Preparation of cellulose nanofibrils by high-pressure homogenizer and cellulose-based composite films. *J. Ind. Eng. Chem.* 15, 50–55. doi:10.1016/j.jiec.2008.07.008
- Lee, H. V, Hamid, S.B.A., Zain, S.K., 2014. Conversion of Lignocellulosic Biomass to Nanocellulose : Structure and Chemical Process. *Sci. World J.* 2014, 1–21. doi:10.1155/2014/631013
- Lehninger, A.L., Nelson, D.L., Cox, M.M., 2004. *Principles of Biochemistry*, 4th ed.
- Leitner, J., Hinterstoisser, B., Wastyn, M., Keckes, J., Gindl, W., 2007. Sugar beet cellulose nanofibril-reinforced composites. *Cellulose* 14, 419–425. doi:10.1007/s10570-007-9131-2
- Leticia, A., Pereira, M., Zanon, C.D., Menegalli, F.C., 2017. Isolation and characterization of cellulose nanofibers from cassava root bagasse and peelings. *Carbohydr. Polym.* 157, 962–970. doi:10.1016/j.carbpol.2016.10.048
- Li, B., Xu, W., Kronlund, D., Määttänen, A., Liu, J., Smått, J., Peltonen, J., Willför, S., Mu, X., Xu, C., 2015. Cellulose nanocrystals prepared via formic acid hydrolysis followed by TEMPO-mediated oxidation. *Carbohydr. Polym.* 133, 605–612. doi:10.1016/j.carbpol.2015.07.033
- Li, H., McDonald, A.G., 2014. Fractionation and characterization of industrial lignins. *Ind. Crop. Prod.* 62, 67–76. doi:10.1016/j.indcrop.2014.08.013
- Li, H., Sun, S., Zhou, X., Peng, F., Sun, R., 2015. Structural characterization of hemicelluloses and topochemical changes in Eucalyptus cell wall during alkali ethanol treatment. *Carbohydr. Polym.* 123, 17–26. doi:10.1016/j.carbpol.2014.12.066
- Li, J., Henriksson, G., Gellerstedt, G., 2007. Lignin depolymerization/repolymerization and its critical role for delignification of aspen wood by steam explosion. *Bioresour. Technol.* 98, 3061–3068. doi:10.1016/j.biortech.2006.10.018
- Li, J., Xu, Q.H., Jin, L.Q., 2013. Research Development on Hydrophobic Modification of Cellulose Nanofibrils. *Adv. Mater. Res.* 785–786, 440–443. doi:10.4028/www.scientific.net/AMR.785-786.440
- Li, R., Fei, J., Cai, Y., Li, Y., Feng, J., Yao, J., 2009. Cellulose whiskers extracted from mulberry: A novel biomass production. *Carbohydr. Polym.* 76, 94–99. doi:10.1016/j.carbpol.2008.09.034
- Li, Y.-Y., Wang, Bin, Ma, M.-G., Wang, Bo, 2018. The Influence of Pre-treatment Time and Sulfuric Acid on Cellulose Nanocrystals. *BioResources* 13, 3585–3602.
- Li, Y., Zhang, R., He, Y., Liu, X., Chen, C., Liu, G., 2014. Thermophilic Solid-State Anaerobic

- Digestion of Alkaline-Pretreated Corn Stover. *Energy and Fuels* 28, 3759–3765. doi:10.1021/ef5005495
- Lisperguer, J., Perez, P., Urizar, S., 2009. Structure and thermal properties of lignins; Characterization by infrared spectroscopy and differential scanning calorimetry. *J. Chil. Chem. Soc.* 54, 460–463.
- Liu, C., Li, B., Du, H., Lv, D., Zhang, Y., Yu, G., 2016. Properties of nanocellulose isolated from corncob residue using sulfuric acid, formic acid, oxidative and mechanical methods. *Carbohydr. Polym.* 151, 716–724. doi:10.1016/j.carbpol.2016.06.025
- Liu, C., Wyman, C.E., 2003. The Effect of Flow Rate of Compressed Hot Water on Xylan, Lignin, and Total Mass Removal from Corn Stover. *Ind. Eng. Chem. Res.* 42, 5409–5416. doi:10.1021/ie030458k
- Liu, K., Li, H., Zhang, J., Zhang, Z., Xu, J., 2016. The effect of non-structural components and lignin on hemicellulose extraction. *Bioresour. Technol.* 214, 755–760. doi:10.1016/j.biortech.2016.05.036
- Liu, Q., 2017. Isolation and characterization of nanocelluloses from wheat straw and their application in agricultural water-saving materials. University of Liège.
- Liu, Q., Lu, Y., Aguedo, M., Jacquet, N., Ouyang, C., He, W., Yan, C., Bai, W., Guo, R., Goffin, D., Song, J., Richel, A., 2017. Isolation of High-Purity Cellulose Nanofibers from Wheat Straw through the Combined Environmentally Friendly Methods of Steam Explosion, Microwave-Assisted Hydrolysis, and Microfluidization. *ACS Sustain. Chem. Eng.* 5, 6183–6191. doi:10.1021/acssuschemeng.7b01108
- Liu, Y., Ng, P.K.W., 2016. Relationship between bran characteristics and bran starch of selected soft wheats grown in Michigan. *Food Chem.* 197, 427–435. doi:10.1016/j.foodchem.2015.10.112
- Liu, Y., Ng, P.K.W., 2015. Isolation and characterization of wheat bran starch and endosperm starch of selected soft wheats grown in Michigan and comparison of their physicochemical properties. *Food Chem.* 176, 137–144. doi:10.1016/j.foodchem.2014.12.023
- Liu, Y., Wang, H., Yu, G., Yu, Q., Li, B., Mu, X., 2014. A novel approach for the preparation of nanocrystalline cellulose by using phosphotungstic acid. *Carbohydr. Polym.* 110, 415–422.
- López-rubio, A., Lagaron, J.M., Ankerfors, M., Lindström, T., Nordqvist, D., 2007. Enhanced film forming and W Im properties of amylopectin using micro- W brillated cellulose. *Carbohydr. Polym.* 68, 718–727. doi:10.1016/j.carbpol.2006.08.008
- Lorenz, M., Sattler, S., Reza, M., Bismarckab, A., Kontturi, E., 2017. Cellulose nanocrystals by acid vapour: towards more effortless isolation of cellulose nanocrystals. *R. Soc. Chem. Faraday*

- Discuss. 202, 315–330. doi:10.1039/c7fd00053g
- Lourenço, A., Pereira, H., 2018. Compositional Variability of Lignin in Biomass. *Intech* 65–98. doi:10.5772/intechopen.71208
- Lu, P., Hsieh, Y.-L., 2012. Preparation and characterization of cellulose nanocrystals from rice straw. *Carbohydr. Polym.* 87, 564–573. doi:10.1016/j.carbpol.2011.08.022
- Luzi, F., Puglia, D., Sarasini, F., Tirillò, J., Ma, G., Zuorro, A., Lavecchia, R., Kenny, J.M., Torre, L., 2019. Valorization and extraction of cellulose nanocrystals from North African grass: *Ampelodesmos mauritanicus* (Diss). *Carbohydr. Polym.* 209, 328–337. doi:10.1016/j.carbpol.2019.01.048
- Maiti, S., Jayaramudu, J., Das, K., Mohan, S., Sadiku, R., Sinha, S., Liu, D., 2013. Preparation and characterization of nano-cellulose with new shape from different precursor. *Carbohydr. Polym.* 98, 562–567. doi:10.1016/j.carbpol.2013.06.029
- Majzoobi, M., Abedi, E., 2014. Effects of pH changes on functional properties of native and acetylated wheat gluten. *Int. Food Res. J.* 21, 1219–1224.
- Malladi, R., Nagalakshmaiah, M., Robert, M., Elkoun, S., 2018. Importance of Agricultural and Industrial Waste in the Field of Nanocellulose and Recent Industrial Developments of Wood Based Nanocellulose: A Review. *ACS Sustain. Chem. Eng.* 1–23. doi:10.1021/acssuschemeng.7b03437
- Mandal, A., Chakrabarty, D., 2011. Isolation of nanocellulose from waste sugarcane bagasse (SCB) and its characterization. *Carbohydr. Polym.* 86, 1291–1299. doi:10.1016/j.carbpol.2011.06.030
- Mao, J.Z., Zhang, L.M., Xu, F., 2012. Fractional and structural characterization of alkaline lignins from *Carex meyeriana* Kunth. *Cellul. Chem. Technol.* 46, 193–205.
- Martelli-tosi, M., Masson, M.M., Silva, N.C., Esposto, B.S., Barros, T.T., Assis, O.B.G., Tapia-blácido, D.R., 2018. Soybean straw nanocellulose produced by enzymatic or acid treatment as a reinforcing filler in soy protein isolate films. *Carbohydr. Polym.* 198, 61–68. doi:10.1016/j.carbpol.2018.06.053
- Matavire, T.O., 2018. Extraction and Modification of hemicellulose from Wheat bran to produce entrapment materials for the controlled release of chemicals and bioactive substances. Stellenbosch University.
- Max, B., María, A., Belén, A., Converti, A., Manuel, J., 2009. Ferulic acid and p -coumaric acid solubilization by alkaline hydrolysis of the solid residue obtained after acid prehydrolysis of vine shoot prunings: Effect of the hydroxide and pH. *Biochem. Eng. J.* 43, 129–134.

doi:10.1016/j.bej.2008.09.015

- McIntosh, S., Vancov, T., 2011. Optimisation of dilute alkaline pretreatment for enzymatic saccharification of wheat straw. *Biomass and Bioenergy* 35, 3094–3103. doi:10.1016/j.biombioe.2011.04.018
- Megazyme, 2016. Total Starch Assay Procedure (Amyloglucosidase/ α -Amylase Method) 11, 1–10.
- Menon, V., Prakash, G., Rao, M., 2010. Value added products from hemicellulose : Biotechnological perspective. India.
- Merali, Z., Ho, J.D., Collins, S.R.A., Gall, G. Le, Elliston, A., Käsper, A., Waldron, K.W., 2013. Characterization of cell wall components of wheat bran following hydrothermal pretreatment and fractionation. *Bioresour. Technol.* 131, 226–234. doi:10.1016/j.biortech.2012.12.023
- Modenbach, A., 2013. Sodium hydroxide pretreatment of corn stover and subsequent enzymatic hydrolysis : An investigation of yields , kinetic modeling and glucose recovery. University of Kentucky.
- Monavari, S., Galbe, M., Zacchi, G., 2009. Impact of impregnation time and chip size on sugar yield in pretreatment of softwood for ethanol production. *Bioresour. Technol.* 100, 6312–6316. doi:10.1016/j.biortech.2009.06.097
- Montane, D., Farriol, X., Salvado, J., Jollez, P., Chornett, E., 1998. Application of Steam Explosion to the Fractionation and Rapid Vapor-Phase Alkaline Pulping of Wheat Straw. *Biomass and Bioenergy* 14, 261–276.
- Morais, J.P.S., Rosa, M.D.F., Filho, M. de sá M. de S., Nascimento, L.D., Nascimento, D.M. do, Cassales, A.R., 2013. Extraction and characterization of nanocellulose structures from raw cotton linter. *Carbohydr. Polym.* 91, 229–235. doi:10.1016/j.carbpol.2012.08.010
- Moran, J.I., Alvarez, V.A., Cyras, V.P., Vazquez, A., 2008. Extraction of cellulose and preparation of nanocellulose from sisal fibers. *Cellulose* 15, 149–159. doi:10.1007/s10570-007-9145-9
- Mosier, N., Wyman, C., Dale, B., Elander, R., Lee, Y.Y., Holtzapple, M., Ladisch, M., 2005. Features of promising technologies for pretreatment of lignocellulosic biomass. *Bioresour. Technol.* 96, 673–686. doi:10.1016/j.biortech.2004.06.025
- Mussatto, S.I., Dragone, G., Roberto, I.C., 2007. Ferulic and p -coumaric acids extraction by alkaline hydrolysis of brewer ' s spent grain. *Ind. Crops Prod.* 25, 231–237. doi:10.1016/j.indcrop.2006.11.001
- Nechyporchuk, O., 2015. Cellulose nanofibers for the production of bionanocomposites. Université

Grenoble Alpes.

- Nenkova, S., Vasileva, T., Stanulov, K., 2008. Production of Phenol Compounds By Alkaline Treatment of Technical Hydrolysis Lignin and Wood Biomass 44, 144–146.
- Neudoerffer, T.S., Smith, R.E., 1969. Enzymic degradation of wheat bran to improve its nutritional value for monogastrics. *Can. J. Anim. Sci.* 49, 205–214.
- Nilsson, C., 2017. Preparation and characterization of nanocellulose from wheat bran. Lund University.
- Olsson, C., Westman, G., 2013. Direct Dissolution of Cellulose : Background , Means and Applications. Intech 143–178.
- Onipe, O.O., Jideani, A.I.O., Beswa, D., 2015. Composition and functionality of wheat bran and its application in some cereal food products. *Int. J. Food Sci. Technol.* 50, 2509–2518. doi:10.1111/ijfs.12935
- Orts, W.J., Shey, J., Imam, S.H., Glenn, G.M., Guttman, M.E., Revol, J.F., 2005. Application of cellulose microfibrils in polymer nanocomposites. *J. Polym. Environ.* 13, 301–306. doi:10.1007/s10924-005-5514-3
- Ou, S., Luo, Y., Xue, F., Huang, C., Zhang, N., Liu, Z., 2007. Separation and purification of ferulic acid in alkaline-hydrolysate from sugarcane bagasse by activated charcoal adsorption / anion macroporous resin exchange chromatography. *J. Food Eng.* 78, 1298–1304. doi:10.1016/j.jfoodeng.2005.12.037
- Ou, S.Y., Teng, J.W., Zhao, Y.Y., Zhao, J., 2012. p-Coumaric acid production from lignocelluloses. *Phenolic Acids Compos. Appl. Heal. Benefits* 63–71.
- Oun, A.A., Rhim, J.W., 2016a. Isolation of cellulose nanocrystals from grain straws and their use for the preparation of carboxymethyl cellulose-based nanocomposite films. *Carbohydr. Polym.* 150, 187–200. doi:10.1016/j.carbpol.2016.05.020
- Oun, A.A., Rhim, J.W., 2016b. Characterization of nanocelluloses isolated from Ushar (*Calotropis procera*) seed fiber: Effect of isolation method. *Mater. Lett.* 168, 146–150. doi:10.1016/j.matlet.2016.01.052
- Paakko, M., Ankerfors, M., Kosonen, H., Nykanen, A., Ahola, S., Osterberg, M., Ruokolainen, J., Laine, J., Larsson, P.T., Ikkala, O., Lindstrom, T., 2007. Enzymatic Hydrolysis Combined with Mechanical Shearing and High-Pressure Homogenization for Nanoscale Cellulose Fibrils and Strong Gels. *Biomacromolecules* 8, 1934–1941.
- Palmarola-Adrados, B., Chotěborská, P., Galbe, M., Zacchi, G., 2005. Ethanol production from non-

- starch carbohydrates of wheat bran. *Bioresour. Technol.* 96, 843–850. doi:10.1016/j.biortech.2004.07.004
- Pan, G.X., Bolton, J.L., Leary, G.J., Street, K.C., Tn, C., 1998. Determination of Ferulic and p - Coumaric Acids in Wheat Straw and the Amounts Released by Mild Acid and Alkaline Peroxide Treatment. *J. Agric. Food Chem.* 46, 5283–5288. doi:10.1021/jf980608f
- Park, S., Baker, J.O., Himmel, M.E., Parilla, P.A., Johnson, D.K., 2010. Cellulose crystallinity index: measurement techniques and their impact on interpreting cellulase performance. *Biotechnol. Biofuels* 3, 10. doi:10.1186/1754-6834-3-10
- Patel, V.R., Agrawal, Y.K., 2011. Nanosuspension : An approach to enhance solubility of drugs. *J. Adv. Pharm. Technol. Res.* 2, 81–88. doi:10.4103/2231-4040.82950
- Peng, F., Bian, J., Ren, J., Peng, P., Xu, F., Sun, R., 2010a. Fractionation and characterization of alkali-extracted hemicelluloses from peashrub. *Biomass and Bioenergy* 39, 20–30. doi:10.1016/j.biombioe.2010.08.034
- Peng, F., Ren, J., Xu, F., Bian, J., Peng, P., Sun, R.-C., 2010b. Fractional Study of Alkali-Soluble Hemicelluloses Obtained by Graded Ethanol Precipitation from Sugar Cane Bagasse. *J. Agric. Food Chem.* 58, 1768–1776. doi:10.1021/jf9033255
- Peng, Y., Wu, S., 2010. The structural and thermal characteristics of wheat straw hemicellulose. *J. Anal. Appl. Pyrolysis* 88, 134–139. doi:10.1016/j.jaap.2010.03.006
- Penttilä, Paavo A., Várnai, A., Fernández, M., Kontro, I., Liljeström, V., Lindner, P., Siika-aho, M., Viikari, L., Serimaa, R., 2013. Small-angle scattering study of structural changes in the microfibril network of nanocellulose during enzymatic hydrolysis. *Cellulose* 20, 1031–1040. doi:10.1007/s10570-013-9899-1
- Penttilä, Paavo A, Várnai, A., Pere, J., Tammelin, T., Salmén, L., Siika-aho, M., Viikari, L., Serimaa, R., 2013. Xylan as limiting factor in enzymatic hydrolysis of nanocellulose. *Bioresour. Technol.* 129, 135–141. doi:10.1016/j.biortech.2012.11.017
- Pereira, P.H.F., Waldron, K.W., Wilson, D.R., Cunha, A.P., Brito, E.S. De, Rodrigues, T.H.S., Rosa, M.F., Azeredo, H.M.C., 2017. Wheat straw hemicelluloses added with cellulose nanocrystals and citric acid . Effect on film physical properties. *Carbohydr. Polym.* 164, 317–324. doi:10.1016/j.carbpol.2017.02.019
- Perez, S., Bertoft, E., 2010. The molecular structures of starch components and their contribution to the architecture of starch granules : A comprehensive review. *Starch* 62, 389–420. doi:10.1002/star.201000013

- Petrofsky, K.E., Marquart, L., Ruan, R., 2012. Improving The Functionality and Bioactivity of Wheat Bran. *J. Chem. Inf. Model.* 53, 1689–1699. doi:10.1017/CBO9781107415324.004
- Phanthong, P., Reubroycharoen, P., Hao, X., Xu, G., 2018. Nanocellulose : Extraction and application. *Carbon Resour. Convers.* 1, 32–43. doi:10.1016/j.crcon.2018.05.004
- Phongthai, S., Lim, S.-T., Rawdkuen, S., 2016. Optimization of microwave-assisted extraction of rice bran protein and its hydrolysates properties. *J. Cereal Sci.* 70, 146–154. doi:10.1016/j.jcs.2016.06.001
- Pino, M.S., Rodríguez-jasso, R.M., Michelin, M., Flores-gallegos, A.C., Morales-Rodriguez, R., Teixeira, J.A., Ruiz, H.A., 2018. Bioreactor design for enzymatic hydrolysis of biomass under the biore fi nery concept. *Chem. Eng. J.* 347, 119–136. doi:10.1016/j.cej.2018.04.057
- Pu, Y., Hu, F., Huang, F., Davison, B.H., Ragauskas, A.J., 2013. Assessing the molecular structure basis for biomass recalcitrance during dilute acid and hydrothermal pretreatments. *Biotechnol. Biofuels* 6, 1–13. doi:10.1186/1754-6834-6-15
- Pu, Y., Zhang, D., Singh, P.M., Ragauskas, A.J., 2008. The new forestry biofuels sector. *Biotechnol. Bioprod. Biorefining* 6, 246–256. doi:10.1002/bbb
- Quesada-Medina, J., López-Cremades, F.J., Olivares-Carrillo, P., 2010. Organosolv extraction of lignin from hydrolyzed almond shells and application of the d-value theory. *Bioresour. Technol.* 101, 8252–8260. doi:10.1016/j.biortech.2010.06.011
- Rabetafika, H.N., Bchir, B., Blecker, C., Paquot, M., Wathelet, B., 2014. Comparative study of alkaline extraction process of hemicelluloses from pear pomace. *Biomass and Bioenergy* 61, 254–264. doi:10.1016/j.biombioe.2013.12.022
- Rebouillat, S., Pla, F., 2013. State of the Art Manufacturing and Engineering of Nanocellulose : A Review of Available Data and Industrial Applications. *J. Biomater. Nanobiotechnol.* 4, 165–188.
- Reisinger, M., Tirpanalan, Ö., Huber, F., Kneifel, W., Novalin, S., 2014. Investigations on a wheat bran biorefinery involving organosolv fractionation and enzymatic treatment. *Bioresour. Technol.* 170, 53–61. doi:10.1016/j.biortech.2014.07.068
- Rezanezhad, S., Nazanezhad, N., Asadpur, G., 2013. Isolation of Nanocellulose from Rice Waste via Ultrasonication. *Lignocellulose* 2, 282–291.
- Ribeiro, R.S.A., Pohlmann, B.C., Calado, V., Bojorge, N., Junior, N.P., 2019. Production of nanocellulose by enzymatic hydrolysis: Trends and Challenges. *Eng. Life Sci.* 1–33. doi:10.1002/elsc.201800158

- Rojas, J., Bedoya, M., Ciro, Y., 2015. Current trends in the production of cellulose nanoparticles and nanocomposites for biomedical applications. *Intech* 194–228.
- Roman, M., Winter, W.T., 2004. Effect of sulfate groups from sulfuric acid hydrolysis on the thermal degradation behavior of bacterial cellulose. *Biomacromolecules* 5, 1671–1677. doi:10.1021/bm034519+
- Rosa, M.F., Medeiros, E.S., Malmonge, J.A., Gregorski, K.S., Wood, D.F., Mattoso, L.H.C., Glenn, G., Orts, W.J., Imam, S.H., 2010. Cellulose nanowhiskers from coconut husk fibers: Effect of preparation conditions on their thermal and morphological behavior. *Carbohydr. Polym.* 81, 83–92. doi:10.1016/j.carbpol.2010.01.059
- Rosa, S.M.L., Rehman, N., De Miranda, M.I.G., Nachtigall, S.M.B., Bica, C.I.D., 2012. Chlorine-free extraction of cellulose from rice husk and whisker isolation. *Carbohydr. Polym.* 87, 1131–1138. doi:10.1016/j.carbpol.2011.08.084
- Saad, W.M., Ridwan, R., Lasim, N.S., Liyana, N., Rapi, M., Salim, F., 2019. Determination and Quantification of p - Coumaric Acid in Pineapples (*Ananas comosus*) Extracts using Gradient Mode RP-HPLC. *Pharmacogn. Res.* 11, 78–82. doi:10.4103/pr.pr
- Sabiha-Hanim, S., Aziatul-Akma, A., 2016. Polymer characterization of cellulose and hemicellulose. *Polym. Sci. Res. Adv. Pract. Appl. Educ. Asp.* 404–411.
- Saha, B., 2004. Lignocellulose biodegradation and applications in biotechnology. *ACS Symp. Ser.* 889, 2–34. doi:10.1021/bk-2004-0889.ch001
- Saha, B.C., 2003. Hemicellulose bioconversion. *J. Ind. Microbiol. Biotechnol.* 30, 279–291. doi:10.1007/s10295-003-0049-x
- Saito, T., Hirota, M., Tamura, N., Kimura, S., Fukuzumi, H., Heux, L., Isogai, A., 2009. Individualization of nano-sized plant cellulose fibrils by direct surface carboxylation using TEMPO catalyst under neutral conditions. *Biomacromolecules* 10, 1992–1996. doi:10.1021/bm900414t
- Samir, A., Alloin, F., Dufresne, A., 2005. Review of recent research into cellulosic whiskers, their properties and their application in nanocomposite field. *Biomacromolecules* 6, 612–626. doi:10.1021/bm0493685
- Sánchez-Bastardo, N., Cocero, M.J., Alonso, E., 2013. Heterogenous Catalysis for the Extraction of Arabinoxylans From Wheat Bran. *J. Chem. Inf. Model.* 53, 1689–1699. doi:10.1017/CBO9781107415324.004
- Santos, J.I., Martín-sampedro, R., Fillat, Ú., Oliva, J.M., Negro, M.J., Ballesteros, M., Eugenio, M.E.,

- Ibarra, D., 2015. Evaluating Lignin-Rich Residues from Biochemical Ethanol Production of Wheat Straw and Olive Tree Pruning by FTIR and 2D-NMR. *Int. J. Polym. Sci.* 2015, 1–11.
- Satyamurthy, P., Jain, P., Balasubramanya, R.H., Vigneshwaran, N., 2011. Preparation and characterization of cellulose nanowhiskers from cotton fibres by controlled microbial hydrolysis. *Carbohydr. Polym.* 83, 122–129. doi:10.1016/j.carbpol.2010.07.029
- Saunders, R.M., Walker, H.G.J., 1968. *The Sugars of Wheat Bran*.
- Saxena, A., 2013. *Nanocomposites Based on Nanocellulose Whiskers*. Georgia Institute of Technology.
- Scheller, H.V., Ulvskov, P., 1871. Hemicelluloses. doi:10.1146/annurev-arplant-042809-112315
- Shak, K.P.Y., Pang, Y.L., Mah, S.K., 2018. Nanocellulose: Recent advances and its prospects in environmental remediation. *Beilstein J. Nanotechnol.* 9, 2479–2498. doi:10.3762/bjnano.9.232
- Shibuya, H., Hayashi, T., 2008. *Manufacture of cellulose nanofibers by enzymatic treatment* 13.
- Siddiqui, N., Mills, R.H., Gardner, D.J., Bousfield, D., Siddiqui, N., Mills, R.H., Gardner, D.J., Bousfield, D., 2011. Production and Characterization of Cellulose Nanofibers from Wood Pulp Production and Characterization of Cellulose Nanofibers from Wood Pulp. *J. Adhes. Sci. Technol.* 25, 709–721. doi:10.1163/016942410X525975
- Silverstein, R.A., Chen, Y., Sharma-Shivappa, R.R., Boyette, M.D., Osborne, J., 2007. A comparison of chemical pretreatment methods for improving saccharification of cotton stalks. *Bioresour. Technol.* 98, 3000–3011. doi:10.1016/j.biortech.2006.10.022
- Sinha, A.K., Kumar, V., Makkar, H.P.S., Boeck, G. De, Becker, K., 2012. Non-starch polysaccharides and their role in fish nutrition – A review. *Food Chem.* 127, 1409–1426. doi:10.1016/j.foodchem.2011.02.042
- Sipponen, M.H., Pihlajaniemi, V., Sipponen, S., Pastinen, O., Laakso, S., 2014. Autohydrolysis and aqueous ammonia extraction of wheat straw: effect of treatment severity on yield and structure of hemicellulose and lignin. *RSC Adv.* 4, 23177–23184. doi:10.1039/c4ra03236e
- Siro, I., Plackett, D., 2010. Microfibrillated cellulose and new nanocomposite materials: A review. *Cellulose* 17, 459–494. doi:10.1007/s10570-010-9405-y
- Sluiter, A., Hames, B., Hyman, D., Payne, C., Ruiz, R., Scarlata, C., Sluiter, J., Templeton, D., Wolfe, J., 2008a. Determination of total solids in biomass and total dissolved solids in liquid process samples. *Natl. Renew. Energy Lab.* 1–6. doi:NREL/TP-510-42621
- Sluiter, A., Hames, B., Ruiz, R., Scarlata, C., Sluiter, J., Templeton, D., 2008b. Determination of Ash in Biomass. *Natl. Renew. Energy Lab.* 1–5.

- Sluiter, A., Hames, B., Ruiz, R., Scarlata, C., Sluiter, J., Templeton, D., Crocker, D., 2012. Determination of Structural Carbohydrates and Lignin in Biomass Determination of Structural Carbohydrates and Lignin in Biomass. *Natl. Renew. Energy Lab.* 1–15.
- Sluiter, A., Ruiz, R., Scarlata, C., Sluiter, J., Templeton, D., 2008c. Determination of Extractives in Biomass. *Natl. Renew. Energy Lab.*
- Stelte, W., Sanadi, A.R., 2009. Preparation and characterization of cellulose nanofibers from two commercial hardwood and softwood pulps. *Ind. Eng. Chem. Res.* 48, 11211–11219. doi:10.1021/ie9011672
- Stephens, C.H., Whitmore, P.M., Morris, H.R., Bier, M.E., 2008. Hydrolysis of the amorphous cellulose in cotton-based paper. *Biomacromolecules* 9, 1093–1099. doi:10.1021/bm800049w
- Strømme, M., Mihranyan, A., Ek, R., 2002. What to do with all these algae? *Mater. Lett.* 57, 569–572. doi:10.1016/s0167-577x(02)00831-5
- Sun, F., Sun, Q., 2015. Current Trends in Lignocellulosic Analysis with Chromatography. *Ann. Chromatogr. Sep. Tech.* 1, 1–8.
- Sun, R., Lawther, J.M., Bank, W.B., 1996. Fractional and structural characterization of wheat straw hemicelluloses. *Carbohydr. Polym.* 29, 0–6.
- Sun, R., Lawther, J.M., Banks, W.B., 1995. Influence of alkaline pre-treatments on the cell wall components of wheat straw. *Ind. Crops Prod.* 4, 127–145.
- Sun, R., Sun, X.F., Wang, S.Q., Zhu, W., Wang, X.Y., 2002. Ester and ether linkages between hydroxycinnamic acids and lignins from wheat , rice , rye , and barley straws , maize stems , and fast-growing poplar wood. *Ind. Crop. Prod.* 15, 179–188.
- Sun, R., Tomkinson, J., 2002. Comparative study of lignins isolated by alkali and ultrasound-assisted alkali extractions from wheat straw. *Ultrason. Sonochem.* 9, 85–93.
- Sun, R., Tomkinson, J., Wang, S., Zhu, W., 2000. Characterization of lignins from wheat straw by alkaline peroxide treatment. *Polym. Degrad. Stab.* 67, 101–109.
- Sun, R.C., Sun, X.F., Ma, X.H., 2002. Effect of ultrasound on the structural and physiochemical properties of organosolv soluble hemicelluloses from wheat straw. *Ultrason. Sonochem.* 9, 95–101.
- Sun, R.C., Tomkinson, J., Wang, Y.X., Xiao, B., 2000. Physico-chemical and structural characterization of hemicelluloses from wheat straw by alkaline peroxide extraction. *Polymer (Guildf).* 41, 2647–2656.

- Sun, X.-F., Sun, R., Fowler, P., Baird, M.S., 2005. Extraction and Characterization of Original Lignin and Hemicelluloses from Wheat Straw. *J. Agric. Food Chem.* 860–870. doi:10.1021/jf040456q
- Sun, X.F., Sun, R.C., Su, Y., Sun, J.X., 2004. Comparative Study of Crude and Purified Cellulose from Wheat Straw. *J. Agric. Food Chem.* 52, 839–847. doi:10.1021/jf0349230
- Sun, Y., Cheng, J., 2002. Hydrolysis of lignocellulosic materials for ethanol production: a review. *Bioresour. Technol.* 83, 1–11. doi:10.1016/S0960-8524(01)00212-7
- Šutka, A., Kukle, S., Gravitis, J., Grave, L., 2013. Characterization of Cellulose Microfibrils Obtained from Hemp, in: *Conference Papers in Materials Science*. pp. 1–7.
- Svagan, A.J., Samir, M.A.S.A., Berglund, L.A., 2007. Biomimetic Polysaccharide Nanocomposites of High Cellulose Content and High Toughness. *Biomacromolecules* 8, 2556–2563.
- Tahir, M.I., Khalique, A., Pasha, T.N., Bhatti, J.A., 2002. Comparative Evaluation of Maize Bran , Wheat Bran and Rice Bran on Milk Production of Holstein Friesian Cattle. *Int. J. Agric. Biol.* 4, 559–560.
- Tanahashi, M., Takada, S., Aoki, T., Goto, T., Higuchi, T., Hanai, S., 1982. Characterization of Explosion Wood. *Wood Res.* 66, 36–51.
- Tanpichai, S., Quero, F., Nogi, M., Yano, H., Young, R.J., Lindstro, T., Sampson, W.W., Eichhorn, S.J., 2012. Effective Young's Modulus of Bacterial and Microfibrillated Cellulose Fibrils in Fibrous Networks. *Biomacromolecules* 13, 1340–1349.
- Tapin, S., Sigoillot, J.-C., Asther, M., Petit-Conil, M., 2006. Feruloyl Esterase Utilization for Simultaneous Processing of Nonwood Plants into Phenolic Compounds and Pulp Fibers. *J. Agric. Food Chem.* 54, 3697–3703.
- Teixeira, E. de M., Correa, A.C., Manzoli, A., Leite, F. de L., Oliveira, C.R. de, Mattoso, L.H.C., 2010. Cellulose nanofibers from white and naturally colored cotton fibers. *Cellulose* 17, 595–606. doi:10.1007/s10570-010-9403-0
- Thermowoodhandbook, 2003. *ThermoWood Handbook*. Finnish ThermoWood Association.
- Thiripura Sundari, M., Ramesh, A., 2012. Isolation and characterization of cellulose nanofibers from the aquatic weed water hyacinth - *Eichhornia crassipes*. *Carbohydr. Polym.* 87, 1701–1705. doi:10.1016/j.carbpol.2011.09.076
- Thring, R.W., 1994. Alkaline degradation of ALCELL® lignin. *Biomass and Bioenergy* 7, 125–130. doi:10.1016/0961-9534(94)00051-T
- Tian, C., Yi, J., Wu, Y., Wu, Q., Qing, Y., Wang, L., 2016. Preparation of highly charged cellulose

- nanofibrils using high-pressure homogenization coupled with strong acid hydrolysis pretreatments. *Carbohydr. Polym.* 136, 485–492. doi:10.1016/j.carbpol.2015.09.055
- Tibolla, H., Maria, F., Cecilia, F., 2014. Cellulose nanofibers produced from banana peel by chemical and enzymatic treatment. *LWT - Food Sci. Technol.* 59, 1311–1318. doi:10.1016/j.lwt.2014.04.011
- Tibolla, H., Pelissari, F.M., Rodrigues, M.I., Menegalli, F.C., 2017. Cellulose nanofibers produced from banana peel by enzymatic treatment : Study of process conditions. *Ind. Crop. Prod.* 95, 664–674. doi:10.1016/j.indcrop.2016.11.035
- Tirpanalan, Ö., Reisinger, M., Huber, F., Kneifel, W., Novalin, S., 2014. Wheat bran biorefinery: An investigation on the starch derived glucose extraction accompanied by pre- and post-treatment steps. *Bioresour. Technol.* 163, 295–299. doi:10.1016/j.biortech.2014.04.058
- Tutt, M., Kikas, T., Olt, J., 2012. Influence of different pretreatment methods on bioethanol production from wheat straw. *Agronoy Res. Bioystem Engineering Spec.* 269–276.
- USDA, 2015. World Agricultural Supply and Demand Estimates. United States Dep. Agric. 1–40. doi:WASDE-525
- Vanderfleet, O.M., Osorio, D.A., Cranston, E.D., 2017. Optimization of cellulose nanocrystal length and surface charge density through phosphoric acid hydrolysis. *Philos. Trans. R. Soc. A* 376, 1–17.
- Vijayalaxmi, S., Jayalakshmi, S.K., Sreeramulu, K., 2014. Polyphenols from different agricultural residues: extraction, identification and their antioxidant properties. *J. Food Sci. Technol.* 52, 1–9. doi:10.1007/s13197-014-1295-9
- Visakh, P.M., Matthew, A.P., Oksman, K., Thomas, S., 2014. Starch-based bionanocomposites: processing and properties, in: Habibi, Y., Lucia, L.A. (Eds.), *Polysaccharide Building Blocks: A Sustainable Approach to the Development of Renewable Biomaterials*. John Wiley & Sons, Inc., pp. 289–309.
- Waga, J., 2004. Structure and allergenicity of wheat gluten proteins – a review. *Polish J. Food Nutrition Sci.* 13, 327–338.
- Wan, C., Zhou, Y., Li, Y., 2011. Liquid hot water and alkaline pretreatment of soybean straw for improving cellulose digestibility. *Bioresour. Technol.* 102, 6254–6259. doi:10.1016/j.biortech.2011.02.075
- Wang, H., Roeder, R.D., Whitney, R.A., Champagne, P., Cunningham, M.F., 2015. Graft Modification of Crystalline Nanocellulose by Cu (0) -Mediated SET Living Radical Polymerization. *J. Polmer*

- Sci. 53, 2800–2808. doi:10.1002/pola.27754
- Wang, J., Sun, B., Liu, Y., Zhang, H., 2014. Optimisation of ultrasound-assisted enzymatic extraction of arabinoxylan from wheat bran. *Food Chem.* 150, 482–488. doi:10.1016/j.foodchem.2013.10.121
- Wang, K., Jiang, J.X., Xu, F., Sun, R.C., 2009. Influence of steaming pressure on steam explosion pretreatment of lespedeza stalks (*Lespedeza cyrtobotrya*). II. Characteristics of degraded lignin. *J. Appl. Polym. Sci.* 116, 1617–1625. doi:10.1002/app.31529
- Wang, N., Ding, E., Cheng, R., 2007. Thermal degradation behaviors of spherical cellulose nanocrystals with sulfate groups. *Polymer (Guildf)*. 48, 3486–3493. doi:10.1016/j.polymer.2007.03.062
- Warren, F.J., Gidley, M.J., Flanagan, B., 2015. Infrared spectroscopy as a tool to characterise starch ordered structure- a joint FTIR-ATR, NMR, XRD and DSC study. *Carbohydr. Polym.* 15, 1–26. doi:10.1016/j.carbpol.2015.11.066
- Watkins, D., Nuruddin, M., Hosur, M., Tcherbi-narteh, A., Jeelani, S., 2015. Extraction and characterization of lignin from different biomass resources. *J. Mater. Res. Technol.* 4, 26–32. doi:10.1016/j.jmrt.2014.10.009
- Werner, K., Pommer, L., Broström, M., 2014. Thermal decomposition of hemicelluloses. *J. Anal. Appl. Pyrolysis* 110, 130–137. doi:10.1016/j.jaap.2014.08.013
- Whitford, D., 1961. Proteins structure and function, *Deutsche medizinische Wochenschrift* (1946).
- Wild, P.J. De, Huijgen, W.J.J., Heeres, H.J., 2012. Pyrolysis of wheat straw-derived organosolv lignin. *J. Anal. Appl. Pyrolysis* 93, 95–103. doi:10.1016/j.jaap.2011.10.002
- Wrigley, C.W., Corke, H., Faubion, J., 2016. The Grains that Feed the World, in: Reference Module in Food Science. doi:<http://dx.doi.org/10.1016/B978-0-08-100596-5.00003-2>
- Wu, H., Li, H., Xue, Y., Luo, G., Gan, L., Liu, J., Mao, L., 2017. High efficiency co-production of ferulic acid and xylooligosaccharides from wheat bran by recombinant xylanase and feruloyl esterase. *Biochem. Eng. J.* 120, 41–48. doi:10.1016/j.bej.2017.01.001
- Xiao, B., Sun, X.F., Sun, R., 2001. Chemical, structural, and thermal characterizations of alkali-soluble lignins and hemicelluloses, and cellulose from maize stems, rye straw, and rice straw. *Polym. Degrad. Stab.* 74, 307–319.
- Xu, F., Liu, C.F., Geng, Z.C., Sun, J.X., Sun, R.C., Hei, B.H., Lin, L., Wu, S.B., Je, J., 2006. Characterisation of degraded organosolv hemicelluloses from wheat straw. *Polym. Degrad. Stab.* 91, 1880–1886. doi:10.1016/j.polymdegradstab.2005.11.002

- Xu, F., Sun, J.X., Liu, C.F., Sun, R.C., 2006. Comparative study of alkali- and acidic organic solvent-soluble hemicellulosic polysaccharides from sugarcane bagasse. *Carbohydr. Res.* 341, 253–261. doi:10.1016/j.carres.2005.10.019
- Xu, J., Chen, Y., Cheng, J.J., Sharma-Shivappa, R.R., Burns, J.C., 2011. Delignification of switchgrass cultivars for bioethanol production. *BioResources* 6, 707–720.
- Xue, B., Wen, J., Xu, F., Sun, R., 2012. Structural characterization of hemicelluloses fractionated by graded ethanol precipitation from *Pinus yunnanensis*. *Carbohydr. Res.* 352, 159–165. doi:10.1016/j.carres.2012.02.004
- Yang, H., Xie, Y., Zheng, X., Pu, Y., Huang, F., Meng, X., Wu, W., 2016. Comparative study of lignin characteristics from wheat straw obtained by Comparative study of soda-AQ and kraft pretreatment and effect on the following enzymatic hydrolysis process. *Bioresour. Technol.* 207, 361–369. doi:10.1016/j.biortech.2016.01.123
- Yu, H., Qin, Z., Liang, B., Liu, N., Zhou, Z., Chen, L., 2013. Facile extraction of thermally stable cellulose nanocrystals with a high yield of 93% through hydrochloric acid hydrolysis under hydrothermal conditions. *J. Mater. Chem. A* 1, 3938–3944. doi:10.1039/c3ta01150j
- Yuan, T., Xu, F., He, J., Sun, R., 2010. Structural and physico-chemical characterization of hemicelluloses from ultrasound-assisted extractions of partially delignified fast-growing poplar wood through organic solvent and alkaline solutions. *Biotechnol. Adv.* 28, 583–593. doi:10.1016/j.biotechadv.2010.05.016
- Yuan, Z., Kapu, N.S., Beatson, R., Feng, X., Martinez, D.M., 2016. Effect of alkaline pre-extraction of hemicelluloses and silica on kraft pulping of bamboo (*Neosinocalamus affinis* Keng). *Ind. Crop. Prod.* 91, 66–75. doi:10.1016/j.indcrop.2016.06.019
- Zeni, M., Favero, D., Mc, A.G., 2015. Preparation of Microcellulose (Mcc) and Nanocellulose (Ncc) from Eucalyptus Kraft Ssp Pulp. *iMed Pub Polym. Sci.* 1, 1–5. doi:10.21767/2471-9935.100007
- Zhai, R., Hu, J., Saddler, J.N., 2018. Bioresource Technology The inhibition of hemicellulosic sugars on cellulose hydrolysis are highly dependant on the cellulase productive binding , processivity , and substrate surface charges. *Bioresour. Technol.* 258, 79–87. doi:10.1016/j.biortech.2017.12.006
- Zheng, H., 2014. Production of fibrillated cellulose materials - effects of pretreatments and refining strategy on pulp properties. Aalto University School of Chemical Technology.
- Zheng, Q., Zhou, T., Wang, Y., Cao, X., Wu, S., Zhao, M., 2018. Pretreatment of wheat straw leads to structural changes and improved enzymatic hydrolysis. *Sci. Rep.* 8, 1321. doi:10.1038/s41598-

018-19517-5

- Zhu, L., O'Dwyer, J.P., Chang, V.S., Granda, C.B., Holtzaple, M.T., 2008. Structural features affecting biomass enzymatic digestibility. *Bioresour. Technol.* 99, 3817–3828. doi:10.1016/j.biortech.2007.07.033
- Zimmermann, T., Bordeanu, N., Strub, E., 2010. Properties of nanofibrillated cellulose from different raw materials and its reinforcement potential. *Carbohydr. Polym.* 79, 1086–1093. doi:10.1016/j.carbpol.2009.10.045
- Zuluaga, R., Putaux, J., Restrepo, A., Mondragon, I., Ganan, P., 2007. Cellulose microfibrils from banana farming residues: isolation and characterization. *Cellulose* 14, 585–592. doi:10.1007/s10570-007-9118-z

Appendix A: Infrared Band Assignment

Table 6.2 Peak assignments for various functional groups found in various extracts

Wavenumber (cm ⁻¹)	Peak Assignments	Reference
3345 - 3200	O—H stretching	Rosa et al. 2010
2924 - 2901	C—H ₂ stretching	Rosa et al. 2010
2893	C—H stretching	Rosa et al. 2010
1745 - 1731	C=O stretch of hemicelluloses and lignin/ acetyl and uronic ester groups of the hemicelluloses or the ester linkage of carboxylic group of the ferulic and <i>p</i> -Coumaric acids of lignin and/or hemicelluloses	Rosa et al. 2012; Sun & Tomkinson 2002
1709	C=O stretch of hemicelluloses and lignin	Rosa et al. 2010
1652 - 1646	H—O—H bending of absorbed water /Amide I peak of protein	Garidel & Schott 2006; Warren et al. 2015
1634 - 1639	C=O stretching conjugate with aromatic ring of lignin	Rosa et al. 2010
1597 - 1590	C=C aromatic vibration of lignin	Rosa et al. 2010
1543 - 1539	C=C aromatic vibration of lignin/ Amide II peak of protein	Warren et al. 2015; Rodrigues et al. 1998; Warren et al. 2015
1519 - 1505	C=C aromatic vibration of lignin	Rosa et al. 2010
1428 - 1408	C—H deformation of cellulose and lignin	Rosa et al. 2010
1386 - 1370	C—H ₃ symmetric bending	Garidel & Schott 2006
1368- 1359	C—H deformation of cellulose, hemicelluloses and lignin	Rosa et al. 2010
1335 - 1327	Weak C—O stretching or O—H in plane deformation of cellulose	Rosa et al. 2010
1319 - 1313	C—H ₂ wag of cellulose	Rosa et al. 2010

1278 - 1242	C—C, C—O, C=O stretching of hemicelluloses and G ring condensation of lignin	Adapa & Canam 2011; Hu & Ragauskas 2012
1221 - 1201	O—H deformation of cellulose	Rosa et al. 2010
1160 - 1120	C—O—C assymetric stretch of cellulose, hemicelluloses and lignin	Rosa et al. 2010
1078 - 1050	C—O stretch of hemicelluloses and lignin	Rosa et al. 2010
1036 - 1015	C—O stretch of cellulose, hemicelluloses and lignin	Rosa et al. 2010
997 - 981	C—H out of plane deformation of lignin or C—O stretching of hemicelluloses	Rosa et al. 2010; Sun & Tomkinson 2002
897 - 837	β -glucosidic linkage between sugar units, C ₁ —H deformation of celluloses and hemicelluloses	Rosa et al. 2010
668 - 660	Ring bend of lignin	Rosa et al. 2010

Appendix B: ANOVA Analysis Tables

Table 6.3 ANOVA table for hemicellulose purity of mild alkaline treatment optimisation of wheat straw

Factors	Sum of squares	df	Mean square	F value	P value
(1) Temperature, °C(L)	10.1652	1	10.1652	12.2293	0.024963
Temperature, °C(Q)	243.2234	1	243.2234	292.6116	0.000069
(2) NaOH Concentration, wt%(L)	53.3325	1	53.3325	64.1621	0.001318
NaOH Concentration, wt%(Q)	14.29	1	14.29	17.1916	0.014303
1L by 2L	14.8709	1	14.8709	17.8905	0.013373
Lack of Fit	15.0085	3	5.0028	6.0187	0.057804
Pure Error	3.3249	4	0.8312		
Total SS	343.0306	12			

$R^2 = 0.95$

Table 6.4 ANOVA table for hemicellulose yield of mild alkaline treatment optimisation of wheat straw

Factors	Sum of squares	df	Mean square	F value	P value
(1) Temperature, °C(L)	108.1992	1	108.1992	1149.186	0.000005
Temperature, °C(Q)	27.5634	1	27.5634	292.752	0.000068
(2) NaOH Concentration, wt%(L)	283.2458	1	283.2458	3008.359	0.000001
NaOH Concentration, wt%(Q)	79.7984	1	79.7984	847.541	0.000008
1L by 2L	22.7154	1	22.7154	241.261	0.0001
Lack of Fit	54.4956	3	18.1652	192.933	0.000088
Pure Error	0.3766	4	0.0942		
Total SS	565.8115	12			

$R^2 = 0.90$

Table 6.5 ANOVA table for *p*-coumaric acid yield of mild alkaline treatment optimisation of wheat straw

Factors	Sum of squares	df	Mean square	F value	P value
(1) Temperature, °C(L)	2732.213	1	2732.213	22740.76	0
Temperature, °C(Q)	218.509	1	218.509	1818.69	0.000002
(2) NaOH Concentration, wt%(L)	37.937	1	37.937	315.76	0.000059
NaOH Concentration, wt%(Q)	977.848	1	977.848	8138.82	0
1L by 2L	47.097	1	47.097	392	0.000038
Lack of Fit	1639.285	3	546.428	4548.03	0
Pure Error	0.481	4	0.12		
Total SS	5551.452	12			

$R^2 = 0.70$

Table 6.6 ANOVA table for hemicellulose purity of mild alkaline treatment optimisation of wheat bran

Factors	Sum of squares	df	Mean square	F value	P value
(1) Temperature, °C(L)	203.6931	1	203.6931	210.6916	0.000131
Temperature, °C(Q)	0.8797	1	0.8797	0.9099	0.394151
(2) NaOH Concentration, wt%(L)	37.1189	1	37.1189	38.3942	0.003449
NaOH Concentration, wt%(Q)	0.0025	1	0.0025	0.0026	0.961722
1L by 2L	0.0134	1	0.0134	0.0138	0.912113
Lack of Fit	16.9495	3	5.6498	5.844	0.06055
Pure Error	3.8671	4	0.9668		
Total SS	262.552	12			

$R^2 = 0.92$

Table 6.7 ANOVA table for hemicellulose yield of mild alkaline treatment optimisation of wheat bran

Factors	Sum of squares	df	Mean square	F value	P value
(1) Temperature, °C(L)	1101.278	1	1101.278	133.6684	0.00032
Temperature, °C(Q)	12.988	1	12.988	1.5764	0.277617
(2) NaOH Concentration, wt%(L)	113.901	1	113.901	13.8248	0.020507
NaOH Concentration, wt%(Q)	8.398	1	8.398	1.0194	0.369785
1L by 2L	10.103	1	10.103	1.2262	0.330249
Lack of Fit	109.43	3	36.477	4.4274	0.092323
Pure Error	32.956	4	8.239		
Total SS	1392.194	12			

$R^2 = 0.90$

Table 6.8 ANOVA table for ferulic acid yield of mild alkaline treatment optimisation of wheat bran

Factors	Sum of squares	df	Mean square	F value	P value
(1) Temperature, °C(L)	222.06	1	222.06	358.254	0.000046
Temperature, °C(Q)	1077.53	1	1077.53	1738.4	0.000002
(2) NaOH Concentration, wt%(L)	27.859	1	27.859	44.945	0.002576
NaOH Concentration, wt%(Q)	0.87	1	0.87	1.404	0.301627
1L by 2L	50.034	1	50.034	80.72	0.000849
Lack of Fit	545.655	3	181.885	293.438	0.000038
Pure Error	2.479	4	0.62		
Total SS	1953.253	12			

$R^2 = 0.72$

Table 6.9 Treatment conditions and response from alkaline delignification treatment of wheat straw for production of cellulose-rich pulp and lignin extraction

Time, min	NaOH Conc., wt%	Residue Cellulose, %	Residue Lignin, %	<i>Residue Hemicelluloses, %</i>	Lignin Yield/ MAWS	Extracted Original Lignin, %
30	8	65.44	18.34	<i>4.39</i>	41.87	
30	12	57.63	14.23	<i>3.31</i>	63.11	
90	8	59.82	17.57	<i>4.04</i>	43.85	
90	12	59.47	14.32	<i>3.13</i>	50.55	
60	10	78.91	11.90	<i>3.78</i>	88.63	
60	10	<i>77.67</i>	11.53	<i>3.44</i>	86.04	
60	10	75.80	12.42	<i>3.74</i>	88.24	
60	7.17	70.34	14.69	<i>4.16</i>	65.10	
60	12.83	51.61	13.74	<i>2.33</i>	64.74	
17.57	10	71.93	20.42	<i>2.98</i>	56.65	
102.43	10	68.35	20.48	<i>2.86</i>	27.89	

Italicised values not included in model as response

Table 6.10 ANOVA table for residue cellulose content of alkaline delignification treatment optimisation of wheat straw

Factor	SS	df	MS	F	p
(1) Time, min(L)	9.7747	1	9.7747	3.9879	0.183917
Time, min(Q)	135.7649	1	135.7649	55.3894	0.017579
(2) NaOH Conc., wt%(L)	150.1065	1	150.1065	61.2405	0.01594
NaOH Conc., wt%(Q)	507.7624	1	507.7624	207.157	0.004793
1L by 2L	13.9129	1	13.9129	5.6762	0.140085
Lack of Fit	91.7303	3	30.5768	12.4747	0.075122
Pure Error	4.9022	2	2.4511		
Total SS	805.7558	10			

$R^2 = 0.88$

Table 6.11 ANOVA table for residue lignin content of alkaline delignification treatment optimisation of wheat straw

Factor	SS	df	MS	F	p
(1) Time, min(L)	0.0443	1	0.04427	0.2215	0.68426
Time, min(Q)	87.9186	1	87.91858	439.8128	0.002266
(2) NaOH Conc., wt%(L)	9.4652	1	9.46523	47.3498	0.020473
NaOH Conc., wt%(Q)	3.8789	1	3.87885	19.404	0.047866
1L by 2L	0.1849	1	0.1849	0.925	0.437656
Lack of Fit	7.5584	3	2.51948	12.6037	0.074401
Pure Error	0.3998	2	0.1999		
Total SS	106.2564	10			

$R^2 = 0.93$

Table 6.12 ANOVA table for lignin yield of alkaline delignification treatment optimisation of wheat straw

Factor	SS	df	MS	F	p
(1) Time, min(L)	328.372	1	328.372	168.393	0.005886
Time, min(Q)	3150.961	1	3150.961	1615.85	0.000618
(2) NaOH Conc., wt%(L)	94.002	1	94.002	48.206	0.020121
NaOH Conc., wt%(Q)	853.668	1	853.668	437.771	0.002277
1L by 2L	52.853	1	52.853	27.104	0.034972
Lack of Fit	242.795	3	80.932	41.503	0.02362
Pure Error	3.9	2	1.95		
Total SS	4049.24	10			

$R^2 = 0.94$

Table 6.13 Treatment conditions and response from alkaline delignification treatment of wheat bran for production of cellulose-rich pulp and lignin extraction

Time, min	NaOH Conc., wt. %	Residue Cellulose, %	Residue Lignin, %	<i>Residue Hemicelluloses, %</i>	Lignin Yield/MAWB %	Extracted Lignin, %
30.00	6.00	40.00	6.33	<i>31.77</i>	19.36	
30.00	10.00	39.58	5.98	<i>32.11</i>	40.88	
90.00	6.00	38.48	6.80	<i>31.03</i>	51.51	
90.00	10.00	42.70	6.25	<i>30.67</i>	62.68	
17.57	8.00	39.79	7.09	<i>33.84</i>	35.97	
102.43	8.00	43.58	7.58	<i>31.96</i>	79.63	
60.00	5.17	45.32	7.89	<i>35.77</i>	17.38	
60.00	10.83	47.24	5.97	<i>33.59</i>	51.31	
60.00	8.00	49.70	6.53	<i>33.93</i>	46.42	
60.00	8.00	48.53	6.73	<i>34.61</i>	49.48	
60.00	8.00	47.49	6.64	<i>34.12</i>	47.33	

Italicised values not included in model as response

Table 6.14 ANOVA table for residue cellulose content of alkaline delignification treatment optimisation of wheat bran

Factor	SS	df	MS	F	p
(1) Time, min(L)	6.0398	1	6.0398	4.92856	0.156591
Time, min(Q)	108.9032	1	108.9032	88.86602	0.011066
(2) NaOH Conc., wt%(L)	5.3209	1	5.3209	4.34188	0.172573
NaOH Conc., wt%(Q)	24.7605	1	24.7605	20.20477	0.046098
1L by 2L	5.3757	1	5.3757	4.38659	0.17124
Lack of Fit	30.7271	3	10.2424	8.35787	0.108737
Pure Error	2.451	2	1.2255		
Total SS	162.7973	10			

$R^2 = 0.80$

Table 6.15 ANOVA table for residue lignin content of alkaline delignification treatment optimisation of wheat straw

Factor	SS	df	MS	F	p
(1) Time, min(L)	0.259994	1	0.259994	27.9826	0.033928
Time, min(Q)	0.132062	1	0.132062	14.2136	0.063706
(2) NaOH Conc., wt%(L)	1.634252	1	1.634252	175.8908	0.005637
NaOH Conc., wt%(Q)	0.013831	1	0.013831	1.4886	0.346771
1L by 2L	0.010366	1	0.010366	1.1157	0.401601
Lack of Fit	1.664398	3	0.554799	59.7118	0.016516
Pure Error	0.018583	2	0.009291		
Total SS	3.774824	10			

$R^2 = 0.55$

Table 6.16 ANOVA table for lignin yield of alkaline delignification treatment optimisation of wheat straw

Factor	SS	df	MS	F	p
(1) Time, min(L)	1673.543	1	1673.543	679.1767	0.001469
Time, min(Q)	109.984	1	109.984	44.635	0.021678
(2) NaOH Conc., wt%(L)	813.4	1	813.4	330.1034	0.003016
NaOH Conc., wt%(Q)	302.069	1	302.069	122.589	0.008059
1L by 2L	26.8	1	26.8	10.8764	0.080937
Lack of Fit	49.03	3	16.343	6.6327	0.133821
Pure Error	4.928	2	2.464		
Total SS	3136.146	10			

$R^2 = 0.98$

Table 6.17 Treatment conditions and response factors for hydrochloric acid treatment of alkaline delignified wheat straw cellulose to produce nanocellulose

Time, h	Temperature, °C	Yield, %	ZP, mV	PdI	Length, nm	Diameter, nm	Aspect Ratio
4	80	9.31	-13.6	0.69	542	21	26
4	120	18.23	-19.1	0.65	478	22	22
8	80	12.94	-15.5	0.30	651	21	31
8	120	20.25	-19.5	0.35	668	18	38
6	71.72	8.03	-12.0	0.49	529	10	53
6	128.28	17.50	-21.6	0.83	496	15	33
3.17	100	17.23	-13.1	0.55	595	14	41
8.83	100	24.39	-18.1	0.32	638	14	46
6	100	21.31	-13.2	0.92	376	13	29
6	100	20.87	-15.3	0.85	425	15	28
6	100	22.38	-14.6	0.75	459	12	39
6	100	22.17	-15.4	0.82	479	14	33
6	100	20.92	-13.2	0.80	458	13	36

Italicised values not included in model as response variables. Where ZP is zeta potential; PdI is polydispersity index

Table 6.18 ANOVA table for nanocellulose yield optimisation after hydrochloric acid treatment of wheat straw cellulose pulp

Factor	SS	df	MS	F	p
(1) Time, h(L)	31.1143	1	31.1143	62.5979	0.001381
Time, h(Q)	4.0223	1	4.0223	8.0924	0.046644
(2) Temperature, °C(L)	109.6889	1	109.6889	220.6798	0.00012
Temperature, °C(Q)	159.2022	1	159.2022	320.2942	0.000057
1L by 2L	0.648	1	0.648	1.3037	0.317241
Lack of Fit	8.6521	3	2.884	5.8023	0.061233
Pure Error	1.9882	4	0.497		
Total SS	311.4236	12			

$R^2 = 0.97$

Table 6.19 ANOVA table for nanocellulose zeta potential optimisation after hydrochloric acid treatment of wheat straw cellulose pulp

Factor	SS	df	MS	F	p
(1) Time, h(L)	10.9802	1	10.98022	9.32107	0.037915
Time, h(Q)	4.5746	1	4.57464	3.88339	0.120082
(2) Temperature, °C(L)	66.5635	1	66.56354	56.50555	0.001676
Temperature, °C(Q)	13.8589	1	13.85886	11.76473	0.026536
1L by 2L	0.5625	1	0.56250	0.47750	0.527565
Lack of Fit	5.9739	3	1.99129	1.69040	0.305533
Pure Error	4.7120	4	1.17800		
Total SS	105.4292	12			

R²=0.90

Table 6.20 ANOVA table for nanocellulose polydispersity index optimisation after hydrochloric acid treatment of wheat straw cellulose pulp

Factor	SS	df	MS	F	p
(1) Time, h(L)	0.128821	1	0.128821	32.44853	0.004693
Time, h(Q)	0.303808	1	0.303808	76.52588	0.000941
(2) Temperature, °C(L)	0.030110	1	0.030110	7.58444	0.051165
Temperature, °C(Q)	0.064857	1	0.064857	16.33683	0.015580
1L by 2L	0.002025	1	0.002025	0.51008	0.514569
Lack of Fit	0.049410	3	0.016470	4.14860	0.101472
Pure Error	0.015880	4	0.003970		
Total SS	0.564000	12			

R²=0.88

Table 6.21 ANOVA table for nanocellulose length optimisation after hydrochloric acid treatment of wheat straw cellulose pulp

Factor	SS	df	MS	F	p
(1) Time, h(L)	16177.1	1	16177.05	9.91666	0.034545
Time, h(Q)	60951.1	1	60951.05	37.36348	0.003626
(2) Temperature, °C(L)	1096.7	1	1096.74	0.67231	0.458295
Temperature, °C(Q)	12060.6	1	12060.64	7.39327	0.053039
1L by 2L	1640.3	1	1640.25	1.00549	0.372726
Lack of Fit	7925.3	3	2641.75	1.61942	0.318733
Pure Error	6525.2	4	1631.30		
Total SS	100437.1	12			

R²=0.86

Table 6.22 Treatment conditions and response factors for enzymatic treatment of wheat straw cellulose to produce nanocellulose

Time, h	FibreCare R Dosage, ECU/g	Viscozyme L Dosage, FBG/g	Glucose Concentration, g/L	ZP, mV	PdI	Mean Diameter, nm
6	50	10	14.0	-14.1	0.92	22.74
6	100	10	15.1	-13.6	0.93	18.49
10	50	10	16.9	-8.9	1	23.61
10	100	10	18.0	-7.8	1	26.89
4.64	75	15	15.3	-15.4	0.91	12.04
10.36	75	15	23.2	-11.8	0.96	12.52
8	32.955	15	19.7	-13.8	0.93	13.16
8	117.045	15	20.4	-15.0	1	16.78
8	75	15	19.2	-15.3	0.95	14.58
8	75	15	19.4	-13.4	0.94	14.61
8	75	15	20.0	-14.4	0.94	14.82
8	75	6.59	12.8	-13.1	0.97	18.35
8	75	23.41	24.8	-13.8	1	15.90
6	50	20	22.8	-12.8	0.94	14.47
10	50	20	23.9	-11.7	1	21.44
6	100	20	22.5	-14.2	0.98	15.25
10	100	20	25.8	-11.6	1	15.23
8	75	15	18.6	-14.0	0.96	14.86
8	75	15	18.8	-14.1	0.95	14.57

Where ZP is zeta potential; PdI is polydispersity index

Table 6.23 ANOVA table for nanocellulose glucose concentration optimisation after enzymatic treatment of wheat straw cellulose pulp

Factors	SS	df	MS	F	p
(1) Time, hrs(L)	37.2094	1	37.2094	122.07	0.000382
Time, hrs(Q)	0.1133	1	0.1133	0.3718	0.574961
(2) FibreCare R Dosage, ECU/g(L)	1.7468	1	1.7468	5.7307	0.074851
FibreCare R Dosage, ECU/g(Q)	1.7293	1	1.7293	5.6733	0.075836
(3) Viscozyme L Dosage, FBG/g(L)	192.6386	1	192.6386	631.975	0.000015
Viscozyme L Dosage, FBG/g(Q)	0.1045	1	0.1045	0.3429	0.589584
1L by 2L	0.6574	1	0.6574	2.1568	0.215866
1L by 3L	0.2677	1	0.2677	0.8781	0.401771
2L by 3L	0.0556	1	0.0556	0.1823	0.691416
Lack of Fit	8.0176	5	1.6035	5.2606	0.066422
Pure Error	1.2193	4	0.3048		
Total SS	245.6252	18			

$R^2 = 0.96$

Table 6.24 ANOVA table for nanocellulose zeta potential optimisation after enzymatic treatment of wheat straw cellulose pulp

Factors	SS	df	MS	F	p
(1) Time, hrs(L)	40.04146	1	40.04146	79.67401	0.000871
Time, hrs(Q)	11.50924	1	11.50924	22.90095	0.00874
(2) FibreCare R Dosage, ECU/g(L)	0.17714	1	0.17714	0.35247	0.584661
FibreCare R Dosage, ECU/g(Q)	1.05632	1	1.05632	2.10185	0.220721
(3) Viscozyme L Dosage, FBG/g(L)	3.67504	1	3.67504	7.31255	0.053861
Viscozyme L Dosage, FBG/g(Q)	5.09807	1	5.09807	10.14408	0.033376
1L by 2L	0.58808	1	0.58808	1.17016	0.340226
1L by 3L	6.48122	1	6.48122	12.89625	0.022939
2L by 3L	0.98082	1	0.98082	1.95162	0.234932
Lack of Fit	8.83961	5	1.76792	3.51779	0.123353
Pure Error	2.01026	4	0.50257		
Total SS	71.68305	18			

$R^2 = 0.85$

Table 6.25 ANOVA table for nanocellulose polydispersity optimisation after enzymatic treatment of wheat straw cellulose pulp

Factors	SS	df	MS	F	p
(1) Time, hrs(L)	0.007384	1	0.007384	105.4899	0.000507
Time, hrs(Q)	0.000011	1	0.000011	0.1639	0.706268
(2) FibreCare R Dosage, ECU/g(L)	0.00206	1	0.00206	29.4273	0.0056
FibreCare R Dosage, ECU/g(Q)	0.000803	1	0.000803	11.4754	0.027593
(3) Viscozyme L Dosage, FBG/g(L)	0.001062	1	0.001062	15.1772	0.017604
Viscozyme L Dosage, FBG/g(Q)	0.002989	1	0.002989	42.7046	0.002833
1L by 2L	0.000312	1	0.000312	4.4643	0.102158
1L by 3L	0.000613	1	0.000613	8.75	0.041635
2L by 3L	0.000112	1	0.000112	1.6071	0.273666
Lack of Fit	0.001297	5	0.000259	3.7065	0.114234
Pure Error	0.00028	4	0.00007		
Total SS	0.017316	18			

$R^2 = 0.91$

Table 6.26 ANOVA table for nanocellulose mean diameter optimisation after enzymatic treatment of wheat straw cellulose pulp

Factors	Sum of squares	df	Mean square	F value	P value
(1) Time, hrs(L)	34.1160	1	34.11600	1726.817	0.000002
Time, hrs(Q)	10.7994	1	10.79943	546.625	0.000020
(2) FibreCare R Dosage, ECU/g(L)	0.0079	1	0.00789	0.400	0.561667
FibreCare R Dosage, ECU/g(Q)	18.2261	1	18.22612	922.534	0.000007
(3) Viscozyme L Dosage, FBG/g(L)	63.6365	1	63.63649	3221.028	0.000001
Viscozyme L Dosage, FBG/g(Q)	50.4718	1	50.47181	2554.684	0.000001
1L by 2L	0.0375	1	0.03747	1.897	0.240484
1L by 3L	0.6768	1	0.67681	34.258	0.004251
2L by 3L	2.4862	1	2.48619	125.841	0.000360
Lack of Fit	132.4091	5	26.48181	1340.405	0.000002
Pure Error	0.0790	4	0.01976		
Total SS	298.0208	18			

$R^2 = 0.56$

Appendix C: Models at Different Stages for Wheat Straw and Wheat Bran Treatments

Mild Alkaline Treatment Models for Wheat Straw

The multiple regression models for the various responses for mild alkaline treatment of wheat straw are given by the equations 6.1 to 6.3, with temperature (x_1) and NaOH concentration (x_2) as the independent factors

MAWS Hemicellulose purity model equation

$$Y = -4.97616 + 0.85360x_1 - 0.01479x_1^2 + 20.38303x_2 - 5.73291x_2^2 - 0.19281x_1x_2$$

(Eqn. 6.1)

MAWS Hemicellulose yield model equation

$$Y = -44.9523 + 0.1055x_1 - 0.0050x_1^2 + 56.5581x_2 - 13.5474x_2^2 - 0.2383x_1x_2$$

(Eqn. 6.2)

p-Coumaric acid yield model equation

$$Y = -184.000 + 2.732x_1 - 0.014x_1^2 + 199.065x_2 - 47.424x_2^2 - 0.343x_1x_2$$

(Eqn. 6.3)

Mild Alkaline Treatment Models for Wheat Bran

The multiple regression models for the various responses for mild alkaline treatment of wheat bran are given by the equations 6.4 to 6.6, with temperature (x_1) and NaOH concentration (x_2) as the independent factors

MAWB Hemicellulose purity model equation

$$Y = 18.09765 + 0.33501x_1 - 0.00089x_1^2 + 4.23459x_2 + 0.07615x_2^2 - 0.00578x_1x_2$$

(Eqn. 6.4)

MAWB Hemicellulose yield model equation

$$Y = -12.0830 - 0.0045x_1 + 0.0034x_1^2 + 18.7696x_2 - 4.3950x_2^2 + 0.1589x_1x_2$$

(Eqn. 6.5)

Ferulic acid yield model equation

$$Y = 57.7003 + 2.0458x_1 - 0.0311x_1^2 - 23.5364x_2 + 1.4148x_2^2 + 0.3537x_1x_2$$

(Eqn. 6.6)

Alkaline Delignification Treatment Models for Wheat Straw

The multiple regression models for the various responses for alkaline delignification treatment of wheat straw are given by the equations 6.7 to 6.9, with temperature (x_1) and NaOH concentration (x_2) as the independent factors

SAWS residue cellulose content model equation

$$Y = -136.507 + 0.306x_1 - 0.005x_1^2 + 43.343x_2 - 2.369x_2^2 + 0.031x_1x_2$$

(Eqn. 6.7)

SAWS residue lignin content model equation

$$Y = 49.17019 - 0.56439x_1 + 0.00438x_1^2 - 4.899922x_2 + 0.20703x_2^2 + 0.00358x_1x_2$$

(Eqn. 6.8)

SAWS lignin yield model equation

$$Y = -354.645 + 3.542x_1 - 0.026x_1^2 + 66.774x_2 - 3.071x_2^2 - 0.061x_1x_2$$

(Eqn. 6.9)

Alkaline Delignification Treatment Models for Wheat Bran

The multiple regression models for the various responses for alkaline delignification treatment of wheat bran are given by the equations 6.10 to 6.12, with temperature (x_1) and NaOH concentration (x_2) as the independent factors

SAWB residue cellulose content model equation

$$Y = 1.7775 + 0.4599x_1 - 0.0049x_1^2 + 7.6243x_2 - 0.5235x_2^2 + 0.0193x_1x_2$$

(Eqn. 6.10)

SAWB residue lignin content model equation

$$Y = 7.4931 - 0.0076x_1 + 0.0002x_1^2 + 0.0229x_2 - 0.0124x_2^2 - 0.0008x_1x_2$$

(Eqn. 6.11)

SAWB lignin yield model equation

$$Y = -141.595 + 0.239x_1 + 0.005x_1^2 + 36.885x_2 - 1.828x_2^2 - 0.043x_1x_2$$

(Eqn. 6.12)

Hydrochloric Acid Treatment Models

The multiple regression models for the various responses for hydrochloric acid treatment for nanocellulose production are given by the equations 6.13 to 6.16, with time (x_1) and temperature (x_2) as the independent factors

Yield model equation

$$Y = -135.404 + 4.27132x_1 - 0.18994x_1^2 + 2.63809x_2 - 0.0119628x_2^2 - 0.0100625x_1x_2$$

(Eqn. 6.13)

Zeta potential model equation

$$Y = -33.3657 + 0.90762x_1 - 0.202561x_1^2 + 0.505427x_2 - 0.00352957x_2^2 + 0.009375x_1x_2$$

(Eqn. 6.14)

Polydispersity index model equation

$$Y = -33.3657 + 0.90762x_1 - 0.202561x_1^2 + 0.505427x_2 - 0.00352957x_2^2 + 0.009375x_1x_2$$

(Eqn. 6.15)

Length model equation

$$Y_2 = 2549.78 - 308.722x_1 + 23.3813x_1^2 - 24.4474x_2 + 0.104122x_2^2 + 0.50625x_1x_2 \quad (\text{Eqn. 6.16})$$

Enzymatic Treatment Models

The multiple regression models for the various responses for enzymatic treatment for nanocellulose production are given by the equations 6.17 to 6.20, with time (x_1), FiberCare dosage (x_2) and Viscozyme dosage (x_3) as the independent variables

Glucose concentration model equation

$$Y = 4.4207 + 0.305873x_1 + 0.0275375x_1^2 - 0.106301x_2 + 0.000564933x_2^2 + 1.0516x_3 - 0.00347171x_3^2 + 0.00573333x_1x_2 - 0.0182917x_1x_3 - 0.000666667x_2x_3 \quad (\text{Eqn. 6.17})$$

Diameter model equation

$$Y = 4.4207 + 0.305873x_1 + 0.0275375x_1^2 - 0.106301x_2 + 0.000564933x_2^2 + 1.0516x_3 - 0.00347171x_3^2 + 0.00573333x_1x_2 - 0.0182917x_1x_3 - 0.000666667x_2x_3 \quad (\text{Eqn. 6.18})$$

Zeta potential model equation

$$Y = 4.9873 + 2.56082x_1 - 0.277504x_1^2 + 0.0721474x_2 - 0.0000441526x_2^2 - 0.0990711x_3 - 0.0242447x_3^2 - 0.00542255x_1x_2 + 0.0900085x_1x_3 + 0.00280117x_2x_3 \quad (\text{Eqn. 6.19})$$

Polydispersity index model equation

$$Y = 0.853139 + 0.0307745x_1 + 0.000277105x_1^2 - 0.000785088x_2 + 1.21756e^{-005}x_2^2 - 0.0110986x_3 + 0.000587083x_3^2 - 0.000125x_1x_2 - 0.000875x_1x_3 + 3e^{-005}x_2x_3 \quad (\text{Eqn. 6.20})$$

Appendix D: Crystallinity and Thermogravimetric analysis at Different Treatment Stages

Table 6.27 Crystallinity measurement at various stages of two-stage alkaline treatment of wheat straw and bran

Sample	Crystallinity Index, %
Untreated Wheat Bran	-
Destarched Wheat Bran	17
Mild Alkaline Treated Wheat Bran (MAWB)	34
Alkaline Delignified Treated Wheat Bran (SAWB)	41
Untreated Wheat Straw	44
Mild Alkaline Treated Wheat Straw (MAWS)	50
Alkaline Delignified Treated Wheat Straw (SAWS)	55

Table 6.28 Thermogravimetric analysis of mild and alkaline delignified wheat straw and wheat bran hemicelluloses

Sample	Onset Decomposition Temperature (T_{onset} , °C)	Maximum Decomposition Temperature (T_{max} , °C)	Moisture Content (%)	Char at 600 °C (%)
MAWS Hemicelluloses	203	288	10	26
MAWB Hemicelluloses	219	305	9	15
SAWS Hemicelluloses	188	270	2	32
SAWB Hemicelluloses	205	292	11	13

Where MAWS is mild alkaline wheat straw; MAWB is mild alkaline wheat bran; SAWS is alkaline delignified wheat straw; SAWB is alkaline delignified wheat bran

Table 6.29 Thermogravimetric analysis of mild alkaline and alkaline delignified wheat straw and wheat bran lignin

Sample	Onset Decomposition Temperature 2 nd stage (T_{onset}), °C	Maximum Decomposition Temperature 2 nd stage (T_{max}), °C	Completion Temperature 3 rd Stage (T_{comp}), °C	Moisture Content (%)	Char at 600 °C (%)
MAWS Lignin	171	295	448	7	49
MAWB Lignin	147	276	338	5	29
SAWS Lignin	141	291	452	7	29
SAWB Lignin	176	256	442	8	34

Where MAWS is mild alkaline wheat straw; MAWB is mild alkaline wheat bran; SAWS is alkaline delignified wheat straw; SAWB is alkaline delignified wheat bran

Table 6.30 Thermogravimetric analysis at various stages of two-stage alkaline treatment of wheat straw and wheat bran

Sample	Decomposition Temperature (T_{onset}), °C	T_{max} , °C	Moisture Content (%)	Char at 600 °C (%)
Untreated Wheat Straw	264	402	6.6	15.2
Mild Alkaline Treated Wheat Straw	272	400	6.2	13.3
Alkaline Delignified Treated Wheat Straw	288	406	6.1	9.5
Untreated Wheat Bran	224	349	8.3	20.6
Destarched Wheat Bran	232	350	8.3	18.1

Mild Alkaline Treated Wheat Bran	252	350	8.6	17.4
Alkaline Delignified Treated Wheat Bran	242	336	8.9	22.8

Table 6.31 Crystallinity measurement for commercial and produced nanocellulose samples

Sample	Crystallinity Index, %
Commercial CNC	74
Commercial CNF	56
SCN	75
HCN	70
ECN	48

Where CNC is cellulose nanocrystals; CNF is cellulose nanofibers; SCN is sulphuric acid nanoparticles; HCN is hydrochloric acid nanoparticles; ECN is enzymatic cellulose nanoparticles.

Table 6. 32 Thermogravimetric analysis of different nanocellulose samples.

Sample	Decomposition Temperature (T_{onset} , °C)	T_{max} , °C	Moisture Content (%)	Char at 600 °C (%)
Commercial CNC	271	345	2.7	19.3
Commercial CNF	212	401	2.1	10.3
SCN	180	309	2.2	24.9
HCN	205	380	2.2	32.3
ECN	174	378	2.0	16.5

Where CNC is cellulose nanocrystals; CNF is cellulose nanofibers; SCN is sulfuric acid nanoparticles; HCN is hydrochloric acid nanoparticles; ECN is enzymatic cellulose nanoparticles.

Appendix E: SEM Images

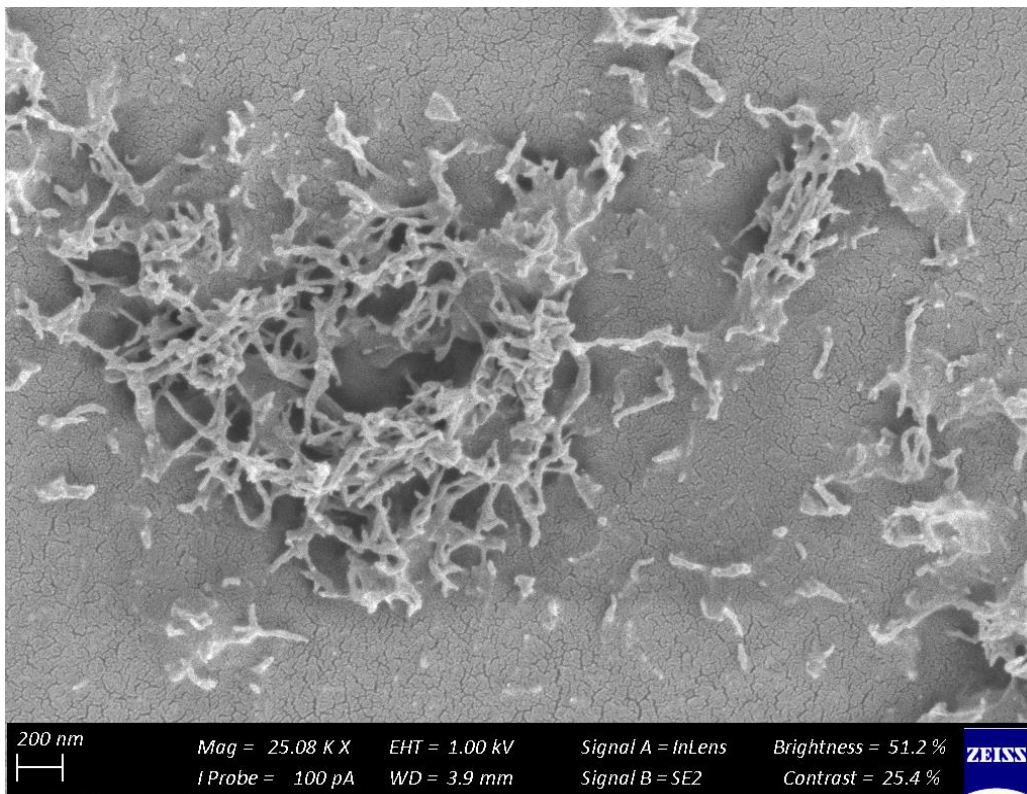


Figure 6.1 SEM image of SCN

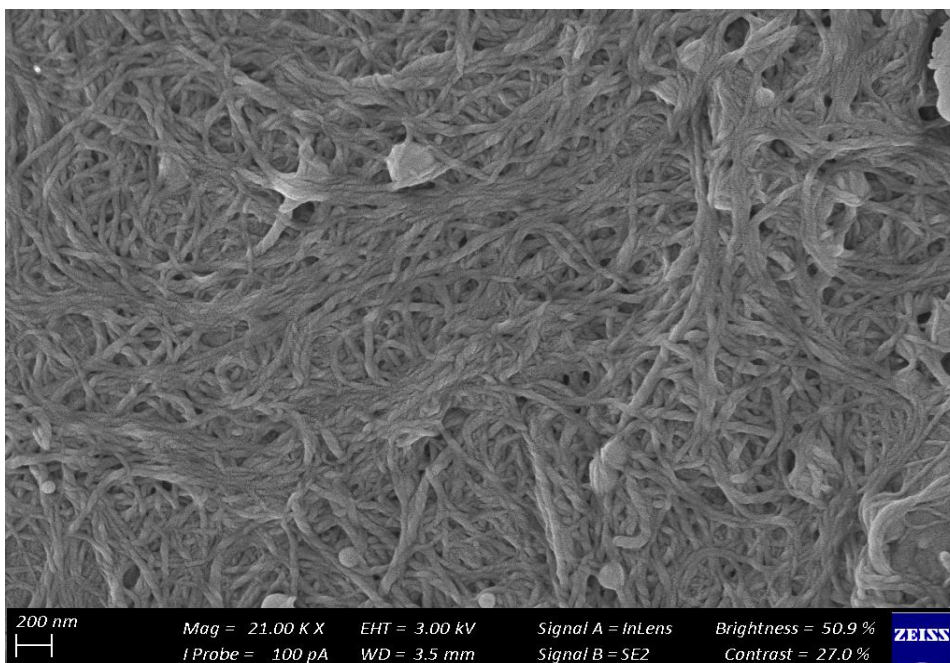


Figure 6.2 SEM image of HCN at optimum conditions

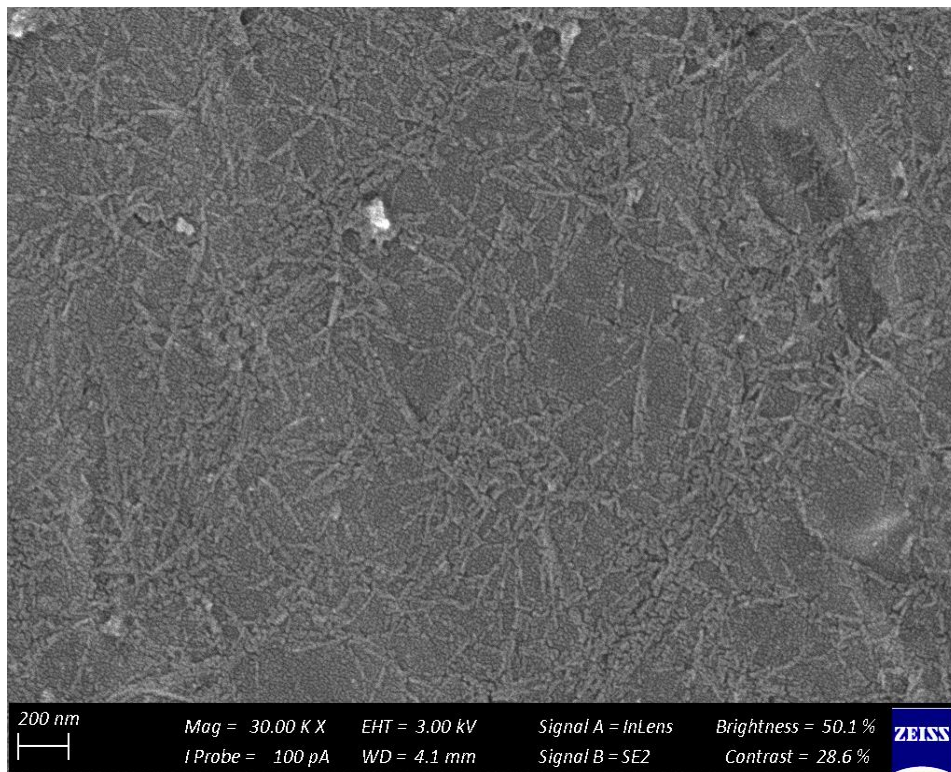


Figure 6.3 SEM image of ECN at optimum conditions